

# Quantification and Mitigation of the Impacts of Extreme Weather on Power System Resilience and Reliability

A Thesis Submitted to  
**Imperial College London**  
For the Degree of Doctor of Philosophy

*By*

**Magnus Rory Jamieson**

**Department of Electrical and Electronic Engineering**  
**Control and Power Group**  
**EPSRC CDT in Future Power Networks and the Smart Grid**  
**Imperial College London**

**18 June 2020**

## **Declaration**

This is to declare that:

1. The substantial material contained within this thesis is my own work.
2. All other work is appropriately referenced.

**Magnus Rory Jamieson**

## Copyright

*The copyright of this thesis rests with the author. Unless otherwise indicated, its contents are licensed under a Creative Commons Attribution 4.0 International Licence (CC BY).*

*Under this licence, you may copy and redistribute the material in any medium or format for both commercial and non-commercial purposes. You may also create and distribute modified versions of the work. This on the condition that you credit the author.*

*When reusing or sharing this work, ensure you make the licence terms clear to others by naming the licence and linking to the licence text. Where a work has been adapted, you should indicate that the work has been changed and describe those changes.*

*Please seek permission from the copyright holder for uses of this work that are not included in this licence or permitted under UK Copyright Law.*

## Abstract

*Modelling the impact of extreme weather on power systems is a computationally expensive, challenging area of study due to the diversity of threats, complicatedness of modelling, and data and simulation requirements to perform the relevant studies. The impacts of extreme weather – specifically wind – are considered. Factors such as the distribution of outage probability on lines and the potential correlation with wind power generation during storms are investigated; so too is sensitivity of security assessments involving extreme wind to the relationships used between failures and the natural hazard being studied, specifically wind speed. A large scale simulation ensemble is developed and demonstrated to investigate what are deemed the most significant features of power system simulation during extreme weather events.*

*The challenges associated with modelling high impact low probability (HILP) events are studied and demonstrate that the results of security assessments are significantly affected by the granularity of incident weather data being used and the corrections or interpolation being applied to the source data.*

*A generalizable simulation framework is formulated and deployed to investigate the significance of the relationship between incident natural hazards, in this case wind, and its corresponding impact on system resilience. Based on this, a large-scale simulation model is developed and demonstrated to take consideration of a wide variety of factors which can affect power systems during extreme weather events including, but not limited to, under frequency load shedding, line overloads, and high wind speed shutdown and its impact on wind generation.*

*A methodology for quantifying and visualising distributed overhead line failure risk is also demonstrated in tandem with straightforward methods for making wind power projections over transmission systems for security studies. The potential correlation between overhead line risk and wind power generation risk is illustrated visually on representations of GB power networks based on real world data.*

# Table of Contents

|   |    |
|---|----|
| List of Figures .....   | 10 |
| List of Tables .....  | 13 |
| Publications, Prizes, and Contributions .....   | 14 |
| List of Abbreviations .....   | 15 |
| List of Symbols .....   | 18 |
| Acknowledgements.....   | 19 |
| Dedications .....   | 20 |
| Chapter 1 Introduction .....  | 21 |
| 1.1 Motivations .....   | 21 |
| 1.1.1 Climate change means a more extreme, more variable planet.....  | 21 |
| 1.1.2 Understanding the importance of the data used in system security evaluations.....                         | 22 |
| 1.1.3 Understanding potential impact of decarbonisation on the power system security...                         | 23 |
| 1.1.4 Understanding the difference between reliability and resilience .....                                     | 23 |
| 1.1.5 Consequences of failures to prepare for high impact events.....   | 24 |
| 1.1.6 Tackling issues of sustainability and resilience in the power system for remote communities .....         | 25 |
| 1.2 Scope and research questions .....  | 25 |
| A. Data challenges associated with modelling weather-related impacts on power systems...                        | 26 |
| B. Challenges associated with power system simulation during extreme weather events .....                       | 27 |
| C. Quantifying and understanding the differences between reliability and resilience .....                       | 28 |
| D. Improving resilience and reliability.....  | 28 |
| E. Modelling the effects of climate change on the power system .....  | 29 |
| 1.3 Primary areas of concern .....  | 30 |
| 1.4 Novelty of work and thesis structure.....   | 30 |
| Chapter 2 Review of relationships between climate, weather, resilience, reliability, and associated issues..... | 32 |
| 2.1 Introduction .....  | 33 |
| 2.2 Quantifying impact of extreme weather on power systems .....  | 33 |
| 2.3 Understanding resilience and reliability .....  | 41 |
| 2.3.1 Qualitative descriptions of reliability and resilience.....   | 41 |
| 2.3.2 Quantitative metrics for describing reliability and resilience.....                                       | 44 |
| 2.3.3 Security standards for resilience and reliability.....  | 45 |
| 2.4 Modelling interactions between weather and the power system .....   | 46 |
| 2.4.1 Quantifying failure rates on overhead lines due to wind .....   | 47 |
| 2.4.2 Estimating wind power output from wind speeds .....   | 49 |

|  |    |
|--|----|
| 2.5 Modelling system perturbations.....  | 52 |
| 2.5.1 Overhead line faults.....  | 52 |
| 2.5.2 Loss of infeed and generation faults.....  | 53 |
| 2.5.3 Frequency response regimes .....   | 55 |
| 2.5.4 Sources of frequency response.....   | 57 |
| 2.5.5 Demand response .....  | 59 |
| 2.6 Conclusion.....  | 62 |
| Chapter 3 A simulation framework to investigate the effect of extreme wind on a power system and sensitivity to weather-fault relationships..... | 63 |
| 3.1 Introduction .....   | 64 |
| 3.2 Simulation Frameworks .....  | 65 |
| 3.3 Implementation of simulation framework and description of components .....   | 69 |
| 3.3.1 Network Builder module.....  | 69 |
| 3.3.2 Data Processing module .....   | 71 |
| 3.3.3 Weather and Climate Models .....   | 72 |
| 3.3.4 Fault Simulator .....  | 73 |
| 3.3.5 Fault Analyser module .....  | 74 |
| 3.4 Models and data used within model and implementation .....   | 74 |
| 3.4.1 Cost function modelling of generators .....  | 75 |
| 3.4.2 Non-weather failure and repair modelling .....   | 75 |
| 3.4.3 Weather-related fault, repair modelling .....  | 75 |
| 3.5 Case Study – truncated GB Network representation.....  | 78 |
| 3.6 Discussion and key findings .....  | 83 |
| 3.7 Conclusion.....  | 84 |
| Chapter 4 Quantification and visualisation of impact of wind data accuracy on failure rates on overhead lines and wind power output.....         | 86 |
| 4.1 Introduction .....   | 87 |
| 4.2 Modelling relationships between weather and line outages .....   | 87 |
| 4.3 Definition and quantification of line exposure to weather conditions.....  | 89 |
| 4.4 Computing failure rate on overhead lines for given exposure and wind speed.....  | 90 |
| 4.5 Correcting spatial wind speed data for differing applications.....   | 91 |
| 4.6 Correcting wind speed for altitude of asset.....   | 92 |
| 4.7 Interpolation of weather data for use in simulations.....  | 93 |
| 4.8 Projecting wind power for given incident wind conditions .....   | 94 |
| 4.9 Case study on Reduced GB and SHETL grid representations.....   | 95 |
| 4.9.1 Development of the SHETL grid representation .....   | 96 |

|   |     |
|---|-----|
| 4.9.2 Implementation of Reduced GB.....   | 99  |
| 4.9.3 Simulation methodology.....   | 100 |
| 4.9.4 Results – SHETL grid .....  | 101 |
| 4.9.5 Results – Ryan Model.....   | 105 |
| 4.9.6 Grid elevation.....   | 108 |
| 4.10 Discussion and key findings .....  | 111 |
| 4.11 Conclusions .....  | 113 |
| Chapter 5 Comprehensive power system simulation during extreme weather events considerate of mitigation measures and weather impacts on generation..... | 116 |
| 5.1 Introduction .....  | 117 |
| 5.2 Data requirements and problem boundaries .....  | 117 |
| 5.3 Proposed simulation approach .....  | 121 |
| 5.4 Data sources and assumptions for simulation.....  | 125 |
| 5.5 Model implementation .....  | 128 |
| 5.5.1 Mathematical Formulations.....  | 128 |
| 5.5.2 Perturbation State Generation .....   | 147 |
| 5.5.3 Check Islands and Trip Disconnected Assets .....  | 149 |
| 5.5.4 System Frequency Response features .....  | 150 |
| 5.5.5 System Frequency Response simulation.....   | 153 |
| 5.5.6 Load flow calculation and optimisation.....   | 159 |
| 5.5.7 Trip Assets simulation block.....   | 159 |
| 5.5.8 Restoration action simulation – Redispatch OPF.....   | 161 |
| 5.5.9 Restoration action simulation – Unit Commitment.....  | 162 |
| 5.6 Case Studies – Cyclone Friedhelm .....  | 162 |
| 5.6.1 Baseline: economic dispatch, very vulnerable double circuits .....  | 164 |
| 5.6.2 Loss of B6 .....  | 168 |
| 5.6.3 Large loss of generation.....   | 171 |
| 5.7 Discussion and key findings .....   | 175 |
| 5.6.1 Baseline cases .....  | 177 |
| 5.6.2 B6 cases.....   | 178 |
| 5.6.3 Large generation loss cases .....   | 179 |
| 5.6.4 Summary of cases and resilience quantification .....  | 180 |
| 5.8 Conclusion.....   | 181 |
| Chapter 6 Conclusions and future work .....   | 184 |
| 6.1 Summary of contributions and achievements.....  | 184 |

|  |     |
|--|-----|
| 6.1.1 Defining approaches and frameworks in which to simulate dependent, weather induced faults in a power system and investigate model sensitivities.....                     | 184 |
| 6.1.2 Demonstrating sensitivity of power system analysis to changes in failure rate-weather relationships.....   | 186 |
| 6.1.3 Illustrating potential correlations between overhead line fault risk and wind power .....  | 186 |
| 6.1.4 Linking spatially resolved weather data to power system modelling and simulation.....  | 187 |
| 6.1.5 Integrating simulation of frequency response with weather fault simulation and demand response.....  | 187 |
| 6.1.6 Establishing methods for assessing the effect of changing frequency response regimes on system reliability and resilience performance.....                               | 188 |
| 6.1.7 Demonstrating significance of spatial disaggregation and interpolation of weather data for use in power system simulations.....  | 189 |
| 6.1.8 Demonstrating the potential value of Flexible Demand Response solutions for containing HILP events or large loss of infeed events in frequency response simulations..... | 189 |
| 6.1.9 Understanding the potential importance of features such as Unit Commitment restrictions in resilience simulations.....   | 190 |
| 6.1.10 The significance of initial dispatch when subsequent fault events happen .....  | 190 |
| 6.1.11 Industrial co-operation and academic impact .....   | 190 |
| 6.2 Future work.....   | 191 |
| 6.2.1 Incorporation of alternative kinds of distributed renewables generation .....  | 191 |
| 6.2.2 Improved frequency response modelling.....   | 192 |
| 6.2.3 Incorporating the investment-side problem.....   | 192 |
| 6.2.4 Examining effects of other weather impacts on the power system .....   | 193 |
| 6.2.5 Effects of climate change and other externalities on system resilience .....   | 193 |
| 6.2.6 Comparator studies.....  | 194 |
| 6.2.7 Improvement of model efficiency.....   | 194 |
| 6.2.8 Optimal OHL routing planning .....   | 194 |
| 6.2.9 Improved mitigation planning .....   | 195 |
| 6.2.10 Three-dimensional OHL modelling and wind direction consideration .....  | 195 |
| 6.3 Concluding remarks .....   | 195 |
| References .....   | 197 |
| Chapter 7 - Appendices.....  | 203 |
| 7.1 Socioeconomic constraints on energy developments in Scotland .....   | 203 |
| 7.1.1 Historical underdevelopment .....  | 203 |
| 7.1.2 Perceptions of the rural environment .....   | 203 |
| 7.1.3 Consequences of underdevelopment and opposition to development.....  | 204 |
| 7.2 Model deployment on simple test case.....  | 205 |

|  |     |
|--|-----|
| 7.2.1 Scenario summary.....  | 205 |
| 7.2.2 Stage 1 - Dispatch.....  | 207 |
| 7.2.3 Stage 2 – Perturbation generation.....                         | 208 |
| 7.2.4 Stage 3 – SFR-load-flow loop .....                             | 208 |
| 7.2.5 Stage 4 – Redispatch and Unit Commitment OPFs.....             | 210 |
| 7.2.6 Stage 5 –Results and termination .....                         | 211 |
| 7.3 EWPS Outputs .....   | 211 |
| 7.3.1 Tabulated results .....  | 211 |
| 7.3.2 Comparison of flexible demand versus non-flexible demand ..... | 214 |
| 7.3.3 Frequency response versus EENS .....                           | 214 |

## List of Figures

|   |     |
|---|-----|
| Figure 2.1 - Percentage change in exceedances of 90th, 98th percentile max temperatures for test license area; each cross represents a different climate model projection and the diamonds the mean ..... | 40  |
| Figure 2.2 - "Bow-tie" model of risk planning.....  | 42  |
| Figure 2.3 - "Swiss cheese" representation of disaster propagation.....   | 43  |
| Figure 2.4 - Example resilience trapezium used in ERP report .....  | 44  |
| Figure 2.5 - fault modelling concept with regards to natural hazards.....   | 48  |
| Figure 2.6 - Ofgem derived power curve example .....  | 50  |
| Figure 2.7 - wind turbine cut-out scheme example.....   | 51  |
| Figure 2.8 - example primary frequency response curves on hypothetical system .....   | 54  |
| Figure 2.9 - frequency response regimes over time deployed in GB.....   | 55  |
| Figure 2.10 - example primary frequency response curves for varying H factors.....  | 56  |
| Figure 2.11 –frequency response for loss of 1320MW with varying k, with H = 5s, total load of 30GW, PFR of 800MW .....  | 58  |
| Figure 2.12 - LFDD disconnection thresholds on GB system and indicative percentage of time spent at frequency level in 2016-17 .....  | 60  |
| Figure 2.13 - Successful LFDD actions as %age w.r.t. system inertia.....  | 61  |
| Figure 3.1 - Approach for modelling cascading large-scale outage events .....   | 65  |
| Figure 3.2 - Approach for simulating cascading outages considering frequency response .....   | 66  |
| Figure 3.3 - Simulation framework for resilience analysis associated with natural hazard demonstrated by Panteli et al .....  | 67  |
| Figure 3.4 - Proposed simulation structure to be demonstrated .....   | 68  |
| Figure 3.5- high level flow diagram of Network Builder .....  | 71  |
| Figure 3.6- High-level representation of Data Processing algorithm.....   | 72  |
| Figure 3.7 - example of deployment of Data Processing module.....   | 72  |
| Figure 3.8- high level flow diagram of Fault Simulator module.....  | 74  |
| Figure 3.9 - TADS data extract showing representative data values .....   | 77  |
| Figure 3.10 - representative data illustrating causes of faults in TADS data .....  | 77  |
| Figure 3.11 - Failure, restoration rates w.r.t wind speed for $S_{Max}$ test case .....   | 78  |
| Figure 3.12 - Illustrative network topology with relative positions of nodes.....   | 79  |
| Figure 3.13 - Wind speed profiles used in study.....  | 79  |
| Figure 3.14 - Comparison between Smed, Smax results for EENS.....   | 82  |
| Figure 3.15 - Comparison between Smed, Smax results for EMLS.....   | 82  |
| Figure 3.16 - Empirical probability that ENS exceeds given thresholds for Ext cases.....  | 83  |
| Figure 4.1 – Fragility curves to be used in study, graph taken from [16] and [64].....  | 88  |
| Figure 4.2 - Arbitrary representation of line exposure to natural hazard .....  | 90  |
| Figure 4.3 - vertical displacement parameter "d", vertical axes arbitrary scale and regression (with d = 0m) .....  | 93  |
| Figure 4.4 - Wind power curve used in study as derived.....   | 95  |
| Figure 4.5 - Network representation of SHETL grid .....   | 96  |
| Figure 4.6 - Raw single level w-resolved wind speed data .....  | 97  |
| Figure 4.7 - Interpolated three-level wind speed data at 10m.....   | 97  |
| Figure 4.8 - Estimated total line exposure of OHL on SHETL grid .....   | 98  |
| Figure 4.9 - Wind farm capacities and locations in Scotland.....  | 98  |
| Figure 4.10 - Visualisation of reduced GB network model known as the "Ryan Model" .....   | 99  |
| Figure 4.11 - Wind farms connected to main GB system, as of December 2018 .....   | 100 |

|  |     |
|--|-----|
| Figure 4.12 - 132kV and 275kV/400kV network fault probabilities on SHETL grid .....  | 101 |
| Figure 4.13 - Total OHL failure probability on SHETL.....  | 102 |
| Figure 4.14 - Aggregated wind farm output across Scotland, together with line failure probability for 275kV and 400kV networks. ....   | 103 |
| Figure 4.15 – Failure probability on OHL overlaid with installed windfarm capacities in SHETL, Scotland .....  | 104 |
| Figure 4.16 - Simulation results for Ryan model with three-level dataset .....   | 105 |
| Figure 4.17 - Wind farm capacities and OHL failure probabilities, three-level data on Ryan Model .   | 106 |
| Figure 4.18 - Single-level incident wind speed data [left] compared to data at 10m from three-level data set .....   | 107 |
| Figure 4.19 - Estimated line failure probability due to wind, single-level data [left] compared with that using the three-level data [right] .....   | 107 |
| Figure 4.20 - Total line failure probability overlaid with installed capacity of windfarms in GB.....  | 108 |
| Figure 4.21 - Estimated maximum grid elevation across Ryan and SHETL grid representations .....  | 109 |
| Figure 5.1 - Diurnal demand curve taken from realtime data from National Grid ESO data .....   | 120 |
| Figure 5.2- Simulation framework for weather-induced cascade modelling with OPFs shown.....  | 123 |
| Figure 5.3 - Graphical representation of windfarm mapping .....  | 126 |
| Figure 5.4 - relevant section of simulation algorithm.....   | 129 |
| Figure 5.5 - location of frequency response simulation in wider model framework .....  | 138 |
| Figure 5.6 - location of load flow OPF in context of wider framework.....  | 140 |
| Figure 5.7 - location of redispatch, UC-OPFs in simulation framework.....  | 141 |
| Figure 5.8 - timescales of different simulations within framework.....   | 147 |
| Figure 5.9 - Typical generator tripping scheme .....   | 151 |
| Figure 5.10 - LFDD scheme used in model.....   | 152 |
| Figure 5.11- representative frequency response curve from model.....   | 157 |
| Figure 5.12 - representative frequency response curve inclusive of flexible demand response .....  | 157 |
| Figure 5.13 - load profile used in case studies, representing a winter peak day.....   | 164 |
| Figure 5.14 - ENS histograms for "base case" economic dispatch scenario .....  | 165 |
| Figure 5.15 - ENS histograms for "base case" N-1 dispatch scenario, 1320MW of reserve spread across system, no FDR, $\Psi = 0$ .....   | 166 |
| Figure 5.16 - ENS histograms for case with 2000MW frequency response and FDR, no locational constraints, $\Psi = 50\text{MW}$ , empty contingency list .....   | 167 |
| Figure 5.17 - ENS histograms for case with 2000MW of frequency response south of B6, empty contingency list, $\Psi = 50\text{MW}$ , no FDR.....  | 167 |
| Figure 5.18 - ENS histograms for "base case" dispatch scenario, N-1 dispatch, interpolated weather data, 1320MW frequency response, no FDR, $\Psi = 0$ , no locational constraint, interpolated data set ..... | 168 |
| Figure 5.19- boundaries around the Central Belt of Scotland, South of Scotland, and North of England .....   | 168 |
| Figure 5.20 - ENS histogram of B6 scenario with N-1 dispatch and 1320MW frequency response, $\phi = 50\text{MW}$ , no locational constraints, interpolated data, no FDR .....                                  | 169 |
| Figure 5.21 - ENS histogram of scenario with economic dispatch, empty contingency list, 0MW frequency response dispatched, $\phi = 0$ , no FDR.....  | 170 |
| Figure 5.22 - ENS histogram for case with 500MW frequency response scheduled in North and 820MW scheduled in South, $\phi = 0$ , no FDR, empty contingency list .....  | 170 |
| Figure 5.23 - ENS histogram with constrained flow, 500MW north of boundary, 820MW located south, $\phi = 0$ , no FDR, empty contingency list.....  | 171 |

|  |     |
|--|-----|
| Figure 5.24 - ENS histogram with case with unconstrained flow, trips, 500MW in north, 2000MW in south, pre-programmed wind generation trips, no FDR, empty contingency list.....       | 171 |
| Figure 5.25 - ENS histogram for case with large generation loss and system in economic dispatch, $\phi = 0$ , no frequency response, empty contingency list, no FDR.....               | 172 |
| Figure 5.26 - ENS histogram for scenario with 2000MW of net response in South, $\phi = 50$ MW, no FDR .....  | 173 |
| Figure 5.27 - ENS histogram of results from case with 500MW net frequency response in North, 2000MW in South, with FDR.....  | 173 |
| Figure 5.28 - ENS histogram of results from case with 500MW net frequency response in North, 2000MW in South, no FDR.....  | 174 |
| Figure 5.29 - ENS histogram [right] for case where there is a large loss of infeed but no constraint on generator up/down times, compared with baseline case in economic dispatch..... | 174 |
| Figure 6.1 - chain of causality for effects of weather on power system.....  | 185 |
| Figure 7.1- approximate location of B6 boundary shown on "Ryan Model" .....  | 206 |
| Figure 7.2 - outage locations indicated on Ryan Model .....  | 207 |
| Figure 7.3 - stage 1 of simulation; dispatch and storage of dispatch state .....   | 208 |
| Figure 7.4 - stage 2; generation of perturbation state .....   | 208 |
| Figure 7.5 - cascade simulation loop.....  | 209 |
| Figure 7.6 - SFR simulation for loss of B6 event.....  | 209 |
| Figure 7.7 - redispatch/UC OPF locations in framework .....  | 210 |
| Figure 7.8- frequency response for second perturbation event .....   | 211 |
| Figure 7.9 - termination of model.....   | 211 |
| Figure 7.10 - performance of different scenarios with given metrics .....  | 213 |
| Figure 7.11 - performance metrics for given scenarios .....  | 214 |
| Figure 7.12 - frequency response dispatched versus EENS .....  | 215 |

## List of Tables

|  |     |
|--|-----|
| Table 3.1 - Sensitivity parameters used in simulation .....                    | 77  |
| Table 3.2 - Output results of case studies.....                                | 81  |
| Table 5.1 - parameters used in DC-SCOPF formulation .....                      | 129 |
| Table 5.2 - variables used in DC-SCOPF formulation .....                       | 130 |
| Table 5.3 - summary of simulation timescales and features .....                | 147 |
| Table 5.4 - failure rates used in model .....                                  | 148 |
| Table 5.5 - tabulated results of case studies.....                             | 175 |
| Table 5.6 - tabulated results for "unresilience metric" from simulations ..... | 180 |
| Table 7.1 - tabulated summary of case studies .....                            | 212 |

## Publications, Prizes, and Contributions

**M. Jamieson, G. Strbac, S. Tindemans, K. R. W. Bell**, "A Simulation Framework to Analyse Dependent Weather-Induced Faults", in *IET Conference on Resilience of Transmission and Distribution Networks*, Birmingham, 2017

**M. Jamieson, G. Strbac, K. R. W. Bell**, *Quantification and Visualisation of Extreme Wind Effects on Transmission Network Outage Probability and Wind Generation Output*, IET Smart Grid Special Issue on Definition, Quantification, Analysis and Enhancement of Grid Resilience (Publication due December 2019)

Prize-winner, best presentation in session, *ETP Conference, Dundee, 2019*

*EPSRC HubNet* poster presenter, 2017 (Bath), 2018 (Manchester)

*Smarter FuturES* conference, Glasgow, presenter, 2018

Presented research at various stages to industrial partners and external organisations such as: SSE, Perth/Glasgow (various times, 2019), Risk Management Solutions (London, October 2019), Ofgem (2019).

## List of Abbreviations

|       |  |
|-------|--|
| AGC   | Automated generator control                        |
| AGW   | Anthropogenic global warming                       |
| API   | Application programming interface                  |
| AV    | Absolute value                                     |
| CCGT  | Closed cycle gas turbine                           |
| CDT   | Centre for Doctoral Training                       |
| CHP   | Combined heat and power                            |
| CVaR  | Conditional value at risk                          |
| DADS  | Demand response availability data system           |
| DER   | Distributed energy resources                       |
| DG    | Distributed generation                             |
| DLR   | Dynamic line rating(s)                             |
| ECWMF | European Centre for Medium-Range Weather Forecasts |
| EENS  | Expected energy not served                         |
| EFL   | Expected fault location                            |
| EFR   | Enhanced frequency response                        |
| ENS   | Energy not served                                  |
| EENS  | Expected energy not served                         |
| EMLS  | Expected maximum load shed                         |
| ERCOT | Electric Reliability Council of Texas              |
| ERP   | Energy Research Partnership                        |
| ETYS  | Electricity Ten Year Statement                     |
| EWPS  | Extreme Weather Perturbation Simulator             |
| FR    | Frequency response                                 |
| GADS  | Generating availability data system                |
| GB    | Great Britain, i.e. the mainland UK power system   |
| GSP   | Grid service point                                 |
| HIHP  | High impact high probability                       |
| HILP  | High impact low probability                        |

|        |   |
|--------|---|
| HWSS   | High wind speed shutdown  |
| IPCC   | Intergovernmental Panel on Climate Change                                 |
| LCC    | Line commutated convertor   |
| LFDD   | Low frequency demand disconnection  |
| LIHP   | Low impact high probability   |
| LOLP   | Loss of load probability  |
| MCMC   | Markov Chain Monte Carlo  |
| MITS   | Main interconnected transmission system                                   |
| NAO    | North Atlantic Oscillation  |
| NERC   | North American Electric Reliability Corporation                           |
| NG ESO | National Grid Electricity System Operator                                 |
| OCGT   | Open cycle gas turbine  |
| OHL    | Overhead lines  |
| PFR    | Primary frequency response  |
| PNS    | Power not served  |
| RIIO   | Revenue = Incentives + Innovation + Outputs<br>(Ofgem regulatory regime). |
| RoCoF  | Rate of change of frequency   |
| RPD    | Renewables Planning Database  |
| SFR    | System frequency response   |
| SHETL  | Scottish Hydro Electric Transmission Ltd.                                 |
| SMPS   | Switched mode power supply  |
| SSB    | Snow, sleet and blizzards   |
| SSE-N  | Scottish and Southern Electricity Networks                                |
| SYS    | (National Grid) Seven Year Statement                                      |
| TADS   | Transmission availability data system (NERC<br>data source)               |
| UFLS   | Under frequency load shedding   |
| USNAS  | United States National Academy of Sciences                                |
| VaR    | Value at risk   |
| VoLL   | Value of lost load  |



## List of Symbols

Where necessary, these are defined in the relevant sections or in-text.

## Acknowledgements

I would like to firstly, of course, thank my supervisory team, in no particular order, of Simon Tindemans, Goran Strbac, and Keith Bell. I literally could not have done this without them.

I would also like to extend my thanks to the many individuals who have helped with the research over the past few years, including Rodrigo Moreno, Calum MacIver, Jochen Cremer, Magnus Davidson, Jacob Kelly, Fiona Irwin, David Brayshaw, and Leon Thurner and the *Pandapower* team.

This work was funded as part of the EPSRC CDT in Future Power Networks and the Smart Grid, a joint effort between Strathclyde University and Imperial College London.

## Dedications

For Rosaleen Nora Elizabeth, James Scott, Florence Rhua, Findlay James, and Mia Rose; otherwise known as the Jamieson family.

# Chapter 1 Introduction

## 1.1 Motivations

### 1.1.1 Climate change means a more extreme, more variable planet

When discussing the impact of weather on power systems, it is important to be clear about how weather actually impacts power systems. For the sake of this dissertation, the ‘network’ should be taken to refer to *the lines, cables, and associated infrastructure which physically facilitates power transfer between nodes*. The ‘system’ in this thesis pertains to *the physical infrastructure involved with the generation, transmission, and consumption of electrical power, inclusive of physical assets such as generation facilities, loads, protection, control, and ancillary services such as demand response or reactive power compensation*.

For context, the definition of the “system” used by the Energy Research Partnership (ERP) in [1] refers to *“the assets, businesses, services and supply chain that facilitate the transport of electricity from the point of generation to the point of consumption; and the political, societal, economic and technological environment in which they operate.”*

The definition used here differs due to the slightly different focus on this thesis. The concern here is primarily on the electromechanical power system itself and its operability in the context of adverse operating conditions, rather than a socioeconomic analysis of the drivers which may operate externally from the power system. While people, the economy, and wider society do have material impacts on the power system, that is considered outwith the scope of the subject matter.

Climate change is a multi-faceted problem which will impact society in innumerable ways. The robustness or scientific veracity of the theory behind anthropogenic climate change (AGM) is not within the scope of this project and the assumption is that AGM is accepted knowledge, in accordance with modern scientific consensus on the issue [2].

What this work is particularly concerned with is the actual *effects* extreme weather will have on power systems; how we model those impacts, and what potential avenues we have to mitigate those impacts. Extreme weather is treated as a vector through which climate change may manifest- the impacts of climate change are many and complex, and shall be discussed in finer detail in due course.

Climate change can be considered as impacting both the frequency and intensity of high impact low probability events (HILPs) [3], and the associated ability of power system operators to deliver power during both everyday operation and during *force majeure* weather events. Storm events such as Storm Desmond [4], and high wind events such as described as in [5], mean an understanding of the relationship between storms and power system risk during intense storm periods is needed so they can be adequately prepared for.

Similarly, extreme and prolonged heatwaves or cold snaps also present complementary challenges to power system planners and operators. Whilst the planet may warm, meaning an increase in average temperatures, changes in the jet stream and associated phenomena may still mean temperate countries such as the UK are subject to extreme cold events such as “the Beast from the East”, a sustained period of cold weather which affected Europe in 2018 following a summer of extended and record-breaking heatwaves [6].

Planners have to both account for an increase in cooling demand in large demand centres and cities during the summer while still ensuring the power system has adequate margin for the winter peak or protracted cold spells. This will have a significant impact on how power systems are operated and designed in the future and approaches for handling these challenges will be heavily dependent on very

uncertain projections of future climatological scenarios and future power system conditions. This diversity of problems can, of course, not all be addressed within the scope of a single research project, but individual aspects of these challenges can and must be identified and addressed.

There is significant uncertainty surrounding the interactions between weather, climate, and the power system. Further, there is uncertainty as to what to then do in order to mitigate the impacts of these interactions, both in terms of exogenous and endogenous aspects in the network.

Weather conditions introduce aleatory uncertainty to any modelling performed on resilience in the context of climate, whereas the abstractions and assumptions made in the simulation of what then happens are from where the epistemic uncertainty emerges.

How often things are going to be broken by storms, or what generation will be available to planners and operators, will change. The ability of the energy system to supply adequate and reliable electricity, by force of regulation, market demands, and political imperative, cannot be further jeopardized by any move to address climate change. Therefore, the capacity of the system to resist, survive, and recover from such outages and impacts must reasonably be expected to, at least, not degrade.

No single solution will be perfect to address all of the challenges faced by the power system, and depending on what level of abstraction or cheap methods are used the optimal portfolio of investments may vary significantly across studies, as will the optimal operational strategies considered. This then suggests a diversity of responses and minimisation of up-front investment is desirable, but it is difficult to know without being able to test the benefits these investments may have in actual “resilience” scenarios.

A significant challenge of dealing with the concept of resilience lies in the significant uncertainty and low probabilities being considered for more extreme events, or the difficulties involved with quantifying the probabilities involved. Given climate change’s impacts, then, may be considered relatively indirect in terms of altering the underlying conditions which create HILPs, the focus should be on the analysis of HILPs and how these may be altered in time. How to then demarcate what is “reliability”, “resilience”, LILP, and HILP, then intersect with the challenge of how to mitigate these HILPs when they do occur. Any alteration to the system to deal with resilience could, naturally, also provide operational benefits to reliability and improve system operability more generally.

Climate change fundamentally, then, alters the cost-benefit analysis of what measures we choose in mitigating HILPs, and so methods are needed to analyse these HILPs at least to understand the potential contribution of such HILPs to future security challenges.

### 1.1.2 Understanding the importance of the data used in system security evaluations

Investigating the interactions between weather and power systems requires significant amounts of data and modelling. That is, weather has a wide variety of impacts on power systems that all need to be quantified and considered- or, at least, justifications need to be made as to why the scope of a simulation problem is defined in a certain manner. Any modelling that is performed will be sensitive to both the precision and accuracy of the data, which will in turn impact the results of such studies.

Simulation boundaries need to be clearly defined and understood but, equally, as many consequential elements need to be incorporated in simulations as possible to fully consider the factors at play. While some surface-level investigations have been performed with statistical analysis and regression using climate projections to evaluate potential failure rates w.r.t different weather conditions, these did not consider the impacts of the relevant outage effects [7] – though it does serve as a useful means of illustrating the uncertainties involved in such projections.

Data quality is also important for ensuring results are applicable in the real world and represent plausible scenarios, so any research in this field has to be done with the validity and veracity of the assumptions behind the data used in mind. Improvements to techniques involving the use of weather data are clearly an area worth investigation, at least in terms of understanding the potential uncertainties and errors which may emerge.

The sensitivity of any findings from studies based on a wide variety of data need to be understood to appreciate from where error or uncertainty can emerge. Therefore this offers a compelling reason for further research in the area to understand this.

### 1.1.3 Understanding potential impact of decarbonisation on the power system security

In light of reports from organisations such as the Intergovernmental Panel on Climate Change (IPCC) [8] and increasingly strict legislation and decarbonisation targets, the power system has been, and will continue to be, increasingly aggressively decarbonised. This is likely to mean a loss of synchronous machinery on which the power system relies to maintain stability, in tandem with an increasing proliferation of power-electronic connected devices, changing system demand profiles, and power generation increasingly reliant on weather conditions- particularly wind and solar. This shall be explored in more detail in the literature review.

Coal power in particular in the mainland UK network (henceforth referred to as the Great Britain (GB) network/system) has shown a precipitous drop in utilisation [9] in recent years. Aggressive decarbonisation on the power system should be considered as much of an impact as climate change itself insofar as the effects that manifest on the power system have a direct impact on planning and operational conditions, as well as future energy demand scenarios, generation portfolios, and system security. Factors such as heat electrification and electric vehicle uptake also have significant potential to disrupt traditional approaches to planning and operating the power system.

Increased penetration of renewables creates increased interdependencies between system operational risk, system adequacy, reliability, and resilience that need to be understood to ensure continued system performance to expected standards. Methods, then, for quantifying the impact of weather on generation and system risk are therefore necessary for robust security assessments considerate of these factors.

### 1.1.4 Understanding the difference between reliability and resilience

Reliability and resilience are both concepts which are fundamentally grounded in an understanding of risk, they just deal with different aspects of probability and impact.

Risk can be represented mathematically, simply, as:

$$r_t = \sum_{e=1...e} p_e \times i_e \quad (1.1)$$

Where  $r_t$  is some metric representing the total system risk across all states,  $p_e$  is the probability of a given event  $e$ , and  $i_e$  is the impact of the given event. This may be, for example, a dollar value, or a performance metric such as expected energy not served (EENS). A wide range of metrics are used to quantify the impact of adverse events on power systems, which shall be discussed in Chapter 2. The challenge with modelling risk associated with power system is that, while there are well-established models for understanding system *impact* pertaining to e.g. fault events, generator outages, overloads,

etc., understanding of the *probabilities* associated with weather-driven faults can be incomplete due to the sparsity of data and uncertainty associated with climate projections.

Reliability as understood in this thesis typically, in simplistic terms, can pertain to low impact high probability (LIHP) or low impact low probability (LILP) events (but is not limited to them), or events the system is expected to handle in day-to-day operation. Resilience, alternatively, but not exclusively, pertains to HILP events which are much more difficult to analyse. Classifying exactly when this goes from being a question of *reliability* to one of *resilience*, then, becomes a particular concern when performing security analyses and investment decisions. Therefore to *improve* any system's resilience, we have to actually understand what its "resilience" actually *is*. Both involve challenges or adverse operating conditions associated with how electricity is delivered from provider to customer, be that due to an everyday, mundane, and predictable event, or a more uncommon, difficult to predict, or particularly hazardous eventuality or emergent risk.

With these assumptions in mind, there must therefore be some point between HILP and LILP where a line can be drawn distinguishing reliability from resilience – and there is work to be done determining exactly where that line is, and why it is there.

#### 1.1.5 Consequences of failures to prepare for high impact events

Resilience in a power systems context is of particular interest because of the magnitude of interdependencies and systems which rely on the system's capability to deliver electricity in an exactly-as-it-is-needed manner. The implications of power system failure and the need for grid resilience is addressed in great detail in [10], and some of the main facets of resilience and reliability will be discussed in Chapter 2, but the need for resilience will specifically be discussed here.

Supply and demand must always be in equilibrium to ensure system stability, and this is where the concepts of reliability and resilience emerge. Basic economic function requires electricity to power tills, or to keep lights and communication equipment on in offices, and for the banking network to continue functioning. Ecommerce and banking transactions would be impossible without telecommunications and the ability of devices to access the internet, which itself requires electricity.

Water and gas pumps require electricity to operate, and Line Commutated Converter (LCC) technology power converters require commutating via external grids before they can power the grid – creating the situation where, in order to get more power onto the network, there already needs to be power on the network in the first place. Similarly, nuclear generation is unsuitable for black start generation because it also relies on external supplies to support it.

Generation such as natural gas (if it should happen to have on-site reserves), coal, and hydroelectric (be it via pumped storage or run-of-river) is necessary to support restoration of the grid from a total loss, or "black start", but as the fossil-fuel based generation is gradually phased out from the grid, this makes maintaining system operation and avoiding such "black start" situations all the more critical to avoid being in the position of requiring black start generation in the first instance- though of course planning to avoid black start situations is always of paramount importance

Whilst GB has not yet had to endure such an event on a scale beyond localised, regional outages, nonetheless it has to be prepared for such an eventuality, regardless of how exactly such a system-wide blackout occurs. In the UK, storms are one such source of potential black-start events, capable of major socioeconomic disruption- such as in the wake of Storm Desmond, which at the time was estimated to have cost in the order of £500m [11]. In the USA, the 2003 New York blackout was reported in 2008 to have cost almost \$6bn [12]. This was attributed to a combination of human failures and equipment failures following a series of lines faulting due to vegetation-related trips. This

cascaded into an event which disconnected 50m people. Though not comparable in scale of socioeconomic impacts, large-scale outages have occurred in both the UK [13] and Australia [14] in recent years. In both cases there was high wind penetration in the network and a cascading series of outages – individually of moderate probability but cumulatively highly unlikely – led to a series of trips of generation and eventually to large scale loss of load, and a localised total blackout in the South Australian case and frequency-related disconnection of demands – including public electric trains – in London.

In the case of the US outage, much of the Northeast of the USA and even Canada were affected and it took some three months of investigations to determine the cause. It should be noted that the referenced article makes mention of the need for a “smart grid” to prevent such incidents occurring again. With an increased penetration of renewables leaving the grid increasingly vulnerable, and the frequency and intensity of HILP weather events changing globally, this need is only further emphasised for islanded, relatively weak networks such as GB. “Weak” in this context refers to parameters such as system inertia, which has gradually been declining in GB for many years.

Given the need for grid “smartness” to enhance resilience then was being discussed as far back as 2008, and given the emergent threat from climate change and the variety of challenges facing the power sector it remains an important area of study.

#### 1.1.6 Tackling issues of sustainability and resilience in the power system for remote communities

Weakly connected systems in networks such as rural Scotland are particularly susceptible to high wind events, leading to disconnection of highland and island communities which already may have limited access to electricity. Improving the resilience of such networks could materially improve living standards of people living in proximity to such networks, particularly in areas such as the West Coast of Scotland.

The companies which operate these networks, SSE as would be the case in Northern Scotland, have significant experience in managing disparate, weak networks but the economies of scale may not exist for non-load-related reinforcement on networks and so alternative means of improving system resilience are interest to such companies, as is quantifying the risk associated with natural hazards such as wind.

Co-operating with industrial partners such as SSE will be essential in understanding the threat extreme weather poses to different kinds of systems and defining the broad scope of the issues, as well as to ensure maximum impact of any research completed. Throughout this project, co-operation was sought with such partners to try and ground research in realistic presumptions and to try and get useful outputs.

## 1.2 Scope and research questions

The primary concern of this thesis is how to model high impact weather events on the power system, with clear frameworks and relationships between simulations and data pertaining to relevant natural hazards. This is to quantify the potential impacts which will manifest as a result of extreme weather, improving on existing methods by using more detailed simulations and more comprehensive modelling of both failure-weather relationships and fault-consequence relationships than are typically presently used.

That then suggests various primary areas of concern, particularly related to how to model the interactions between weather and the power system, how to quantify the impact, and what can then be done to improve these metrics. In order to *quantify* the effect of extreme weather on the power

system, there needs to be robust modelling of the relationship between extreme weather and system risk, but this is inherently dependent on the quality of data used and what information one is trying to extract from the simulation.

To *mitigate* these risks, one needs to have a robust model of what actually happens during and after an event to see the impact of such mitigation strategies, and this is dependent on the scale and boundaries of the power system simulation. The decisions made as a result of such simulations may therefore be inherently dependent on the level of abstraction used in system simulations, and to what extent needs to be understood and investigated.

If it is understood that climate change manifests as a change in frequency and intensity of HILP events, this then ties the outcome of our modelling to the frequency and probability of the events analysed in such simulations. A solution that is cost-effective for an event that has an occurrence probability of once in ten years may not be so for events which are only once in fifty years, for example, and so establishing at what level of probability a solution becomes cost-effective or having methods which enable such investigations are clearly desirable. These aspects can then be summarised in the following research questions which the research within this thesis attempts to address in the manners described.

A. *Data challenges associated with modelling weather-related impacts on power systems*

1. *How should modelling of resilience and reliability be approached in the context of extreme weather?*

To quantify and understand the impact of weather and climate on the power system, the interactions between different facets of modelling and data types needs to be clearly defined and understood in order to evaluate the sensitivities and potential limitations of any modelling done, and to clearly illustrate, in such cases, where improvements can be made. This should be done by clear definition of modelling frameworks and algorithms used in the simulation of such scenarios. It should be understood that in “extreme” cases, the compounding probabilities mean that averaged results such as EENS will obfuscate the impact of the most extreme events at the tail end, and so care should be taken when discussing how these results change both in terms of event severity and frequency.

2. *How sensitive are models of weather impacts on the power system to the quality of data used?*

Different aspects of input data will have different impacts on the results of system simulations, and some will clearly be more significant than others. In order to optimise modelling and simulation of HILP events, one has to understand what the most important factors involved in the modelling actually are. Changing the relationship between e.g. the wind speed experienced by a line and its failure rate can have impacts in the scale of orders of magnitude on both the probability of failure of lines in the sampling, and in terms of risk metrics such as EENS, so results taken from reliability and resilience studies are clearly strongly dependent on the precision and reliability of the data used to drive them. Further, the granularity of the data also matters. More coarse datasets will mean more of the network exposed to the most extreme values of the parameters associated with a natural hazard, inherently biasing the results towards more pessimistic outcomes.

3. *Are the models we use to represent outage risk adequate, and how could they be improved?*

Any power system simulation will require a certain level of abstraction to make the problem tractable. There are standard simplifications that are commonly made, such as the linearised DC approximation used in optimal power flows, but there are also other simplifications and abstractions made that may significantly affect findings, some of which may be suboptimal or unrepresentative of real-world impacts. Current homogenous representations of overhead line risk fail to take into account geographical and meteorological diversity network branches are subject to, but the methods proposed offer a robust platform for improving this by spatially disaggregating overhead lines such

that risk can be quantified spatially, which is more appropriate in the context of understanding risk associated with spatiotemporally diverse phenomena such as weather.

Current models, then, can be understood to represent reasonable proxies based on the methodologies available presently, but improvements to weather data used in power system modelling mean that these methods can be improved to take consideration of the spatial disaggregation of overhead line risk and other vulnerable system assets when considering dependent, weather-induced faults.

Fault events which can generally be considered agnostic of wind itself (e.g. non-wind generation) and as such any simulation which incorporates these in a wind-related simulation can likely use failure rates independent of external weather conditions. In the case studies performed, for example, substation faults themselves were not examined but these, in reality, could also be subject to faults due to extreme wind associated with e.g. vegetation, debris.

*B. Challenges associated with power system simulation during extreme weather events*

*4. What level of detail or abstraction is necessary in simulations to understand the risk associated with a high impact weather event?*

This depends on various factors, and is largely constrained by factors such as the granularity of available data and the computational expense of the simulations being undertaken. A key factor is to understand how these different models interact, the associated data requirements, and the significance of the sensitivities of different datasets used. Even if a relationship between a natural hazard and failure rate for a particular asset is well understood, translating this to an electromechanical impact on a power system is still a nontrivial problem. That is, a fragility curve may provide a probability for a given fault on a given line which is representative on a population level, but there may be situations where further abstractions and assumptions need to be made. For instance, if wind causes a fault on a double-circuit, some assumption needs to be made about the relationship between a fault on a single line and how that translates to the risk of a fault on an adjacent line. A “line” is just a connecting conductor between two points, but a “branch” can be a cable, single, or dual circuit and if a fragility curve just represents the failure probability of a line, assumptions then need to be made about how line faults translate to branch faults. This is symptomatic of the many challenges associated with resilience analysis more generally.

*5. How do we represent the spatial impact of storms on a network-based power system model?*

Weather events are inherently varied and distributed, in that they affect wide regions of a system simultaneously via different mechanisms and with different magnitudes of impacts. Ideally, then, representation of adverse weather events and conditions should attempt to be representative of the events themselves as possible, or at least as far as available data resolution and granularity will allow.

In reality, current practise does not always reflect this, particularly representations of overhead line failure risks due to extreme weather. The demonstrated methods in this thesis use the available weather data as the basis on which to disaggregate the representation of overhead lines such that the representation of risk on OHL is as precise as the weather data on which it is based. This acts as a reasonable approximation and offers a clear mechanism for improving such granularity – simply increasing the resolution of the incident natural hazard data via interpolation. The risk associated with overhead lines is represented by converting a point-to-point branch representation into a 2-dimensional array to better reflect the diversity of weather conditions which may be experienced by OHL during storm conditions, but even this is incomplete for reasons which shall be addressed in Chapter 4.

C. Quantifying and understanding the differences between reliability and resilience

6. *How can resilience be quantified and classified?*

Metrics such as VaR and cVaR are used in Chapter 5 to quantify resilience, which are becoming increasingly popular metrics. A new metric is also introduced to demarcate reliability from resilience in which a threshold ENS is introduced above which the proportion of states where the fault event is N-2 or worse are counted. An arbitrary value is chosen, in this case 10MWhr, and the percentage of N-2+ events which exceed this threshold are given as a percentage, effectively to give an idea of the proportion of sampled events which exceed an “acceptable” severity and to compare this across scenarios. An acceptable proportion could then be asserted to classify if the system is acceptably “resilient” for a given sample scenario sampled across a set of broadly consistent events.

7. *Where do we draw the line distinguishing reliability and resilience?*

In this work, a hypothetical threshold is inferred whereby anything greater than an N-1 falls under the mantle of “resilience”. Resilience is still a term, in a power systems context, which has yet to be fully classified and defined and work is ongoing in this area, but the definition used is useful for the analysis and research performed within the scope of this thesis. Resilience can refer to factors such as operational or human resilience, or to infrastructural resilience. These, however, can be difficult phenomena to include in power system simulations directly.

8. *What are the main drivers of power system resilience?*

In the modelling performed, various factors stand out as being significant influences on the results of security studies. The granularity of data used impacts how much of the system is subject to the most severe weather conditions, in turn affecting the probability of concentrated faults in the areas subject to the most extreme conditions. The operation of the system, particularly what generation is used and the dispatch of frequency response, also significantly impact system resilience. Different types of events will affect the power system differently and will be affected by different factors: that is, if faults are primarily network-related (i.e. line outages), frequency response may not help improve system resilience if it is in the wrong place, and cannot help if load centres are isolated by system faults. However, if fault events are generally associated with large losses of infeed, frequency response becomes far more significant, but less dependent on its location and more dependent on the type of frequency response used- unless the loss of infeed is associated with a generator which was scheduled to supply frequency response itself.

Therefore, resilience in the context understood here is linked heavily to the types of events affecting the system, the preventative and corrective measures in place, and the fault-weather modelling used to generate the fault events being analysed. Other factors such as the constraints and abstractions applied to the model also affect the resilience – in terms of performance metrics – of the power system. An immediate example studied within the research is the influence of unit commitment constraints applied to the system being examined within a larger scale simulation.

D. Improving resilience and reliability

9. *Can resilience be improved simply by operating the network differently?*

As demonstrated in the various case studies performed, for the states observed and the scenarios generated there is a clear linkage between the different dispatch scenario and the frequency and intensity of large-loss events. That is, the performance of the system in adverse conditions can be related to the dispatch scenarios used during those events as well as the resources (in these cases, frequency/demand response) available to the system to mitigate the impacts of the outages and perturbations to that system. Therefore it is reasonable to infer that system performance can be improved by changing where, how much, and what kind of frequency response is utilised during large-

scale outage events dependent *on the nature of those events which are reasonable expected to occur*. Equally, however, suboptimal scheduling of frequency response can not only not improve resilience, but can actively reduce it.

10. *Can we expect network resilience to improve or degrade with added diversity and penetration of renewables?*

Without knowing how wider system operability will change in the face of increasing renewables, it is difficult to determine. Decreasing inertia certainly makes systems such as GB more susceptible to large frequency deviations and frequency-related cascade events, but the system operator has largely managed to avoid major disruption to the system associated with this. Renewable energy development and integration in the system is happening in tandem with more widespread changes such as digitisation and proliferation of smart devices and forms only a part of the wide array of challenges facing the power system. The answer, then, depends on the *manner* in which renewable integration is pursued.

Using inverters with suboptimal or overly conservative protection settings, such as the former Engineering Recommendation G59 125mHz RoCoF setting. Distributed generation using such protection schemes may not respond optimally to system perturbations and may disconnect during fault events, when the system is most in need of support, carrying a risk that such generation in turn feeds into cascading events and system disruption. This in itself contributed to the large-scale system disruption in August 2019 in the UK, but such devices could also help support system security if deployed suitably.

E. *Modelling the effects of climate change on the power system*

11. *How might climate change impact on our modelling and quantification of risk associated with these events?*

There is always a cost-benefit analysis involved with distinguishing between threats that must be prepared for versus those which can be regarded either as out of scope – either due to being suitably improbable, or so egregiously harmful little can be done to stop them. If money is invested in preventing a problem that never manifests, this is associated with wasted money, stranded assets, and loss of reputation. Conversely, failure to adequately prepare for adverse operating conditions can lead to situations similar to the South Australian Blackout in 2016, where for a lack of knowledge about how groups of wind-turbines would respond and ride-through faults during a high-wind condition led to cascading outages and a black-start condition. Methods for more clearly and justifiably categorising threats to the system would better prepare operators and give better accountability and trust in services.

Climate change introduces significant uncertainty into projections across multiple time horizons regarding the impact of weather and other natural hazards on the power system, often in nonlinear manners. As can be observed in the wildfires seen in California and Australia, the potential for climatic damage to power system infrastructure can be outwith the control of the power system altogether even if the actions of individual actors may be associated with causing individual e.g. wildfire events.

Floods, national-scale wildfires, droughts, etc. will all have profound impacts on power systems in ways which are difficult to quantify and it is difficult to conceive of a way to adequately protect a power system against the threats posed by such events in a cost-effective manner, or whether such damage should just be seen as inevitable with planners just learning to live with a “new normal”. That is not to say it should be acceptable to disregard reliability and resilience standards simply because the operational conditions become more difficult, however.

Legislators, businesses, and other stakeholders are going to have to decide among themselves what reasonable balance to strike to balance the energy trilemma is, such as it is. This will affect the focus of analysis – whether it lies with longer term changes in e.g. water availability or on shocks like the Australian wildfires or Beast from the East. Both short and long term resilience need to be addressed, and addressing one will, naturally, in some way potentially benefit wider system resilience, but the immediacy of events such as wildfires and the political fallout thereafter will almost certainly weight heavily - addressing the most immediate, distressing threats will almost certainly take precedent. How this could impact resilience studies remains open to study.

### 1.3 Primary areas of concern

The focus of the work performed concerns subjects relevant to the impact of wind specifically on the GB network and understanding the ways in which the impact of extreme wind manifests on the power system. This is due to GB's significant penetration of wind power at multiple levels of the network, and the significant variability and complexity of weather-related modelling in this area.

The UK, being a temperate nation, tends not to experience the most extreme manifestations of climate change – widespread droughts, hurricanes, monsoons, etc. – but will still be subject to more gradual aspects of climate change such as changing weather patterns and water availability. The UK, having a significant wind resource, is acutely vulnerable to the effects of changes in wind resource across the northern hemisphere, and so quantifying these relationships is of paramount importance.

The methods described in this thesis are intended to be tractable and generic enough to be universally applicable with lessons learned from the specific GB context. The unique nature of GB's system – an island nation with limited interconnection undergoing rapid decarbonisation with significant imbalance between producing and consuming regions – makes it a particularly interesting case study for different analysis methods and technologies.

There is a significant amount of work in this area, as will be described in Chapter 2, but this tends to be in different areas of analysis (e.g. frequency response requirements given varying wind, modelling relationships between wind parameters and failure rates) which make assumptions and abstractions about other areas that would benefit from further detail and investigation, and a joining together of these different areas of research in a more comprehensive fashion.

The availability and completeness of wind data, and the solid foundation of work on which to build, means there is a good balance of challenging work that still needs to be done as regards understanding the impact of extreme wind on the UK grids but with a solid direction laid out by such research as to where future work actually needs done.

It is for these reasons the bulk of research done has been focussed on understanding both how to link weather models to power system representations, and how to then model what happens when those models interact.

### 1.4 Novelty of work and thesis structure

Various different aspects of power system analysis are considered in this thesis, which independently are understood and developed to varying degrees. Among one of the most significant challenges involved with addressing climate change is how to combine disparate and diverse styles of analysis and expertise in a productive manner.

Electrical engineers are typically not economists or policymakers, nor are they climate scientists. To address climate change and its effects on the power system some level of understanding is needed in all of these different areas. However, answers should also not be obfuscated by unnecessary

complication and should remain as straightforward as possible whilst not compromising on the value of information provided by such research.

In order to model the impact of weather on the power system a wide variety of factors need to be considered; the relationship between a given weather parameter and its corresponding effect on a component; the effect on the system if that asset drops out of service; the necessary granularity of the simulation; whether or not the weather data being used representative of the conditions actually present or incident upon a given asset.

To investigate this properly, then, it is necessary to investigate the potential factors which may affect representations of, for instance, the relationship between a given wind speed in the data being used and what a given asset is actually subject to, considering environmental effects. If then modelling this outage, an appropriately detailed simulation model is needed to realise the consequences of the outage properly. The work put forward in this thesis attempts to begin to define these interactions and quantify their significance in the context of power systems.

The work presented carries contributions to various different domains of power system analysis in the context of weather and climate, which are discussed in Chapters 3, 4, and 5 with Case Studies demonstrating the applicability of these approaches in Chapter 5.

Chapter 3 establishes and discusses a method of approaching weather-related fault modelling on a power system in the context of uncertainty about the actual relationships between a given weather parameter – in this case wind – and the impact on the system – specifically failure rates on OHL. This attempts to set up a framework for simply analysing dependent fault scenarios, as laid out in [15]. It is from the themes established in this work that future directions of work were determined.

In this work it became evident that any analysis performed on the system associated with weather impacts is dependent on, as previously mentioned, the links between weather and failure probability – and that in turn has a major impact on the reliability metrics we use to measure such risk. Therefore, Chapter 4 discusses and demonstrates novel techniques for quantifying and visualising failure probability on overhead lines as well as projections about wind power output, correcting for the varying weather conditions experienced across overhead lines, which has been published and is presented in [16].

Once we have these more robust and data-driven methods for quantifying failure probability, it is then important to model and understand the consequences these outages actually have on the system once they have occurred and what interventions can then be made to mitigate the consequences of them, and what ability the network inherently has for coping with such outages. This is investigated in Chapter 5 which demonstrates the importance of taking consideration of factors such as frequency response in simulation due to the potential contribution of distributed energy resources to contribute to power system resilience. The methodologies demonstrated are then used for various test cases. Chapter 6 summarises and concludes the thesis with the Appendix in 7.

## **Chapter 2 Review of relationships between climate, weather, resilience, reliability, and associated issues**

### **Abstract**

*Climate and extreme weather are set to have a wide range of impacts on the power system across varied timescales with local, regional, and international effects on power systems. Issues like water scarcity, thermal shocks, storms and hurricanes are identified as having potentially significant impacts. A literature review is performed to understand what threats the power system faces associated with natural hazards associated with weather and how these may impact power system reliability and resilience as well as investigating the material differences between resilience and reliability as concepts and why those differences matter.*

*Extreme wind is chosen as the natural hazard of most significance to be taken forward in this thesis due to the significant body of work supporting future research paired with the correspondingly significant amount of research which is still needed to understand its impact on the power system. Reliability and resilience can generally be distinguished in terms of the understanding of risk associated with each of the terms, with reliability more driven by perennial, reasonably expected outage scenarios and events with resilience driven by the “long tail”. Qualitative and quantitative descriptions of reliability and resilience are provided.*

## 2.1 Introduction

Clearly, high impact low probability event simulation is a complicated domain, particularly when it comes to defining the scope of the problem. Quantifying risk necessitates a robust appreciation of both the probability of events and their impacts, both of which can be difficult to quantify.

Establishing the necessary scope of the problem, in terms of areas where analysis is weaker and where gaps exist for further research means an examination of a wide array of natural hazards is necessary. That is not to say natural hazards are the only threats to power system security, as the Ukraine power system cyberattacks of 2015 illustrated hostile actors can be significant threats to power system operation as well [17]. A look at how the impacts and probabilities associated with modelling these natural hazards is therefore to be conducted.

Individual natural hazards such as wind can manifest as a wide array of threats to a power system, so both the kinds of threats which can be present and the actual impacts these threats have on the power system need to be considered. To put it simply, one has to understand both how likely a power line is to fail during a storm, and the impact such an outage would have on the wider system.

## 2.2 Quantifying impact of extreme weather on power systems

Different aspects of the system and network interact with the natural environment in different ways which can prove to be either beneficial or detrimental. Weather can be a source of energy for renewable electricity generation- such as wind, solar, or wave - or more indirect benefits such as cooling of heavily loaded lines to allow greater load transfer during cold weather in winter or during less severe windy conditions. This can be realised via techniques such as dynamic line ratings (DLR), the benefits of which are explored in the context of managing uncertainty in networks [18].

Different kinds of weather also present different threats to the system and networks. The threats and opportunities presented by different weather kinds will be described hence. Wider range studies into the impacts of weather and extreme events have been carried out by IMechE in [19], as well as in [7] and [10]. A comprehensive literature review into the impact of climate change in a renewables-heavy system has also been carried out by the Met Office amongst others led by L. Dawkins [6]. National Grid Electricity Transmission, even before NG's reforms and segregation into National Grid TO and National Grid ESO, also produced materials investigating its preparedness for climate-related threats such as drought and flooding [20]. This section discusses specific facets of power system interactions with the power system and how threats may manifest from these natural hazards.

### *2.2.1 Lightning-related effects on the power system*

Thunderstorms and lightning are associated with convective available potential energy (CAPE) in the upper atmosphere and manifests as a burst of extremely high voltage flow from Earth to ground, and this can cause a variety of problems to the power system. Standards are well established to quantify the risk associated with lightning strikes on the power system [21]. As an inherently random act, planning for lightning-related investment carries significant uncertainty, as does quantifying the risk associated with such storms, which in [22] is done with assistance from a method known as *stratified sampling*.

Lightning, as well as causing flashovers and overloads on lines – leading to transient outages – can also cause permanent damage associated with overloading key assets, or lead to cascading outages if multiple key assets are struck in a short period of time.

Lightning strikes during dry periods of weather can also lead to wildfires, which can cause widespread damage to systems for a long duration of time which is difficult to contain or control. Strikes to vegetation can also cause permanent or transient faults due to falling branches or trees. For these

reasons and more, vegetation management is an area necessitating study and research [23] to prevent damage caused by e.g. overgrowth leading to phase-ground faults.

As climate change is expected to cause an increase of heat – and hence energy – in the atmosphere, this is anticipated to lead to an increase in the amount of lightning-related weather events globally, which one could anticipate as leading to, in turn, an increase in lightning related faults and outages on the power system [24].

The variability of lightning across the European continent and its frequency is also associated with the North Atlantic Oscillation (NAO) [25], a climatological phenomenon which drives high and low pressure events across the North Atlantic and shapes weather events across Northern Europe, with significant impacts on renewable energy resources.

In [7] it is projected that most climate change scenarios at the time of writing would see a significant increase in the frequency of lightning-related faults on the power system in GB. Again, the projections vary significantly by model, and this presents significant challenges to planners with lower end estimates suggesting increases in the range of 5% with more extreme projections suggesting an over 30% increase in lightning-related faults by the 2080s.

With the rate of change of the operation of power networks and the complete overhaul experienced even in the last decade, attempting to model future fault rates on the system with the combined uncertainty of both climate projections and the inherent assumptions necessary concerning power system operation render such predictions of fault rates essentially meaningless in terms of what it means for present day operation of the system, particularly in terms of quantitative assessments of the precise estimators of such values. Nonetheless, the relative changes and errors across fault vectors and weather types nonetheless are useful for being indicative of relative risk.

### *2.2.2 Wind-related impacts on the power system*

Wind's interaction with the power system, particularly at extreme values, presents a wide range of challenges. Wind can cause mechanical failure of components, shearing of lines from connectors and insulators, transient faults associated with wind-induced oscillations and clashing of conductors as lines collide with each other, or "galloping" which relates to line oscillations exacerbated by line icing [26]. As with lightning, vegetation can cause permanent or transient faults due to falling branches and trees, though most significantly at distribution level [27]. Wind is also typically associated with other extreme weather events such as flooding, lightning, rain, and snow, and so explicitly analysing the impact of wind on the system can be particularly challenging as it will not always be singularly acting on the power system. Classifying the cause of faults is in of itself a non-trivial data challenge, investigated in the context of the GB transmission system in [28].

At extreme values of wind speed, wind power must be curtailed to prevent mechanical failure or damage to turbines and windfarms. This is known as High Wind Speed Shutdown (HWSS). This can affect windfarms over a wide area of a region simultaneously, but will affect individual turbines and windfarms to differing extents due to localised weather conditions [29]. Therefore, considerations must be made for these geographic effects and sensitivities of windfarms to such phenomena.

Low wind will also result in reduced output from windfarms, which can coincide with heatwave conditions and times when there may be acute cooling demand, introducing new interdependencies and sensitivities to the network. This will again impact wide areas of the network simultaneously and potentially for extended periods of time. High wind can also coincide with sunny conditions, however, causing the system to become saturated with renewable energy making system management more complicated [6].

Climate change, while being linked to changing intensities and frequencies of HILP events, may also be associated in a reduction in the output of wind power generation in the northern hemisphere [30] as wind speeds fall due to climate change. Further, climatological phenomena such as El Nino, La Nina, and the NAO also impact future wind scenarios and cost projections – by as much as 10% of output year on year in GB [31]. This illustrates very clearly how important it is to understand, then, the relationship between climate, weather, and the power system. Investment decisions on wind power plant will potentially be significantly impacted not just by local conditions but global and trans-national climate events, affecting rates of return on a macroeconomic scale, but also the penetration and distribution of wind generation on the power system more specifically, with associated electromechanical consequences both locally and at a macro-system level. That is, increased wind penetration is associated with phenomena such as decreasing system strength and inertia, and loss of frequency response capability on networks. This shall be discussed further in Chapter 4. Other studies however suggest a probable increase in wind energy resource output [32]. This emphasises the need for further research into the significance of such uncertainty. It is reasonable to conclude that the net infeed of wind power across the world is going to increase significantly, but that this generation and its efficiency may be sensitive to climatic events and climate change more generally and this needs to be better understood.

Wind's variability introduces challenges to the network primarily due to its intermittency (that is, periods of high wind can be interrupted by periods of low or zero wind)). That is, wind power output can vary significantly over different time horizons even while still providing power. This intermittency can be compounded by forecasting challenges.

In [33] various concepts are described which are problematic consequences of wind penetration on networks, and some have already been discussed, but one particularly problematic aspect of high penetrations of wind power on networks is associated with the issue of “ramping”. That is, as weather patterns move across areas with significant wind output, there can be large-scale variation in the output of wind farms on the grid, as was quantified in [33]. A wide array of the consequences of high wind penetrations are discussed in [6].

“Ramping”, where there are sudden and significant changes in the output of connected wind generation, in particular is a major concern with potentially gigawatt variations in wind output across a system in very short time scales. The Thames Estuary region in particular can vary in output by as much as 80% in a single day, with system-wide variations of up to 40% in a single day also possible. In [6] it is reported that there could be hourly ramps of as much as 15GW by 2030, with significant regional variation on wind farms. This may not be particularly problematic over diurnal timescales – operators already have to be prepared for significant diurnal shifts in e.g. demand, but could become problematic over shorter timescales. This variability compounds already pre-existing challenges associated with balancing supply and demand, such as ensuring adequate holding of reserve and frequency response.

Ramping can have both short-term and longer-term impacts – the pace of and magnitude of change in output can produce challenges for operators. Shorter-term fluctuations increase demand for frequency response and load-balancing generation, whereas longer-term fluctuations are a system adequacy challenge which manifest as unit-commitment challenges, with generators potentially having to switch on and off in short periods of time to respond to these fluctuations, incurring significant costs to operators in terms of start-up and shut-down costs, or additional costs to switch on or maintain generation which may not have been expecting to be powered on.

There can also be long periods of wind droughts and low wind capacity events, with [34] reporting that in as much as 10% of the time between 1970 and 2003 saw wind farms with zero output due to low wind speeds (defined as  $<4\text{ms}^{-1}$ ), which accounted for 99% of the time in which windfarms had zero output – the remaining 1% of such events being due to HWSS. It is also suggested that  $<0.1\%$  of the UK experiences high-speed wind events (defined as  $>25\text{ms}^{-1}$ ) at any one time, meaning the risk can be considered distributed on a UK-wide scale and the impacts low-risk at any given time, and was only 4% of the data in the sampled time domain of the paper. This emphasises the benefits of having wind generation resource distributed around the UK, however.

It should be noted that such distributions are liable to change non-negligibly in the future regardless of the exact nature of climate change and dependent on its magnitude. As suggested in [31] and [30], average wind speeds are subject to both climate variability – that is, phenomena such as the North Atlantic Oscillation (NAO) which vary year-on-year and drive weather patterns – and AGW, which changes the underlying climatological phenomena which shape weather and climatological events themselves. Wind patterns across the global north will change, and with them the distribution of wind events. If a reduced average wind speed across the global north materialises as more sustained wind droughts in wind-dependent nations such as the UK, this places yet more stress on the power system in having to adjust to the variability of this resource and to be able to securely supply power during extended wind droughts. Work needs to be done in this domain with larger sample sizes to consider more recent climate projections and scenarios, which is referred to in [6]. In [35], however, it is suggested that, as climate change regimes manifest as shifts in the scale of 50-100 years – much longer than a typical renewable energy development – current projections about wind speeds and wind output “will probably be valid for the coming decades”.

There is some complementarity between wind and solar which can mitigate this – the NAO also interacts with solar irradiance [36], and, in very general terms, when it is sunny it tends not to be windy. Similarly, there is a “dipole” effect described in GB, where the north tends to be windier and less sunny than the south, which tends to be sunnier and less windy. These effects can complement each other and mitigate the correlated impact of weather impacts across regions. It is found that beyond distances of 600km [34], the correlation between windfarms’ output is weak and can be considered independent, which infers that supporting grid resilience relies not just on diversity of generation source but location of the generation itself.

Another challenge with wind is in meeting the “residual demand” in the winter – that is, the net demand minus renewables contribution. The complementarity between wind and solar cannot be relied upon to mitigate the variability of each resource as the UK averages only 6 hours of sunlight in winter – and some parts of Scotland see significantly less even than that – and so the UK is more susceptible to the variability of the wind resource, even considering the benefits of diversity across the regional dipole.

### *2.2.3 Flooding, water availability, and associated impacts on the power system*

Flooding can impact the power system via inundation of low lying assets, such as in [4], impacting both the power system itself and the ability for response teams to get to and restore system assets. Much like wind, flooding affects wide areas for extended periods of time. Like wind, the effects of flooding may be impacted by the elevation of system assets (which is to say, low lying, sea-level assets will likely be at far greater risk of flooding than those located in the Cairngorms) and more general geographic conditions. Flood risk is well understood and quantified throughout the EU via the *Water Framework Directive* and associated legislation, meaning the risk of flooding in various areas is quantified in terms of e.g. 1 in 100, 200 year risk, with Ofgem (the energy and markets regulator in

the UK) mandating at-risk assets in flood-prone areas have adequate levels of prevention. This has been done for some time, as can be evidenced in [37] with data going back at least to 2010.

The impact of coastal and inland flooding was also investigated as part of the IMechE report into natural hazards facing the GB network [19] and in the McColl paper the percentage change in the probability of flood-causing rain events was investigated [7]. It can be said with confidence that there will be a significant increase in flood threats to the UK as rain patterns change and the North, in particular, becomes warmer and wetter. There is however significant uncertainty projected in the potential change in flooding in GB – projections ranging from ~25% to over 125% increase in flooding-related rain events by 2080. This suggests significant incentive for flexible flood response solutions, rather than more expensive, fixed solutions which necessitate centralised investment. With such an enormous range in potential risk, being able to defer investment or to invest in solutions which can be used flexibly (e.g. mobile flood barriers, sandbags) may be preferable to those which incur significant CAPEX focussed on a few critical assets – but again this likely depends inherently on the climate projections being used.

Water availability also presents its own issues for generators, planners, and operators. Water shortages can lead to enforced generator shutdowns and reduced utilisation of both hydroelectric and thermoelectric plant [38]. Water distribution globally is likely to become increasingly problematic with many areas becoming more arid, with others seeing more variable, extreme weather and precipitation patterns. Surface water availability in regions with sizeable pumped storage and hydro schemes will be affected, but will also depend on local geographic conditions. Similarly, run-of-river hydro schemes will likely be affected differently compared to surface pumped storage reservations.

Given the capacity for hydroelectric power to provide renewable electricity while retaining properties associated with thermoelectric generation – specifically the provision of inertia and frequency response – with none of the associated drawbacks such as pollution or dangerous by-products one would generally associate with thermoelectric generation such as nuclear or natural gas, this could be problematic in a world trying to move away from such generation to clean energy supported by hydro for storage and inertia support. This is unrealistic in the context of the UK which has limited remaining hydroelectric capacity relative to its electricity demand, but may be achievable in other parts of the world.

#### *2.2.4 Wildfires*

Wildfires can have a wide range of causes and can have devastating socioeconomic and environmental impacts [39]. Wildfires can be caused by human negligence from articles such as glass bottles left on the ground, malicious actions, or intentionally started fires for e.g. barbecues which are not properly controlled. They can also be caused by lightning, or power equipment failure in at-risk areas. This is a contributory factor behind the decision of Californian power company Pacific Gas and Electric to intentionally disconnect customers in at-risk regions to reduce wildfire risk [40].

Some work has been performed to investigate the risk of wildfires to overhead lines and the spread of wildfires on the system in [41] and the effect localised wildfires can have on overhead line temperatures [42]. Wildfires not only can destroy overhead line branches by physically burning down structures and components, but can also have an indirect impact on the operation on the system. Since line ratings are typically determined by thermal limits – for safety reasons, to prevent sagging power-carrying conductors from coming dangerously close to the ground – it is important to control the flow of power to limit the risks posed by such sagging. Wildfires, even at significant distances, can impact local temperatures and affect the actual temperatures of lines, necessitating de-rating of lines even if not directly at risk from the fire itself.

With changing precipitation distributions globally, localised warming, and changing wind patterns, the precise risk posed by wildfires will vary regionally. This makes methods of quantifying and mitigating the risk associated with wildfires an important avenue of research not just because of the effects of wildfires on the power system, but the risks the power system can incur on the natural environment, itself providing a threat vector for the generation of wildfires. The Australian wildfire season of 2019/2020 is a worrying example of the potential for devastating threat wildfires can pose and in a warming climate. With some regions of the world becoming increasingly dry and hot, this threat is only liable to increase and further research in this domain is looking increasingly important as it stands relatively lacking presently.

#### 2.2.5 Extreme cold, snow, and blizzard conditions

Historically, energy systems such as GB can broadly be thought of as being designed around meeting the adequacy requirement of the peak winter demand level within a certain level of LOLP (loss of load probability)- though GB has moved away from such explicit targets towards more diverse incentive schemes such as the *Capacity Market* in recent times [43] In temperate countries like the UK, which can experience both heatwaves and extreme cold events, this presents systemic challenges with planners and operators having to adapt to both sustained hot, dry periods and wet, cold winter conditions, and even freezing snow and ice conditions in more exposed regions. In [27], snow, sleet, and blizzard (SSB) faults are classified as their own phenomenon.

Snow, sleet, and blizzards can cause outages on transmission and distribution systems via a wide range of impacts. Accumulated snow on insulators can cause flashovers due to the accumulated moisture [44], whereas accumulation of snow and ice on lines can cause collapse due to mechanical failure, and accumulation of snow and ice can be difficult to detect while gradually causing degradation of insulators on OHL connections [45]. At higher altitudes, where areas may be prone to snow drifts, substations are at risk of being physically submerged in snow drifts and could be unreachable for extended periods of time due to snow.

Cold weather is also associated with higher electricity and energy demand from heating across the energy system – which is to say, including the gas network – associated with space and water heating in homes and businesses...

There is a correlation in GB between ambient temperature and demand, particularly in winter where electrified heating in particular introduces significant additional demand. According to [46] there is a significant linear relationship between electricity demand such that a 1°C drop in temperature during winter corresponds to an approximately 1% increase in electrical demand. This is not unique to GB with demonstrable relationships between demand and temperature in industrialised nations worldwide, with an example shown in [47] with reference to the USA.

With additional decarbonisation efforts this could become far more significant, as according to [48] energy demand from gas can be as much as triple that of power demand, suggesting an increasingly decarbonised network would be significantly more susceptible to cold temperature shocks at times when it is also susceptible to wide variations in renewable resources, particularly wind.

It is noted in [6] that very little literature exists examining the interactions between demand and temperature in extended cold periods and how this may be affected by climate variation, suggesting a significant gap in knowledge, particularly given system adequacy in GB is inherently tied to such events. Increasing moves to decarbonise heating introduces significant uncertainty to the magnitude of change which will be observed in power networks associated with winter heating, given the variety of approaches and technologies which can be deployed to reduce power demand in such scenarios –

reducing such demand could come from more conventional heating schemes such as CHP (combined heat and power), distributed residential heating schemes as is common in Scandinavia, or via increased energy efficiency in domestic settings, but are not limited to these. The complexity associated with understanding the risk associated with extended cold periods, now and in the future, at a system-level is likely to significantly increase, therefore, but there is a lack of work investigating the interactions between these aspects.

As previously mentioned, a 1°C change in temperature can see a ~1% change in electricity demand – or a 3-4% increase in gas demand as mentioned in [6]. The electricity system is simply not currently equipped to handle such demand in winter months if gas demand during such periods is switched to electricity demand. Climate change may see warmer winters on average, but they do not eliminate the probability of extended cold snaps such as the Beast from the East to which the system still needs to be resilient. This likely could mean significant amounts of peaking generation being unutilized for extended periods of time and being used solely for the winter peak. Such peaking generation would then have to make enough revenue during those short windows that pricing at such times could be egregious for those with exposure to these costs. Given the residual demand on the system will reach its peak around this time of year, the system will also be subject to significant variability of wind resource and relatively diminished solar resource at a time when the system has the greatest need for power capacity in the annual cycle.

#### *2.2.6 Extreme heat*

Extreme heat is problematic across the entire energy system. Ambient temperature impacts the efficiency of thermal engines (that is, any generator reliant on the use of cycles of heating/cooling water) due to the process by which thermal generation works, reducing their output [49]. Though a relatively minor amount (less than a percent per °K above ISO conditions), at a system scale this becomes a non-negligible problem. Similarly, since lines and transformers are generally thermally rated, increases in ambient temperature may force de-rating of assets across the system at a time when distribution networks may be acutely constrained in periods of high distributed generation from solar photovoltaic (PV) supplies and low demand. Extreme heat is also fundamentally related to other aspects such as wildfires and water availability but should be considered in and of itself given the aforementioned reasons.

As with extreme cold, [6] identifies that there is relatively limited knowledge about the effect of increased ambient heat and sustained heatwaves on the GB power system compared to other system stresses. The relationship between falling temperatures and heating has been quantified, as has been discussed previously, but no equivalent level of evidence exists at a GB scale in academic literature to understand the relationship between summer cooling demand and ambient temperature- though individual industrial stakeholders will likely have significant data to support decision-making in these areas

The GB grid may move from having a winter absolute peak at a time of extremely variable wind and limited solar to having both a summer peaking event and a winter peaking event. It is reported in [6] that meteorologists are generally better at forecasting temperature than other weather variables – that is, forecasts of temperature tend to be more accurate than other parameters. This is naturally of significant benefit to planners given sustained low temperature periods are among the most challenging operational conditions with which operators have to be able to survive in the GB system.

At extreme values of temperature, cooling of generation becomes a challenge should water availability become limited at a time when the system may be suffering from acute variability and ramping issues associated with solar and wind penetration on grid. This may be particularly problematic in situations

where inland nuclear reactors cannot use sea-water for cooling and have to rely on river-water cooling. In the worst case scenario, extreme heat can lead to the need to shut down nuclear plants and restrict line flows to prevent overheating and reduce the risk of wildfires at a time when the system is particularly vulnerable to shocks due to high renewable penetrations, reducing system inertia, interconnectivity. This already takes place in California during windy, dry periods [40]. Increased cooling demand also increases the underlying essential load on the system at a time when refrigeration and water pump facilities are at their most stressed and needed.

This is again a case where diversity of location and type of generation can be of clear material benefit – the climatic dipole between Northern and Southern Europe and between Scotland and the rest of GB mean these localised effects can be mitigated by locational diversity. The complementarity of wind and solar across locations and due to different climatological drivers mean a climate event which reduces wind capacity in northern GB/Europe can also increase solar irradiance and increase wind in southern Europe. The exact manifestations and drivers of these are discussed via various papers discussed in [6] and serve to highlight the extreme complexity in modelling the relationships between weather and power systems on continental scales.

In [7] the threat of heat-related faults associated with solar heating and maximum temperature was also carried out to quantify potential increases in associated faults on the system. This analysis projected the percentage increase in which percentile thresholds of solar heating were exceeded on “average” or “extreme heat” days, or the 90th and 98th percentile of temperature. There is once more significant uncertainty in the results of this analysis, which can be seen in Figure 2.1, taken from [7].

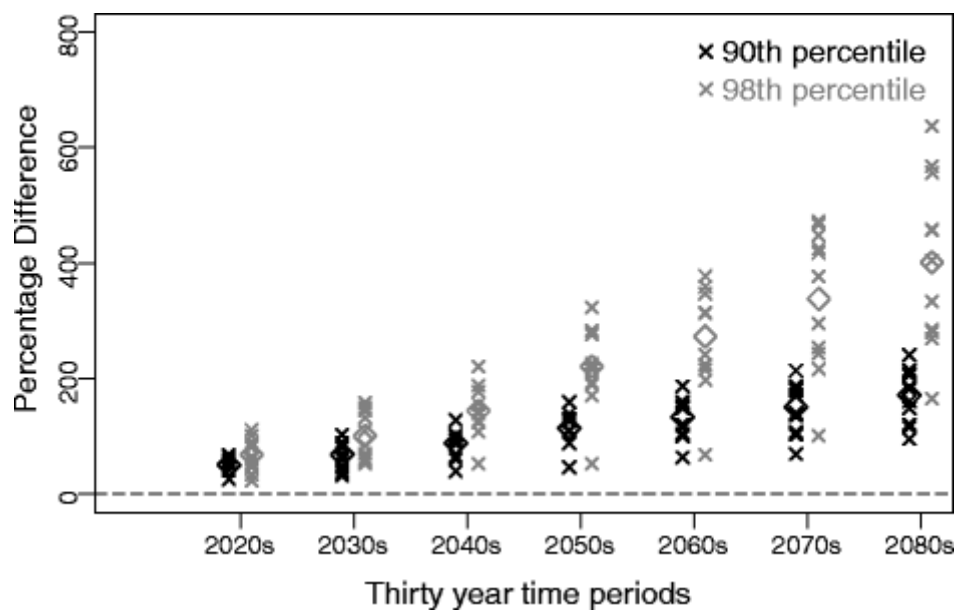


Figure 2.1 - Percentage change in exceedances of 90th, 98th percentile max temperatures for test license area; each cross represents a different climate model projection and the diamonds the mean

### 2.2.7 Common themes

The results for any cost-benefit analysis in attempting to plan for or mitigate climate change rely not only on the climate model used, but the level of aggregation of the model used (the data in the above figure is only for one single license area as solar heating faults were stated to not occur on the transmission network). What may be a suitable investment scheme for one climate projection may be a total waste of money in another.

However, equally, an investment made to prevent the most credible event or scenario is not automatically redundant should the event not come to pass – it may have been an entirely reasonable investment made based on entirely reasonable evidence, but when planning for HILP events there is a high probability that the investment may never actually necessitate deployment. The consequences of not having the right flood defences can be seen in events such as the inundation following Storm Desmond, or in the mishandling of risk management associated with the Fukushima nuclear plant disaster [50].

Resilience planning necessitates risk-averse thinking, but reliability and economic-driven thinking necessitates efficiency-driven and cost-cutting driven investment. Therefore there needs to be clear division drawn between what constitutes a “reliability”-centric investment versus one which could be considered as driven by resilience.

All of the described weather-driven natural hazards will be impacted by climate change, but to differing degrees of severity and with significant regional variation. Furthermore, the quantity and quality of literature that exists to study these impacts also varies significantly and emergent threats like wildfires and drought have not been adequately quantified given the potential harm such events could have in both developed and developing countries and power systems.

It bears repeating that, generally speaking, climate scientists and electrical and electronic engineers are from different academic traditions and so it should not be surprising that studies combining meteorological studies with electrical engineering are, relatively speaking, thin on the ground. This does, however, leave significant academic scope for addressing these areas.

## 2.3 Understanding resilience and reliability

Reliability and resilience are not concepts unique to power systems, and apply across most economic sectors. The exact definitions will vary sector by sector, as will the consequences of failure. The power sector is particularly important, however, in the context of resilience due to the interdependencies that exist between it, wider society, and the economy. Therefore, it is important to be clear about what one is referring to when discussing the terms in this context and the implications involved with strong or weak resilience or reliability.

### 2.3.1 Qualitative descriptions of reliability and resilience

There are a wide variety of given definitions for what constitutes “resilience”. In [1], resilience is defined by the ERP as: *“the ability to withstand and reduce the magnitude and/or duration of disruptive events, which includes the capability to anticipate, absorb, adapt to, and/or rapidly recover from such events”*. This is in contrast to reliability, which is defined by the US National Academy of Sciences (USNAS) within [10] as *“the ability of the bulk power system to withstand sudden disturbances, such as electric short circuits or the unanticipated loss of system elements from credible contingencies, while avoiding uncontrolled cascading blackouts or damage to equipment.”* Or system adequacy, which is defined in [10] as *“The ability of the electricity system to supply the aggregate electrical demand and energy requirements of the end-use customers at all times, taking into account scheduled and reasonably expected unscheduled outages of system elements.”*

Reliability is summarised in [1] as “the daily challenges faced by system and network operators”. That is, it is expected that an organisation should have a given level of performance for daily operation that can be measured against KPIs (key performance indicators) and classified as either satisfactory or unsatisfactory.

Yearly reports of reliability performance, such as those produced by Ofgem [37], offer policymakers and stakeholders useful barometers for whether asset owners or operators in the energy markets are

performing to the expected standards. NERC (North American Electric Reliability Corporation) performs a similar role in the USA, with data tables available for more technical information such as asset availability and outage causes across the USA's grid, such as TADS, DADS, and GADS (Transmission, Demand response, and Generating Availability Data System respectively) [51].

Infamously coined by former US Defence Secretary Donald Rumsfeld, a useful principle by which to appreciate the principles of resilience planning is that “there are known knowns; there are things we know we know. We also know there are known unknowns; that is to say we know there are some things we do not know. But there are also unknown unknowns—the ones we don't know we don't know”.

Reliability can, at a high level, be generally understood as primarily concerning “known knowns”. That is, reliability predominantly concerns predictable phenomena acting in a predictable way which can be readily quantified and understood. Resilience at a very basic level, as well as covering some “known knowns”, particularly begins to manifest in the realms of “known unknowns” or “unknown unknowns”, where either events are being considered where the probability is unknown, irrelevant, or vanishingly small, or where the impact is difficult to quantify or anticipate- or some combination thereof.

Various qualitative concepts have been deployed to describe approaches to resilience in different contexts. The nuclear industry operationalizes safety via the concept of “defence in depth” [52] which describes the physical layers of safety involved in disaster prevention. Each stage has a stated objective of preventing further state degradation on a sliding scale from “normal operation” to “post-severe accident situation”, with prevention at one end of the scale and disaster remediation at the other. This is similar to the “bow-tie” model of planning for resilience shown in , taken from [1].

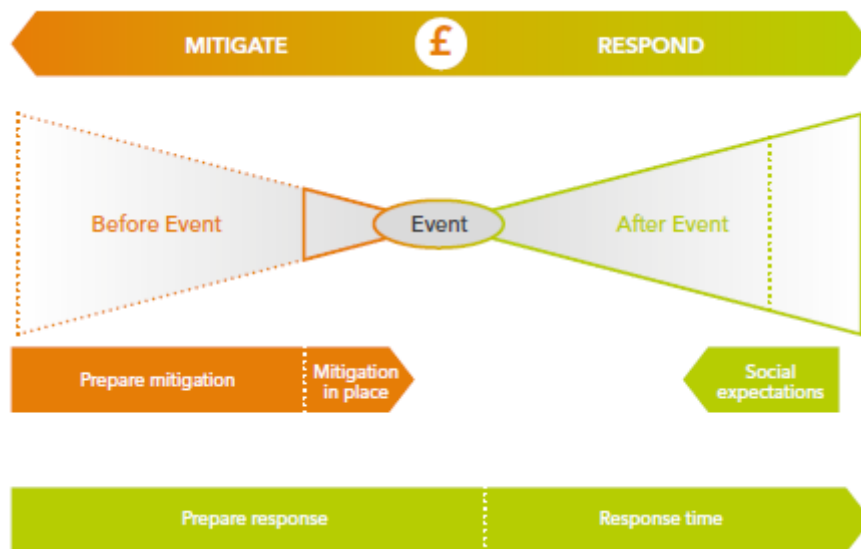


Figure 2.2 - "Bow-tie" model of risk planning

This conceptualises resilience planning as forever being a balancing act between preventative measures, or mitigation measures set in place ahead of time, versus remedial or corrective actions taken after the fact. The importance of posterior remediation varies by sector. The consequences of nuclear safety failures are significant enough such that the emphasis is primarily on disaster prevention – much like with black-start preparations in the GB power systems – but plans still need to be in place to restore the system or mitigate damage should the worst occur.

Similarly, there is the “Swiss cheese” representation of risk and disasters. This conceptualises major adverse events as being a series of aligned “holes” in prevention schemes, attributable to failures or malicious undermining of security, and is comparable to defence in depth in concept and application. A visual representation, taken from [53] and simplified, is shown in Figure 2.3.

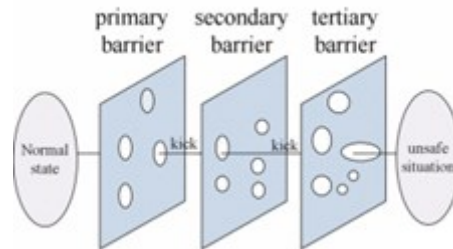


Figure 2.3 - "Swiss cheese" representation of disaster propagation

While these concepts combined provide a means of qualitatively describing the over-arching concepts of reliability and resilience, and its consequences, it does not offer a direct means of comparing outcomes and hence measuring performance improvement or degradation of resilience or reliability. For that, generally quantitative methods and metrics are needed, but these too present their own challenges. The “Swiss Cheese” model represents HILP events or particularly serious disasters as those which various levels of prevention or control fail to adequately protect against. That is, a perturbation can be thought of as some sort of vector which passes through the layers of “cheese” and “holes” represent weaknesses or vulnerabilities which cannot contain the event in question. This illustrates the fact that, typically, disasters happen when a series of failures coincide in a suboptimal manner through misfortune, inadequate preparation, or active sabotage.

One concept that begins to more quantitatively describe resilience is the “resilience trapezoid” as developed in [54]. Also known as the “FLEP” (when translated from Greek to English), it refers to how **F**ast a state degrades, how **L**ow a state’s resilience or performance drops, the **E**xtent of the degraded state, or how long the performance is compromised, and how **P**romptly the system recovers. The exemplar trapezoid used in [1] is shown in Figure 2.4.

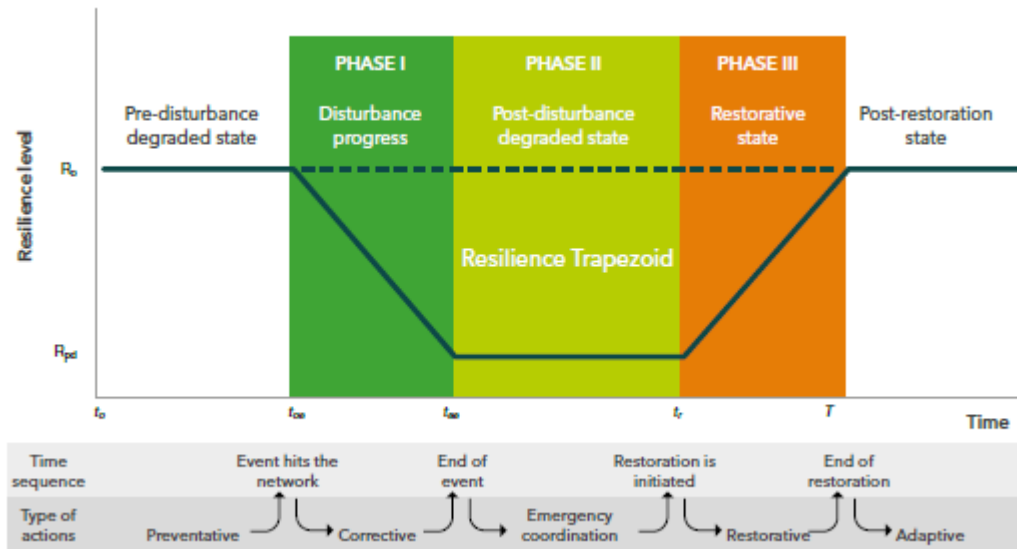


Figure 2.4 - Example resilience trapezium used in ERP report

The challenge, however, remains insofar as the exact metrics being used to quantify the magnitude of each stage of this trapezoid. In order to understand why that is significant, an understanding of how to quantify power system performance and how this relates to power system reliability and resilience will be discussed.

### 2.3.2 Quantitative metrics for describing reliability and resilience

Due to its role as a markets regulator, Ofgem historically has liked to use metrics such as CI (customer interruptions) and CML (customer minutes lost) as metrics for reliability performance of power companies [37]. There are associated targets which change year-on-year to ensure continuous performance improvement in line with the desires of the Government of the day and the expectation that continual technological progression should ensure performance improvement. National Grid, in its role as electricity system operator (ESO) also has its own reliability incentives mandated by Ofgem [55]

On the technical side, the metrics LOLP (loss of load probability), ENS (energy not served), and EENS (expected energy not served) are commonly used to quantify the estimated impact of outage events or scenarios on power systems in cost-benefit analyses. In this context, a pound or dollar value can be assigned to the EENS to determine an expected cost of unreliability and used to justify investments on the power system to improve whichever reliability metric is used. In that sense they can be used as a proxy for economic performance and are rather gross estimators of reliability – the impacts of HILP events are obfuscated by nature of the “averaging” of impacts across whichever sample size is used, meaning they may be inappropriate in the context of resilience. However, in a stable, predictable, system absent of unpredictable or severe shocks managed by rational actors these metrics can reasonably be assumed to nonetheless be useful.

Resilience, given its concern typically laying in shock events with high impacts or difficult to quantify probabilities, is far more difficult to represent using such economic risk metrics. Metrics such as VaR (Value at Risk) or CVaR (Conditional Value at Risk) can be used to more explicitly examine the tail of the distribution of outcomes. In [56], VaR and cVaR are defined as follows: “[by] definition with respect to a specified probability level  $\beta$ , the  $\beta$ -VaR of a portfolio is the lowest amount  $\alpha$  such that, with probability  $\beta$ , the loss will not exceed  $\alpha$ , whereas the  $\beta$ -CVaR is the conditional expectation of losses

above that amount  $\alpha$ ." The "loss" referred to by VaR and cVaR may be, for instance, a dollar amount or a value of ENS.

When considering some HILP events of acutely low probability, or uncertain probability, it remains challenging to capture such events and represent those events using conventional Monte Carlo state sampling methods. This shall be discussed further in Chapter 5.

EENS, CVaR, and VaR are all risk metrics in the sense that they are dependent on the probability and impact of the events of which they describe, which in resilience studies can be acutely problematic. It may be the case, then, that for resilience studies, rather than sampling across a wide variety of possible states, specific eventualities are analysed on the basis purely on impact or on the basis of avoiding events we judge, be it by expert elicitation or heuristics, to be undesirable enough such that planners or operators must prepare for them, regardless of probability. This shall be discussed in Section 2.3.3.

### 2.3.3 Security standards for resilience and reliability

Deterministic security standards, such as "N-1", effectively operate in a manner whereby the risk horizon can be interpreted as being set by the lowest probability of any single outage event, adverse condition, or loss of asset. That is, the lowest probability which concerns the operator is the one representative of the single outage with the lowest probability. The definition of an "event" can vary: it can be an adverse operating state introduced by a demand surge, loss of infeed from a generator, or loss of a network branch. The "event" could also encapsulate a given weather state which induces a perturbation to the optimal running of the system, with the simulation and realisation of that perturbation constituting another "event". It is judged that the loss of any single system asset, no matter how improbable that specific outcome may be, is deemed sufficiently adverse as to require adequate preventative or corrective actions to be in place to deal with it.

There may well be N-2, N-3 events that approach probabilities comparable to the loss of e.g. an underground cable, but that are not considered in reliability planning scenarios or conventional deterministic security criteria. The limitations of this are examined by R. Moreno in [57] and more generally in [58], and work is ongoing at the time of writing in reviewing security standards in GB and the Security and Quality of Supply Standard (SQSS) [59].

In the context of resilience, planning for specific eventualities becomes far more difficult, making the need for robust data, system analysis tools, and heuristics all the more important. Failure to appropriately identify credible system threats can lead to widespread blackout conditions such as were seen in South Australia, as previously mentioned in [14]. It was also noted that a lack of understanding about the actual resilience capabilities of assets on the system – specifically wind turbine ride-through capabilities – contributed to the black-start condition, suggesting that network awareness and visibility are key resilience factors.

Approaches taken towards reliability cannot then be directly applied in the context of resilience, as one cannot directly translate the understanding expected for "known-knowns" to "known-unknowns" or "unknown-unknowns".

Similarly, in planning to be secure against N-1 events, the system may then be protected against a wider array of events than those which have actually been selected in the credible contingency list (that is, setting up the system for N-1 security may also render it secure against a variety of N-2+ conditions), and so often there is an added, unseen, security benefit to security decisions made at dispatch. Clearly quantifying and understanding the drivers of resilience should clearly then be a focus of trying to improve a system's resilience.

## 2.4 Modelling interactions between weather and the power system

As has been established, there are a wide variety of ways in which the weather can affect power systems. Tractability and defining the scope of a power system simulation then becomes acutely challenging due to the intricate ways in which these models may need to interact with each other, and the varying sensitivities of results to different aspects of these models.

A fundamental way to look at the interaction between the weather and the power system is to look at it in terms of *causal weather events*, *system perturbations*, and *resultant system outcomes*. That is, the primary causal weather which affects the power system, the perturbations on the system this causes (e.g. variations in wind power output, line failures, etc.), and the corresponding impact these outages then have on a power system. The natural hazard chosen for further examination here is extreme wind. As will be described going forward, though there is significant research investigating the impacts of wind on the power system – and thus a robust foundation on which to build – there is still plenty of work to be undertaken to address gaps. Given the UK is a temperate nation, wind is one of the few dangerous natural hazards it is exposed to. Its increasing deployment of onshore and offshore wind also mean that it is important to understand how power system risk and wind are associated on the system more generally.

For example, when modelling a wind storm, there needs to be models linking that wind to the network and to generation. There then need to be corresponding relationships between the impacts these effects have on the system, and how that actually manifests in the power system. It then becomes necessary to clearly define the scope of the power system being analysed to understand what the relevant causal relationships actually are and their significance.

As a more abstract example, greenhouse gas emissions drive climate change which, in turn, will change the distribution of wind speeds in a given region- but it is not CO<sub>2</sub> that causes mechanical failure in lines, but wind. Therefore, the scope of our problem should be limited to the actual interaction between wind and lines, if our concern is the simulation of wind faults on lines. Climate change acts as a driver for the wind, it is not the cause of the fault itself.

Similarly, when relating a wind speed to a given failure rate on a line or asset, factors such as directionality or location of line also may need to be taken into consideration. A wind gust acting perpendicularly to a line may have a more significant impact than one acting in parallel; a sudden, intense gust of wind may have more impact than a sustained period of extreme wind such as a hurricane.

Once a line has then faulted, this then actually has to be translated into an effect on the power system. For instance, a loss of infeed will see an imbalance between generation and supply, resulting in a frequency deviation and the need for frequency response or redispatch of generation [60]. However, even various assumptions need to be made about the manner in which the system responds to this deviation in frequency and how spinning generators will react, versus power electronic devices. System inertia may change with time as e.g. factory machines connect and disconnect, just as connected demand across the system will change the way in which demand responds to deviation in frequency in tandem with changes in connected generation infeed along the diurnal cycle.

The restoration of this line, or reconnection of a generator, then too needs to be considered. Some assets, such as transformers, take weeks (or even months) to repair compared to overhead lines which, for simpler and smaller connections such as wooden poles, can be repaired in a matter of hours [61]. This then could factor into how exactly the system is prepared for a resilience-related event – enduring a little pain for a short time will always be preferable to a lot of pain for a long time, which

is the basis of schemes such as under-frequency load shedding (UFLS) and low frequency demand disconnection (LFDD). These are both different names for a strategy undertaken by system operators to keep frequency within bounds and prevent low-frequency disconnection of generators, which can cascade to system-wide blackouts. Then a metric is still needed to quantify exactly how significant the damage has been to the system as a result of the causal event, which is where terms such as Value of Lost Load (VoLL) emerge, which attempt to quantify the economic harm caused by supply interruptions by assigning a monetary value to a risk metric such as EENS.

At every stage, new abstractions and assumptions need to be made about how exactly a power system will react, all to a single event which can be attributed to a weather condition- from the beginning causal event to the end result. These abstractions could significantly affect what mitigation and correction strategies are ultimately used, and are all fundamentally dependent on the data used to drive the simulations, meaning that it is imperative these relationships are clearly defined and the abstractions and simplifications made are appropriate.

#### 2.4.1 Quantifying failure rates on overhead lines due to wind

Failure rates on lines due to weather have been represented in several ways, and techniques continue to be developed to improve upon them. In reliability analyses this can be in terms of using adjusted failure rates for “normal”, “adverse”, or “extreme” weather conditions – but this then introduces the complexity of quantifying exactly when a weather condition goes from normal to adverse, or adverse to extreme. Such methods are shown in [62] and [63].

The number of years between these sources’ publication (almost 40) illustrates how standard this approach has been. In lieu of more data-driven approaches, it is not an unreasonable method to use – the increased failure rates are intended to replicate the “bunching” effect on faults that weather causes on power systems – more things break, and they break at the same time, due to the weather acting upon them. However, this, effectively, bunches all experience of weather into three “bins”, when in reality the probability of failure of a given asset of line will be subject to an enormous variety of factors –geographic conditions, varying exposure to weather conditions along the path of a line, and so on.

Such representations and approaches to modelling line failure rates also typically apply the modified failure rate homogeneously across a system, which therefore obscures regional impacts of extreme weather on a power system. For more acute or extreme events, where we are particularly concerned with locational impacts of extreme weather, such analysis is an inadequate representation of failure probability on networks and more granular methodologies may be necessary; both to represent failure probability and the consequences of failures when they actually happen.

For example, lines across the coast will experience different fault mechanisms than those in an arid desert region. Coastal assets can suffer flashovers due to moisture and sediment thrown onto them from the sea during storms, whereas in a desert there is no such moisture but there may be more dust and debris which may cause different operational challenges. Lines above the tree-line in mountainous regions will be less likely to suffer vegetation-related losses, as there is no vegetation to fall on the lines. However, in hilly regions with little to no vegetation, lines, towers, and substations may be more susceptible to landslips, which offer a completely different mechanism of damaging equipment. None of these are captured by such adjusted failure rates purely defined in terms of “stormy” weather conditions.

Fundamentally, what is needed is a method of converting an incident natural hazard – in this case a wind speed – into a corresponding impact on the network, specifically whether a line is in or out of service. This can be conceptualised as shown in Figure 2.5, with an incident hazard with a presumed relationship between a natural hazard and the natural hazard itself acting on a system asset to generate a new asset state.

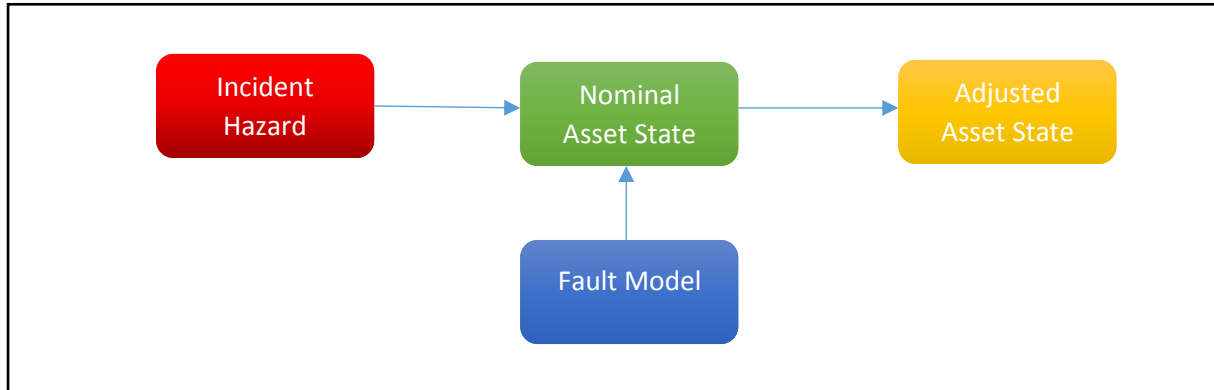


Figure 2.5 - fault modelling concept with regards to natural hazards

An improvement on this methodology in recent years has been based on more data-driven models in an attempt to make more portable, tractable methodologies based on improvements in data collection and availability and completeness of weather data. Hindcasted datasets such as MERRA-2 and ERA-5 from NASA in the USA or ECWMF (European Centre for Medium-Range Weather Forecasts), which shall be discussed in Chapter 4, offer spatiotemporally complete datasets which can be used to quantify the probability of line failures given a set of weather parameters, such as was done by K. Murray in [27]. Similar techniques were utilised by P. Mancarella and M. Panteli in a number of works including [54], with K. Murray’s work developed further in [64] by F. Fan to break fragility curves down by voltage level.

These effectively use Bayesian methods to determine a cumulative probability curve of the failure of a given asset given a weather parameter to the project the failure probability of an asset in a Monte-Carlo simulation. A challenge with using these methods, however, is that data can be sparse meaning significant uncertainty in the long tail of the results. Also, assumptions need to be made about the homogeneity of assets – the resilience of assets may change with age, location, construction, and voltage level (the latter being the metric by which F. Fan separated their fragility curves in [64]). Therefore, there can always be improvements made to the granularity of the curves which are constructed using such methods but only up until the point there is actually sufficient data to have confidence in the samples.

In the context of resilience this is a major challenge because in many cases that data simply does not exist in the extreme cases, and so projecting based on historic data has to be a compromise between granularity and data availability. This is addressed [64] by using different sized bins of data to increase sample sizes in given bins, and extrapolating the data accordingly to develop the fragility curves. Alternatively mechanical models of towers can be used in tandem with data-driven models of lines to generate fragility curves, as are used by Panteli et al in [54].

Understanding the relationship between weather and power system conditions is limited both by the granularity and completeness of the data and how the interaction with the power system itself is modelled. Different datasets and reanalysis data will give different relationships between faults and weather parameters because of the different underlying methods involved with how these reanalysis datasets are actually formed. Even the datasets used to generate the fragility curves in [27] and [64]

have this limitation, in that the sample sizes of faults, years, and data are limited – and the samples are geographically limited to Scotland and its network.

It would be useful to compare fragility curves across different reanalysis datasets, different geographical regions, and different biomes, and with different corrections to see the corresponding variability in the curves generated by such data. Further, translating those faults onto a power system model also introduces challenges regarding how to model the outages themselves or translate the presence of a “fault” to a power system consequence.

A fragility curve can identify, in a Monte Carlo simulation, whether a fault or failure has occurred in a given sample. This still presents a challenge as to how to translate that “fault” into some new network state. In a DCOPF, for instance, this would mean taking a line out of service – however, in transient analysis the consequence of a line failure may instead be a short-circuit (e.g. phase-phase, phase-earth transient faults). Further, if  $n$  lines are identified as having faulted in a sample hour, the fragility curve tells us nothing about in which order these lines faulted, or whether the faults manifested as single or double circuit faults, or whether the fault was permanent or transient. Certain assumptions have to be made in order to compensate for this, but there was no literature found investigating this directly.

Similarly, the fault mechanisms in a region like Scotland with relation to wind speeds will be different from those in a more arid region such as the southern United States. It cannot be assumed that a fragility curve derived in a temperate, windy nation such as Scotland would be equally applicable to, for instance, the ERCOT (Electricity Reliability Council of Texas) power system in Texas.

Further, some factors are not directly considered in the derivation of the fragility curves used in [27] and [64] – specifically the directionality of wind, or impact of factors such as precipitation. As has been discussed, different weather and climatological phenomena in GB manifest in different ways – e.g. turbulent, chilly easterly winds; stable, high wind speeds from the west. These two may cause different fault scenarios and fault conditions which mean a model of fragility curve in Scotland may simply not be applicable in e.g. Southwest England, but the comparator data does not exist.

The best way to address this would be continental-wide datasets of aggregated data which could be separated by biome and corrected for e.g. voltage levels, age of assets, construction, etc. - but this level of aggregation simply does not yet exist. The frameworks and data analysis techniques to generate such models, however, have already been demonstrated at small scale and could be upscaled accordingly for wider-scale modelling of continental-scale interconnections and grids.

#### 2.4.2 Estimating wind power output from wind speeds

Wind output on wind farms for a given wind speed at a given site can vary significantly. This may be due to different manufacturer power curves for different turbines, local microclimates, varying geographic conditions if the wind farm is built in a particularly windy or hilly location, or due to varied turbine sizes with groups on a given wind farm. A “power curve” is a model relating the incident weather, in this case wind, on a given wind turbine or wind farm with an associated capacity factor for the power output of that wind turbine or wind farm. Exemplar wind power curves will be shown in Chapter 4.

Developing a relationship between a forecast – or, indeed, hindcasted- wind velocity and the anticipated output of a wind farm is important because it impacts how much wind power can be anticipated to be feeding into the network at any given time – and, the more wind there is on the network, the more significant any error in this forecasting potentially is. That is, even a 1% error if there is 10GW of power on the network could mean a difference in infeed of hundreds of Megawatts of power. Underestimating the amount of infeed on the network could lead to additional curtailment

costs, or even over-voltage and frequency deviation issues if the system cannot respond appropriately to the variability of wind resources should there be insufficient balancing reserve on the system.

Conversely, overestimating the amount of wind power which may be on the network could also lead to problems – power shortfalls, high balancing costs, or even load curtailment if there is insufficient available response to respond to unexpected, sudden shortfalls of supply.

Ofgem have in the past produced characteristic power curves linking the capacity factor of wind farms to an incident wind speed, as described in [65], with an example shown in Figure 2.6. Similarly, at an EU level, in 2009 *TradeWind* developed characteristic wind power curves for different types of wind farm – e.g offshore versus inland. These are described in [66]. This will be discussed in further detail in Chapter 4 and Chapter 5.

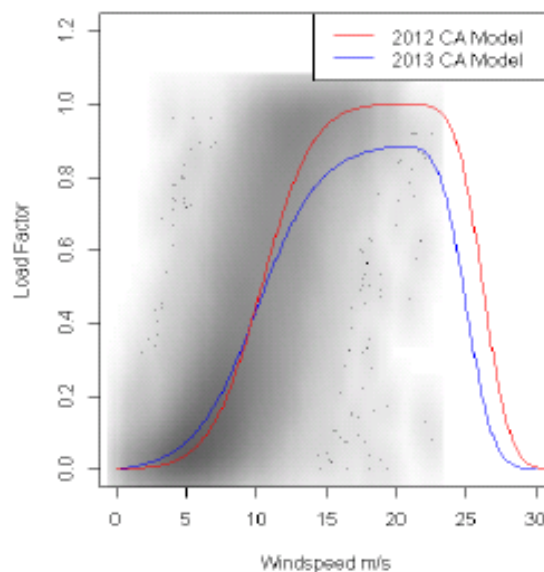


Figure 2.6 - Ofgem derived power curve example

As with modelling the effect of extreme wind on overhead line failures, challenges emerge in the extremes of wind speed distributions due to the lack of data available. For this reason, in the curve shown, Ofgem fitted the cut-out feature on the curve using a Gaussian filter by inspection in lieu of a significant amount of data.

At an individual turbine level, turbines will have a minimum “cut-in” speed which the wind must be blowing at for a certain amount of time before the turbine starts feeding power into the grid. At high wind speeds, wind turbines also have mechanisms to reduce their power output or rotational speed to prevent mechanical damage or overloads. This may be done by adjusting the angle of the blades, via electromagnetic brakes, or, on smaller turbines, altering the angle of the hub away from the wind. An example scheme is shown in Figure 2.7, taken from [29].

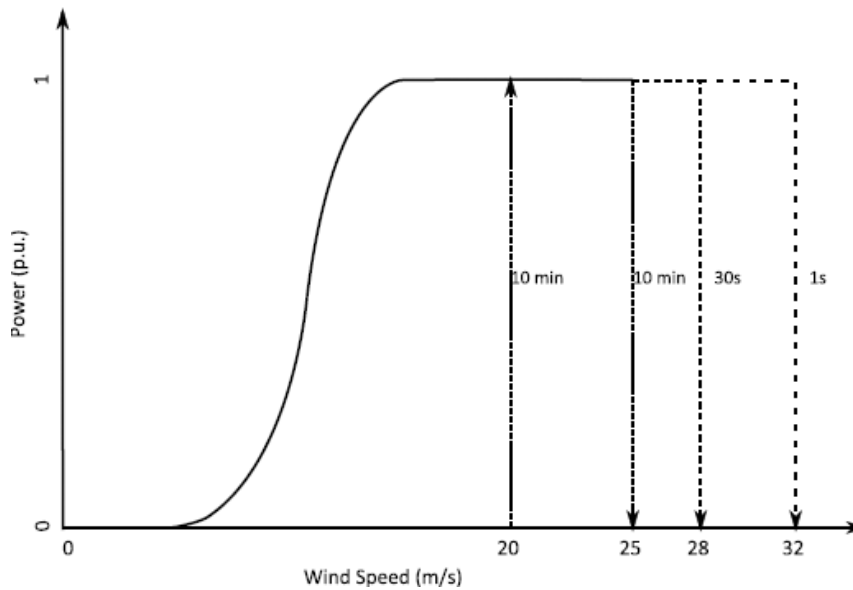


Figure 2.7 - wind turbine cut-out scheme example

While this can then be easily understood and quantified for individual turbines, at a population level on a wind farm grouping, groups of turbines may cut in and out at different paces, as well as some turbines being unavailable due to faults or maintenance work. Therefore, either individual turbines can be sampled in a Monte Carlo fashion to estimate the output of a wind farm, or a wind farm can be aggregated with some estimate made of the capacity factor of the entire wind farm, reducing the computational expense and sampling requirements of a simulation or projection.

The effect of HWSS is considered in the power curves described in Ofgem’s capability assessment referred to in [65] and in [66]. Such curves can then be used to aid in dispatch decisions for operators, but are still subject to uncertainty over both short and long terms. Work analysing exactly how windfarms can be impacted by extreme weather events is invaluable in understanding the links between system risk, security, and operability during force majeure weather events.

Although the wind farm may be physically fine itself with protection systems operating as expected in such extreme wind events, this can nonetheless lead to a significant loss of infeed for however long the extreme wind event is affecting a system.

This affects both operational decisions in control rooms in the short term and, longer term, affects planning decisions for investors due to uncertainty in the actual output of windfarms. If the frequency and intensity of extreme wind events changes, this then affects investment and planning decisions in wind farms by reducing their availability and annualised capacity factors. This emphasises the need for robust and data-driven methods for quantifying these relationships precisely both for economic reasons, and for network operability reasons. As more wind generation penetrates the network at multiple levels, this becomes a problem for both distributors and planners.

Wind power tends to be distributed across regions, making generation susceptible to regional extreme weather events such as storms or anti-cyclones, which can cause either extreme highs or lows in terms of wind output that need to be planned for and accommodated for. This, however, also distributes the impact of extreme weather events. Due to the diversity of geographic conditions across, in particular, Scotland, this means a wide variety of weather conditions – so if extreme wind forces a wind farm to shut down in one location that does not necessarily mean all of them will be forced to curtail their output, but effects will be correlated regionally [6].

Climate change, as previously mentioned, is also likely to affect regional wind capacity factors on wind farms, which will affect future planning decisions and could change the types, location, or capacity of wind farm capacity installed on the network. In [6] it is discussed that windfarms ~600km apart tend to show very weak correlation in outputs, emphasising the value of locational diversity of wind generation.

Due to the lack of easily acquirable data to quantify HWSS at extreme wind speeds, compromises have been made in curve fitting to make workable and useful curves. This highlights two things: the value of data from generators and producers themselves, as they will have experience operating their generation facilities and will likely be able to produce more accurate projections of output than an aggregated system-wide model could; also, the difficulties involved with translating given weather datasets to physical phenomena on the power system, in this case the projected output of a given windfarm or group of windfarms. Population-level models of power curves are just that – at a system-wide level they may be representative, but for individual windfarms are at best gross estimators of real output.

## 2.5 Modelling system perturbations

When a line drops out of service or a generator drops out from the network, there will be a corresponding impact on the system, regardless of what the cause of that outage was in the first instance. Substation or transformer faults connecting multiple parts of the network, too, can lead to disconnections of large numbers of customers for extended periods of time due to the concentration of connection assets at such locations.

A “perturbation” on a network can refer to a wide range of things which all require different protection and mitigation measures. Control and protection of power systems is an major field of study in its own right and too broad in scope to be covered in particular depth in this section alone and can be studied in a wide variety of texts, for instance [60], but some general themes and the most significant aspects, within the scope of this project, shall be discussed in this section.

### 2.5.1 Overhead line faults

In the context of resilience studies pertaining to wind, there are various failures which immediately present themselves as threats. Wind can cause “galloping” of OHL or clashing and swinging of conductors, leading to transient short-circuit phase-to-phase faults [26]. Alternatively, mechanical failure of connectors can lead to shearing of lines and phase-ground faults and permanent outages. Vegetation falling on lines or pole collapse can sever connections reducing power flow between areas. Transient faults can be resolved by auto-re-closer actions, whereby a breaker opens and closes after allowing time for ionized particles to disperse or remains open until manually reclosed if the fault is not resolved.

Loss of lines can also lead to cascading faults should overloads be caused on nearby lines, particularly if there are widespread common-mode faults on the network. This is one of the reasons behind deterministic security criteria such as N-1 – to prevent the network from degrading beyond a single fault condition to a far more serious, uncontrollable state. Arresting such faults through preventative measures such as security constrained dispatch has been, in GB, a very effective means of avoiding more serious cascading failures and outage scenarios, with no black-start conditions ever having affected the entire GB system at the time of writing.

As well as causing customer interruptions or disconnections due to loss of connections to the MITS (main interconnected transmission system), line outages can separate parts of the grid into “islanded” sections and cause loss of synchronism between these islands, making system restoration and

reconnection after repairs have been carried out more difficult. Also, for these separated grids, there may then be an imbalance between supply and demand (assuming those islands have both supply and demand and do not immediately fall into blackout conditions), and managing frequency and the supply-demand balance will be significantly more challenging in islanded conditions because there will be fewer assets available compared to the main system.. This is related to the effect of loss of infeed in a power system more generally. OHL faults primarily act as limiting the ability of the network, then, to transport power from supply to demand sources.

There are also other issues associated with overhead lines – e.g. reactive power consumption by heavily loaded lines[60]. High reactive power draw can limit power transfer between constrained networks and require compensation with capacitor banks, for example. Voltage and reactive power are inherently linked and so voltage levels can be controlled to manage reactive power to a limited extent for power factor regulation.

The reason OHL faults are a concern is because the loss of many concurrently can create desynchronised islands, so regions are created where there is loss of infeed and others may be created where there is a surplus of supply – ergo it is not the loss of the lines themselves which solely cause the problems but the restrictions this then places on the power balance in the remaining, surviving networks. Focus should therefore then be on the impact of power imbalances on these networks.

#### 2.5.2 Loss of infeed and generation faults

In a power system, imbalance between supply and demand manifests as voltage and frequency deviations, and effects may be distributed across the network with localised voltage and frequency excursions. This, in turn, can lead to further overloads or equipment damage should protection equipment fail to deploy, particularly if there are significant imbalances due to large transfer across the affected branches [60].

When there is an imbalance between supply and demand on a network, governors on suitably equipped synchronous machines, or controllers on power-electric connected devices, can adjust their outputs to restore the system frequency to the nominal value or within statutory limits (between 49.5Hz and 50.5Hz in GB) while also ensuring the rate of change of frequency (RoCoF) is within limits to prevent cascading outages. An example frequency response curve is shown in Figure 2.8, taken from [67] (note that it is using a US system model, so frequency base is 60Hz rather than 50Hz).

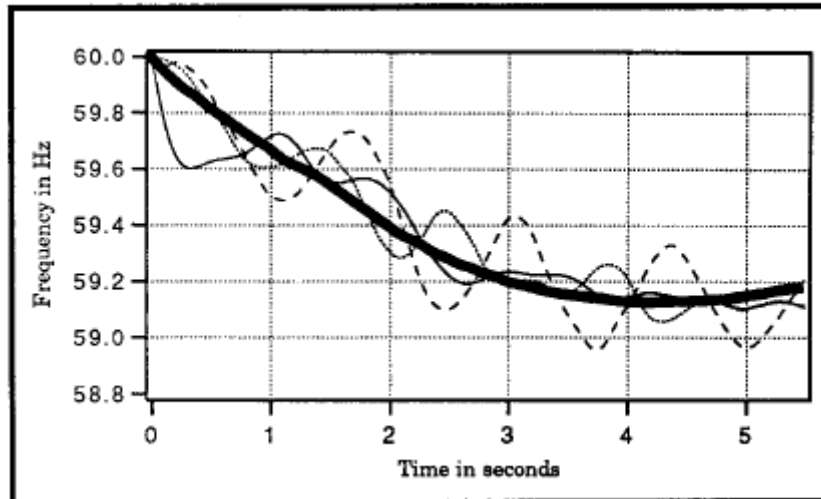


Figure 2.8 - example primary frequency response curves on hypothetical system

Frequency response will vary at different points in the network as different machines respond differently to the deviation, shown as hashed lines, with an averaged system-wide frequency response shown as the bold line. This introduces new error into the modelling, as an aggregated system frequency response will potentially miss more extreme deviations in areas with less local system inertia and system strength which will in turn have localised impacts. There is again a balance that needs to be struck between computational complexity and simulation refinement.

Frequency response is a manifestation of the impacts of an imbalance between supply and demand, but this in turn will also be impacted wider system operability challenges, for example the ability to transfer extra output from frequency-responsive generation to other parts of the network. There are also other stability-related concerns such as rotor angles of generators and “vector shift” protection on connected assets, but these are localised rather than system-wide impacts. Frequency response is generally, however, modelled using a single bus representation with various assumptions about how generator governors or controllers will respond to a given frequency deviation. The formulation of such problems and examples of its implementation shall be quantified in detail in Chapter 5.

There are a wide range of techniques used in the simulation of frequency response, and these can involve the use of specialised coding libraries such as *MatLab SimuLink* or proprietary software such as *DigSILENT/PowerFactory*. One drawback of using such software packages is the licensing requirements and cost thereof, as well as the need for training or significant time investment in order to effectively utilise and understand these software packages or incorporate them with larger scale simulations or analyses. This can be assumed, for larger companies, to simply be part of the cost of doing business, but may act as an impediment for research by reducing the ease of access to support and reducing the number of users in the wider population.

There may be benefits to directly modelling power system simulations from first principles in a more specialised manner in linear programming languages such as *python*. Using representations of frequency response from sources such as [60] and [67] incorporated in wider network models, considerate of weather conditions and other network phenomena such as have been described in previous sections, may allow the analysis of the impacts of, for instance, increased wind penetration on power system stability and frequency response requirements. Such research was carried out in [68], examining the changing frequency response requirements in GB with increasing penetrations of wind and changing system inertia.

### 2.5.3 Frequency response regimes

Frequency response can broadly be divided into three different regimes – primary, secondary, and tertiary. In GB, primary and secondary response differ in that primary frequency response is expected to arrest immediate frequency deviations within 10 seconds, and act up to 30 seconds, whereas secondary response is designed to restore the frequency to statutory limits – or as close as possible – and sustain this response for up to 30 minutes [69]. National Grid uses a broader range still of frequency related services which each specifically refer to a specific kind of response e.g. “Fast Frequency Response” or “Enhanced Frequency Response”, but for the purposes of the modelling herein the general abstractions used are deemed appropriate for the level of analysis undertaken.

Tertiary response can be considered response which acts more slowly, once the immediate frequency deviation has been controlled – to restore balance between supply and demand and ready the system for future perturbations or adverse operating conditions. This can be represented graphically in Figure 2.9, taken from [68].

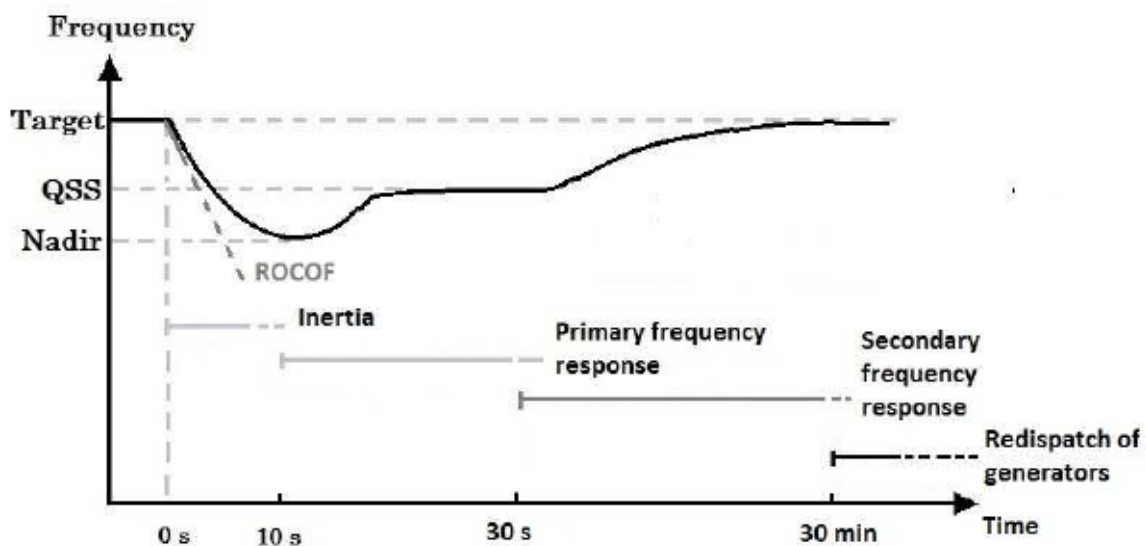


Figure 2.9 - frequency response regimes over time deployed in GB

The study in [68] focussed solely on primary and secondary frequency requirements with varying degrees of wind penetration and changing system responsiveness and inertia. In the paper it is assumed that primary response deploys linearly within 10 seconds, is replaced at 30 seconds by secondary response which deploys to a target level within 1 second. This is done on a single bus representation of the system, ignoring network constraints and assuming homogenous frequency response across the system. Such an approach will be used in Chapter 5.

An example primary frequency response curve, for varying system inertia factors found using the methods deployed in [68] is shown in Figure 2.10. The significance and mathematical formulations relevant to the grid inertia factor shall be discussed in detail in Chapter 5, but for now can be understood as representing the “stiffness” of the network and resistance to changes in frequency, which can be seen in the figure as being represented by the greater deviations in systems with lower frequencies – they are “bouncier”.

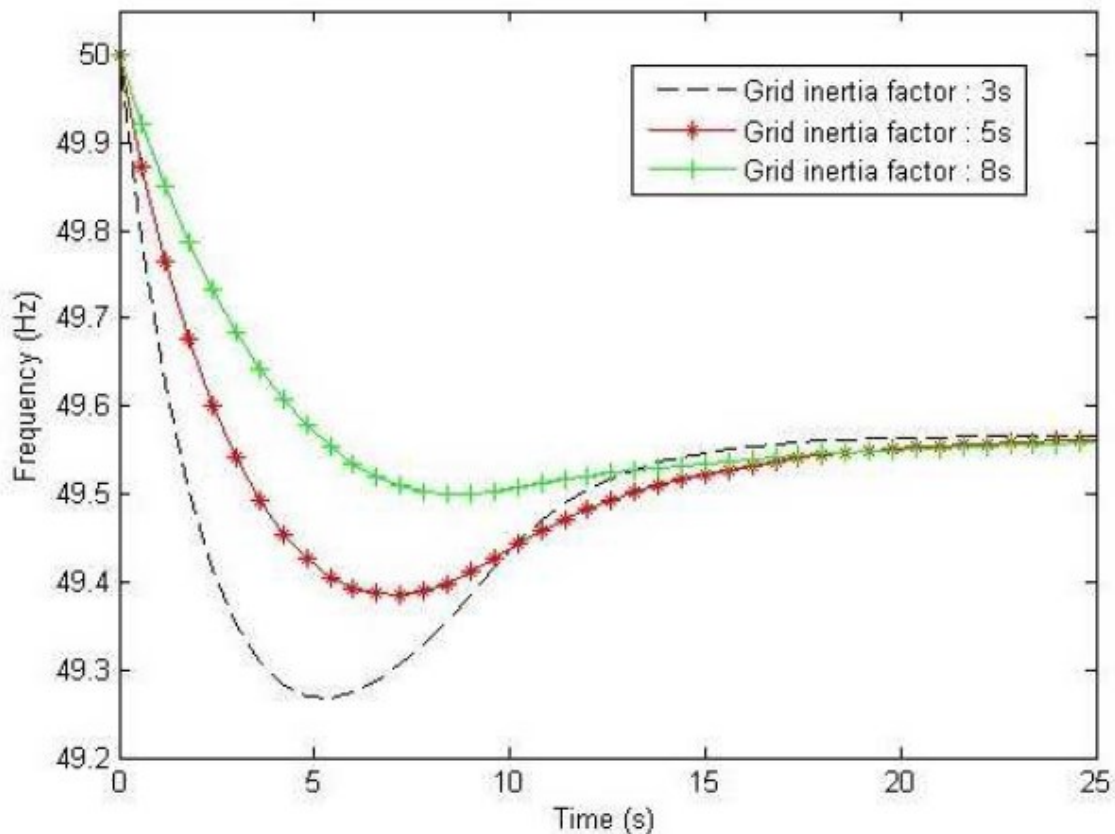


Figure 2.10 - example primary frequency response curves for varying H factors

The frequency response curves shown represent the loss of infeed of 1320MW with a primary frequency response (PFR) of 800MW for a total system load of 30GW. Primary frequency response acts to arrest the fall in frequency and contain it within statutory bounds; the recovery that occurs after the frequency nadir occurs because primary response may not be fully delivered until 10s after the event. Secondary response replaces primary response as it falls away after 30s is delivered to maintain the new system equilibrium while other operational decisions are made (e.g. redispatch, load curtailment). It should also be noted that system inertia affects only the stiffness of the network – not its ability to restore equilibrium after the transient event. Inertia is of primary concern for controlling RoCoF, not adequacy of frequency response itself in the longer term of any system perturbation.

System frequency response requirements in GB are governed primarily by the SQSS [59] to be constrained within normal operation, or following an N-1 event, within the bounds of 49.5Hz and 50.5Hz. Following the largest possible loss of infeed (loss of the 1320MW nuclear station or a double circuit from a heavily exporting area), frequency is allowed to fall as low as 49.2Hz so long as it is restored to within statutory bounds within 60s. Therefore, there must always be enough reserve to respond to the single largest loss of infeed on the system.

Fundamentally, frequency has to be controlled on the grid to protect spinning machines and generators. If there is too much generation on the system and frequency surges, synchronous machines' rpm increases as a consequence until protection activates to shut the machine off from the grid – known as an “overspeed trip”. Conversely, if the frequency drops too low machines can be

strained by the need to perform extra work, which may result in, again, machines tripping off from the grid for self-preservation, known as an “underspeed trip” [70].

Losing generators due to frequency deviations then can lead to cascading outages and widespread blackouts, regardless of any natural hazards acting on the network. Although the initial outage may be caused by an exogenous natural hazard, frequency response is an inherent electromechanical property of the system affected by generator governors, automated generator control (AGC) (though this is not deployed in GB), power electronic device response, and system inertia.

#### 2.5.4 Sources of frequency response

Response can be provided by generators themselves, with a certain expectation of response mandated by technical regulations such as the Grid Code, or auxiliary/ancillary services can be provided by, for instance, demand aggregators or distributed energy resources (DER) to provide enhanced frequency response (EFR) or other response requirements for the system.

Frequency response and inertia capabilities vary by generator type and scale. Nuclear generation, for instance, has significant inertia but may only have limited response capabilities to adjust its output to meet changes in supply and demand due to the nature of nuclear generation requiring strict control of thermal conditions and limited controllability of graphite moderators. Coal, open-cycle gas turbines (OCGT), or closed-cycle gas turbines (CCGT) can adjust actuators and burn rates to adjust their outputs to respond to system requirements with relative ease. Similarly, hydro plant (both pumped storage and run-of-river) can adjust its output from zero to full relatively quickly (in as few as 2 or 3 minutes dependent on location, scale, etc) to meet changes in demand.

Power electronics, due to their use of semiconductor devices, can quickly (even relative to the frequency of the power system) adjust power outputs and voltage in response to system events, but cannot directly supply inertia to the system in a manner comparable to spinning machinery. Cheaper or older power convertors may also trip off during system perturbations if they are not designed or capable of handling voltage or frequency deviations, introducing uncertainty into system response. This can particularly be an issue during major outage events and loss of infeed may happen randomly across the system as local frequency deviations vary and converters from different manufacturers or different topologies drop off at different voltage or frequency thresholds for self-preservation, or due to loss-of-mains protection. This was a contributory factor in the outages in the UK in August 2019 [13]

The changing dynamics of devices connected to the power system also has an impact on the response of a given power system to loss of infeed. That is, spinning machinery and synchronous engines connected to the power system react differently from DC motors and power electronic devices, particularly to changes in frequency. In a frequency response simulation, this can be represented via a factor  $k$  which represents the percentage change in demand given an associated change in frequency. In [68] this is illustrated as shown in Figure 2.11.

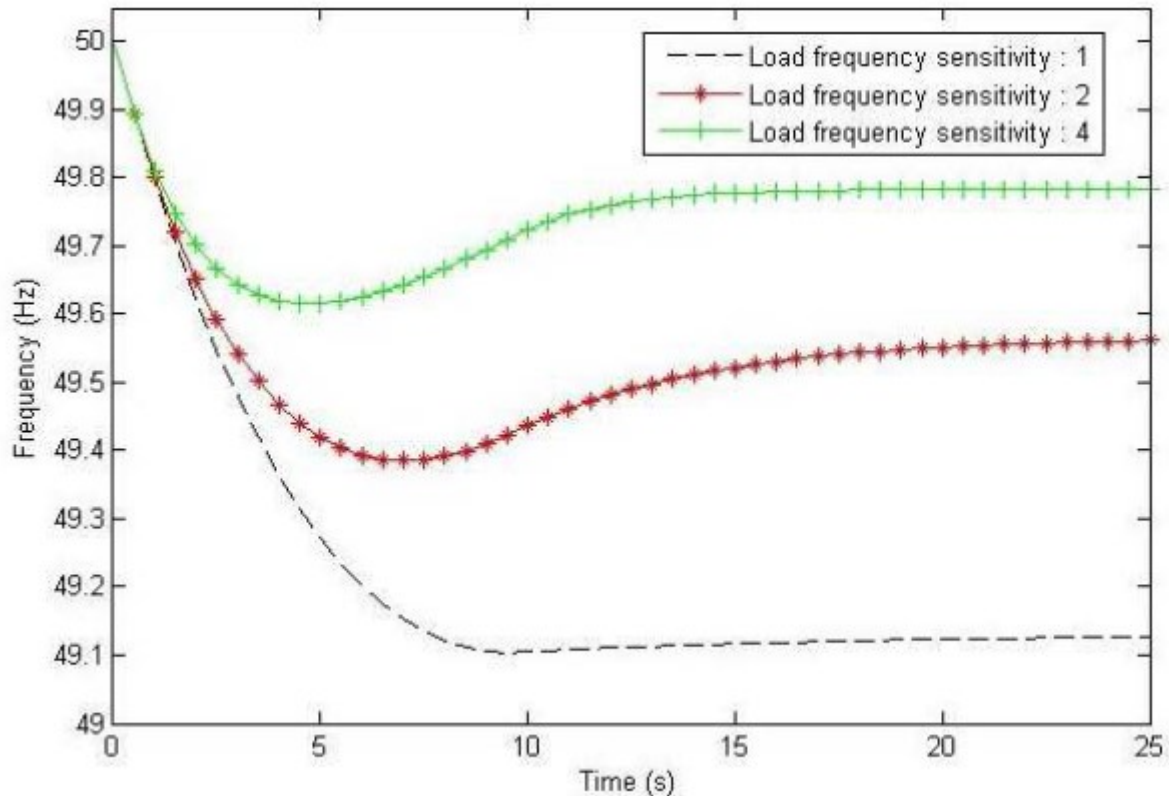


Figure 2.11 –frequency response for loss of 1320MW with varying  $k$ , with  $H = 5s$ , total load of 30GW, PFR of 800MW

It can be observed that this has a significant impact on both the nadir to which the frequency drops, and the final frequency at which the system settles after primary response has deployed. This should be unsurprising – inertia merely impacts the rate of change of frequency and the ability of the system to resist *sudden* changes – in the figure shown the initial rate of change of frequency is consistent across all 3 regimes, but the settling frequency recovers much better – or, rather, degrades less - for systems with greater load frequency sensitivity.

This is because some devices' power consumption drops with frequency – e.g. machines connected with AC motors such as fridge and freezer compressors. Constant-power devices, such as switch mode power supplies (SMPS) connected to phone chargers maintain their power consumption regardless of the system frequency, reducing the system load responsiveness to frequency deviations. A system with more responsive load, then, will have lower frequency response requirements – but these will change with time in the day, and across locations on the network.

The amount of frequency response available to restore supply-demand will in turn be impacted by the properties of the network on which a supply imbalance happens, and the location of the generation on the system. However, this is not represented in single bus or low-order representations of frequency response models such as those used in [60], [67], [68], or [71]. However, tying frequency response simulation to network simulation is a complex computational problem typically suited to specialised software, as previously discussed, and performing reliability or resilience studies considerate of these factors has simply not been done in significant detail, particularly in consideration of the impacts of wind generation or low system inertia.

### 2.5.5 Demand response

In [1] it is noted that the economy of the UK has significantly moved from manufacturing to a more heavily deindustrialised, service-based economy. This has meant a reduction in large loads associated with industrial machinery on the grid with the end result being the loss of significant amounts of spinning machinery, which can provide some inherent support to system stability through machines' inertia. This is of course also dependent on the industrial context of the machinery – paper mills, for instance, require extreme precision and consistency.

Instead of manufacturing being the driver of electricity demand in GB, then, it is cities. This presents its own challenges – cities have diverse demand centres, and different requirements from factories. If a factory loses power supply for an extended period of time, this causes economic damage for which the regulator may hold the relevant actors accountable. If a city loses supply, there can be widespread socioeconomic disruption, social unrest, and potentially fatalities. Business, residences, and industrial facilities all may be affected and restoration may be difficult and complicated if there is significant distributed DER on the system.

Distributed generation can be observed as a depression in system demand when observed from the operational point of view. This presents distinct problems for planners during loss-of-infeed events as disconnecting load will also result in disconnection of generation, and it can be difficult to estimate what the gross demand in a given section of network is.

One method of limiting the damage of major system disturbances is rota disconnections or load curtailment, whereby the system operator will disconnect load that cannot be met by available generation and will cycle through regions in turn disconnecting demand as necessary. During frequency deviations following large loss of infeed, however, automatic LFDD relays may activate to disconnect loads at distribution centres when given thresholds are exceeded to contain frequency within set bounds and prevent further system degradation. Such regimes are described in [72] and in the Grid Code itself [73].

Changing frequency responsiveness of the network, increased penetration of constant-power devices, and loss of inertia make LFDD schemes of critical importance in such times. Their primary aim is to curtail load to keep frequency above levels at which generators might start to disconnect due to underspeed protection – the principle being that it is better to endure a bit of pain to save the majority of the system than to try and save the whole network, fail, and suffer a total blackout. Such large scale deviations necessitating these interventions are generally associated with multiple concurrent losses of infeed and interconnectors in a short period of time, with LFDD acting as a “last resort” intervention on the system. The last time such a measure was deployed in the GB, at the time of writing, was August 2019, though the last time previous was as far back as 2008.

When LFDD relays are allocated and deployed on the network, they are done so on the expectation that each relay will disconnect a given percentage of total system load and so at each threshold there will be an expected level of demand reduction to return the system to a more stable state. If there is inadequate load shed at a given stage of tripping, the frequency may continue to degrade to a further stage, resulting in further shedding of load. In the worst case, incorrect setting of LFDD levels could see a “ping-pong” effect between UFLS and over-speed tripping of generators leading to a system blackout. Therefore, it is critical that the expected level of load shed planned for such events corresponds with what is actually likely to happen on the network during such an outage.

However, given the correlation between weather conditions and DG output, the percentage of load which could be tripped from a given network feeder will vary over the year. In networks with

significant DG penetration, distribution feeder flows can become bi-directional, for example in residential areas with significant solar PV during the summer. Tripping such feeders would not only not *decrease* system load, it could have the net effect of *decreasing* net system infeed by tripping off distributed generation in tandem with load, exacerbating the problem. Conversely, if there is simply less demand than expected at the connected load, this would lead to larger frequency deviations, and further frequency degradations and tripping events. The thresholds used in the GB LFDD scheme are shown in Figure 2.12, taken from [72].

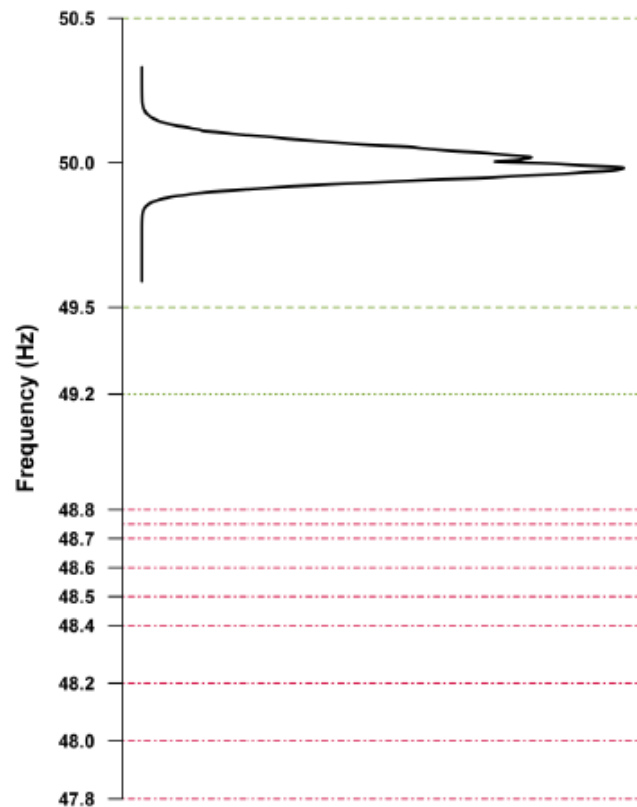


Figure 2.12 - LFDD disconnection thresholds on GB system and indicative percentage of time spent at frequency level in 2016-17

It can be observed that GB spends the majority of the time hovering around the 50Hz mark, as would be expected. Any failure to constrain frequency deviations at each threshold could lead to unnecessary, extraneous load disconnections or a cascading series of outages and events culminating in a black start event. Therefore, it is important that relays are set at appropriate locations, and expected return of load curtailment matches what is actually happening on the network.

Unfortunately, as highlighted in [72], these LFDD arrays are not 100% effective at arresting frequency deviations and the problem gets worse with increased penetration of DG and falling levels of system inertia. Higher levels of inertia are associated with more successful LFDD actions in the simulations undertaken in [72], shown in Figure 2.13.

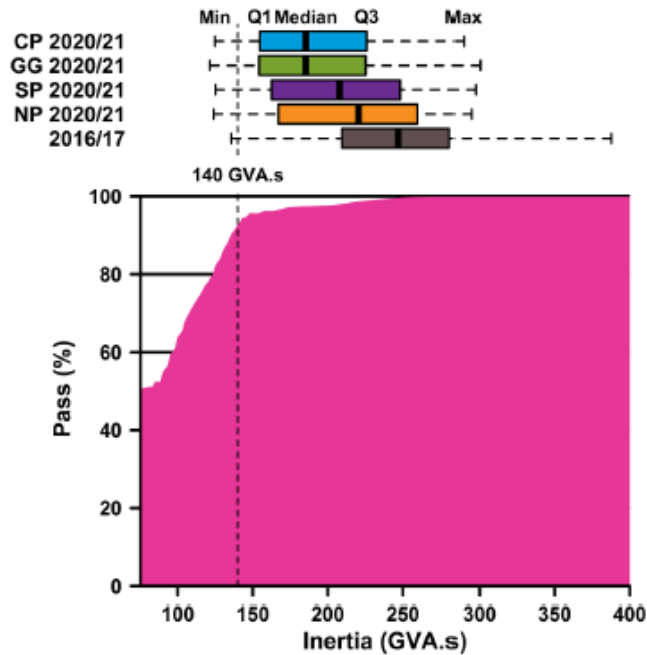


Figure 2.13 - Successful LFDD actions as %age w.r.t. system inertia

As t lower levels of system inertia, the RoCoF relays are triggered by the loss of infeed. This reiterates the importance of having either strong system inertia or frequency response capable of mitigating the impacts of large-scale infeed losses.

Work has been performed examining the potential of “wet devices” – washing machines, tumble dryers etc. – or thermostatic loads such as refrigeration for frequency response, with an example demonstrated in [74], and principles for estimating response from such response regimes investigated in [75]. A challenge with such methods is getting consumer buy-in and estimating the firm response capability of such techniques. As much of 4% of total active demand reduction via wet appliances is possible according to [74], assuming 29% of households take part. However, retrofitting devices to be able to take part in such demand aggregation services could be inherently costly with significant uncertainty as to the potential return for investors.

Similarly, those who can afford the luxury of being able to purchase new “smart” technology may simply not respond to changing price signals incentivising them to shift load overnight or to allow their devices to be used as flexible demand. Research needs to be done on understanding the necessary drivers to incentivise users to take up such devices to allow greater penetration of demand aggregation of such devices at a system level, as well as the contractual and economic frameworks to allow trading of such resources in a way which does not disproportionately increase system risk. Research has been performed on incorporating such demand response into the formulation of security constrained optimal power flows, however, as demonstrated in [76].

Interconnectedness and smartness of network-connected devices, and the proliferation of smart metering and control devices on networks, offer ample opportunity for improving resilience without the requirement of major investment in system assets, be that of the form of line reinforcement or investment in new generation facilities.

## 2.6 Conclusion

Clearly, modelling weather-related system perturbations is a complicated and challenging task which covers a wide range of factors – even without going into significant detail concerning repair times and how networks are represented in the modelling. Further, even with the substantial scale of the issues discussed here some have still had to be excluded and deemed out of scope, e.g. protection, resonance/harmonics, etc.

The factors chosen and discussed here represent the factors which were deemed to be most relevant for subsequent analysis and those which were likely to be the most significant in the context of resilience studies. For instance, the outages in Australia and England and Wales which were described were associated with random outages paired with frequency-related demand disconnections or trips at times of relatively high wind power infeed. This implies that areas of significance in resilience, in these cases, were; frequency response, impacts of wind on the power system, cascading outage simulation- the protection on the grid side actually generally acted as it should have.

Therefore, factors which in some way could be most easily related to the phenomena driving these outages were chosen and examined. Clearly more work could be done in areas such as thermal shock, flooding, and lightning, particularly in the context of climate change, but system boundaries have to be drawn somewhere. Hence, given the focus on power system reliability and resilience associated with extreme wind understanding what drives these wind outages and the impacts they have on the system itself should be prioritised.

As has been previously discussed, in the context of weather-related outages on the system an “event” can relate to any number of different things. The “event” could be the storm which drives the failures on the system, but equally the “event” could be everything that happens after a line or generator falls out of service. The “event” could simply be a line falling out of service. Therefore any analyst should be clear in defining what exactly the scope of the modelling being undertaken actually is.

In the rest of this thesis, the themes raised and discussed in this section will in turn be explored to understand the most significant features involved with modelling dependent, extreme-weather related faults and the challenges which arise from this; how we can model the relationships between extreme wind and system risk; how to quantify that risk; and potential means of mitigating that risk operationally.

## Chapter 3 A simulation framework to investigate the effect of extreme wind on a power system and sensitivity to weather-fault relationships

### Abstract

*In order to begin to investigate the relationships between extreme weather and corresponding impacts on power systems, a clear framework needs to be established to allow investigation of such events and the relationships between different data types and the corresponding outputs of simulation models. To that end, a framework for simulating weather-induced dependent faults across networks is proposed and demonstrated on a truncated GB network representative of the Scottish and Northern English network.*

*Different weather scenarios are simulated on the test network considering location and wind-speed intensity, analysed using Monte-Carlo simulation. The sensitivity of the network to co-occurrence of faults is adjusted by changing the sensitivity of network assets to wind speed via an exponential function. Greater sensitivity to wind speed induces a significant increase in outages, as reflected by risk metrics, specifically Expected Energy Not Served and Expected Maximum Load Shed. This model is intended to be tractable and portable to other natural hazards but the context considered herein is extreme wind. The abstractions and approximations used are demonstrably broad and simple, but are illustrative of the challenges associated with data collection and are intended as placeholders for more robust models and implementations.*

**Relevant Publication:** *M. Jamieson, G. Strbac, S. Tindemans, K. R. W. Bell, "A Simulation Framework to Analyse Dependent Weather-Induced Faults", in IET Conference on Resilience of Transmission and Distribution Networks, Birmingham, 2017*

### 3.1 Introduction

Combining weather, climatological, and power system simulations then presents a complex challenge for planners and those who wish to investigate these phenomena in any great level of detail. The interactions between these models will vary significantly, as will the sensitivity of the metrics used to quantify system risk to the input data. Historically in computer science the concept of *GIGO* or “garbage in garbage out” has been used to describe the relationship between input data with the results which come out of it. In other words, the results extracted from any data-driven simulation framework or model are generally only as reliable and robust as the data on which those models are based.

Conclusions drawn from inadequate data or models, if the data is of poor quality, have to be viewed and understood with an understanding of the flaws inherent in the source data and conclusions drawn with that in mind. As a first step in the research project, an attempt was made to clarify exactly what data is necessary, how that data interacts with each other data in a given simulation, and what kinds of results are useful to extract.

Typical outputs from reliability and risk assessments take the form of values such as EENS and expected costs associated thereof. This will inherently be sensitive to both the modelling of the probability of such events, and of the quantifying of the impacts and costs associated with those events which have been simulated. Therefore there is a relationship between the costs associated with mitigation of events and the probabilities of the events a planner wishes to defend the system against.

What an “event” constitutes also has to be clearly defined. An “event” could be a “ramping” event where the demand suddenly increases across the power system due to a concurrent, system-wide event. For example, half time during the world cup final with people all over the country putting on their kettles; or between 5 and 7 PM in countries like the UK, when 9-to-5 workers begin to return home and put on ovens and heating to prepare food and rest and lighting loads increase across domestic, commercial, and industrial properties. These events are largely predictable and can be scheduled for well ahead of time with knowledge of the sporting events’ schedules or other television schedules themselves, and can be assumed to act relatively homogeneously across the network dependent on viewing habits of the population (though, naturally, there will be regional variation – one may not expect as significant ramping in Scotland in a World Cup final in which England was playing compared to in England itself due to historic sporting rivalry).

Another type of event could be “ramping” of wind or solar power – that is, significant variation in the output of renewable energy sources due to variations in the weather systems driving them, as described in [6]. This has different degrees of predictability in tandem with modern meteorology’s capacity for short to long-term predictions of weather and climate phenomena. Moving cloud and high wind speed shutdown can cause significant fluctuations in the power output of renewable generation. Similarly, cold or warm fronts could cause regional variations in heating demand, particularly given the relationship in temperate countries such as the UK between heat demand and cold temperatures.

The events to be analysed in this section are more distinct, however. Specifically, wind-induced overhead line failures and random outages on generators concurrent with this shall be simulated for given incident weather events with a variety of synthesised relationships between wind speed and OHL failure rates to, first of all, set out a modelling framework to investigate the relationship between

incident extreme wind events and OHL failures, and the sensitivity of the simulation of such events to variation in the relationship between given weather conditions and the metrics used to quantify the impact of such events.

This section shall outline a generalised framework for the analysis of climate and weather related events on a power system, and use that framework to investigate an assortment of weather events on a power system with changing relationships between the incident natural hazard and the test system. This work was presented at the *IET International Conference on Resilience of Transmission and Distribution Networks 2017* and an associated conference paper can be found in [15].

### 3.2 Simulation Frameworks

There are multiple different approaches that can be used when simulating dependent, weather induced failures. The simulation of specific features such as OHL failures shall be discussed in more detail in Chapter 5, as well as a discussion on the strengths and weaknesses of these approaches, but this Chapter shall look at the features at a more high level.

An example of a simulation structure for examining fault events and cascading is shown in [77], and is shown in Figure 3.1. This approach is more commonly known as the “Manchester Model”, from 2002/03.

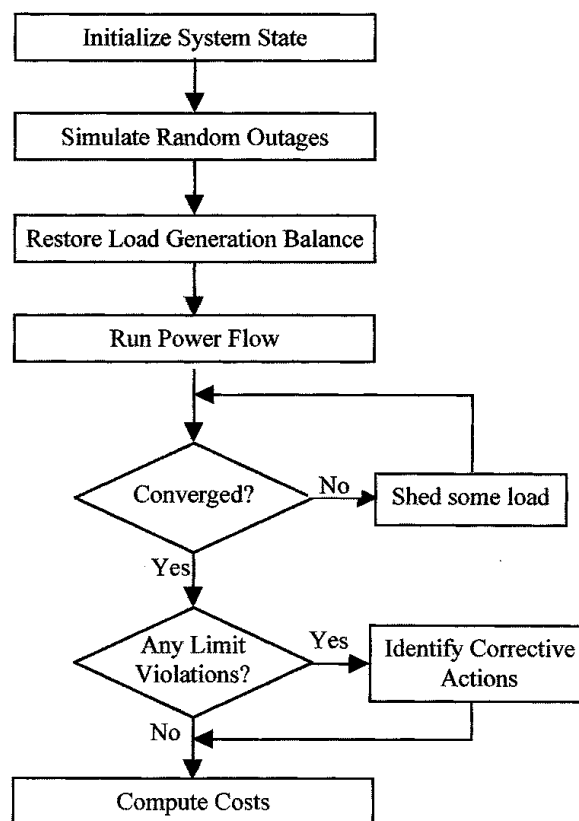


Figure 3.1 - Approach for modelling cascading large-scale outage events

A more recent example can be observed in [78], which takes consideration not just of corrective actions and load flow but of frequency response also. This is illustrated in Figure 3.2.

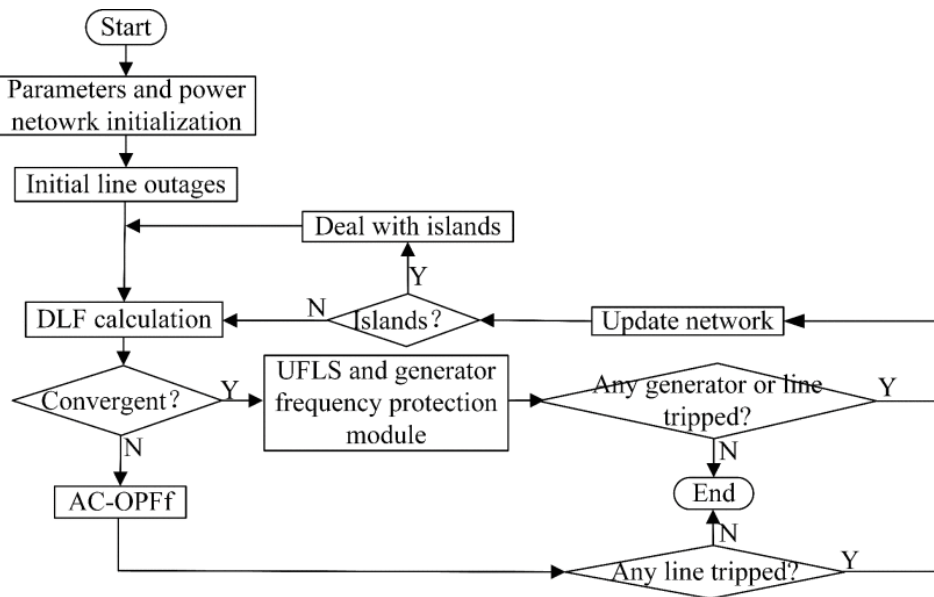


Figure 3.2 - Approach for simulating cascading outages considering frequency response

Between them, these approaches outline how one may simulate the degradation and cascading outage of a system given a set of line or generator outages, but they do not outline specifically how weather or climate may interact with these models, rather the simulation of these events once the outages have already taken place. This is discussed in [54] in the context of quantifying resilience with their approach illustrated in Figure 3.3.

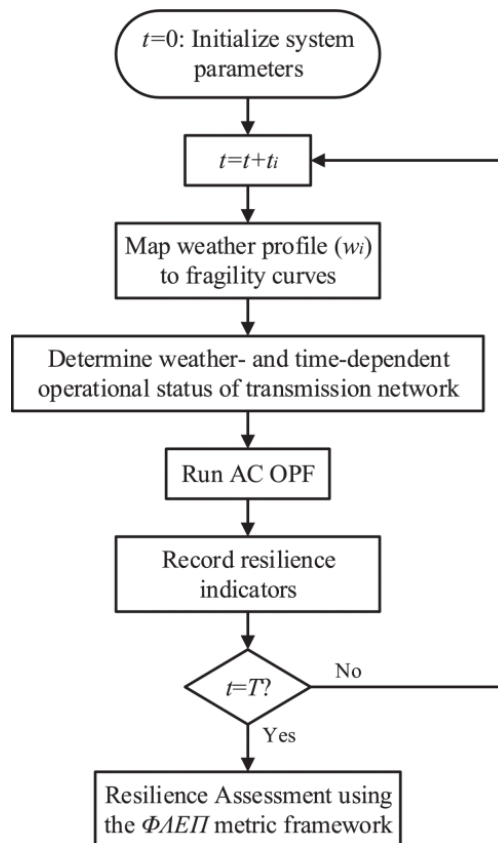


Figure 3.3 - Simulation framework for resilience analysis associated with natural hazard demonstrated by Panteli et al

It should be noted that the Greek characters refer to specific performance metrics for resilience used in the referenced paper (anglicised as “FLEP”). These, at a high level, refer to how long an event lasts, how quickly it degrades, how bad the event becomes, and how swiftly the system recovers from the initial event.

Unlike the other iterations, this does take consideration of weather-related factors in the simulation, but does *not* take consideration of frequency response or cascading events in the analysis. So while there are overlaps in these analyses, there are also gaps. The following simulation structure is proposed to cover these associated features, taken from the paper presented in [15].

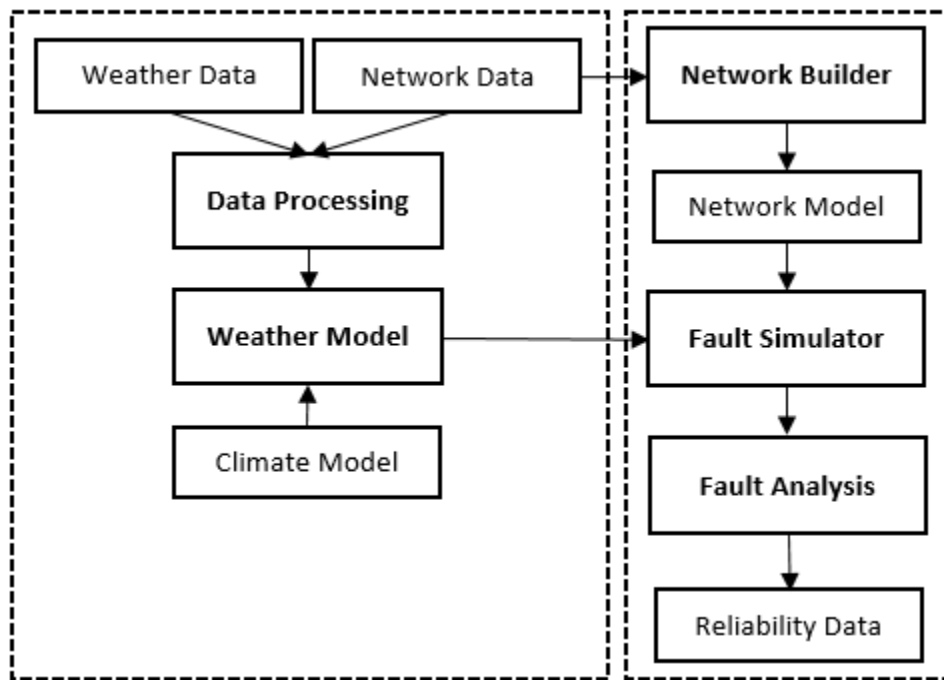


Figure 3.4 - Proposed simulation structure to be demonstrated

Unlike the other structures illustrated, this combines the possibility for climate-based analysis, simulation of common-mode perturbations (in however much detail the user desires as detailed in the *Fault Simulator*, and illustrates clearly the flow of data within such a simulation and a generalizable software approach for future analysis. The rest of this Chapter will outline specifically the significance of each block and how they fit into the structure, and the types of result which can be extracted.

The representation shown implies a single pass “scenario” simulation, but equally loops could be applied between the *Reliability Data* block and the *Fault Simulator* block for multiple runs or sensitivity tests where climate models are used to modify the incident weather data used for the scenario/fault simulation. The titles of the blocks represent high-level descriptors of the functions being undertaken. For example, *Fault Analysis* as a block is used to analyse and process the outputs of the scenario simulation such that results can be computed into a format useable and presentable e.g. visually.

The use of the *Climate Model* could arguably be applied to the weather data rather than the weather model directly. However, this depends on what the intended interpretation of the results are, and whether the focus is on sampling from weather data and adjusting it for changes in climate or whether modelling changes in climate and using that to determine what the weather state might be in the analysed scenario. That is, whether the sample is drawn from the weather data and modelled for climate or drawn from a climate projection and a weather state is implied. In this case, a weather scenario was generated but unmodified by any climate model, and so the *Climate Model* block is indicative.

The system boundaries can also be clearly identified via the hashed outlines. These separate what is acting as an exogenous force on the power system – the natural hazard, driven by external factors – and the power system itself. In this sense, the natural hazard can be understood as a threat acting upon vulnerabilities inherent in the system, such as is described in [79]. This is comparable to a *Swiss-Cheese* model of resilience, insofar as the natural hazard is acting on the power system via whatever aspects of that power system are vulnerable to it. In the analysis undertaken herein, this can be understood as extreme wind acting as a threat upon a vulnerability, specifically exposed overhead

lines. The blocks of the model shall be discussed in greater detail later in this section but a brief summary is provided here.

The framework is broadly separated into data sources or outputs and scripts/software processing. In order to begin to simulate the impacts of extreme weather and natural hazards on a power system, fundamentally, one requires an understanding of both the network on which the weather is acting and the weather model itself. Thereafter, assumptions can be made about the fundamental relationships between these two.

In this case, with some sourced *Network Data*, a module is necessary to convert this source data into a format which can be utilised by any subsequent analysis – the *Network Builder*. The *Weather Data* also needs to be in a format such that can be applied to the power system in any subsequent simulation and linked with the *Network Model* in such a way as there are clear fault-parameter relationships. For longer term simulations or modelling, a *Climate Model* could also be used to modify the *Weather Model* in some fashion to make future projections, as is done in e.g. [7].

The *Fault Simulator* in many ways reflects an aggregate of the models previously described but contained within one “package” and placed in the context of the wider analysis, and the nature of this simulator will vary based on the type of analysis being undertaken and the types of result one wishes to extract from the modelling being performed.

Finally, the *Fault Analysis* module collates results from different samples or scenarios generated or computed within the *Fault Simulator* and outputs them in a productive or informative manner dependent on the context. For reliability analyses this could be, for instance, a distribution of ENS values or specific EMLS/EENS values. The ENS represents the aggregated load curtailment in a given situation or single sample. Conversely, the expected maximum load shed represents the average largest value encountered of load curtailment recorded in each simulation, averaged across all simulations. The EENS is the average energy not served, averaged across all simulations. For resilience these metrics will require more refinement than typical, gross estimators of performance such as LOLP (loss of load probability) or EENS, but that will be discussed further in Chapter 5.

### 3.3 Implementation of simulation framework and description of components

The implementation of the model utilised here, and for all subsequent modelling performed in this research, was done so in the *python* programming language. This is due to the fact *python* is an open source, accessible language with a wealth of supporting online literature, a broad range of functionality and libraries, and many power-system specific libraries available for researchers. The specific tools used in the power system analysis shall be described in the *Fault Simulator* section. The framework and flowcharts described here should be interpreted as illustrative, rather than exhaustive, descriptions of the underlying processes.

As only a very basic implementation was developed at this stage, representing a simplified representation of many phenomena, the power flow calculations were performed by an open-source power-flow library developed for *python* called *pandapower* [80]. Further, as only a very basic representation of the spatial distribution of weather was used, historic data for a specific location (Glasgow) was chosen to synthesise hypothetical events, taken from NOAA [81]. This was initially half-hourly resolved but was reduced to hour-resolution to match with the failure rates and restoration rates used within the software.

#### 3.3.1 Network Builder module

This component of the framework pertains to taking network data from raw data files, such as .dat or .csv files, and processing it into a format which is usable in a *python* package. Within *pandapower* the

linearised DC approximation was used for the load flows, which requires information on the following features of a power system:

- Generators
  - Maximum, minimum real power (kW)
  - Bus connection
  - Fuel cost
- Loads
  - Real power demand (kW)
  - Bus connection
- Branches
  - Connectivity (to, from busses)
  - Reactance  $X$  (p.u.)
  - Capacity/rating (kW)
- External grid connections
  - Bus connection
- Buses
  - Reference bus
  - Location or weather “region”

This data was extracted from .csv files into the *python* software into a format useable by *pandapower*-the module effectively acting as a consolidator for disparate data sources into a more compact representation that can be utilised more specifically. This module could also be called for changes to network topology. The module is also used to reconnect disconnected islands following line restoration. The generalised construction of this module of the framework is as illustrated in Figure 3.5.

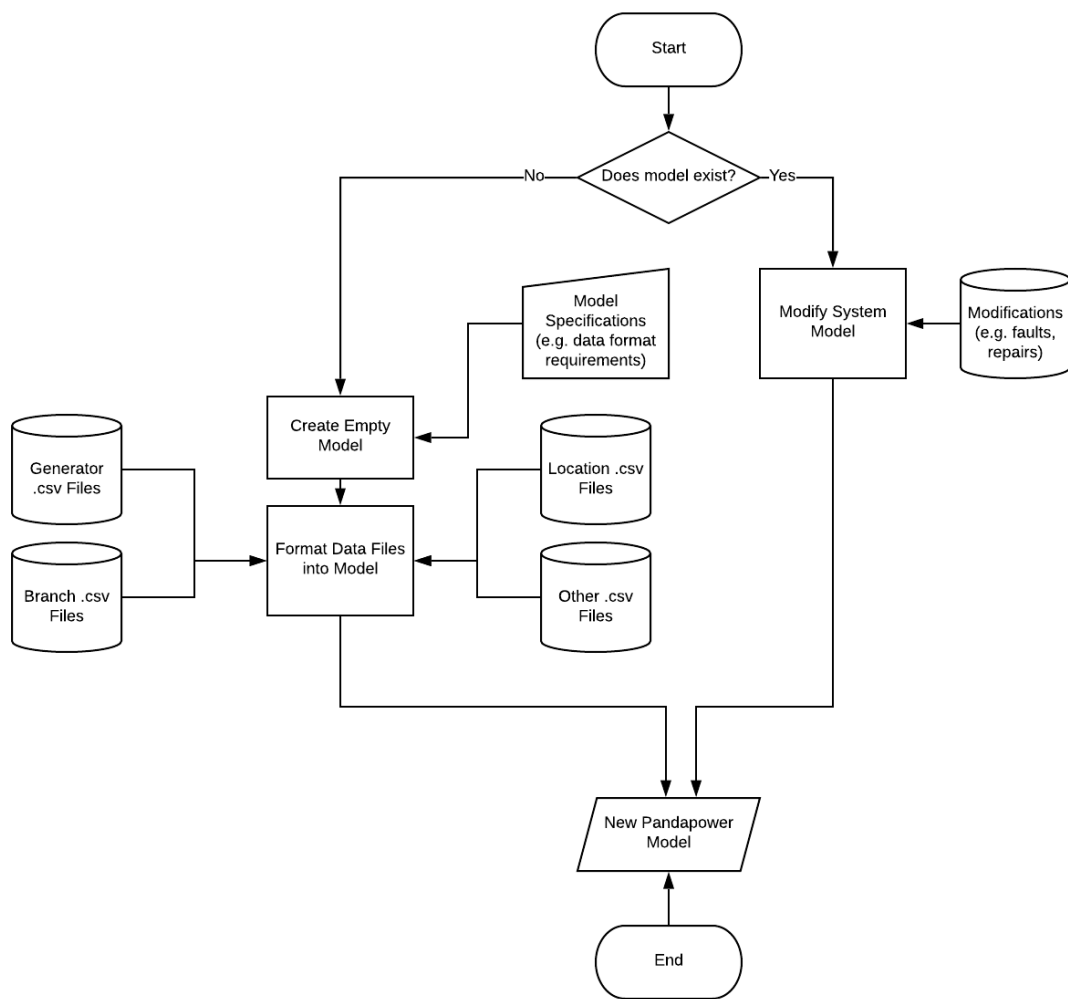


Figure 3.5- high level flow diagram of Network Builder

These features allow the calculation of the power flow via means of a linearized DCOPF, but the next step then – to perform reliability or resilience analyses – requires information on the failure mechanics of different assets on the system.

### 3.3.2 Data Processing module

This is a broader purpose module which, for instance, is used to modify or extract features from the source data – for example to sample the 30-minute resolved data into hourly blocks.

This can broadly be described in the general form as shown in Figure 3.6.

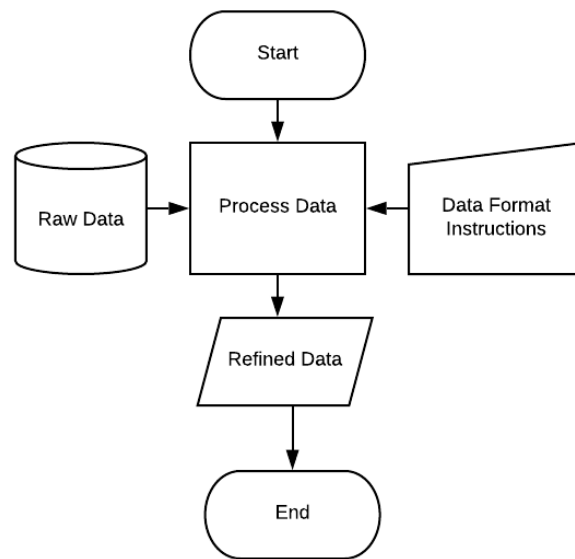


Figure 3.6- High-level representation of Data Processing algorithm

An example is shown for the processing of weather data into hourly format to demonstrate the general principle in Figure 3.7.

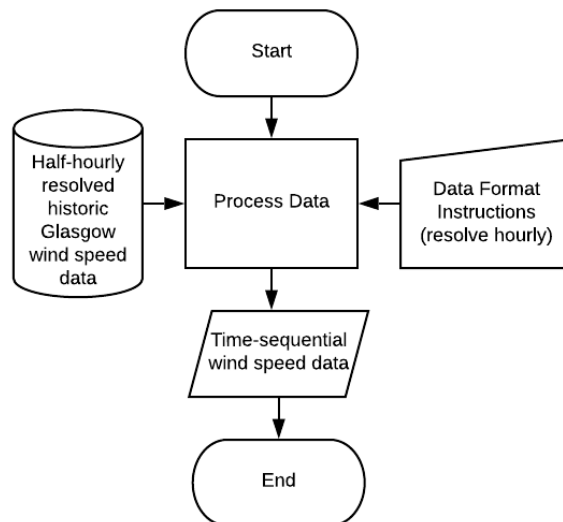


Figure 3.7 - example of deployment of Data Processing module

Different types of data will require different levels of processing and will interact with each other in a different way so this diagram is intended to be indicative of the general process at work.

### 3.3.3 Weather and Climate Models

Weather and climate, though related, are different concepts which should, in large scale simulations, be treated as separate concepts. That is, weather is an expression of underlying climatic drivers which change the distribution, frequency, and magnitude of weather events. In this case, only weather is being considered but it was deemed important to include reference to the higher-level climate models

which can affect the weather-systems which may impact a power system. These have already been discussed – the NAO, for example.

In order to perform subsequent analysis, these weather models then require a relationship with failure rates on the system so that dependent, weather-related faults can be simulated across the system. In a larger scale analysis, weather conditions at a given location can be sampled from a distribution of weather generated from historic data, which can then be shifted by a climate model. For this implementation, representative 24-hour weather “events” were synthesised as examples of typical, or indicative, events.

### 3.3.4 Fault Simulator

The *Fault Simulator* block combines weather and network models, with a given relationship between the two, to generate credible fault scenarios for subsequent simulations and to simulate the consequences of these outcomes. In this implementation the actual simulation of these perturbations is relatively basic- using a DCOPF and heuristics to calculate the load curtailment, and hence ENS, associated with a given fault state.

This requires a relationship between the weather and network models to generate credible failure scenarios with known probabilities. In this case, an exponential distribution of faults is assumed which can be represented by the standard formula;

$$p(\text{fault}) = 1 - e^{-\lambda_g \delta t} \quad (3.1)$$

where  $\delta t$  is the size of time-interval in which the fault probability is being computed (assumed to be 1 hour),  $\lambda_g$  is the failure (or, indeed, restoration rate) of a given asset, and  $p(\text{fault})$  is the probability of fault (or restoration). That is, in this case, the probability that a given asset fails or is restored within a sampled hour.

The following approach and heuristics are used to simulate fault scenarios in this model. Some factors involved working around the limitations of the software as it was implemented at the time, which, in future implementations, may not be necessary (and, indeed, in Chapter 5, are addressed wholesale).

- Import network state data and weather data
- Sample across assets to generate perturbation state
- Determine if discrete fault state has already occurred
  - If so, load results from memory
  - If not, continue
- Perform simulation (load flow) on network state
  - If converges, supply can meet demand
  - If not
    - “Generators” representative of load shedding are created on buses without generation with cost function representative of value of lost load (VoLL) to attempt load shedding until convergence
    - If this does not work, load is uniformly shed in 5% increments until system convergence or until no further load available to shed
- The results of the state are then recorded

This implementation was built around *pandapower*'s DCOPF functionality at the time of writing of the paper to demonstrate the principles of the approach, which treated loads as fixed and minimised generation dispatch cost. The total load curtailment used in each sample was then aggregated to get performance metrics for the simulation as a whole. The generalised approach is shown in Figure 3.8.

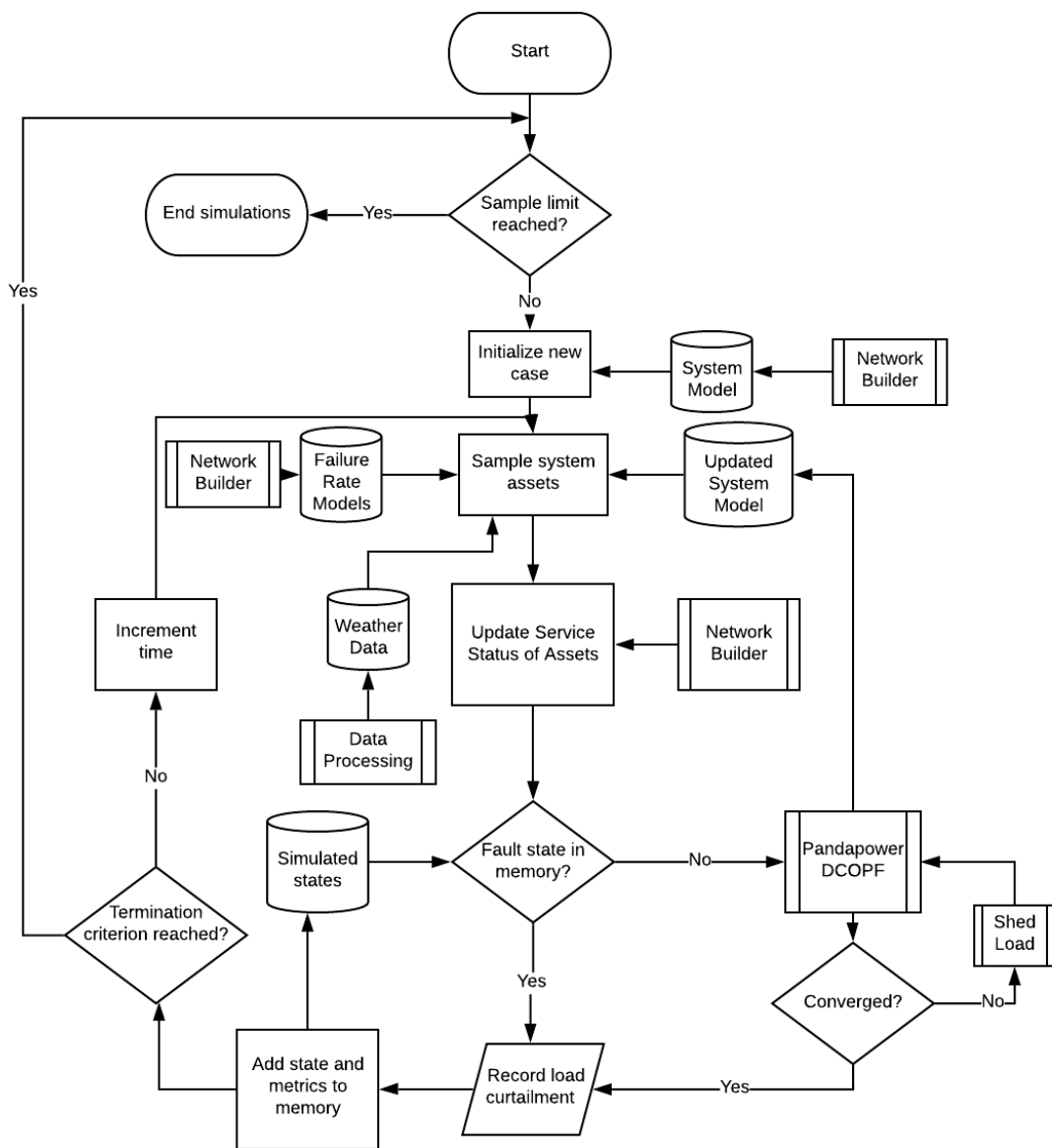


Figure 3.8- high level flow diagram of Fault Simulator module

### 3.3.5 Fault Analyser module

This module simply takes results from the samples simulated within the *Fault Simulator* and computes reliability and performance metrics accordingly. These results can then be used to compare the performance of different system topologies, or to compare the severity of different weather events assuming different incident natural hazards or relationships between failure rates and incident weather conditions. For instance, the relationship between a natural hazard and failure rates can be modified to determine the sensitivity of an output metric to that relationship.

## 3.4 Models and data used within model and implementation

The data sources and approaches used within the model and its implementation are detailed here. It is worth emphasising that the aim of this framework was to investigate the assumptions and challenges necessary in weather-related power system modelling, and the volume of data required

meant that assumptions and abstractions on all levels were necessary. The emphasis was on getting a functional framework in place which demonstrated the principles of the approach where each aspect could then subsequently be improved upon as the interactions between models and data could be more clearly understood in the context of a wider simulation framework. Nonetheless, the specific data sources, abstractions, and assumptions are outlined here with a discussion of the strengths and weaknesses which shall be further discussed in the *Discussion and Key Findings* section of this chapter.

#### 3.4.1 Cost function modelling of generators

Cost functions for generators were derived from the Reduced GB network model developed at the University of Strathclyde according to principles set out in [82] to the requirements set out by the software [80]. The analysis in this implementation is not intended to be a fully-fledged economic analysis, rather a comparative study for different sensitivities to network-hazard models, and so the priority was not on ideal representations of cost-functions on generators, rather having estimates which were at least broadly representative.

The OPFs in this stage of the implementation were only intended to determine whether a feasible solution for a given perturbation state could be determined to make an estimate of the total load curtailment. While non-optimal load flows could be used, using OPFs was deemed to be appropriate for future developments which may require more stringent, robust economic modelling. The emphasis was on developing a framework and structure which *worked* and could then be improved once the interactions and modelling were clearly identified and defined.

The *pandapower* casefile in the implementation of the simulation aggregates generators at nodes to single generators utilising the maximum cost function at the given node. Again, this was for simplicity and simulation efficiency and further detail on such simulations is developed and described in Chapter 5.

#### 3.4.2 Non-weather failure and repair modelling

Line and generator service status are modelled as two-state Markov models, parameterised by time-dependent fault and repair rates. Failure rates for OHL were derived from reliability system taken from the Transmission Availability Data System [51]. A failure rate  $\lambda_f$  of  $4.57 \times 10^{-6}$  /hr/km ( $\sim 1$  per 25 years) was used with a restoration rate  $\lambda_r$  of 0.03 (or a mean time to repair (MTTR) of 33hr) for OHL. The failure rate and restoration rates associated with generators were derived from the IEEE 1996 Reliability Test System (hence referred to as the 1996-RTS) [61]. These values equate to  $5 \times 10^{-4}$ /hr (or  $\sim 1$  per 12 weeks) with an associated repair rate of  $5.95 \times 10^{-3}$ /hr (or a MTTR of  $\sim 1$  week).

The “external grid” representations used represent the boundary connections to England and the rest of NGET and are assumed 100% reliable (though their connecting branches to the rest of the network are not). Loss of these is assumed to induce a blackout condition on the subset network modelled (the nature of this network will be explained in the relevant section). This also helps to represent how significant the North-South boundary is in such investigations, but also may represent an inherently conservative assumption given it may be possible, with adequate planning, to run Scotland as an independent island from the rest of the GB MITS.

#### 3.4.3 Weather-related fault, repair modelling

In order to simulate the effects of extreme wind on OHL, relationships between observed wind speed and failure risk are postulated. As demonstrated in [27] and [64] this can be achieved by using Bayesian methods and data clustering to form data-driven models of the relationship between a natural hazard and failure rates but is heavily dependent on data availability for the specific natural hazard being investigated.

Though extreme wind is not uncommon on GB, failures of double circuits or transmission assets, relatively speaking, are, particularly in terms of the timescales in which climatic reanalysis weather data is available (typically around 30 years). This means significant uncertainty in the long tail of the data which can make projections made based on this data problematic dependent on the context in which the analysis is being performed.

Collecting the data for analysis and Bayesian analysis presents its own challenges, and the quality and quantity of data collection varies significantly between network operators and owners [27]. Further, demarcating weather faults from non-weather faults can also be difficult, as well as classifying fault states where multiple fault-driving phenomena may be acting (e.g. wind and snow, snow and ice, etc.). This is a strength of fragility curves in that they can be formulated to clearly separate different fault drivers and impacts, e.g. to more clearly separate weather and non-weather faults.

Incorporating geographical data for buses and lines, weather conditions can be distinguished across sections of networks to be considerate of different weather systems (as opposed to homogenous “adverse” storm failure ratings applied across a system). These different methods shall be examined in detail in Chapter 4, but in general two standard approaches can be defined:

- Assigning buses to weather zones or regions with homogenous conditions, for example as is done in [83], and taking the more extreme weather parameter for lines which traverse different regions
- Assigning weather to individual nodes and taking weather conditions from the more extreme end on branch connections

Reliability parameters – failure, restorations, etc. – can be corrected for individual asset types or aggregated to be representative of entire asset classes. In this implementation, all lines were assumed to have the same per-km failure rates. Failure-weather relationships were postulated to give reasonable relationships with comparable values to similar research – for example in [84].

The fault rate is an exponential function of the incident wind speed with the relationship between wind speed and line failure rate postulated as

$$\lambda_{wf}(t) = l * e^{\alpha_f(w(t) - \bar{w})} * \lambda_f \quad (3.2)$$

where  $\lambda_{wf}$  is the weather-related failure rate,  $\lambda_f$  is the non-weather rate (or, equivalently, the failure rate at mean wind speed),  $l$  is line length,  $w(t)$  is the wind speed observed and  $\bar{w}$  is the mean wind speed over the entire yearly “Glasgow” dataset from [81];  $\alpha$  is a sensitivity parameter.. This allows the sensitivity of lines to wind-related faults to be adjusted and compared across different scenarios. The formulation used for asset restoration rates is

$$\lambda_{wr}(t) = \begin{cases} \lambda_r, & w(t) < \bar{w} \\ e^{\alpha_r(w(t) - \bar{w})} * \lambda_r, & w(t) \geq \bar{w} \end{cases} \quad (3.3)$$

whereby an assumption is made of a baseline level of performance upon which cannot be improved, but steadily degrading restoration rates for increasingly adverse weather conditions. The sensitivity parameters to be used in the simulation are as shown in Table 3.1.

Table 3.1 - Sensitivity parameters used in simulation

| Sensitivity              | $\alpha_r(\text{sm}^{-1})$ | $\alpha_f(\text{sm}^{-1})$ |
|--------------------------|----------------------------|----------------------------|
| Max ( $S_{Max}$ )        | -0.01                      | 0.159                      |
| Medium ( $S_{med}$ )     | -0.01                      | 0.123                      |
| Negligible ( $S_{neg}$ ) | 0                          | 0                          |

This allows different levels of sensitivity to wind to be tested in the simulation to get an indication of the significance of the hazard-failure-rate relationship. A positive  $\alpha_n$  value infers an increasing rate w.r.t the weather parameter, with a negative rate implying a falling rate. In practical terms, this means increasing failure rates w.r.t increasing sensitivity of weather, but falling restoration rates as repair efforts are hindered by inclement weather conditions.

The values were selected and validated such that the longest line under the highest observed wind speed  $w$  ( $56\text{ms}^{-1}$  in the selected data set) was associated with a failure probability of 0.99 in the sample hour for the Max case, 0.50 for the Medium case, and equivalent to the probability of random failures based on the TADS data for the Neg case. TADS data discriminates by cause but a generalised failure rate was presumed for portability and such that the comparisons were based on consistent assumptions. Gross values are given for e.g. mean time to repair (MTTRs) for different asset classes. An extract of the data used to derive these values is shown in Figure 3.9.

| Region | Element    | Voltage Class | Oh/UG       | Elemental Outage Frequency (13) |      |      | Elemental Outage Duration, Repair time, and Update Time (47) |             |             |
|--------|------------|---------------|-------------|---------------------------------|------|------|--|-------------|-------------|
|        |            |               |             | TOF                             | SOF  | MOF  | SODT   | MTTR P(5%)< | MTTR P(5%)> |
| NERC   | AC Circuit | 200-299 kV    | Overhead    | 0.61                            | 0.36 | 0.25 | 12.05  | 33.39       |             |
| NERC   | AC Circuit | 300-399 kV    | Overhead    | 0.99                            | 0.5  | 0.49 | 8.38   | 16.8        |             |
| NERC   | AC Circuit | 400-599 kV    | Overhead    | 1                               | 0.66 | 0.33 | 20.11  | 30.24       |             |
| NERC   | AC Circuit | 600-799 kV    | Overhead    | 0.75                            | 0.39 | 0.36 | 3.36   | 8.56        |             |
| NERC   | AC Circuit | 200-299 kV    | Underground | 0.2                             | 0.2  | 0    | 48.8   | 244.48      |             |
| NERC   | AC Circuit | 300-399 kV    | Underground | 0.47                            | 0.47 | 0    | 28.57  | 59.85       |             |
| NERC   | AC Circuit | 400-599 kV    | Underground |                                 |      |      |  |             |             |
| NERC   | AC Circuit | 600-799 kV    | Underground |                                 |      |      |  |             |             |
| NERC   | DC Circuit | 200-299 kV    | Overhead    | 10.75                           | 6.5  | 4.25 | 20.89  | 3.18        |             |

Figure 3.9 - TADS data extract showing representative data values

TADS also provides data regarding what is driving these events by cause. An illustrative example, extracted from the data, is shown below in Figure 3.10.

| Sustained Outages by Cause Code 2008 |            |               |   |             |             |                     |             |         |         |
|--------------------------------------|------------|---------------|---|-------------|-------------|---------------------|-------------|---------|---------|
| Gran_Value                           | Element    | Voltage Class | Outage Cause Code                       | # Initiated | Initiated % | # Sustained Outages | Sustained % | # Hours | Hours % |
| NERC                                 | AC Circuit | 200-299 kV    | Weather, excluding lightning            | 300         | 19.40       | 189                 | 12.2        | 10648.2 | 18.8    |
| NERC                                 | AC Circuit | 200-299 kV    | Lightning                               | 147         | 9.50        | 72                  | 4.6         | 145.8   | 0.3     |
| NERC                                 | AC Circuit | 200-299 kV    | Environmental                           | 0           | 0.00        | 0                   | 0           | 0       | 0       |
| NERC                                 | AC Circuit | 200-299 kV    | Contamination                           | 16          | 1.00        | 5                   | 0.3         | 51.5    | 0.1     |
| NERC                                 | AC Circuit | 200-299 kV    | Foreign Interference                    | 73          | 4.70        | 58                  | 3.7         | 391     | 0.7     |
| NERC                                 | AC Circuit | 200-299 kV    | Fire                                    | 79          | 5.10        | 69                  | 4.5         | 5977.9  | 10.6    |
| NERC                                 | AC Circuit | 200-299 kV    | Vandalism, Terrorism, or Malicious Acts | 6           | 0.40        | 3                   | 0.2         | 64.5    | 0.1     |
| NERC                                 | AC Circuit | 200-299 kV    | Failed AC Substation Equipment          | 150         | 9.70        | 126                 | 8.1         | 13135.8 | 23.2    |
| NERC                                 | AC Circuit | 200-299 kV    | Failed AC/DC Terminal Equipment         | 1           | 0.10        | 1                   | 0.1         | 72.1    | 0.1     |
| NERC                                 | AC Circuit | 200-299 kV    | Failed Protection System Equipment      | 97          | 6.30        | 89                  | 5.7         | 874.3   | 1.5     |
| NERC                                 | AC Circuit | 200-299 kV    | Failed AC Circuit Equipment             | 169         | 10.90       | 194                 | 12.5        | 11233   | 19.9    |
| NERC                                 | AC Circuit | 200-299 kV    | Failed DC Circuit Equipment             | 0           | 0.00        | 0                   | 0           | 0       | 0       |

Figure 3.10 - representative data illustrating causes of faults in TADS data

Wind itself is not identified as a key driver of the data in TADS which suggests it is not the prevailing driver behind the failure rate and so the value used for Neg can be assumed to be largely independent of the effects of wind relative to other factors identified in the modelling. Discussions with the, at the time, project's industrial partners and comparison with typical values found within the spreadsheet for transmission OHL were used to ensure the presumed values were appropriate for the application.

Restoration rate sensitivity was arbitrarily assigned to infer a lowering of restoration rates, with the assumption that in real world case-studies this could be more definitively adjusted based on data on restoration times.

As an illustration of the failure rates, the  $S_{Max}$  failure and restoration rate correction factors are shown in Figure 3.11, taken from the published paper associated with this Chapter [15].

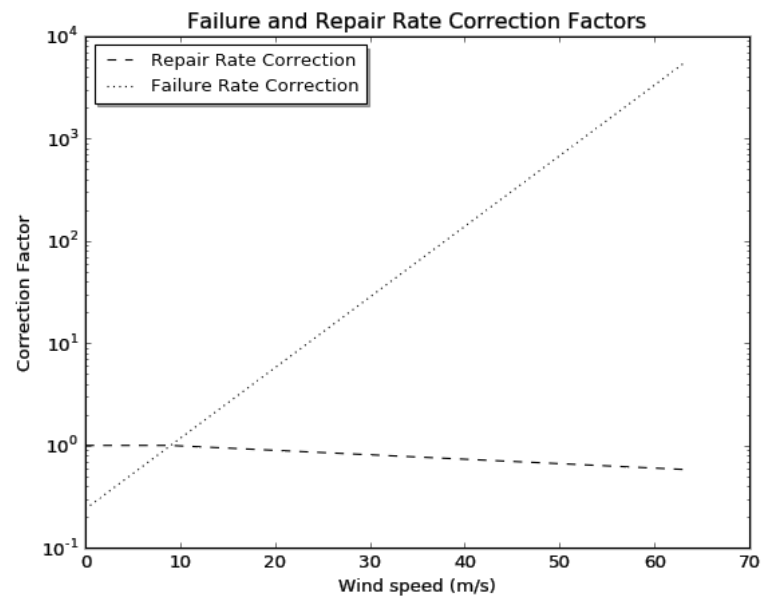


Figure 3.11 - Failure, restoration rates w.r.t wind speed for  $S_{Max}$  test case

The intersection of the lines occurs at the mean wind speed of the sample set,  $\sim 9\text{ms}^{-1}$ . With the given weather and failure/restoration models, and infrastructure in place to perform a study of a given test network, all that remains is to determine a test network on which the implementation can be tested and specific weather events which can be used to examine hypothesised weather events.

### 3.5 Case Study – truncated GB Network representation

Filling in each of the “blocks” alluded to in Section 3.2 leads to the final parts required to perform the study – a network model and weather data which can be assigned to this weather model. Owing to the rudimentary implementations of the simulator used thus far, only a basic abstraction of the GB network was used for a case study to demonstrate the fundamental principles of the simulation approach that would be tractable enough to be useful in a security assessment. To that end, an implementation of the Reduced GB network model developed at Strathclyde University was used [82], and adapted to be suitable for *pandapower* implementation. This represents a very basic proxy of the Scottish and Northern English networks with the B6 boundary approximated by two “external grid”, distributed slack buses at the southernmost points represented at buses 9 and 10 in Figure 3.12 again taken from [15], with a representation of the Reduced GB model developed using techniques from Chapter 4 show adjacent to show the approximate geographic locations of the buses. The line illustrates the cut-off point from GB.

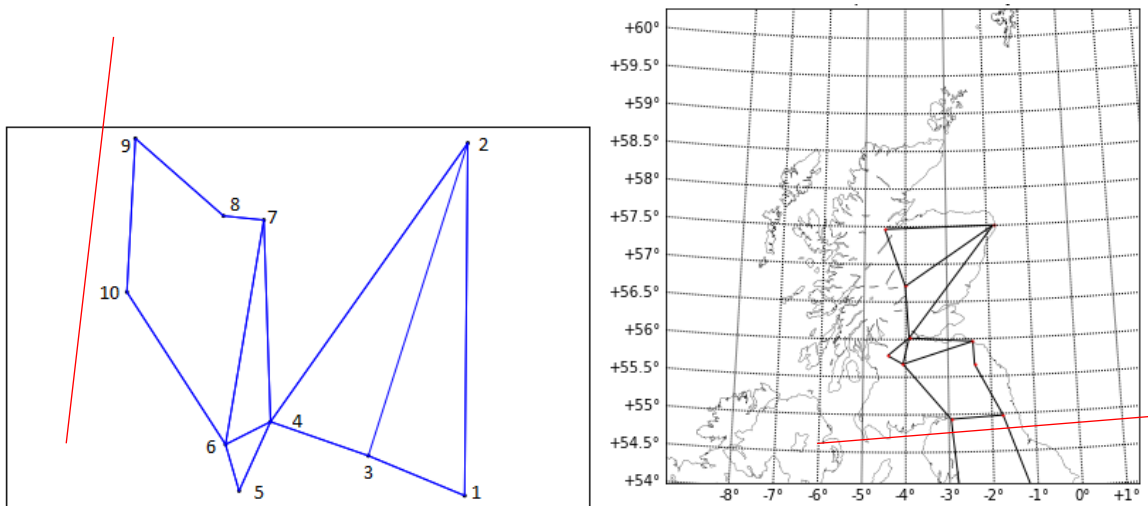


Figure 3.12 - Illustrative network topology with relative positions of nodes

Line lengths were estimated using the 2011 National Grid Seven Year Statement (SYS) by determining line routes and summing up the associated line lengths manually. These values were then used to determine the associated failure rates for different points in time on different lines. The loads were assumed to be constant in time based on the Reduced GB model with a total nominal system load of 8,075.5MW.

Using this network model, different scenarios could be proposed and simulated in the framework, created from historic data and adapted to a format that could be utilised in the simulation model. The wind speed profiles were selected from historic wind speed data and are intended as feasible timelines of weather conditions as opposed to being representative of reanalysis data such as MERRA-2, which is used in Chapter 4. The wind profiles used in the study are shown in, from [15].

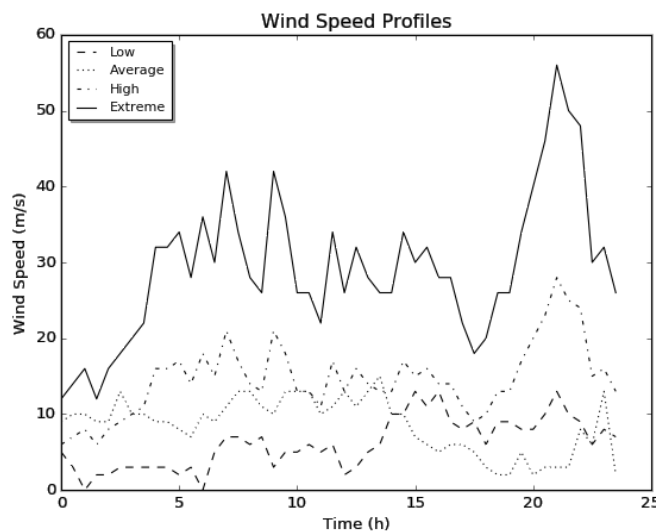


Figure 3.13 - Wind speed profiles used in study

The source data is resolved in 30-min windows and resolved into 1-hour blocks. These were chosen to be representative of different hypothetical scenarios – a “low” wind profile with mean wind speed of  $6\text{ms}^{-1}$ , an “average” representative wind day with mean wind speed of  $9\text{ms}^{-1}$ , a “high” wind speed day with mean of  $15\text{ms}^{-1}$ , and a wind storm created from this by doubling the wind speed values to make

a hypothetical “extreme” wind speed event with mean of  $30\text{ms}^{-1}$  and maximum of  $56\text{ms}^{-1}$ . The portability of this approach means any historic wind data could be used, but these were chosen to slot in to demonstrate the approach’s functionality.

Various different weather storm scenarios were then applied to the test network using these hypothetical wind profiles. These were as follows:

- “Extreme” applied at buses 1, 2, and 3 with “Average” applied everywhere else – **North**
- “Extreme” weather at buses 5 through 10 with “Average” applied everywhere else – **South**
- “Low”, “Average”, “High”, and “Extreme” days applied homogenously across the system

In this sense again it makes sense to clarify the distinction between incident events and subsequent “events”. That is, a storm in itself can be considered a causal “event” which causes a system state with various outages. A perturbed system state can in itself be considered a separate “event” which can have any number of causes. I.e. If  $n$  lines are lost on a system, the causal event can largely be considered separate from the simulation of the outages themselves – the line losses could have been caused by wind, snow, or wildfires – but in this framework effectively the *Fault Simulator* just considers this as an independent perturbed state, agnostic of whatever may have caused it. This is why it is important to clearly define the relationships used within the simulation model in order to make it portable and tractable to consider different simulation types, and different natural hazards.

The simulation scenarios were played out as follows:

- System state initialized assuming all assets in service
- The selected initial 24-hour weather event was applied to the system with lines sampled with calculated failure, restoration rates
- **Low** wind profile then applied to system and system continually sampled until all PNS in final sample = 0. That is, the load curtailment is zero because lines and/or generators on the system have been repaired.

Two metrics are calculated and reported by the simulator – the expected energy not supplied (i.e. the EENS), and a metric called Expected Maximum Load Shed (EMLS). This simulation was performed for 100,000 samples or until the standard error of the EENS observed was  $\leq 5\%$  of the expectation after  $< 100$  samples taken. If error  $>5\%$  in an output value, it can be assumed that this result’s simulation was terminated at 100,000 samples.

The final results of the tested scenarios are tabulated in Table 3.2

Table 3.2 - Output results of case studies

| <b>Case</b>  | <b>EENS (MWh, S<sub>Max</sub>)</b> | <b>EENS (MWh, S<sub>med</sub>)</b> |
|--------------|------------------------------------|------------------------------------|
| <i>North</i> | 275±16                             | 91±12                              |
| <i>South</i> | 3088±154                           | 85±10                              |
| <i>Low</i>   | No events                          | 3±3                                |
| <i>Ave</i>   | 3±3                                | No events                          |
| <i>High</i>  | 6±5                                | No events                          |
| <i>Ext</i>   | 7316±366                           | 217±13                             |
| <b>Case</b>  | <b>EMLS(MW, S<sub>Max</sub>)</b>   | <b>EMLS(MW, S<sub>med</sub>)</b>   |
| <i>North</i> | 62±2                               | 12±1                               |
| <i>South</i> | 72±7                               | 17±1                               |
| <i>Low</i>   | No events                          | 0.1±0.1                            |
| <i>Ave</i>   | 0.1±0.1                            | No events                          |
| <i>High</i>  | 0.2±0.1                            | No events                          |
| <i>Ext</i>   | 62±10                              | 51±2                               |

The resultant metrics can then be observed to be significantly responsive to adjustments in the sensitivity of OHL to wind faults. The increasing sensitivity to faults in this model increases both the probability of adverse states occurring and individual faults, and the probability of multiple faults happening simultaneously. This increases both the EENS and EMLS – that is, the expected “badness” of a fault event, and the expected total energy not served across an event. Further graphical illustration is provided of the EENS and EMLS results in Figure 3.14 and Figure 3.15.

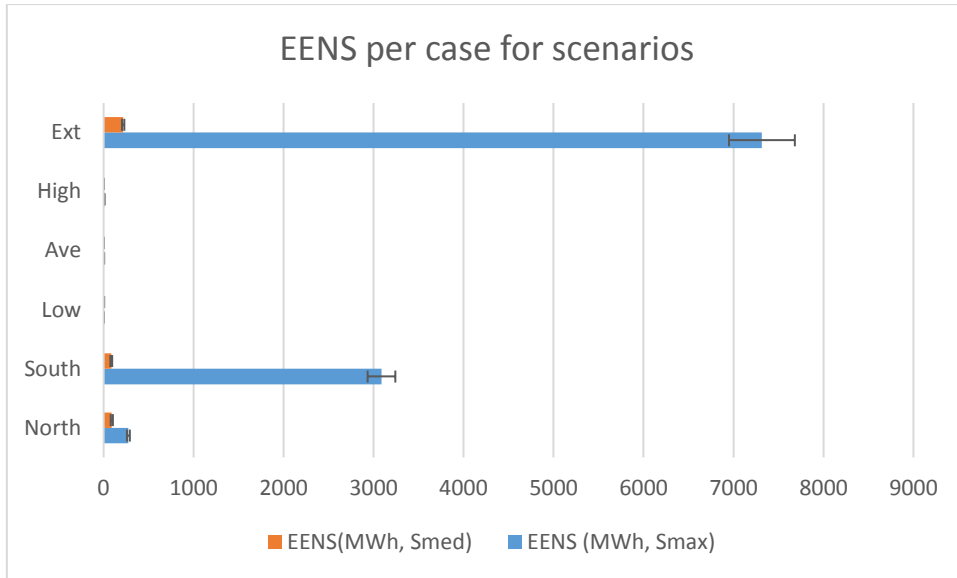


Figure 3.14 - Comparison between Smed, Smax results for EENS

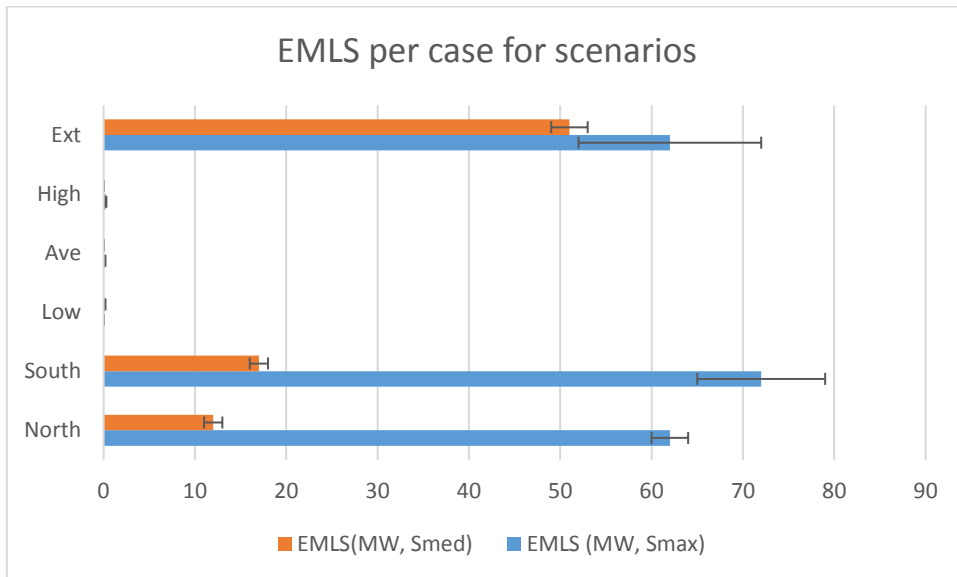


Figure 3.15 - Comparison between Smed, Smax results for EMLS

The locational impact of the weather in this case is particularly significant due to the heuristics used to represent the B6 boundary. That is, the most significant loss events are associated with the loss of branches connecting nodes 9 and 10. When the network is less sensitive to the impacts of weather, or the storm event is away from the South of the network, the resultant risk metrics are accordingly much lower. Lower sensitivity or extremity of weather conditions on buses 9 and 10 are associated with loss of the boundary connections and total loss of infeed from these connections. Though there is increased redundancy in the South, there is also more heavy reliance on the infeed from buses 9 and 10 and greater consequences for the loss of these connections than those in the North, which has longer lines but less severe consequences for system damage. The EMLS for South Max and Ext Max cases are within standard error of each other emphasising the significance of the southern sector of the network on the overall reliability metrics used in this implementation.

Ext cases are significantly greater than the North and South cases because there is a compounding of both the loss of connectivity to the external grids and the loss of load across all sections of the system

homogenously, severely impacting the ability to restore load across the system meaning the severity of events is that much worse.

For the events at lower sensitivities and lower extremity of weather events the results are very sensitive to the lower probabilities of events occurring. That is, no events are recorded for the Ave Med cases or High Med cases, even though the EMLS and EENS for the Low Med cases is nonzero. This will be due to a very small number of loss events occurring at the long tail of the distribution, which is not unsurprising for analysis of HILP events.

There were no loss-creating events recorded for the Neg sensitivity cases, and hence those results are omitted from the results for clarity.

To illustrate the type of results which can be extracted from this methodology, a complementary cumulative probability distribution function of ENS for the Ext case (i.e. the extreme weather event applied homogenously across the system) is shown in Figure 3.16.

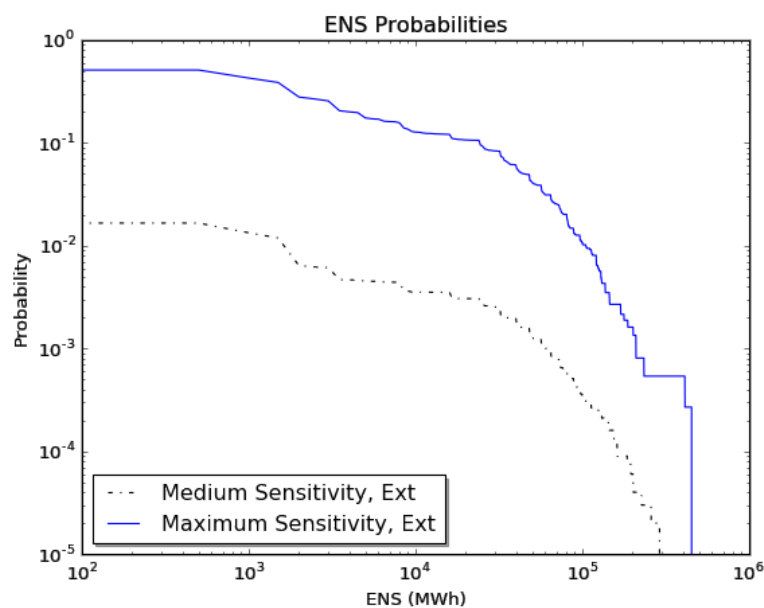


Figure 3.16 - Empirical probability that ENS exceeds given thresholds for Ext cases

As can be determined by inspection, increasing the sensitivity to faults within the model increases both the probabilities of faults, and the extremeness of the potential outage events associated with the increase in coincident, common-mode outages. This specific chart was chosen to illustrate the most significant case differences and the importance of the region particularly above 10<sup>5</sup> MWh, where, for the S<sub>max</sub> Ext case the outcome is heavily affected by a small number of extreme events (as can be determined from the “jagged” nature of the graph at extreme values where very few data points exist).

### 3.6 Discussion and key findings

By recording the EENS associated with different assets it could also be possible for planners and investors to rank the significance of different assets in security assessments to aid in resilience planning to lines associated with high risk. High risk in this context, of course, could mean either a high probability of failure, or significant consequences of outages associated with that outage. In this case the significance of the branches connecting buses 9 and 10 is clear, which suggests either the need for reinforcement of the network surrounding these nodes or that the modelling assumptions used are too conservative.

Alternatively, different heuristics and less conservative modelling could be used to investigate the significance of the data and heuristics used – it may well be possible for the truncated network as represented to operate in islanded conditions, and the heuristics used may be too conservative and weigh the effects of these outages too heavily. But what can be clearly demonstrated is that the relationships used between a natural hazard and the outcomes of simulations associated with those relationships have the potential to have major impacts on the results of simulations and analyses of the impacts of extreme weather events.

Of course the underlying models rely on significant abstractions and broad approximations. These, however, can all be replaced with more granular or appropriate models – the focus was on establishing a clear simulation framework in which the data models could be inserted or replaced, and factors which were not considered or missed in this analysis could subsequently be added to improve the realism of the model.

What can be understood however is that the heuristics and assumptions made about the relationship between natural hazards and failure rates on a system and how those outage events are simulated clearly have a significant impact on the output metrics which can be extracted from the results. In this case faults in the Southern regions of the network drive the reliability metrics in the analysis because their high risk – in the Ext cases they have both high probability and high impact. The faults associated with buses 9 and 10 are particularly significant and highlight the importance of the heuristics used within the simulation itself, because it is assumed that loss of buses 9 and 10 automatically leads to a blackout conditions. However, the impact may be exaggerated by the simplistic representation of the consequences of outages on the system.

Wind power's impact on the system was also not directly considered, and the synthetic weather events generated may not be representative of realistic events in the world. Wind direction, too, was not considered in the analysis, nor was frequency or voltage collapse. The use of DCOPFs in such analysis is computationally convenient but, in reality, cannot fully capture the impacts of such events. The representation of OHL risk, too, was relatively simplistic, considering only point-to-point representations of OHL which cannot capture the spatial variation in risk across OHL on transmission networks.

### 3.7 Conclusion

This chapter demonstrated the development and implementation of a framework that could be used to conceptualise and operationalise analysis of extreme weather's impacts on the power system and could be used in a tractable and portable manner to investigate climate and weather's impact on power systems more broadly, with examples of metrics for analysing the performance of a given power system.

Increasing the sensitivity of OHL to wind-driven faults clearly increases both the probability and impact of wind-related faults on the power system drives an increase in the probability of N-k events. This, accordingly, represents an increase in overall risk. For the same incident weather events, changing the sensitivity of the model to faults from wind can have an impact in the scale of orders of magnitude on the output metrics, meaning having accurate models of both the simulation of the outage events and restoration, and robust understanding of the probability of the events which drive outages, are of major importance.

The strength of the proposed framework is that it clearly identifies the interactions between different models and illustrates, when assembling the simulation model, where improvements can be made. In

this case, at each stage there are clear improvements which can be made and which shall accordingly be addressed in the rest of the presented research in Chapters 4 and 5.

Having a clearly defined framework allows the input data and models to be varied – as illustrated here – to demonstrate sensitivities, but also to allow investigation of what improvements can be made in processes to improve the performance metrics being analysed. Having a clear framework also allows the types of events to be changed to investigate different natural hazards or different events to compare the severity of different threats to power systems.

Climate change presents as changing both the frequency and intensity of threats such as extreme storms and temperatures, and so having frameworks which can be used in a versatile manner to quantify the risk of these events is vital to ensure prevention, corrective, or mitigation investments are appropriately directed. Of course, in the context of reliability and resilience these investments will vary and the weighting of probability and impact may vary across them when directing resources.

So long as there is a robust evidence base to justify why decisions are made, stakeholders can be confident in the decisions they make – especially if things go wrong or prevention plans fail. Investment decisions can then be justified based on the evidence and models that were available *at the time*, and the clearer the modelling is to stakeholders, the easier it is to make such justifications and defence of investment decisions made.

Developing models which can clearly demonstrate the significance of such relationships and allow portability is clearly important, then, to tackle challenges associated with both quantifying and mitigating the challenges associated with resilience and reliability, which this Chapter has set out to do and demonstrated an example of an approach which could be taken to do so.

The next step, then, is to improve on the areas of the implementation which were lacking. As has been mentioned, risk concerns both the *impact* and *probability* of an event. Therefore, in this case, in understanding the threats posed by extreme wind to the power system we need to assess whether current methods of modelling OHL risk are adequate, and whether the simulation of the consequences of those outages, when they occur, is adequate. The next focus then is on improving the representation of OHL risk on the power system in a way which can be meaningful and productive for planners, and also useful for more wide-scale simulations to quantify and analyse risk.

Chapter 4, therefore, seeks to focus on the quantification of OHL risk and improve the representation of weather-related failure rates on power systems using more data-driven methodologies, and demonstrate those methods on more realistic representations of the GB network or sections thereof. This directly addresses one of the weaknesses in this implementation – the rudimentary representation of GB itself. Once a more appropriate representation of OHL risk can be demonstrated, this can then be combined with an improved simulation model for more robust resilience analysis and the lines between reliability and resilience can begin to be more clearly understood. Chapter 5 will concern itself with the power-system simulation associated with this improved representation of OHL risk. Another weakness in the implementation thus far was in the representation of wind power – insofar as it was not represented at all. This is directly addressed in Chapter 4 also, such that the effects of extreme wind on wind power can also be incorporated into resilience analysis at least at a rudimentary level.

## Chapter 4 Quantification and visualisation of impact of wind data accuracy on failure rates on overhead lines and wind power output

### Abstract

*In this chapter, an approach is demonstrated to visualise overhead line failure rates and estimated wind power output during extreme wind events on transmission networks. This is to improve the representation of overhead line fault risk and weather data use on transmission systems based on the weaknesses identified in the methodology deployed in Chapter 3. Reanalysis data is combined with network data and line failure models to illustrate spatially resolved line failure probability with data corrected for asset altitude and exposure. Wind output is estimated using a corrected power curve to account for high speed shutdown with wind speed corrected for altitude. Case studies demonstrate these methods' application on representations of real networks of different scales. The proposed methods allow users to determine at-risk regions of overhead line networks and to estimate the impact on wind power output. Such techniques could equally be applied to forecasted weather conditions to aid in resilience planning. The demonstrated approaches are shown to be particularly sensitive to the weather data used, especially when modelling risk on overhead lines, but are still shown to be useful as an indicative representation of system risk. The techniques also provide a more robust method of representing weather-related failure rates on lines considerate of the altitude, voltage level, and their varying exposure to weather conditions than current techniques typically provide, which can be used to usefully represent failure probability of lines during storms.*

**Relevant Publication:** M. Jamieson, G. Strbac, K. R. W. Bell, **Quantification and Visualisation of Extreme Wind Effects on Transmission Network Outage Probability and Wind Generation Output**, IET Smart Grid Special Issue on Definition, Quantification, Analysis and Enhancement of Grid Resilience (Publication due December 2019)

## 4.1 Introduction

As discussed in Section 2.3, and in Chapter 3, understanding both how likely a fault is, and where it is likely to happen, may have significant impacts on the results of power system security assessments involving the investigation of extreme weather events. That is, resilience and reliability both, as concepts, are reliant upon the robustness of the quantification of both *impact* and *probability*. Further, our ability to plan for and mitigate high impact events is reliant on knowing both *where* and *how likely* faults are to occur.

Presently, methods used to quantify failure probability on lines does not directly consider both facets – rather, fragility curves convert an input parameter representative of a natural hazard into a corresponding failure rate or probability. The focus of this thesis is on extreme wind in particular, and so the drive herein is to understand the potential impact of wind in a power system. The two primary ways in which wind interacts with a power system in this work can then be understood in terms of OHL faults, and the corresponding impact on wind power resources.

No direct correlation was found between wind and demand, for instance, on the power system in [6], rather temperature was found to be the primary driver. The volume of work examining the effect of extreme wind on the power system, both on generation and security, also emphasised that these separate aspects necessitate linking for more refined analysis and simulation of wind-related threats to the system.

Wind failure rates will vary not just between network branches on a system but also across individual lines themselves, particularly if they traverse geographically diverse regions with varied natural hazards. Coastal regions, for instance, will be more vulnerable to coastal flooding and flashovers associated with sediment thrown from seawater onto OHL insulators. Low-lying distribution assets will be more vulnerable to inland flooding and flash-floods, whereas in exposed, mountainous regions with little vegetation OHL may be more vulnerable to lightning and higher wind speeds as e.g. there is less material on the ground to affect wind speeds.

This section details an improved approach to quantifying and visualising OHL risk which is spatio-temporally disaggregated in such a manner as to consider variability across networks and branches. This in turn could allow planners to target specific regions with restoration assets during force majeure weather events to mitigate the worst impacts of extreme weather on the system.

## 4.2 Modelling relationships between weather and line outages

The concept of fragility curves has been discussed in section 2.4.1, along with discussion of more homogenous representations of line failure rates on power systems. The fragility curves used in this Chapter are derived from those calculated in [64]. The utility of these fragility curves derives from the fact they are disaggregated to be in terms of /100km/hr, meaning an appropriately disaggregated line could have its failure rate locally corrected for the local exposure to any given overhead line section, and its failure rate corrected for the size of time-step used. In [64], ERA-Interim weather data was used, with the maximum wind speed experienced by an OHL in a three-hour window through the area which the line traverses used to determine the wind gust which is associated with the recorded wind fault. Therefore, any wind data used to make projections based on the deployed fragility curves must be used with this in mind: different wind speed data reflects different aspects of what wind actually is.

Using maximum gust speed over such an extended period of time may overestimate the wind speed which actually caused the fault – the assumption being the fault would be caused by the highest single

observed wind gust in that window. However, it is noted in [10] that both sustained high wind speeds – that is, high wind speeds averaged over a period of time – can cause significant damage to networks just as readily as short, intense wind gusts can, particularly if those storm systems happen to sit on a given part of the network for an extended period of time such as in hurricane storm systems.

Therefore, using time-averaged wind speed data with a fragility curve derived from maximum wind gust data may be a conservative estimation of the actual wind speeds experienced on the system or associated failure rates, whereas using more extreme maximum gust speeds in a given simulation may overestimate the intensity of a given wind storm to which a power system is subject. Given the pre-existing uncertainty associated with using fragility curves, this infers a need to compare the results for different datasets or a prescription of how results from such fragility curves should be interpreted – as a relative, rather than absolute, indicator of system security, which could be used to aid prioritisation of system assets during storms for system restoration.

The fragility curves in both [27] and [64] are derived from data-driven analysis of faults recorded on the SHETL network in Northern Scotland. In the former, a cumulative probability distribution was determined linking failure probability on a given OHL with an incident wind speed. In the latter, this analysis is extended to break the fragility curves down by voltage level (132kV and 275kV) for improved granularity of results. At improved levels of data granularity, especially for moderate-sized grids, data availability becomes an acute challenge. The fragility curves themselves are also agnostic of wind speed direction. The fragility curves to be used herein are derived from the data tables in [64], and are shown in Figure 4.1, with graph taken from [16].

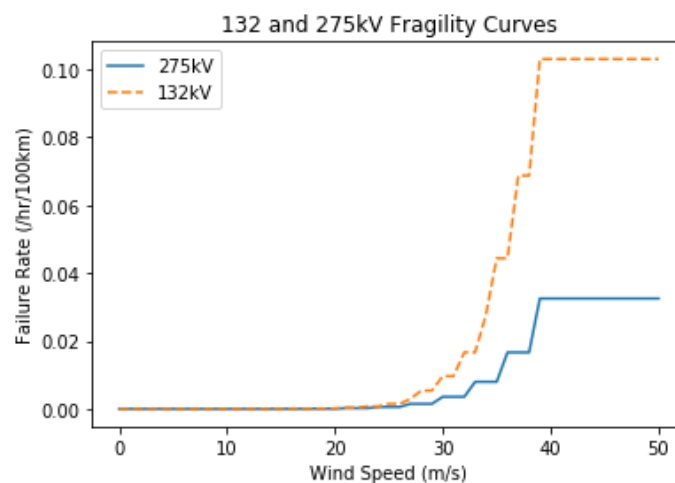


Figure 4.1 – Fragility curves to be used in study, graph taken from [16] and [64]

These are derived from 3-hourly wind speed windows with the maximum wind gust over that 3 hour window being used as the dependent variable. The source data is from the Scottish Hydro Electric Transmission Ltd network – that is, the network in Northern Scotland, herein referred to as SHETL. Both [27] and [64] utilise SHETL to derive cumulative probability distributions relating an incident wind speed to a corresponding failure probability, with the primary difference between the works being that F. Fan in [64] took this a step further and disaggregated the failure probability of lines by voltage level. At the time of writing for the report, SHETL was primarily 132kV and 275kV lines, however since then the network now has a single 400kV connection. For the rest of this section it is assumed the 275kV OHL fragility curve can be applied to 400kV lines in lieu of more accurate data. Further, it is assumed that the fragility curves derived from SHETL can be applied across the whole GB system, at least with an acceptable level of accuracy to be indicative of system risk. The “stepped” nature of

these curves is due to the interpretation of the curves via the data bins used in the source material. As the curves themselves are in terms of failure rate/hour/100km, the actual length of lines exposed to a given weather parameter then needs to be determined.

### 4.3 Definition and quantification of line exposure to weather conditions

In order to convert any branch data to a corresponding failure rate using the fragility curves being used, an estimation of the branch's exposure to the natural hazard being examined (in this case, wind) has to be determined. Conventionally this has involved using an assumed length of line, and the weather speed associated with, for example, the most extreme of the wind speeds at either end of a given network branch such as described in Chapter 3. Buses can also be assigned to weather "zones" with the greatest wind speed of the zones which that branch crosses being assigned to the line being investigated, for instance in [85].

For geographically uniform areas, or particularly short branches, this may be an acceptable approximation should meteorological variation be minor. However, for long lines over diverse geographical regions exposed to a wide variety of natural hazards this plainly may be too broad an approximation to be acceptable, and thus a spatiotemporal disaggregation of lines as demonstrated herein may be necessary in such circumstances.

To correct for the exposure of each line to different weather conditions, each line was spatially disaggregated and converted from two co-ordinate pairs (in latitude, longitude) to a 2-dimensional array. This was achieved using the *python* programming language. For the case studies and examples investigated herein, MERRA-2 (Modern-Era Retrospective analysis for Research and Applications) data [86] is utilised due to its availability and spatiotemporal completeness, and the co-ordinates system it utilises is used for the data resolution.

MERRA-2 is a relatively coarse dataset, resolving to  $0.5^\circ$  by  $0.625^\circ$  latitude and longitude, or approximately 50km by 50km. To estimate the amount of line in each of these given "blocks" of data, two co-ordinate points are set as a "start" and "end, which can be then interpreted as a vector. This vector can be iterated through in a given number of steps – which could be varied based on data granularity – to project a path through the 2d array. Each "step" can be counted as a sample within each data block. Using the resolution of the data and Pythagoras' theorem, the "length" of line within each block can then be determined.

Presuming concern lies with the effect of wind on OHL, then only lines which are above ground and subject to the wind itself are assumed to be vulnerable to wind conditions themselves. That is, underground or undersea cables can be assumed to have no exposure to extreme wind conditions whatsoever (though connecting substations may well be subject to these weather conditions should they too be connected to the grid by OHL).

If it is assumed that there is a 50kmx50km resolution grid, a line going directly East from West across two whole blocks from the far West of the westernmost block to the far East of an adjacent block (i.e. 100km), this could then be disaggregated to be equivalent to two blocks with 50km of line within each in a 2-dimensional representation. A demonstration of the method described here is shown in Figure 4.2. "Exposure" here is defined as "the magnitude of the length of an OHL subject to any incident natural hazard".

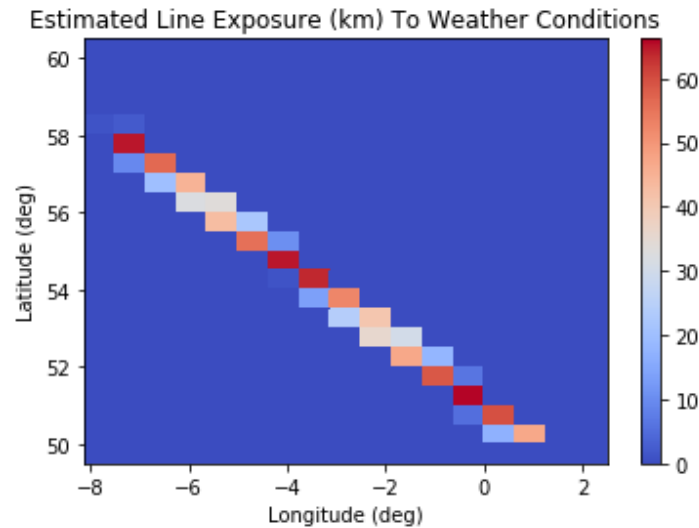


Figure 4.2 - Arbitrary representation of line exposure to natural hazard

This demonstrates in itself that, assuming weather data is overlain over such a line, the OHL will be subject to both varying intensities of weather, and different parts of the line will have different magnitudes of exposure. This, of course, represents the exposure of an OHL to wind – a cable’s exposure to wind would be assumed to be zero across the entirety of the network branch under consideration. A homogenous representation of this line would only consider two values: the total length of the line, and the incident wind speed at either end of the connecting nodes. This tells the user nothing about where the line is most likely to fault, and may be a significant over or underestimation of what the true failure risk on the line actually is.

#### 4.4 Computing failure rate on overhead lines for given exposure and wind speed

The implementation of fragility curves considered here consider the failure probability in terms of “per hour, per 100km”. That is – the fragility curves are agnostic of wind direction. Further, in the source data used to generate the fragility curves a conservative estimation is made such that the maximum estimated wind gust in a three hour window was what caused the associated, recorded fault (based on the fact the source data was 3-hourly resolved maximum wind gust data). OHL faults can be due to sustained, high wind speeds as well as with extreme, sudden wind gusts. This is discussed in [10] in the context of hurricanes, where the initial storm peak, as well as the sustained storm system that may sit on a region for days at a time, both cause damage to the power system.

The reason this is an issue is because when deploying a fragility curve to make projections about future failure rates, the data which is used to make projections may not be a perfect replacement for that which was used to create the natural-hazard-failure-rate distribution. That is, using time-averaged wind speed data with a curve based on maximum wind gust speed may represent an underestimation of the projections of failure rate which are then made. Alternatively, using maximum wind gust speed on fragility curves based on time-averaged wind speed data may overestimate actual failure rate projections. The results garnered from the fragility curves as they are applied herein, then, can be assumed to be useful relative indicators of system risk but may not represent the precise or absolute values of failure probability. The fragility curves are also to be applied consistently across data sets such that analysis is based on the same fundamental data such that clearer comparisons can be made.

To determine the actual failure probability for a section of line, the exposure determined via the methods described above must be combined with weather data and the fragility curve. That is, the failure rate for a given incident weather parameter for a given location must be used to determine the

failure rate per 100km in a given section of line, which must then be corrected for the actual exposure of the line in a given block. This can then be converted back to a failure probability for the subsequent analysis.

An exponential failure probability distribution is assumed, represented by Equation 4.1.

$$p(\text{fault}) = 1 - e^{-\lambda\delta t} \quad (4.1)$$

In this equation,  $p(\text{fault})$  represents the failure probability within a given time period  $\delta t$  (assumed to be 1hr) and based on a failure rate  $\lambda$ . Rearranging to solve for  $\lambda$  from the source data means the failure rate can be corrected to the actual line exposure, then converted back into a failure probability.

Using the combination of these proposed methods, then, a given line can be represented in 2 dimensions with spatially disaggregated exposure to weather patterns and associated failure rates.

#### 4.5 Correcting spatial wind speed data for differing applications

“MERRA-2” data represents a broad spectrum of meteorological hindcasted weather data covering parameters such as solar irradiance, ambient temperature, and, most relevantly, wind speeds. Hindcasted data represents an estimation of the weather conditions at a given region for a point in space and time, which is typically estimated from a mix of satellite data and local historical meteorological measurements, combined to give a complete map of estimated weather conditions. Though other sources are available and are described in sources such as [6], MERRA-2 was chosen because it was deemed the most appropriate for the analysis being undertaken and was judged able to provide, at worst, an indicative representation of historic risk during different events and a variety of data types for analysis.

Two specific subsets of data were chosen;  $u$  and  $v$  resolved wind speed data at heights of 2m, 10m, and 50m, and single level maximum wind speed data [87, 88], henceforth referred to as “three-level” and “single-level” data respectively. The latter dataset is presumed to be the wind speed active at 10m.

The MERRA-2 data effectively treats the globe as a “bumpy-sphere” – that is, a grid of blocks at fixed horizontal displacement with homogenous weather conditions within those 50kmx50km blocks. For geographically uniform, flat regions, as stated, this may be an acceptable approximation for shorter line branches. However, the UK is a geographically diverse country with rugged mountain ranges in Scotland, with lower-lying floodplains in England, creating distinct climatological biomes. These are defined within [6] as falling into three broad categories – the windy North, the windy and sunny Southeast, and the sunny Southwest Peninsula. Geographic diversity within the scale of 50kmx50km ranges may therefore be profound. Homogenous representations of OHL in system studies cannot directly the diversity of weather conditions that may affect network branches; further, the exact mechanisms which drive OHL failures will vary across different geographical and weather conditions. That is, a storm hitting the entire UK at the same time may manifest as extreme winds in Scotland and Northern England, while simultaneously causing flooding and inundation of substations in Southern England and Wales. In Scotland, therefore, in such a context, there would be significantly increased risk of OHL faults at a time where there would be increased risk of flooding on substations in England. This represents one of the major challenges in resilience analysis: during HILP events, a single causal weather pattern could manifest as a variety of natural hazards affecting different areas to different magnitudes simultaneously.

As a first approximation to begin to understand this, estimations about the elevation of the grid were also taken while generating the exposure arrays. This was done using NASA Shuttle Radar Topographic

Mission (SRTM) data [89]. Elevation data is recorded in images in .tif format which were called via an API (application programming interface) [90] which in turn converted a co-ordinate pair to a value representing an estimation of the elevation at that point. While progressing through the vector, as described in Section 4.3, samples of elevation were taken at each point. The highest elevation sampled in each block of data was then recorded. The usage of this data will be discussed in further detail in Section 4.9.

#### 4.6 Correcting wind speed for altitude of asset

Different assets on a system will experience different weather conditions not only because of their location but because of the variety of heights of assets, and the fact wind speed increases as one moves further from the surface of the Earth and away from obstructions which can slow winds. For example, typical 275kV towers in SHETL can be estimated to have heights circa 50m, whereas 132kV towers on GB will have heights of around 30m. Wind tower hub heights, too, vary by manufacturer and capacity with offshore turbines exceeding 100m compared to rooftop turbines which may be less than 10m. Wind turbine hub heights are based on 100m, based on typical commercial-scale wind turbines and on typical values found in the Renewable Energy Planning Database [91]. Though wind turbine hub heights can vary significantly, for the purposes desired in this Chapter it was deemed adequate to assume a typical value applied across the system to be indicative of general trends rather than more precise absolute measurement of wind power infeed on the system.

In [92], wind speeds are corrected using three wind speeds at various heights to extrapolate the wind speed at a given height. A fuller illustration and description of this method can be found in the reference's supplementary materials but a similar approach is utilised here. First, the  $u$  and  $v$  orthogonal components of wind speed at the  $(2+d)m$ ,  $(10+d)m$ , and 50m are taken, as is done in the original methodology, with the  $d$  a value representing vertical displacement  $d$  stored in the raw data. That is, a presumed height at which the data is measured. For the vast majority of observed data in the case studies performed this was at or near zero. Regressing these against the log of their altitude then means the wind speed at height  $h$  can then be estimated using Equation 4.2.

$$w(h) = A \log(h - d) - A \log(z) \quad (4.2)$$

How the  $d$  parameter relates to the vertical heights of the measurements is shown in Figure 4.3, along with an example regression with arbitrary data selected for illustrative purposes.

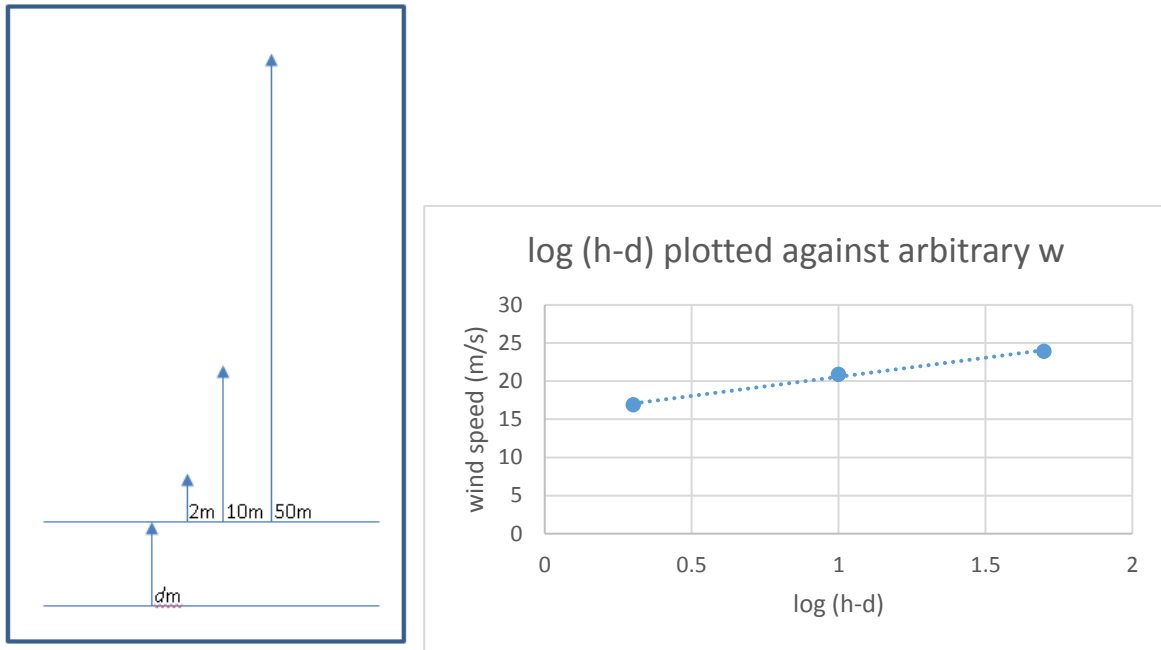


Figure 4.3 - vertical displacement parameter "d", vertical axes arbitrary scale and regression (with  $d = 0m$ )

This presumes a standard linear equation of form  $y = mx + c$ , with known  $x$  values  $\log(h-d)$  taken from the 2m, 10m, and 50m heights with the  $d$  values, and known  $y$  values, the resolved wind speeds at these altitudes. Given  $y$  and  $x$  are known, the other parameters can be simply calculated.

$w(h)$  represents the incident wind speed  $w(\text{ms}^{-1})$  at height  $h(\text{m})$ , or the anemometer height from which the wind speed can be measured. The gradient  $A$  can then be computed via regression, as can  $\log(z)$  which is the  $y$  intercept. This can then be rearranged to extrapolate the wind speed at unknown height, with  $z$  determined using Equation 4.3

$$z = e^{-c/A} \quad (4.3)$$

where  $c$  is simply the  $y$ -intercept of the equation determined from the known data and the regression.

This further emphasises the potential significance of disaggregating fragility curves by voltage levels – 132kV OHL, by virtue of being typically smaller and shorter than their larger 275kV/400kV cousins, may be subject to less extreme weather and better protected by wind shadow, but they are also more vulnerable to inclement weather when it does occur. The taller 275kV/400kV lines, being used for transmission scale and hence being less typically found directly next to heavily populated areas, can reasonably be expected to be subject to more extreme weather conditions will less sheltering from the wind associated with wind shadows and adjacent vegetation. Distribution level OHL will likely be more susceptible still to severe wind conditions, but research was not yet found creating relevant fragility curves and this research more directly pertains to transmission and national scale networks than distribution networks.

#### 4.7 Interpolation of weather data for use in simulations

As previously discussed, MERRA-2 is a particularly coarse dataset. On a global or regional scale, or for climatological analyses, this is not inherently problematic. However in the context of power system analyses a resolution of 50kmx50km is plainly inadequate for systems as diverse and concentrated as GB.

For perspective, it is approximately 100km between Glasgow and Perth, where Scottish and Southern Electricity have their main offices. Using such a resolution would mean the assumption that an OHL connecting these two cities would experience 2 or 3 different weather conditions across the entire line – while this is an improvement on using a homogenous representation of that line (which would represent, of course, the entire line experiencing only a single weather condition), it undermines the value of disaggregating the representation of the line in such a manner to use such a coarse dataset.

In [92], the authors used a form of LOESS regression which they refer to as a “non-parametric locally weighted scatterplot smoother”. 2-dimensional interpolation and regression itself presents a significant computational and academic field in its own right. In this context, an accessible and easily deployable solution was deemed desirable. The *python* function *griddata*, part of the *SciPy* library, was used to perform the interpolation of the incident weather data to improve model granularity [93].

This, naturally, cannot begin to account for local topological factors which may affect wind speed and directions such as valleys or mountaintops, where phenomena such as the *Venturi effect* and wind shadow may have profound localised impacts on wind if the terrain is particularly variable or there are large man-made structures affecting local wind flows (for example, wind farms). Nonetheless it allows a first-order improvement on the raw data available and more granular results to demonstrate the over-arching principles of the proposed methodology.

#### 4.8 Projecting wind power for given incident wind conditions

In extreme weather conditions, wind turbines will engage in self-preservation actions to prevent electromechanical failure, such as deployment of brakes or adjusting angle of turbine blades to reduce the rotational speed of the turbine. This in turn reduces wind turbine output and, when aggregated across wind farm groups or entire windfarms, can cause significant drops in wind power infeed over the scale of minutes or hours, dependent on the duration and intensity of the storm. This is HWSS, as described in Chapter 2, and is investigated in [29].

HWSS can be significant in the context of resilience because such reductions in wind power infeed will occur at times when high wind speeds are also increasing power system risk associated with OHL outages and, in winter, increased life-critical demand from sources like heating. Although an individual turbine will act in a broadly predictable manner with pre-defined manufacturer settings for cut-out and cut-in, the aggregated effects across a wind farm, taking into account local variations in wind conditions and turbine heights, manufacturers, mean aggregating such variation presents a significant challenge; aggregating this to a regional, national, or international scale even more so.

Various different approaches have been taken to project wind power outputs given a set of incident weather conditions. Forming detailed analyses for quantifying HWSS is stymied by factors such as the diversity of kinds of wind farms, constantly evolving technologies in wind farms, and sparsity of data for HWSS conditions, and so forming a generalizable curve which can be applied across a system is in itself a rather gross estimation of the wide variety of factors which can affect wind generation (wind direction can generally be considered less of a factor in this instance than in the context of OHL faults, as wind turbines can be designed to “track” the wind direction to optimise output, however given the impacts of local geography on local wind speeds wind direction may still be a factor).

The approach taken here, and demonstrated in [16], was to use a simple proxy and amalgamation of methods as described in [31], [92], and [33]. A curve representative of a pre-corrected power curve (that is, not considerate of HWSS) was provided by D. Brayshaw of a form used in [33]. A sigmoidal curve was then fitted to this using the form

$$y = \frac{a}{1 + e^{(-f(w)(x-w+\delta))}} \quad (4.4)$$

in which  $a$  is a normalising factor set to 0.9128,  $\delta$  is an x-shift with value -15.  $w, f(w)$  represent the power curve as represented as an  $x, y$  co-ordinate set. The *SciPy* function *curve\_fit* was used for the regression.

In equivalent studies, a Gaussian filter was applied after some maximum value to force the output to be – or approach – zero. In [16] this was not performed, rather a complementary curve was used to curtail the input at higher windspeeds simply by subtracting this complementary curve from the original, as shown in Figure 4.4, taken again used in [IET ref] [16].

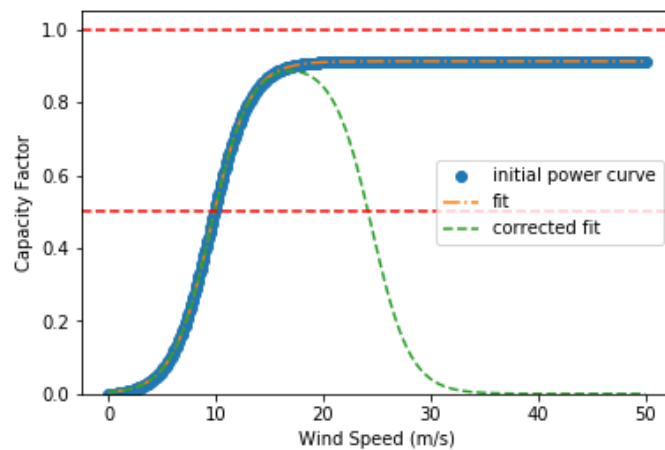


Figure 4.4 - Wind power curve used in study as derived

The scale of challenge presented in producing more representative power curves was, in the context of this research, deemed out of scope insofar as the exact impact of HWSS itself was not sought to be quantified, rather an indication of general trends was sought. That is, ideally a more complete curve based fully on empirical data would be preferred, but the aim was to generate a curve that could be productively used to illustrate general trends across a system, and the simple proxy generated was deemed appropriate and proportionate for that purpose, however future work would hopefully use more data-driven methodologies for more precise measurements. Nonetheless, as is the case with the fragility curves, the curve itself can still be useful for being indicative of relative, rather than absolute, information across the system and is, by inspection, similar enough to the comparator curves to be useful for this research.

#### 4.9 Case study on Reduced GB and SHETL grid representations

The next step, then, was to apply the proposed methodologies described on representations of real networks to demonstrate their value as approaches. The information provided by applying these methods could be utilised to, for example, target placement of restoration assets, backup generation, or, if analysis is performed over inter-annual periods, to simulate investment-side strategies and target investments at either particularly vulnerable or valuable (i.e. operationally significant) connections.

Two networks were chosen for study using the developed approaches: a representation of the Northern Scotland SHETL grid, and a reduced representation of the GB MITS developed at the University of Strathclyde based on work and principles defined in [82].

#### 4.9.1 Development of the SHETL grid representation

As the study in this case is an examination of only OHL risk, and does not contain power system simulations themselves, only a node-branch representation of the network was required for the analysis. Data for transmission lines and interconnectivity was taken from the National Grid ESO Electricity Ten Year Statement (NG ESO ETYS) for the years 2017 and 2018 [94, 95], with data also provided by J. Kelly of Scottish and Southern Electricity Networks (SSE-N). Some minor data cleansing was necessary, performed with consultation with SSE-N, to ensure appropriately representative branches. A node-branch visualisation of the SHETL grid is shown in Figure 4.5. The visualisation of networks and wind speed data herein is produced by a combination of different *python* software libraries, specifically *basemap* [96], *matplotlib* [97], and *NetworkX* [98].

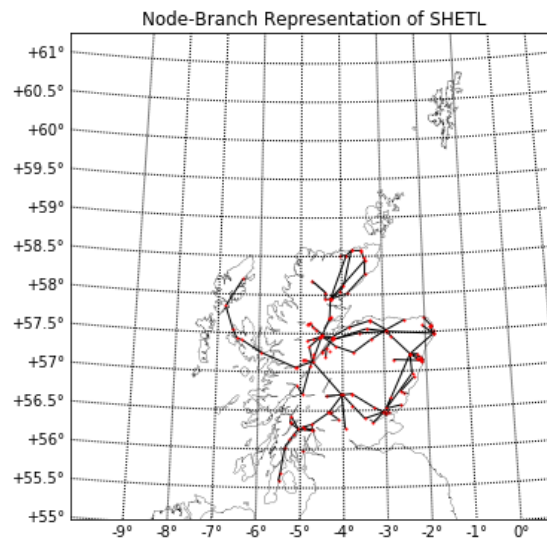


Figure 4.5 - Network representation of SHETL grid

An incident weather event is chosen – specifically Cyclone Friedhelm from December 2011 [5].

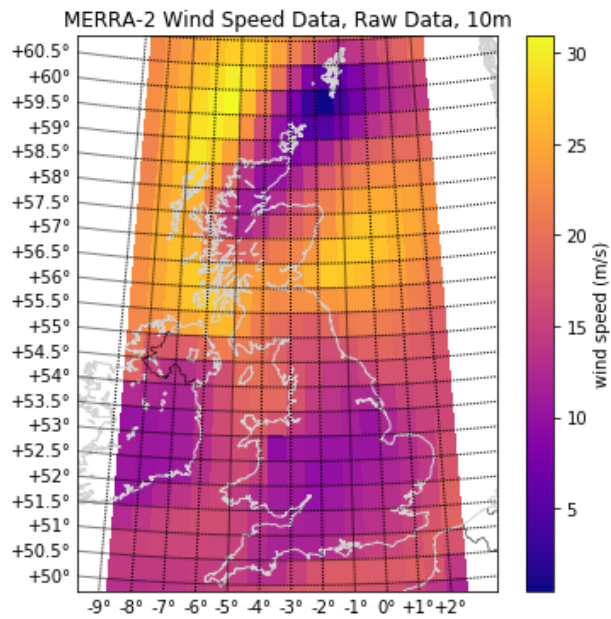


Figure 4.6 - Raw single level w-resolved wind speed data

Interpolating this data to increase granularity by a factor of 5 then provides the wind speed data shown in Figure 4.7.

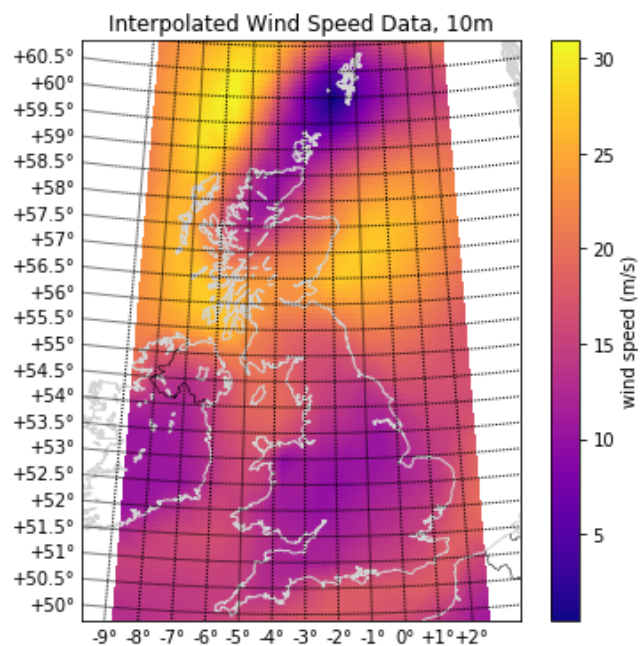


Figure 4.7 - Interpolated three-level wind speed data at 10m

This increased resolution then provides the means to determine the localised exposure of the network to wind, illustrated in Figure 4.8.

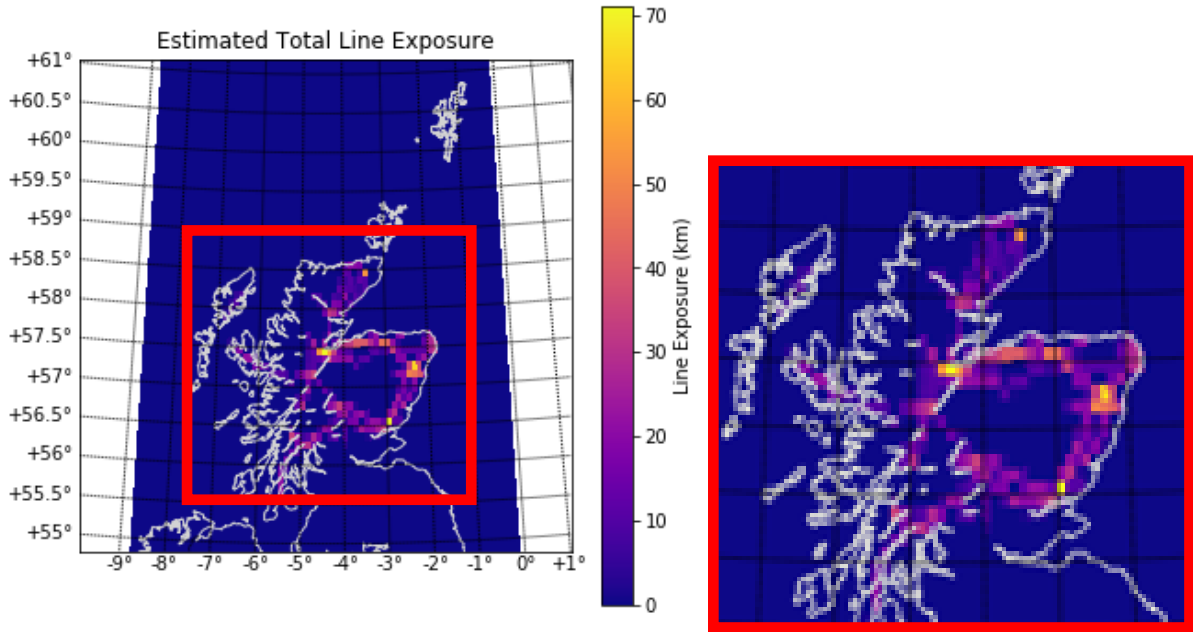


Figure 4.8 - Estimated total line exposure of OHL on SHETL grid

This can then be compared with the distribution of windfarms across Scotland. This data is extracted from the Renewable Energy Planning Database (REPD) December 2018 [91], which provides information such as hub height, farm capacity, and co-ordinates. These were bulk-converted to lat-lon pairs using an online Ordnance Survey bulk co-ordinate conversion tool to get the co-ordinates into an appropriate format [99]. The results are shown in Figure 4.9, with disc colour and radius scaled to windfarm capacity.

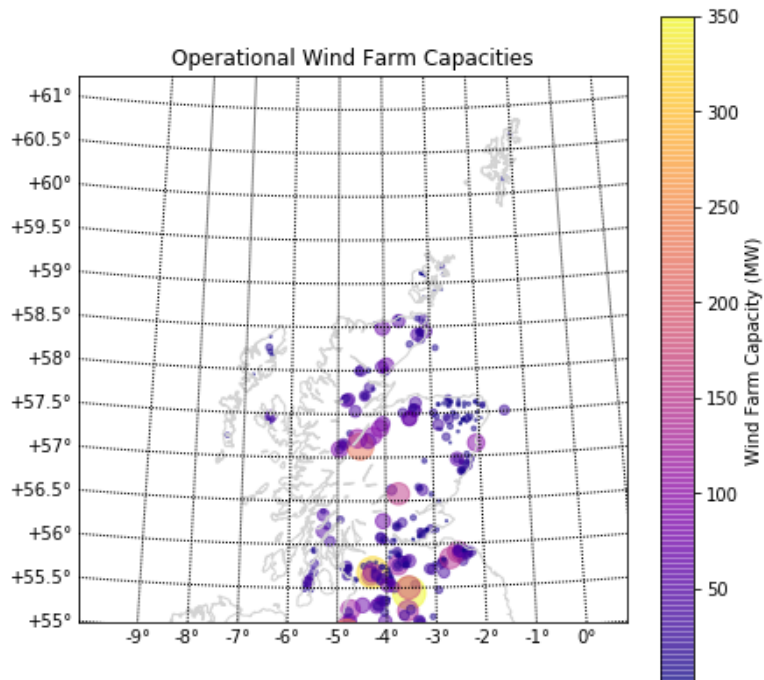


Figure 4.9 - Wind farm capacities and locations in Scotland

It can be observed that there is significant overlap in regions of SHETL where there is grid capacity and where there is installed wind power capacity. This should be unsurprising – power can only be

connected to the grid where a grid exists to which can be connected. In Scotland, the majority of demand is in the South-Central region of the country, also known as the Central Belt, just south of SHETL. This is also where the largest windfarms are connected, again in part because there is significant grid capacity to allow connection of wind resource, however there are also other factors as to why wind development is largely confined to the coasts and south of the country. This is discussed in the Appendix 7.1.

A consequence of the overlap between grid capacity installation and wind power installation is that it creates interdependencies between wind power output and system risk in these locations which is compounded in extreme wind scenarios. This will further be investigated in Section 4.9.3.

#### 4.9.2 Implementation of Reduced GB

The representative GB network was produced with input and contributions from C. MacIver of the University of Strathclyde and J.Kelly. Again, only a node-branch representation was necessary in this instance to be representative of approximate locations and representative of network connections for use in the analysis. This network model represents a consolidation of key interconnection routes and attempts to retain key information about approximate locations of key substations and important network branches, while collapsing smaller branches into larger, representative network branches. Data was provided by C. MacIver in the form of consolidated data tables which were in turn converted into formats usable by the software model. Location data not directly provided was approximated by approximating the locations on the grid using the ETYSs and *Google Maps*.

The result was a representation of the GB network which could provide a useful comparator for the SHETL model. The node-branch representation of the representative GB model, herein referred to as the *Ryan Model* after one of the original architects of the model R. Tumilty, is shown in Figure 4.10.

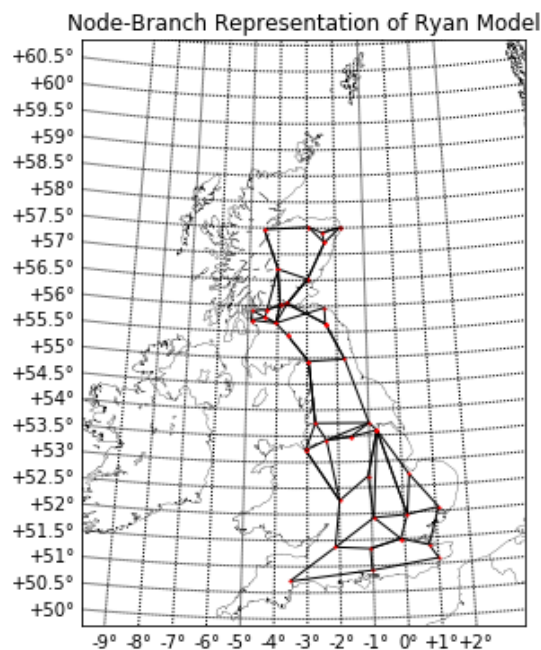


Figure 4.10 - Visualisation of reduced GB network model known as the "Ryan Model"

Similarly to the SHETL model, in Scotland it can be observed the grid is concentrated in the South of Scotland but there is still a significant amount of network in the Northeast. There is little to no grid represented in this representation, however, of the network in the far West coast surrounding Oban, the North coast surrounding Caithness and Sutherland, nor in much of Wales. Northern Ireland is not

represented as it is not part of the GB MITS and is part of the main Irish grid with HVDC interconnection with GB.

A visualisation of wind farms across GB more generally is shown in Figure 4.11.

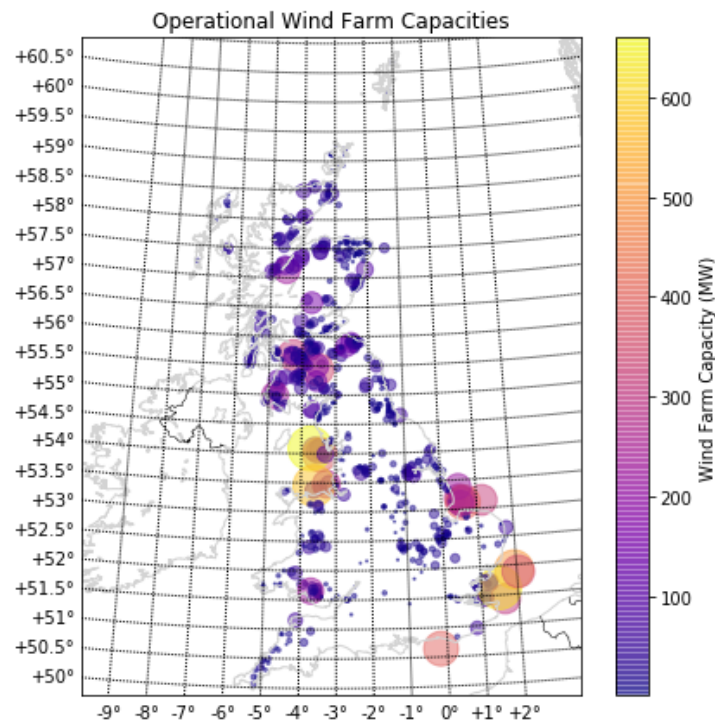


Figure 4.11 - Wind farms connected to main GB system, as of December 2018

It can be observed that wind generation in GB is dominated by large offshore windfarms in the Southeast of England, onshore windfarms in the Southwest of Scotland, and offshore wind farms north of Wales.

The developed methods can then be applied to these renderings to illustrate the linkages between wind power and system-wide OHL risk.

#### 4.9.3 Simulation methodology

A Monte-Carlo simulation method is used to aggregate locational failure probability across the system and produce maps representative of OHL risk across the system. That is, the risk of a failure happening at a given location in a given hour using the models and methodologies formulated thus far. This is done as described in the following pseudocode:

---

```
For sample in sample size:  
  For line in all lines:  
    For section of line:  
      Generate random number between 0 and 1  
      Get failure probability for line section  
      If random number < failure probability:  
        Fault recorded in block  
        Latitude, longitude of fault recorded
```

---

This then generates a 2 dimensional array with fault numbers which occur in each  $\sim 10\text{km} \times 10\text{km}$  pixel of data recorded. Dividing these counts by the sample size provides an estimate of the overall fault probability by block. This means that a line can “fault” across multiple locations, or multiple faults can be recorded within a given block within a given time step if multiple lines intersect. This provides an estimate, then, of how likely *any part of the network* is to fault in a given time step. Individual lines can of course be analysed in this method, as, in a power system simulation, whether a line faults in 10 locations or 1 it is still simply no longer in service. However, the purpose of this exercise is to demonstrate and visualise the overall probability of something breaking in *any given location* on the network, agnostic of the impacts of that incurred fault.

The average of the latitude and longitude of fault locations within the simulation can then also be used to generate a value representative of the expected location of a fault on the system – the *expected fault location* (EFL).

Using the power curve demonstrated in Section 4.8, estimates about locational wind power output can also be made to illustrate the effect of extreme wind on system-wide wind output.

#### 4.9.4 Results – SHETL grid

A sample size of 10,000 is used (but any sample size could be used dependent on desired precision versus computational and time expense). The case study of *Cyclone Friedhelm* with the illustrated weather conditions was used. The three-level data (that is, the data with 2m, 10m, and 50m sets extrapolated to relevant asset altitudes) is used first. The results for the estimated OHL fault probability on the 132kV and 275kV/400kV networks are shown in Figure 4.12.

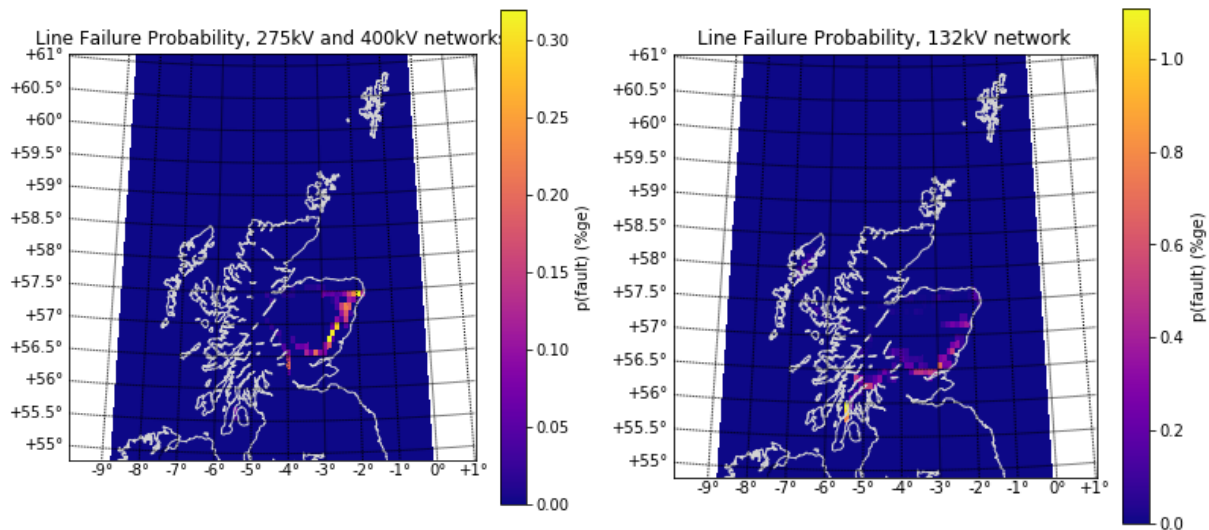


Figure 4.12 - 132kV and 275kV/400kV network fault probabilities on SHETL grid

Using these aggregated grids, the total OHL failure probability across the entire system can then be evaluated, with the results in Figure 4.13.

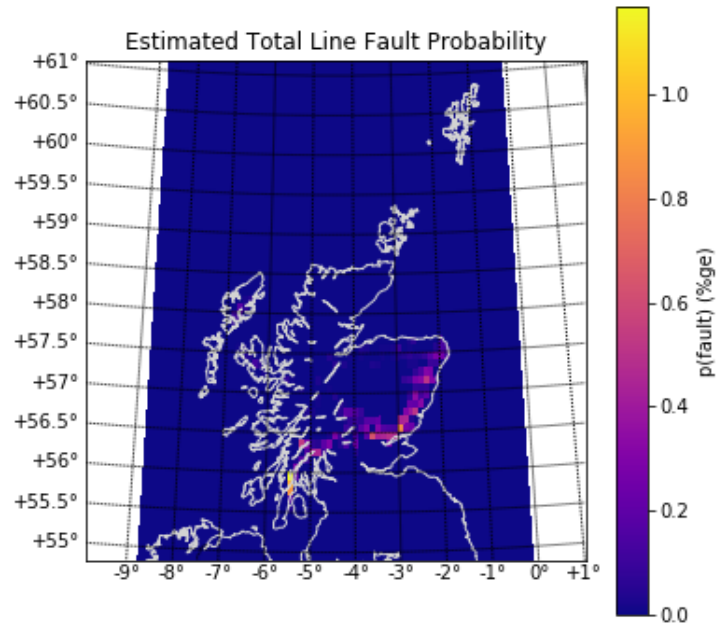


Figure 4.13 - Total OHL failure probability on SHETL

The output of windfarms across the system can be similarly aggregated to visualise windfarm outputs, as illustrated in Figure 4.14.

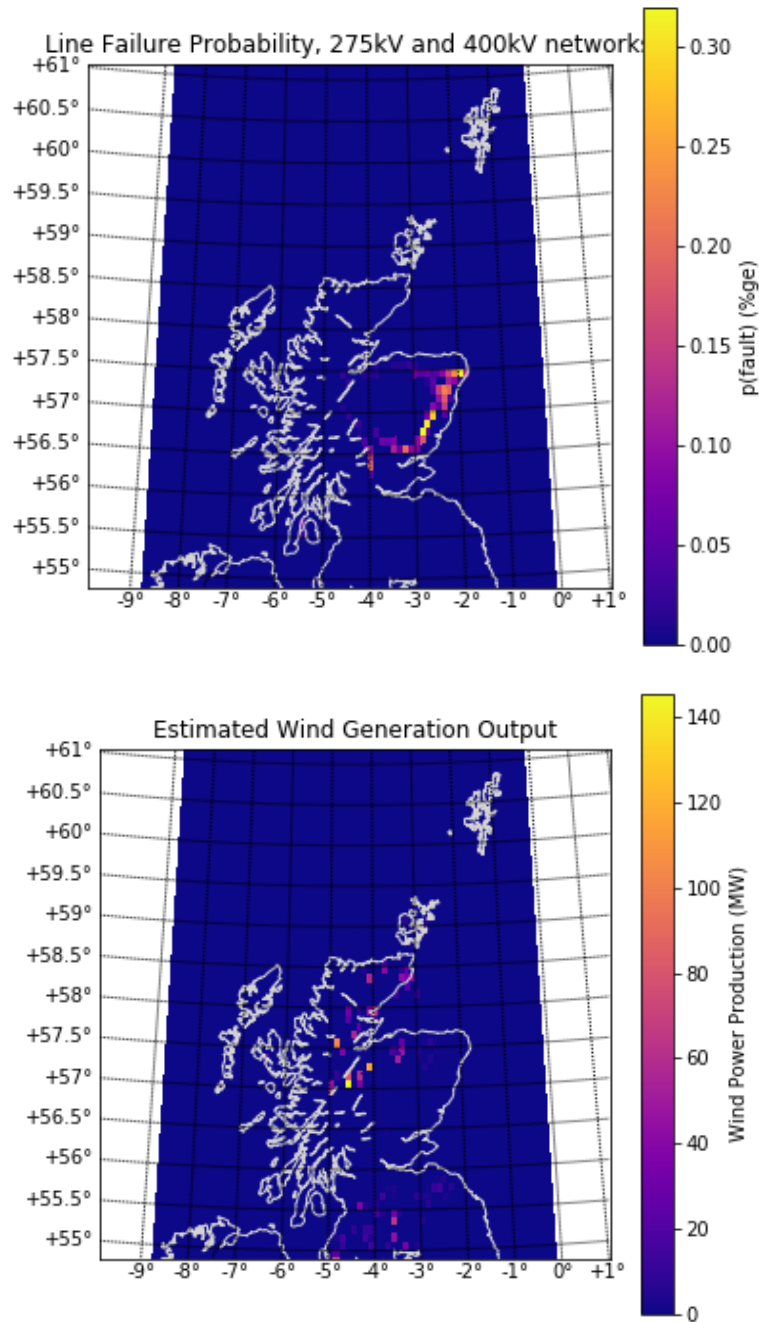


Figure 4.14 - Aggregated wind farm output across Scotland, together with line failure probability for 275kV and 400kV networks.

By inspection it can be seen that, despite there being significant wind farm capacity installed across the East Coast and Southern regions of SHETL, the effects of HWSS have reduced significant amounts of infeed to zero due to the extreme wind speeds. That is, the areas with highest OHL risk will coincidentally have significant loss of wind power due to HWSS. Overlaying the total OHL failure probability with the installed wind farm capacity illustrates this, as can be seen in Figure 4.15. The disc radii have been normalised to the highest capacity single windfarm on the system (350MW, Clyde Wind Farm, though Whitelee is the largest farm facility at >460MW it is separated into multiple separate groups within the data itself).

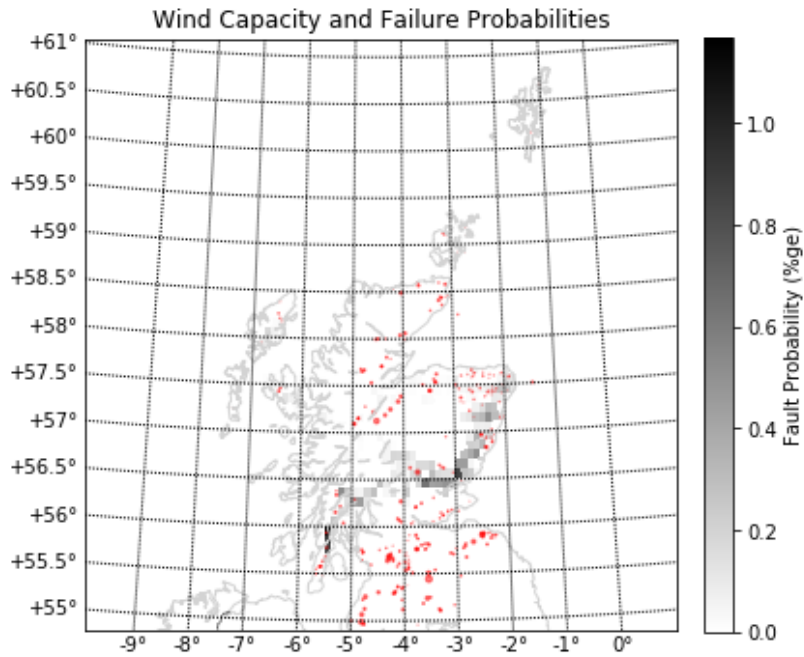


Figure 4.15 – Failure probability on OHL overlaid with installed windfarm capacities in SHETL, Scotland

The EFL from these results is (56.70°, -3.78). Visually, this seems reasonable – the most extreme values are in the South, Southwest, and East of the network- the mean value of these locations should reasonably be expected to be somewhere in the middle of these areas. This tells us where a failure is most likely to happen, which can be useful information if attempting to optimise placement of spares or other emergency response equipment or staff.

Of course, these values are unweighted by the actual impact of any outages – in reality an outage on the East coast would be far more consequential than a loss to the relatively small Southwest peninsula in Scotland, and that would weigh significantly on the planning decisions as regards location of repair teams and resilience assets. Conversely, there is significantly more redundancy on the East coast than on the weakly connected fringes of SHETL, meaning any single outage is less likely to lead to disconnections than the weaker segments of the network. This does, however, provide a useful first-order approximation and indication of what the most at-risk areas of the network would reasonably be.

#### 4.9.5 Results – Ryan Model

The simulation is repeated on the Ryan model to get results across the wider GB system, and across both weather datasets for comparison. The total line failure probability for the three-level wind power dataset and aggregated wind power resource is illustrated in Figure 4.16.

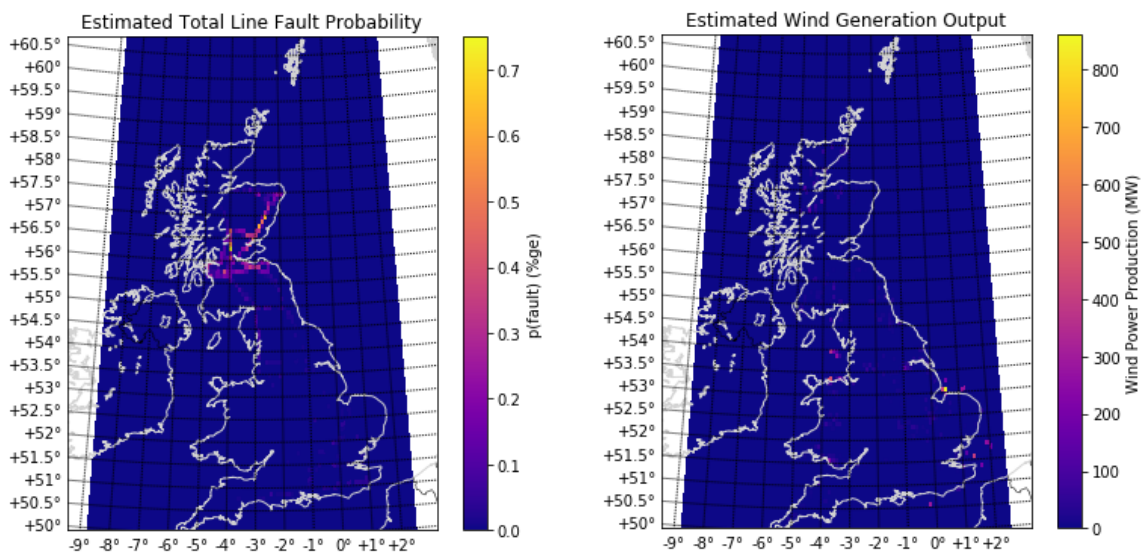


Figure 4.16 - Simulation results for Ryan model with three-level dataset

The estimated total wind power on the system is 10.8GW, with an EFL of (56.02, -3.30)°. It should be noted in the wind generation projection that there is data present but it is dominated by the large outputs of wind generators off of the Southeast coast of England from offshore wind farms and offshore windfarms north of Wales. Due to HWSS the wind output across the system more generally is significantly depressed and is negligible compared to these groups.

Overlaying these results with GB-wide wind capacities produces the following in Figure 4.17.

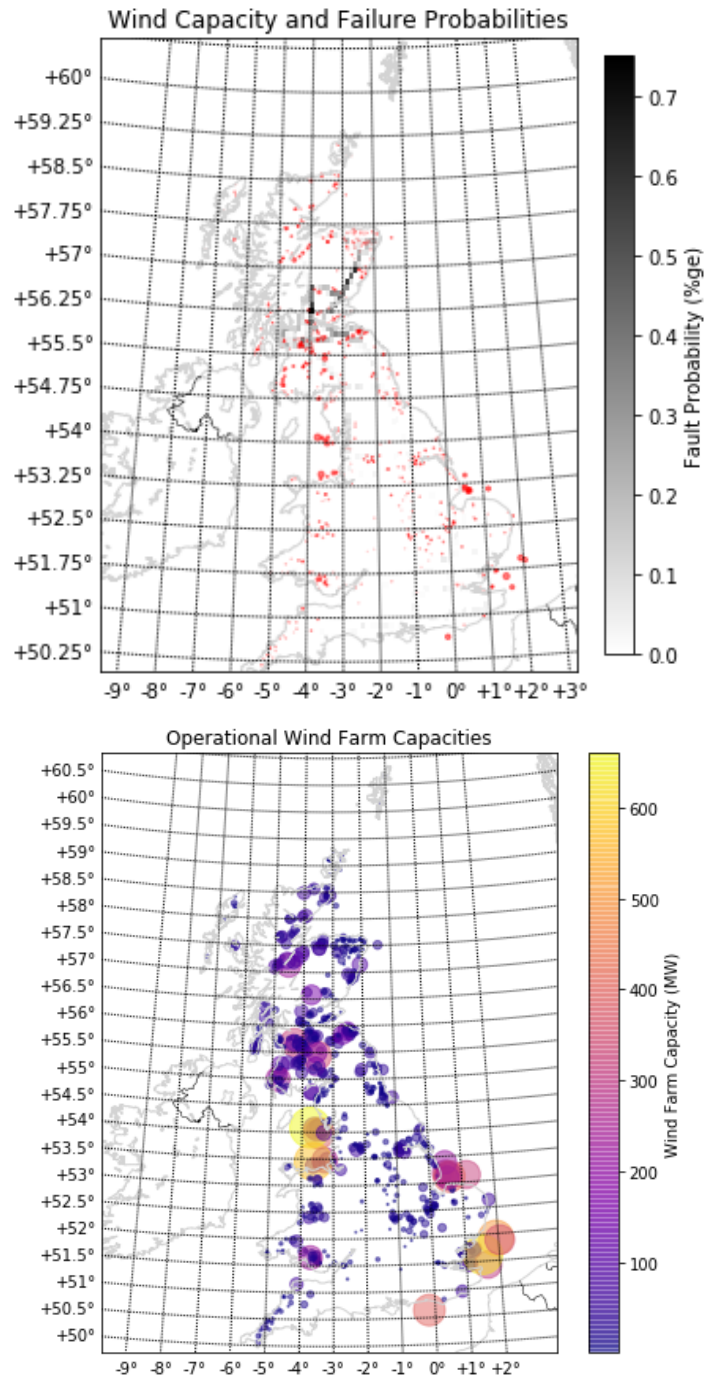


Figure 4.17 - Wind farm capacities and OHL failure probabilities, three-level data on Ryan Model

This can be compared with the results from the single-level dataset (that is the data where only the “maxspeed” wind speed data with all assets treated as being at equivalent height with no vertical extrapolation was performed). The wind speeds incident across the system are shown in Figure 4.18.

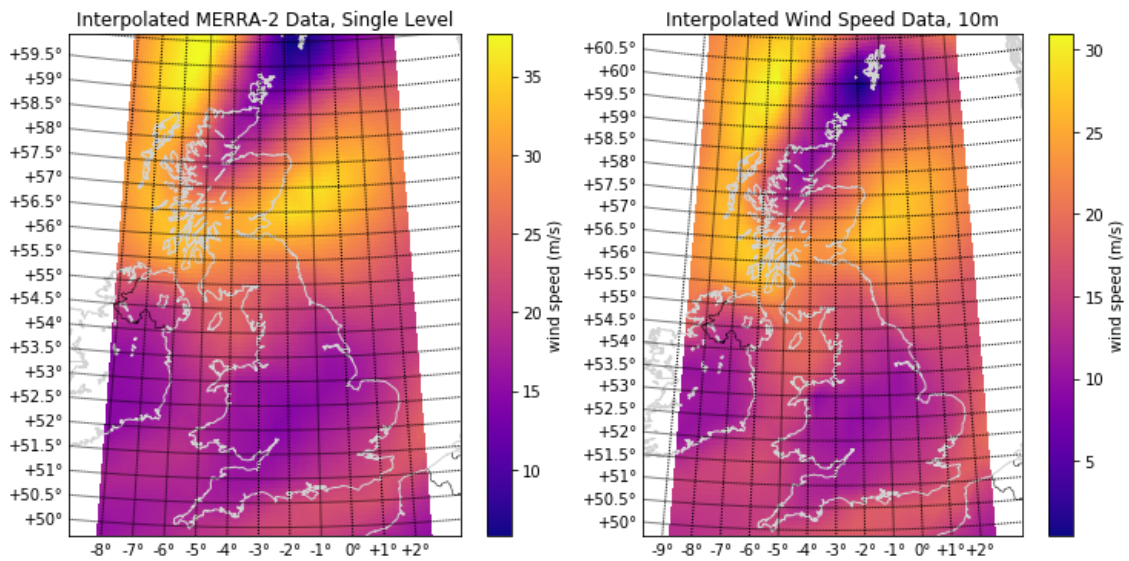


Figure 4.18 - Single-level incident wind speed data [left] compared to data at 10m from three-level data set

The values here can be observed to be more extreme than those of the 10m data extracted from the three-level wind speed data ensemble, though the trend is broadly the same across the two datasets (extreme winds in the South, East, and West Coast of Scotland with moderate winds across the rest of GB).

The results, when using the single-level data for fault location estimation, are in Figure 4.19.

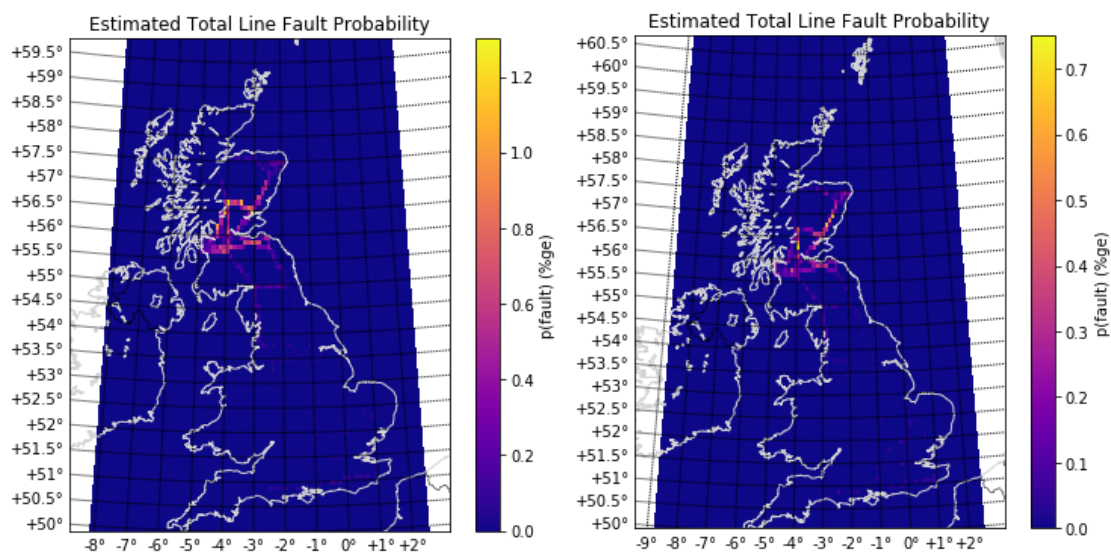


Figure 4.19 - Estimated line failure probability due to wind, single-level data [left] compared with that using the three-level data [right]

It can be observed with examination of the scales that there are more extreme values of failure probability across the system, and particularly concentrated in the Central Belt of Scotland and East Coast which experiences the most extreme values of wind speed, but that the general distribution of failure risk across the systems are comparable.

To understand the reasons for this would require further analysis as to the types of networks in the areas with most extreme weather conditions. That is, presuming the areas have significant penetrations of 132kV OHL and the single-level wind speed is presumed to act at 10m, the more

extreme values of wind speed would naturally correspond with more extreme values of failure probability associated with those lines.

The EFL for this case was (55.97, -3.41)°. As with the three-level data, the general trend is consistent with there being significant risk of failure in the South of Scotland and with areas of significant grid density and high wind speeds, but in the wider context of GB this is a relatively localised storm, as can be observed in Figure 4.20.

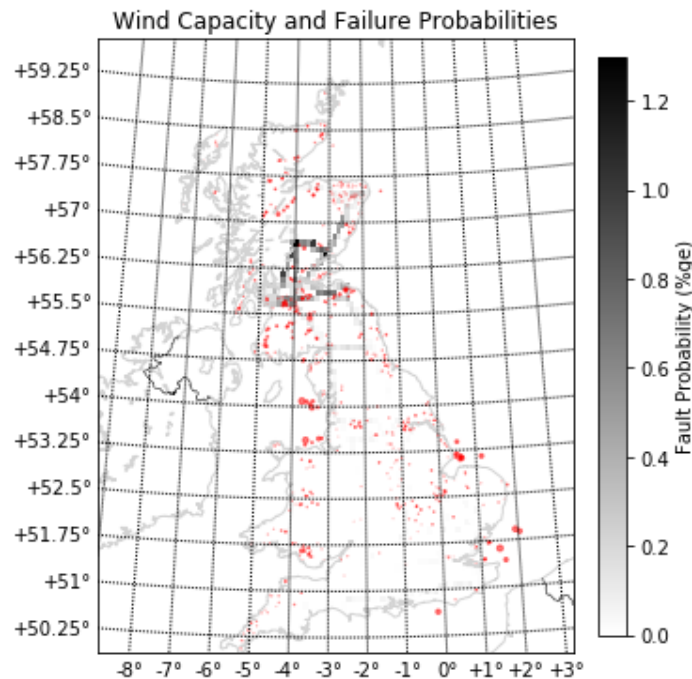


Figure 4.20 - Total line failure probability overlaid with installed capacity of windfarms in GB

Though there is significant failure probability in the Northeast and Central-North of Scotland, in both cases there is shown to be relatively significant risk across the Central Belt, where there is both significant penetration of wind resources and where the most significant population density – and hence domestic and commercial demand – is based. Comparing the estimated wind output across these cases suggests 10.8GW in the three-level dataset but 11.2GW for the single level dataset, a discrepancy of almost 4%. For comparison, if the uncorrected power curve which does not account for HWSS is used, in both cases the estimated wind output across the system is 17.7GW. This suggests HWSS could be responsible for a loss of as much as 6.9GW of wind power output capacity during this event.

#### 4.9.6 Grid elevation

Throughout this section, OHL have been treated as 2-dimensional representations of point-to-point connections. This effectively assumes that the grid is itself flat and the distance between two points can be approximated “as the crow flies”, which is to say the line travels directly from point A to point B. This in itself acts as a new source of error and abstraction – clearly lines do not travel perfectly horizontally between two points on a network, especially over mountainous regions where there may be significant variability in elevation. Further, line pathway planning is affected by local planning concerns as well as topological factors such as hills, local manmade structures, or planning limitations such as Sites of Special Scientific Interest (SSSI) where developments may be restricted for aesthetic or conservational reasons. Further, a purely 2-dimensional representation of lines assumes that the lines are perfectly taut from point-to-point in this representation, whereas in reality lines may sag,

particularly with increasing temperature. In fact, thermal limits on lines are primarily driven by thermal restrictions to prevent overheating lines from becoming health and safety hazards for humans or to prevent phase-earth faults.

To begin to understand the potential variability of grid elevation, as noted in Section 4.3, the elevation data for each block of each line was estimated. Aggregating these estimates across the system to estimate the highest single grid elevation can then give an illustration of the potential variability of environments experienced by network branches, which in turn could have consequences for security analyses. The maximum sampled elevation across the Ryan model and SHETL model are shown

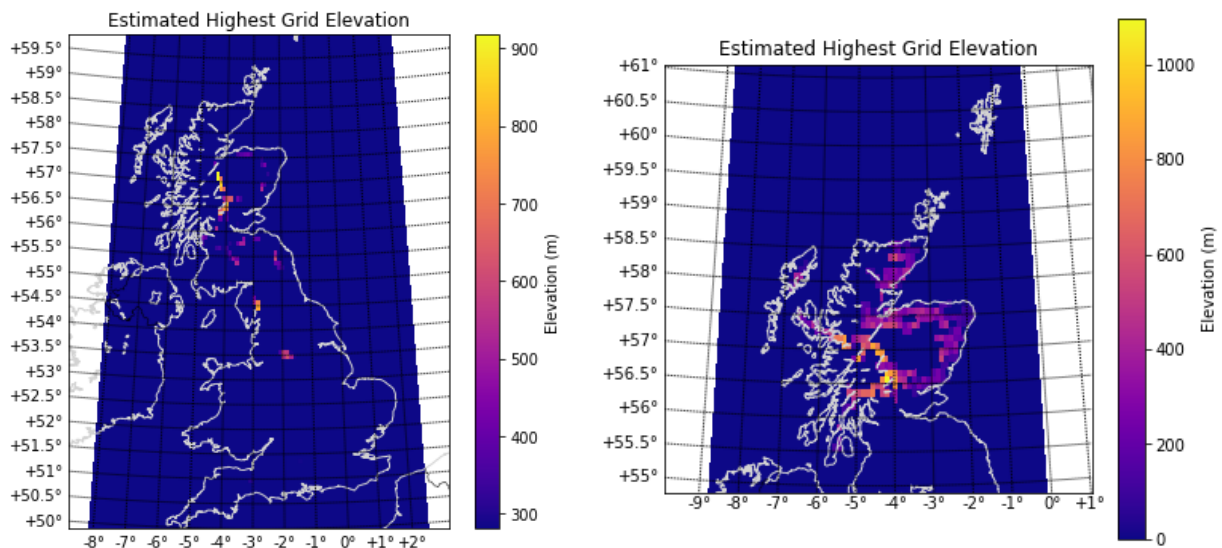


Figure 4.21 - Estimated maximum grid elevation across Ryan and SHETL grid representations

At a high level, it can be concluded that England is a lower lying, flatter country than Scotland. This places it at increased risk of coastal and fluvial flooding, particularly in the case of low-lying substations such as that which was inundated during Storm Desmond [4]. Extreme highs of elevation also present operational challenges, however, for operators. The lines at the most extreme high elevations in Scotland tend to be in underdeveloped, rural areas which will accordingly have relatively poor transport accessibility. This means that, should faults occur, even accessing the transmission or distribution assets which have faulted may be challenging. Further, the exact mechanisms by which OHLs fault will vary across lines and regions with changing topologies and biomes. OHL in more heavily forested areas may have reduced wind speed exposure associated with wind shadow from vegetation, but that same vegetation could present a security hazard associated with falling branches, debris, or collapsing vegetation leading to transient or permanent faults.

The highest values of elevation on the grid in both SHETL and GB are in the Northwest of the grid, where the grid passes through the Highlands past Fort William. With reference to the node-branch representations of these networks, this line is particularly significant in the case study being examined as it has a relatively low estimated risk compared to the East coast lines. In particularly extreme cases it may be necessary to curtail load flow on the East coast and increase power flows on this branch to reduce system risk, but should a fault actually occur then the restoration time could be significantly more than a line which faults in a more populous, developed area. This emphasises the balance which must be found between the potential risk of a contingency state, the plans in place to address it, and the corresponding changes in costs associated with mitigation or prevention.

A consequence of diversity of elevations and biomes across the grid, as discussed before, is that there will be a wide variety of fault-inducing mechanisms across the system. For example, vegetation-related faults can cause common-mode faults on OHL in a wide variety of ways but those faults can only actually happen if there is vegetation present which can cause them. The tree-line in any environment varies with latitude, historic land use, topology, and climate, but in GB is generally between 530m and 600m [100]. Therefore, network sections which travel above this line will be less prone to vegetation-related outages but will be more exposed to natural hazards such as lightning. The lack of vegetation also means that, for shorter towers or distribution networks, lines will not have wind shadow from forestry and could experience more extreme weather conditions. If vegetation-related faults are a major driver of failure events on the SHETL network, in areas where there is less vegetation corrections may therefore be necessary to reflect the different underlying conditions driving the failure mechanics- even though at a population level, i.e. “on average”, system-wide behaviour will still reflect the distributions used to create the fragility curves. Given the source data was not available to consider this factor, it is not possible to make an assertion either way and further investigation may be warranted.

A more direct consequence of the disparity between 2-dimensional and 3-dimensional representation of OHL is a consequence of trigonometry – that is, if elevation is considered, a 2d grid may represent total distance travelled “as the crow flies”, but it does not reflect that actual length of line present in each block. For example, a 2d representation of a line with an increase of elevation between two points of 1km in a 5kmx5km grid going North-South would underestimate the total length of line by as much as ~4%, assuming the line itself is taut and travels perfectly point-to-point.

Tracing the pathways of individual lines to better reflect local topological variety therefore presents itself as the obvious next step for refinement of line exposure calculation, and would manifest as a correction in each block to the length of exposure based on the actual path the line takes vertically as well as horizontally. In the test case examined, a block of elevation 1,099m was found to be the maximum and was adjacent to a block 971m lower than it. This, in a 10kmx10km corresponds to an approximate error of ~0.5% between a 2d representation and a length-corrected 3d representation.

It is also worth noting that a storm system acting across a diverse system such as GB will manifest different weather patterns across different regions of that network simultaneously. For instance, Cyclone Friedhelm in the case study discussed resulted in not just extreme winds in Scotland but flooding in England and Wales. Flooding is not a direct threat to OHL (except in the rare circumstances where storm surges or landslips destroy distribution equipment or towers) but does threaten low-lying distribution substations or low-lying power generation facilities. A particularly major example of this was the inundation of the Fukushima nuclear power plant following a tsunami in Japan [50]. Whilst the UK is not at pre-eminent threat of tsunamis, OHL outages associated with high winds concurrent with substation outages due to flooding could cause widespread and significant damage to system operability. Therefore, analysis only of extreme wind may not by itself comprehensively represent true system risk during such storm events. This ties into how power systems themselves are represented in simulations – in a node-branch model all generators and loads are assumed to connect to given buses with line flows limited by the branch connections. Therefore, representing substation-level faults can be a challenge at such a level of abstraction because, within a substation, there are many potential routes which power may take.

Translating a fault within a substation to an effect on the wider power system carries further levels of abstraction. Representing OHL faults concurrently with substation flooding faults, therefore, requires not simply an understanding of fault levels but a level of refinement in the representation of

substations themselves that goes beyond standard, simplified node-branch representations and into node-breaker representations.

#### 4.10 Discussion and key findings

The main driver of disaggregating OHL and linking visualisation with wind power output in the manner demonstrated is to begin to understand the co-dependencies inherent in resilience to extreme wind events, and weather more generally. It is economically rational to install wind turbines in areas in which there is as much wind as possible to get maximum return and wind power output – but the nature of regions with high winds is, of course, is that there is the increased probability of extreme winds. This in turn creates linkages between the risk of outages on OHL and the risk associated with loss of infeed due to HWSS. High wind can cause line trips, which in situations with high southerly flow can reduce Scottish export capacity. However, if this happens concurrently with HWSS in Scotland then this can ameliorate the situation for the Scottish network's operability.

Conversely, a more serious situation can arise whereby OHL trips can reduce export capacity at a time of high wind, requiring curtailment of wind farms on the exporting side (Scotland) whilst HWSS reduces wind farm output on the importing side (England). The impact of these events is additive in nature

A full analysis of the consequences of these outages would require a complete simulation of the actual outage events themselves, but various conclusions can be drawn by inspection of the charts and from examination of some of the quantitative results from the simulations.

There is approximately 19.5GW of capacity installed in GB in the model used, of which 8.1GW is in Scotland. The actual output estimated according to the model is 2.1GW for the three-level dataset, or 2.3GW should the single-level data be used. This corresponds to an approximately 10% error between the sets.

Overlaying the probability of failure with the wind farm installed capacities illustrates the linkage between wind power and line risk, inasmuch as in this case study fault risk is concentrated in the South, Southwest, and East Coast. Wind power output is concentrated in farms less affected by extreme winds which correspondingly have lower risk networks connecting them. Operators already plan for loss of infeed and variability of power resources, but in occasions such as wind storms, the boundary between what is classified as a "credible" and "non-credible" contingency event becomes important. In cases such as the South Australian blackout [14], the inability of the system to cope with windfarm trips resulted in the tripping of an interconnector, frequency and voltage degradation, and the eventual total collapse of a large section of the power system.

The challenge in such conditions is not only identifying credible contingencies but also identifying potential concurrent faults or faults which may cause cascading, uncontrollable faults with far-reaching consequences. One of the primary aims of the SQSS is to ensure the system is resistant to credible security threats and can be restored to a state where it can survive another adverse state. That is, in an N-1 situation the security standards mandate that the system can not only limit the negative consequences of a natural hazard but potentially prepare the system for another incident, preventing one outage from leading to a series of further outages. In a high-wind scenario such as the test cases here, that becomes particularly important because of the linkages between OHL risk and variability of wind power infeed. HWSS can happen in the scale of minutes or hours dependent on the scale of storm and its progression, but OHL faults and cascades can happen as quickly as protection equipment can operate, so even to the scale of sub-second. In the model used, Scotland accounts for

some 41% of total installed wind capacity- but, not only that, it also has significant hydroelectric resources and two nuclear power plants.

The loss of interconnection between Scotland and England due to a significant storm event would impact not only cross border supplies from Scotland to England associated with high wind power infeed but also the loss of significant operability-related assets – hydroelectricity is a vitally important strategic resource for black start situations. Furthermore, while nuclear power plants cannot be used for black start generation themselves, they are among the largest capacity generators on the system in tandem with international interconnectors and large scale offshore windfarms which are distributed around the UK's coast, as can be seen in Figure 4.17. Being able to quantify precisely the risk associated with flows across the B6 boundary then is of significant importance to operators and planners during storm events not just for Scotland but GB-wide system stability.

The significant penetration of wind in Scotland means Gigawatts of cross-border flows in such situations and, while loss of load in Scotland would be relatively small in the context of the entire GB network, the impact on system operability from the loss of southerly power flows, two nuclear generators at Hunterston and Torness, and the loss of black start facilities such as Foyers could be significant. Further, the SHETL network representation used has significantly more 132kV OHL in it than the Ryan Model, suggesting it is significantly weaker than may be suggested in reduction models. This is why it is important to have a robust quantification of both probability and impact, and why improvements in the complexity and precision of fault probability quantification for OHL could be significant for such studies.

Comparing the failure probabilities and wind power outputs also shows the sensitivity of the modelling to the incident weather data. The single-level data shows more extreme probabilities across the system with almost double the peak failure probability on the system, but with only a 4% shift in wind power output estimation. When modelling only SHETL, the potential change in projected wind power shows an almost 10% discrepancy across datasets. This illustrates the benefits of distributing wind power resources across the power system during extreme wind effects, as, in this case, the most extreme effects are concentrated in a relatively local area allowing affected regions to be supported by pooled resources across the system.

It is also worth noting that the incident weather event being examined in this case study is exactly around the region at which the fragility curves and power curve for windfarms are at their most variable, and thus any minor adjustment to the incident weather has significant consequences for the final output results manifest across the system. Particularly, the fragility curves shown between  $30\text{ms}^{-1}$  and  $40\text{ms}^{-1}$  – i.e. precisely where the peak wind speeds observed across the test case vary between across the data sets – vary by as much as an order of magnitude. Similarly, beyond  $20\text{ms}^{-1}$  the power curve rapidly tends to zero. The combination of these factors means that in the region identified and in the test case used the failure probability across the system is far more susceptible to the variation in weather data than the wind power output, as for wind farms approaching or beyond  $30\text{ms}^{-1}$  their estimated power output will already be approaching zero, meaning any further increase in wind speed will not have major impacts relative to changes in the failure rate.

Simulating the same event with slightly different interpretations of the weather data has been shown to have a significant impact on the calculated failure probabilities across the system with only a minor discrepancy across wind power projections, which in this case is minor in comparison to the, relatively localised, OHL failure risk.

Such results also have to be understood in the context of the abstractions necessary to make the data useable in this context. That is, the fragility curves have been applied in a manner comparable to that in which they were derived, but the derivation was itself agnostic of, for instance, wind direction. Although different failure mechanisms are caused by different aspects of wind – be that a gust or a sustained blast – while the curves have been derived agnostic of wind direction, in reality it is not unreasonable to assume that wind direction will have a significant effect on potential failure mechanics on OHL. That is, gusts or turbulent wind flows perpendicular to an OHL could cause line “galloping” [26], leading to cascading faults or shocks to the structure of a tower, potentially leading to collapse or clashing of conductors, leading to transient faults. Wind in parallel with OHL could still cause tower collapses or debris and vegetation to collide with conductors, damaging network conductivity in that manner.

Similarly, wind has other, indirect effects. Moisture and debris can be thrown onto lines in coastal regions, leading to flashovers on conductors days after the storm itself may have occurred. Similarly, wind paired with line icing and snow could lead to branch collapse or flashovers as the ice melts over insulators. This is accommodated for in some sense with other fragility curves in [64] but not those used in the current analyses demonstrated.

The methods have been used on a transmission scale network but it is likely that distribution assets are even more vulnerable to outages associated with extreme winds, not just due to the construction differences in network assets but because the sheer volume of assets mean there are more assets which could be broken in adverse weather conditions and the economy of scale may not exist for non-load related reinforcement of network branches, particularly in rural areas of grids such as SHETL where grown is in generation rather than demand.

What has also not been captured in the demonstrated methodology is the potential variability of wind output during wind storms at shorter scales. In [6] potential hourly ramping events of up to 15GW are anticipated by 2030, which infers major minute-by-minute variation in wind power generation that is not captured in hourly simulations such as that performed here. These variations will coincide, potentially, with unstable networks as gusts induce transient faults across power networks – potentially aligned with particular gusts with lines which have a common bearing – making the system significantly more difficult to control during wind storms.

Users must be careful in both selecting and interpreting the data used in such studies. This is both to ensure it is appropriate to the context and style of analysis being used and to ensure the application is relevant to the source data and usable for those attempting to make decisions based on study findings. Further, there is a balance that has to be struck between model precision and flexibility – there is potential for obfuscation of results via over-complication should too many inappropriate corrections be applied where conservative approximations may be entirely suitable.

#### **4.11 Conclusions**

The methods demonstrated in this section illustrate a method for presenting OHL risk and visualising wind power output across a system while demonstrating the potential sensitivities of such modelling to changes in the source data and postulated relationships used. This is an example of analysis of extreme weather events on an OHL network using hindcasted data, but the method could equally be applied to forecast data to plan the location of, for example, restoration assets and repair teams during force majeure events to reduce asset downtimes and improve system resilience.

The proposed approaches are designed to be tractable and portable to other kinds of natural hazards and renewable energy generation. For example, rather than wind speed and wind gusts, extremes of

temperature could be used with load flow information, ambient temperature, and solar irradiance to examine the potential of thermal shutdowns of assets such as transformers and the interaction between solar infeed, ambient temperature, and solar irradiance during heatwaves. Similarly, data on precipitation could be used with elevation data and network models to examine the risks associated with flooding and hydroelectricity. Given the links between wind storms and flooding, this analysis could be carried out concurrently to get a more comprehensive analysis of storm-related threats on the power system.

The analysis thus has only considered a single natural hazard and its potential effects on failure rates, but for some natural hazards there is a link between how the system is operated and the failure rates of assets on the system. For example, line loading, ambient temperature, and line icing are all inherently linked. Line ratings are typically associated with thermal/sag limitations of an OHL, and so in hot weather operators will be constrained by the upper bounds of temperature limits on lines. However, in snow or ice conditions it may be the case that operators, where possible, actively try and load lines more heavily to increase their temperature above freezing to prevent additional mechanical loading associated with ice on the lines. To take full consideration of this, therefore, a full simulation model/load flow could be incorporated into the methodology, particularly given the links between elevation, line loading, and temperature. The demonstrated methodologies taken as a comprehensive piece of work allow this sort of analysis and, crucially, the visualisation of such results to begin to productively address such features.

The UK, and Scotland especially, is geographically diverse with a wide range of biomes – from mountainous, barren landscapes in Highland Scotland to more low-lying plains in England and windy, wild coastlines in Western Scotland. Therefore, the application of statistical methods which assume homogenous properties and line structures may not be appropriate in extremes of these regions. That is, if in the data on which such fragility curves are derived it is the case that vegetation-related outages and faults are a primary driver of outages in SHETL, in regions where there is significantly less forest cover these fragility curves may be less appropriate or accurate in practise, and further there may be significant variation and sensitivity of failure rates across longer lines which traverse geographically diverse regions.

Disaggregation of lines allows the analysis of such effects and the consideration of more localised weather and geographic conditions of lines and is a step forward in risk analysis from homogenous representations of OHL, particularly in terms of the phenomena which can be investigated and the results which can be ascertained from analysis. That is, not only can high risk OHL be identified but so can specific high risk regions across the network. Estimations can then be made about the most high-risk regions either across individual lines or system-wide using metrics such as EFL.

Although interpolation of the source data in this case was useful for improving simulation granularity, it does not address the issues identified with local topological variation directly in that extremes associated with local high elevation regions or geographic phenomena such as “wind tunnels”. It is difficult to make such estimations without having a means of directly incorporating such calculations and more detailed modelling of the local topological conditions of the networks beyond the simple visualisation deployed here, but the potential importance of taking consideration of such factors was made evident.

The demonstrated methods have proven a clear advancement in the quantification of failure *probability* on OHL during storms but have not in any way yet considered the *impact* of such outages. Lines which have a high probability of failure in this case study may actually have a low impact and, therefore, a relatively low risk. There may be other lines on the system which have a lower probability

of risk but are much more important for system security; although understanding the probability of outages is important, without a quantification of the impact of such outages the analysis is incomplete.

The main limitation on further improvement on the granularity of the simulations used is computational expense and scalability. The analysis in this Chapter has concentrated on examining a specific hour, to demonstrate the fundamental principles of the approach, but inter-annual or more detailed simulations (to examine, for instance, seasonal variation) exponentially increase the sample size. The benefit of the method is that it allows further detail to be examined, but of course this then increases the number of samples which have to be taken in each iteration of the simulation to increase by, potentially, orders of magnitude compared to homogenous representations of OHL where, effectively, the number of line samples simply =  $n$ , where  $n$  is the number of lines in the system. In the methods shown the detail of the lines scales indirectly with the resolution of the weather data used. However, given the potential for parallelisation of the implementation of the code, it is entirely possible to make the process much more efficient than that which has been demonstrated.

Further, as illustrated in the case study, the primary area of concern is in weather and storm conditions where wind speeds approach or exceed  $20\text{-}25\text{ms}^{-1}$ . This makes sampling techniques such as stratified sampling attractive to more efficiently direct the simulations to representative weather days, periods, or months where we are particularly concerned about wind storms. Something that should be noted is that the most computationally expensive parts of the process are the calculation of the pathways of individual lines, and the simulations themselves. The former need only be performed once, and the latter can be targeted at specific at-risk lines and areas which could be selected via offline analysis to optimise simulation. The methods as demonstrated here are only intended to be indicative of a very simple application of the methods which can be built upon and refined.

Various next steps then present themselves. Refinement of the method to incorporate the methodology for correcting line exposure per block to be three-dimensional; a comparison between homogenous representations of OHL in security studies and the disaggregated methods demonstrated; annual or seasonally targeted analysis for more detailed analysis of risk; or incorporation with a simulation model to more fully quantify the actual risk associated with lines. The latter, in this instance, was chosen, as the other approaches were deemed to be improvements in methodology which would improve the precision of the model and were useful in themselves, but do not fundamentally extend the work. The simulation model to be incorporated with this methodology is described in Chapter 5.

## **Chapter 5 Comprehensive power system simulation during extreme weather events considerate of mitigation measures and weather impacts on generation**

### **Abstract**

A simulation methodology is demonstrated on a representation of the GB network adapted from previous work and incorporating significant wind generation infeed to investigate the impact of changing frequency response dispatch regimes on system security. Changing the amount, location, and type of frequency response scheduled is shown to significantly impact performance metrics used in the quantification of system risk. An “unresilience” metric is proposed and compared across case studies to demonstrate the relative performance of the system following different kinds of outage events – specifically, a loss of a significant cross-boundary interconnection, a large loss of infeed, or more randomised, stochastically generated network faults. Results are also compared across interpolated weather data sets with increased spatial granularity versus using reanalysis data with a coarser resolution. At increased granularity, faults are less concentrated around individual nodes as less of the network is exposed to the most extreme conditions, meaning fewer common mode faults and, accordingly, better system performance. Using Flexible Demand Response is shown to significantly improve system performance as it is not reliant on the transmission network and can act in a more targeted, faster manner.

## 5.1 Introduction

Taking into consideration the findings from Chapters 4 and 5, evidently the results from power system simulations are likely to vary significantly based both on the abstractions of the power system itself and based on how faults such as loss of infeed are represented in power systems, or how to translate overhead line faults into power system simulations.

That is, as has been demonstrated in Chapter 4, there are significant variations in the risk profiles of overhead lines if they are no longer treated as homogenous entities but as an asset with a variety of states connected to each other – much like the power system itself is not a single bus but a network of nodes, lines, loads, and generators. Reducing a line to a homogenous entity is an abstraction of a real, tangible asset in much the same way a single bus representation of a system used in a frequency response simulation is.

It has been demonstrated that correcting the failure rate of lines spatially to recognize varying weather and geographic conditions has a material impact on the failure rates of those lines, as does taking account of different fragility curve models for different voltage levels. How this translates to actual impacts on the power system will be examined in this chapter in the context of a security assessment of an event during a high impact wind speed event, using the same data as is used in Chapter 4.

As was discussed at the end of Chapter 4, there were multiple potential means on which to build on the methodologies developed, but the development of a simulation model was deemed to be the most important. That is, refinements had been made in terms of how to go from a natural hazard and a network node-branch model to a representation of system failure probability on OHL, but this had not been considerate of the actual impacts of those events and thus was an incomplete representation of system risk.

Expanding to inter-annual analyses was deemed to be an expansion, rather than an advancement, of the methodology. The next step then was decided to be to incorporate a comprehensive simulation methodology to more completely represent the risk associated with wind faults on OHL during storm events, considerate of high wind penetration on the systems while also providing a means of simulating different mitigation or prevention measures, at least to a basic level.

This also serves as a means of bringing the analysis back to the original framework defined in Chapter 3 and improving it to be more representative of weather and power system phenomena across the system, showing the progressions that have been made in the methods and approaches used. That is, while Chapter 3 introduced the general framework to be used, Chapter 4 presented a series of refinements to the representation and use of weather data, while this Chapter serves to utilise the improved representation of OHL risk and improve simulation of system perturbations themselves.

This section then presents a simulation model, comprised of a combination of discrete models brought together to represent a whole-system analysis, which take consideration of many of the aspects discussed throughout this thesis. The model herein will be referred to, as a whole, as the Extreme Wind Perturbation Simulator (EWPS), or “the model”, or “the simulation” etc.

## 5.2 Data requirements and problem boundaries

Work on large-scale climatological reliability or resilience studies on power systems tends to use DCOPF approximations for the load flow and power system simulations themselves. This is the case in work already referred to, such as [15, 101, 102]. This is because the linear approximation DCOPF allows greater tractability than ACOPFs due to the reduced complexity of the optimal power flow problem

itself, allowing the problem to be wrapped in a larger-scale optimisation problem or simulation, limiting the computational expense of the problem itself. The assumption is that effects such as voltage deviation and line resistance are effectively negligible relative to other power system phenomena.

In Chapter 3, the simulation considered lines as homogenous entities with failure rates driven only by the length of line and an exponential relationship between that failure rate and an incident wind speed. The weather incident upon these lines was determined based solely on the extreme of the values on either end of the line with very basic groupings of buses upon which that weather was incident. The actual relationship between the failure rate and wind speed were largely synthetic and used to illustrate the sensitivity of risk metrics to changes in relationships between weather and failure rates. Similarly, lines were assumed to have homogenous failure mechanics, which is to say there was no differentiation in voltage levels in the connections themselves. As illustrated in Chapter 4, this is clearly inadequate.

Using the improved methodology determined in Chapter 4, there are greater data requirements for lines – spatial weather data and elevation data in particular. The same sources are used herein as were used in Chapter 4.

Regarding network data, in Chapter 3 network data was based on a highly simplified version of the GB network that did not consider wind generation or the interaction between wind power and the incident weather either. The power curve models used in Chapter 4 and elevation data could again be used in this context to make estimations about the output of individual wind farms.

Similarly, the generators in Chapter 3 were aggregated representations of connected generators at each node which were not representative of individual generators or reactors and were considered freely redispatchable. In reality, generators are constrained over various timescales – by thermal limitations and mechanical constraints in the domains of both frequency response and system balancing. Generators used in an OPF therefore should aim to be as representative of individual units as possible to represent the fact that individual generators can fault without affecting the wider generation site. For instance, during the Three Mile Island incident an entire reactor melted down but the remaining site remained functional after the event [103].

Using only a DCOPF to represent power imbalances may miss phenomenon such as suboptimal UFLS or generator tripping, particularly given the sequence of such events may be of major importance. For example, losing generation can reduce the overall system inertia and make the system more susceptible to frequency deviations which can lead to more damaging frequency deviations in a negative direction. Only simulating ideal load curtailment or generation actions does not capture this potential sequence of events. Studies such as [78] have considered frequency response in the context of power flow analysis but this study did not consider secondary frequency response requirements, nor does it consider the impacts of weather.

The work here attempts to include these factors as using a similar approach, while also improving the representation of overhead line risk. This necessitates data on the frequency response capability and ramp rates of generators, as well as their inertia capabilities. Since such data is frequently considered commercially sensitive, assumptions also have to be made about these as well as about the expected failure rates and mechanisms of generators using appropriate proxies.

The location and distribution of frequency response also is consequential for the ability of a system to respond to system deviations. In a single bus representation of the power system such detail is lost as all load and generation is lumped into representative groups, but if frequency response physically

cannot be pushed onto the network due to network constraints – or leads to overloading of connecting branches and subsequent faults and cascading conditions – it is useless (or, at best, less useful than it should be) during loss of infeed events or acute network degradation events such as during wind storms.

Therefore, data pertaining to both generator failure rates and a relationship between OHL failure rates and weather are necessary to generate feasible fault scenarios on the network. Thankfully, the latter have been investigated in Chapter 4 and can be deployed here as well. For generator faults, the same approach can be taken as was used in Chapter 3, assuming independence between generator failures and wind as a natural hazard.

Getting access to representative GB power system models – as opposed to network models, which can be deduced with sources such as *Google Maps* and access to the NG ETYS [95] – is also a challenge due to the commercially sensitive nature of such data, particularly individual generator stations. Therefore any model used will again involve various assumptions about the nature of various assets and will necessitate compromises and proxies for different assets.

As regarding representation of weather phenomena on the power system, in this case only the interaction between wind and the power system will be considered, and thermal and solar effects will be considered negligible. This is purely to limit the scope of a problem which is already intricate and broad in scale, and so the system boundary must be drawn somewhere. It is also noted that the test case being investigated is in the middle of winter in the UK, so solar power contributions to the grid are expected to be negligible and temperatures in a range that will not *negatively* impede the load flow capabilities of lines or rating of transformers.

The load shedding scheme of the system also needs to be considered – in Chapter 3 it is assumed load is shed uniformly across the system in blocks of 5% but this does not reflect what is done on every network and acted solely as a heuristic to make the problem tractable. In reality such schemes are set by regulations and grid codes, and different TSOs and DSOs will have differing approaches. Generator tripping behaviour will also vary by generator or may be stochastic in nature. Frequency response deployment of individuals may also be stochastic – that is, generators may not respond optimally to signals demanding changes in output or may respond sub-optimally. That is not considered in this analysis directly – again, as scope had to be limited somewhere.

When modelling system behaviour, various assumptions need to be made about exactly what loads are connected across a system, dependent on the scale at which the system is being modelled. The kind of loads which will be connected over the course of a day will naturally vary. On a normal (i.e. non-public holiday), for example, behaviour is largely predictable and follows a generalised diurnal curve, such as that shown in Figure 5.1 [104].

## Demand Last 24 Hrs

Data last updated on : 18/07/2019 15:04:00

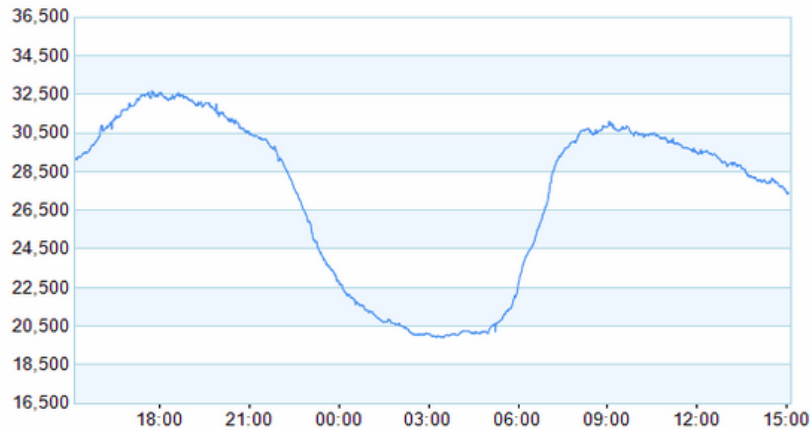


Figure 5.1 - Diurnal demand curve taken from realtime data from National Grid ESO data

That is, in the morning, people will tend to be cooking and preparing breakfast before work. During the day, people will tend to be at work or in offices. In the evening, people will be cooking or relaxing after work, or out socialising. Similarly, industrial demand will tend to be concentrated during office hours when staff are working or using machinery. Demand at weekends will follow different patterns as office workers or workers on a conventional 9-to-5 rotation spend their weekends socialising or away from home.

As was mentioned in [1], the changing nature of the British economy also has implications for load profiles and power usage in the system. Rotating and heavy machinery has become less prevalent as a significant source of demand as the UK moves towards a more service-driven, rather than manufacturing-driven, economy.

Data centres, particularly for ecommerce or banking, require 24 hour uninterruptable power supplies for reliable economic operation, and demand such as refrigeration in summer or heating in winter equally have limited load shifting capabilities without careful planning and monitoring. In the peak of winter, having adequate heating can be a matter of life or death for vulnerable or older citizens, and in warmer seasons food could rapidly become spoiled should refrigeration or freezing devices fail. In more extreme heatwave conditions, cooling may also begin to become a life-critical load in hospitals or care homes for elderly people.

As demonstrated in [46] there is a relationship between temperature and aggregate system demand a strongly linear relationship at lower temperatures - approximately a 1% increase in electrical load and 3-4% increase in gas demand for a 1°C fall in temperature. It is reasonable to expect a similar, weaker relationship for increasing temperatures but there was little literature found to investigate the matter, as reported in [6]. Temperature is a driver of demand in GB, but weather drives supply variability – and the relationships are only weakly quantified in relation to demand at higher temperatures.

Therefore, not only does the amount of load that will be lost at different times of day vary, but the nature of that load and economic cost of the loss of load will vary as well. Using a homogenous VoLL

cost will, therefore, obfuscate these different phenomena – or, at least, their potential costs. It is reasonable to expect a threshold to emerge where increasing temperatures in England and Wales, then, begin to create summer peaks associated with cooling demand and changing customer behaviour, but no such studies in the context of climate change were forthcoming. Therefore, for the purposes of this work, it is generally assumed the system has an aggregated, homogenous load profile across the test system with test cases taking place in scenarios with low or negligible solar infeed. In future studies this may need to be corrected – with demand being sensitive to temperature, it may well be the case that power demand in Scotland, for example, is much more variable to changes in temperature than in England if there is a significant temperature gradient.

### 5.3 Proposed simulation approach

In Chapter 4 a simulation framework was proposed at a high level to deal with modelling weather-related failures. This simulation methodology can be considered to broach various different blocks of the model and act to be a more robust and comprehensive simulation of what transpires when a fault scenario acts on a given network dispatch.

The dispatch itself is independent of the fault simulation and could equally be defined from historic balancing data, but in this case shall be determined via the use of a security constrained optimal power flow (SCOPF) based on the linearized DC approximation with frequency response and unit commitment constraints. The exact formulation will be described in Section 5.5.1 Mathematical Formulations.

In order to reconcile the problems with associating network-related problems with the single-bus representation of a frequency response simulation, these steps should be linked to each other in the simulation somehow so the simulations can be performed independently but the results map onto each other. This requires both a formulation for a suitable load flow, and for an efficient and appropriately robust System Frequency Response (SFR) simulation.

Network faults, as discussed in previous sections of this thesis, are not necessarily of concern in and of themselves – rather, they reduce the capacity of the network to get power from generation to demand which means, both locally and at a system-wide level, supply-demand imbalances. If the network remains contiguous this can be readily considered in conventional analysis such as OPFs, and if the system does not then incur any overloads on lines, there is no issue with the single-bus approximation of the power system used in SFR analysis.

The loss of infeed from generators or disconnection of loads will also cause supply imbalances in themselves should weakly connected assets be disconnected from the MITS, but of more significant concern is the potential for islanded conditions on smaller, less robustly connected networks. Therefore, the necessity to simulate the frequency response of associated islands following islanded events emerges – this is a particular challenge as it requires the linking together of the network models associated with power flows and the single bus representations associated with SFR modelling.

Similarly, in order to approximate the more complete restoration of the system, the frequency response problem should be linked to some simulation of power system restoration as well at least to a basic level of abstraction. That is, system restoration does not just require frequency response to contain deviations from the base frequency but for balance to be restored to the system between generation and demand. This happens over multiple timescales – both as secondary response winds down and the generators return to pre-fault operation via AGC or manual action, and over the hours following the event as faulted lines and generators are returned to operation as demand changes as part of the diurnal cycle. This should be considered because the timing of an event impacts the

expected load on the system, and hence any reliability metric which measures cost in terms of total load disconnected. That is, the absolute and relative amount of load connected will vary based on e.g. the time of day at which the fault occurs, the ambient weather conditions, and the type of generation connected.

Further, some assets can hypothetically be relatively quickly repaired (e.g. LV wooden poles and conductors) whereas others can take weeks, or even months (transformers and substations). Therefore, even if in a simulation window as narrow as one day the restoration of lines may have begun to occur. Algorithms or approaches should be incorporated to include this at least to a basic level of abstraction to account for the fact that there will be situations where there is a significant outage or fault condition which can be rapidly repaired, versus an outage which may affect only a small area or result in a small ENS but which results in a long outage and hence the cumulative impact is comparable to the more significant event. This matters because the consequences for longer term outages are likely to be far more significant than those of shorter term outages which can be swiftly restored, particularly in, for example, acute cold scenarios. At least some basic consideration must therefore be made for this in the simulation, therefore.

Considering all of these factors, then, the simulation framework can be generally summarised in the format shown in Figure 5.2.

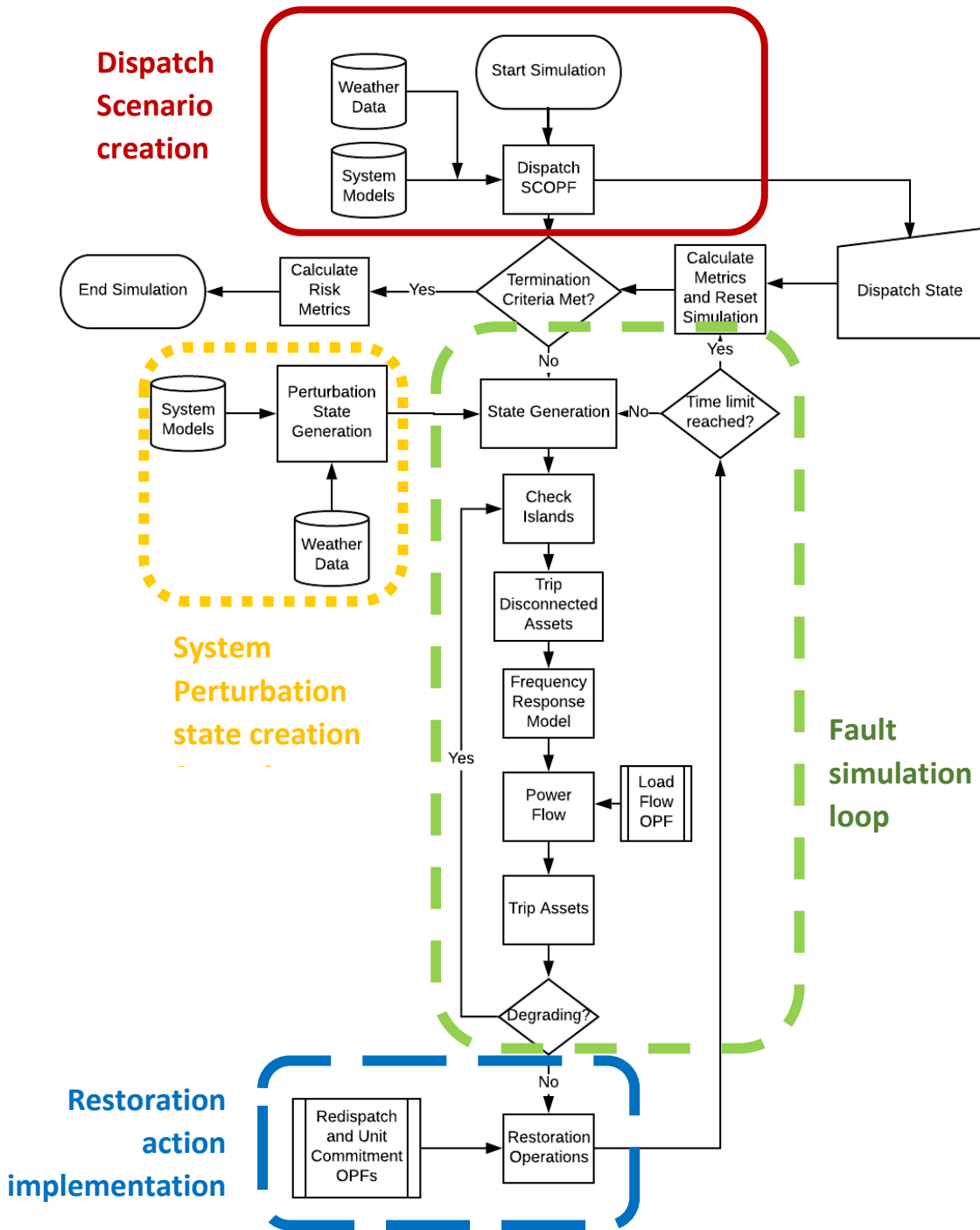


Figure 5.2- Simulation framework for weather-induced cascade modelling with OPFs shown

This draws on concepts from both [77] and [78]. In this case it can be seen that there are four main areas where analysis or simulations are performed. It can also be understood as an expansion of the *Fault Simulator* and *Fault Analysis* blocks demonstrated in Chapter 3. The blocks can be grouped together for a more clear understanding as to the overall structure of the simulation methodology.

The red, solid box is where the dispatch scenario is created. This is generated using forecast or hindcasted weather data paired with system models using relevant data to create a dispatch scenario which will be subsequently perturbed in the simulation model.

The yellow box with the smallest dashes generates a perturbation state based on the incident weather conditions and the asset fault models inherent in the network model.

The green box with the mid-sized dashes is where the actual simulation and processing of the fault event occurs. The perturbation generated by the fault scenario generator is actually implemented in the power system model, and simulated from start to finish of the perturbation itself until the system settles into a state where no further degradation occurs. This is essentially simulating the perturbation from initial fault scenario through to it settling in a degraded, but stable, state.

Finally, in the blue box, restoration actions are scheduled and performed, such as unit recommitment and redispatch. The output from the blue box will be values such as the ENS of the tested state and the perturbation itself (including the revised generation pattern). These are pure economic metrics in absence of any probability-based weighting. The nature of the risk metrics calculated at the end of the simulation depends on the type of simulation being conducted and the information being sought.

There are multiple loops in this framework which should be observed, in particular:

- The loop within the green box for simulating cascade tripping while the system degrades, before the redispatch and unit-commitment OPFs are performed
- The loop from the blue box into the green box, where perturbation states are generated for each hour and the model carries on simulating, accumulating perturbations as the incident event progresses.

This framework is broadly comparable to the work in [78] and serves as an expansion of the *Fault Simulator* block, except it includes consideration of secondary response simulation, system redispatch, system restoration, and weather-related impacts on the system both in terms of the risk of assets and in the contribution of wind power to overall system risk.

The aim of this approach is to integrate a wide array of analysis techniques together to get useful information about the potential variability of risk metrics in a given scenario when changing the input data, or corrections associated with that data.

In [105], it is demonstrated that basing projections of the reaction of the power system on sample sizes which are too small can result in significant inaccuracies in projections based on those samples. For instance, in using a one year sample rather than a larger 25 year sample, Staffell and Pfenninger found that errors in projections of peak demand were around 3% off of the “true” mean, minimum demand net renewables were 13% off, and the error in the number of hours with net negative demand was as much as 23%.

Applying that thinking to simulation of the power system itself, there may be significant errors in the outcomes of power system security evaluations which apply too many simplifications and abstractions to the models which they are simulating, with significant impacts on cost projections and EENS projections. Similarly, as demonstrated in Chapter 4, improving the granularity and resolution of the fragility curves used and representation of line risk on the system may also have a material impact on the simulation of perturbation events as it will change the distribution of simulated events which occur. Similarly, the translation of events generated by the perturbation simulator to the power system model may also have significant impacts on the risk metrics determined from such simulations.

Much as Staffell and Pfenninger examined the potential error associated with under-sampling using a single year and compared it to using a larger sample, in this work case studies will be performed varying the constraints and states of the dispatch scenarios to fully understand the potential variation in output results.

That is, if there is significant variability in the risk metrics associated with a single dispatch state or incident weather scenario when the input parameters are changed, this has consequences for more large-scale resilience and reliability studies which do not go into as much depth in the system simulation as this model attempts to. Alternatively, if changing the level of abstraction does not materially change the results, it implies that these approximations are reasonable and the aspects which have been reduced or ignored are appropriate.

The simulation ensemble as proposed here should be understood as much as concerning the nature of interactions between the different aspects of the simulation model developed as the minutiae of the individual simulation components. That is, given the scale and complexity of the simulation, there are compromises made at each stage that can be iteratively improved on, but at some point the work had to be stopped in order to demonstrate the fundamental principles of the work. Where necessary the reasoning for the compromises made at the time of implementation have been explained, but it is understood that refinements and improvements can always be made to simulations such as this.

A major aspect of the contributions made and novelty of this section of work is the ensemble effort and understanding of how the ensemble of simulations work together and why.

#### 5.4 Data sources and assumptions for simulation

The data required for the comprehensive simulation can be broadly broken down into two separate areas: weather data, and system data. Exact values will be given in the formulation, but the sources and assumptions behind the derivation of these values will be discussed here.

A reasonably detailed analysis and comparison of weather data sources is performed by Dawkins in [6]. System data pertaining to generating facilities, loads, and network parameters for lines and transformers are difficult obtain as, particularly for the GB network, they are distributed across a variety of sources. Network and wind farm data used in Chapter 4 could be used for power system analysis insofar as it provides node, branch, and wind farm location data. However, the wind farm data (location and capacity) must be converted into a format usable in a power systems context- that is, wind farms need to be mapped to nodes and buses on the power system model.

Without knowing the exact network connectivity and data pertaining to individual wind farms (and, given the pace of change in the GB network, this is difficult even for network operators to keep track of), a heuristic method would be needed to at least form a basic approximation of the locations and connectivity of windfarms. Similarly, the wind farm data used in Chapter 4 includes hundreds of individual, commercially connected wind farms e.g. ones connected to an industrial site at the Michelin plant in Dundee which have a total capacity of <5MW. Such data would have to be aggregated in some way to remain useful in the simulation without compromising model tractability.

With the power system model, failure rates for synchronous machine generators were derived from [61]. Conversely, failure rates for wind turbines were taken from the same paper but the data w.r.t. the DC link rather than generators. This is based on the assumption that the power curve in itself carries some representation of the availability of individual turbines aggregated to the level of a wind farm, and the only way total loss of infeed from a windfarm to the grid would be a total failure of the grid connecting power converter or sufficient HWSS to render the net output zero.

For the simulations considered here, only random generator faults or wind-induced OHL faults will be considered. That is, it is assumed failure rates at lower wind speeds are analogous to the rates of random outages, whereas at higher wind speeds the wind-failure mechanisms become dominant and the driver of failures. Therefore, no additional consideration is considered necessary for random outages.

Such data was mapped using a method which involved the use of the Haversine equation to determine the km distance between every single windfarm and each node from the network model. The node to which each windfarm had the lowest distance was the one to which each wind farm was therefore assigned. This can be visually represented as shown in Figure 5.3.

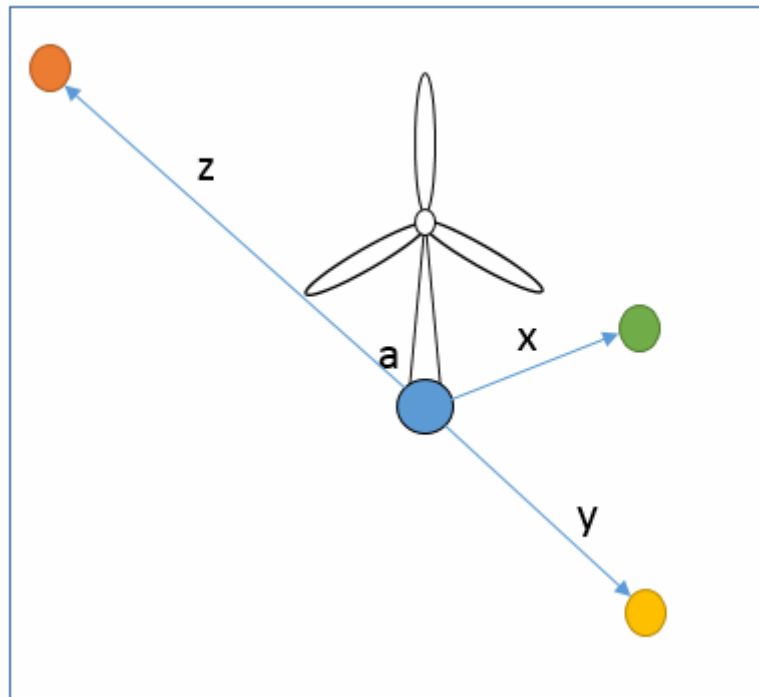


Figure 5.3 - Graphical representation of windfarm mapping

In this case, the Haversine equation is used to estimate the distance  $x$ ,  $y$ , and  $z$  between the origin point  $a$ , and the respective points at which the buses are located. The windfarm is then assigned to the bus which has the minimum distance. The elevation of each point is ignored, only “as the crow flies” distance is considered. The windfarm in this case would, by inspection, be assigned to point  $x$ . Location data for individual buses was simply taken from the model used in Chapter 4. The windfarm is treated as a single point for the derivation of total power capacity given a set weather condition, using the corrected power curve also derived in Chapter 4.

In the simulation model, the fragility curves derived in [64] are used, with the same data bins, adapted for use in the software. This marks a progression in power system simulation as lines have not been represented in such a fashion in the literature examined herein, especially not in the context of security assessments.

The data sources used for the power simulation are again those used in Chapter 4 – namely [87, 88] from the NASA MERRA-2 dataset [86]. These are used due to the spatiotemporal completeness of the data, and as it can be readily corrected to account for geographical features as discussed in Chapter 4.

The locational data, network and system data pertaining to the test networks was taken from multiple sources: the NG ETYS [95], the RPD 2018 [91], and from data provided by C. MacIver of the University of Strathclyde, and with modifications made to update the network and make it appropriate for use in a DCOPF. This covers the basic data necessary for the formulation of a DCOPF, but did not include appropriate example cost functions for generators, nor did it include costs for things such as generator tripping or wind power curtailment. Data on costs was taken from [57], and was intended to be indicative rather than absolute representations of cost.

For the purposes of the SFR simulation, typical constants were used that would reasonably be expected of the GB system based on values taken from [68] and [67]. The system, during a frequency excursion, is assumed to act as a single thermal generator acting with droop control and frequency responsive load – load damping is not considered directly.

Hydroelectric generation and interconnectors are included in this, in that it is assumed their contribution can be bundled into the system-wide “representative” single bus and the specific phenomena associated with these inputs into the system can be ignored at a system scale. Wind generation is assumed to be nonresponsive to frequency deviations (i.e. its output stays fixed during system perturbations), and with interconnectors has zero contribution to system inertia. This is a conservative assumption, as research does show that wind can hypothetically have a contribution to system inertia via so-called “synthetic inertia”, which is discussed in [68], but in the framework being proposed this was deemed, at the time of writing, to be outwith the bounds of investigation and the assumption was deemed appropriate.

In this context it was deemed that in some instances it was better and more useful to be conservative, and given the SFR is only needed to be approximate to the system frequency, and certain proxies and abstractions are already being made, this was deemed to be appropriate if sub-optimal, particularly given the difficulty associated with quantifying what the actual inertial contribution of power-converter technologies actually is. As has been previously discussed, individual loads and generators may “see” a different frequency from the system-wide average, but as a first approximation a single, homogenous frequency profile was used for the single bus representations and all generators were assumed to respond, proportionally, identically and ideally based on the control algorithm used. In reality, a hydro plant will react differently from an inverter, which is different from a nuclear plant. Certain assumptions are made to separate these factors but for frequency-responsive generators these were not directly differentiated. This will be further elaborated in this section and in 5.5.1.6.

Representing UFLS also presents a challenge for system operators as, in GB, the thresholds at which load is shed depend both on the frequency deviation itself and the location of the bus at which LFDD is taking place. Buses therefore need to be classified based on the transmission owner region in which they are located. Thresholds were therefore taken from the Grid Code [73] and buses assigned to regions based on data provided by C. MacIver. The specific values used will be discussed in Section 5.5.4 when relevant to the model formulation. Series compensators are treated as OHL with line ratings corresponding to those of adjacent lines, as a basic approximation. Transformers, too, are treated as connecting branches. The winter ratings associated with the lines are used as their nominal values due to the timing of the test case in question, with an emergency rating corresponding to a 130% of the nominal value. The long-term emergency post-contingency rating was set to the normal winter rating on the assumption that, because the example being used is during a high wind example in the winter, sufficient ambient cooling would be present to allow the line temperatures to drop within acceptable bounds.

Hydroelectric plant – both pumped storage and run-of-river- is assumed to be able to provide primary, secondary, and tertiary response, and is assumed to be able to sustain primary response through to tertiary response.

So too are interconnectors, as it is assumed the power electronics can adjust their output accordingly and maintain the new output.

Nuclear plant is assumed to be unable to act as primary frequency response, but can provide secondary response, but this cannot be sustained into tertiary response. Alternatively it can provide tertiary response without secondary frequency response. In GB, nuclear typically does not directly deploy response- but globally it can be deployed as such.

In order to limit the complexity of the simulation, coal plant is assumed to be able to provide primary, secondary, or tertiary response, but only one for each scenario (that is, it can exclusively provide one form of response to which it is scheduled. In reality it may be able to provide all three.

Gas plant, both open-cycle and closed-cycle, has the same restrictions.

The Ryan Model lists some connected generation as “Other” or “CHP”. This is assumed to act in a similar manner to both Gas and Coal plant, in lieu of more complete information.

Of course these assumptions are imperfect, and there is scope for refinement and adjustment for each of them, but limiting the problem boundaries and avoiding obfuscation via over-complication was a key concern. The assumptions, therefore, were based on discussions with colleagues and what would be deemed reasonable and appropriate for the fundamental work being undertaken to demonstrate the methods.

## 5.5 Model implementation

Taking all of the relevant data sources together, then, the model needs to be implemented. The formulation and implementation shall approximately be considered, then, in terms of the boxes described in Section 5.2.

Prerequisite knowledge about the formulation and deployment of SCOPFs is presumed and important for understanding how various aspects of the model link together, but the mathematical formulations provided, as well as the flow charts, should provide enough information to provide at least a base level understanding of the fundamental processes at play. References to comparable methodologies and studies are also provided for further information.

### 5.5.1 Mathematical Formulations

This part of the simulation model is particularly concerned with generating the state which the user wishes to test. Therefore, a reasonable dispatch state is necessary if a security assessment is to be performed such that the results reflect a reasonable, realistic dispatch scenario one might reasonably expect to experience on the system. One could also take historic balancing data and map it to the system with approximations made as regards the dispatch and location of frequency reserve response, and availability of generators – such data is nontrivial to access and apply to such network models, however.

The power system model generated broadly approximates the GB transmission system such as it was assembled in approximately 2015/16, but updated with 2018 wind data. This corresponds to a peak demand of ~58GW, wind capacity of ~20GW, and total connected synchronous generation of ~68GW.

Sites such as Hinkley Point, whose nominal total output is stated at around 1320MW, were broken down into equal generators of 660MW or less, and this rule of thumb was applied to every large generator on the network. There are a significant number of small wind generators in the data, and so in the model, wind farms were aggregated to equal units of 1GW or smaller based on the assumption the largest single infeed from a farm would be associated with a 1GW feeder or interconnector.

In order to determine an appropriate generation dispatch profile, a DC security constrained OPF (DC-SCOPF) was implemented and deployed. This was based on work in [57], and implementing linearized frequency-related constraints derived from [60], [67], and [68]. Some parameters which are used within the software implementation for data processing purposes – but which are not actually used in the optimization itself – are omitted for clarity. Data types used in *pyomo* [59] are also given. The complexity of the model necessitates it be described in sections for clarity to ensure each step is described for the purposes intended. The constraints and objective functions shall also be given and a description given thereof. The mathematical formulation described hence refers to the *Dispatch SCOPF* highlighted in Figure 5.4.

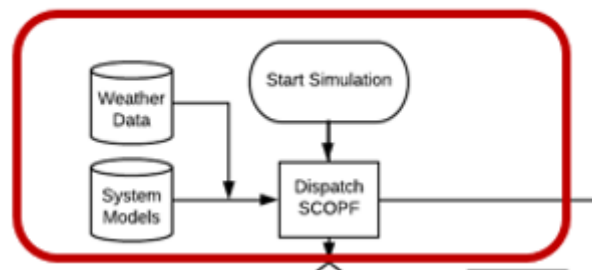


Figure 5.4 - relevant section of simulation algorithm

### 5.5.1.1 Dispatch-SCOPF formulation – parameters

The parameters used in the formulation of the Dispatch-SCOPF dispatch problem are described in Table 5.1. These represent broadly typical parameters used in comparable DC Security-Constrained Optimal Power Flow studies and simulations with some new additions related to the SFR and frequency reserve scheduling, which shall be described in further detail in the implementation of the SFR in Section 5.5.4.

Table 5.1 - parameters used in DC-SCOPF formulation

| Parameter            | Type             | Description                                       |
|----------------------|------------------|---|
| $g$                  | Positive integer | Index of generator in generator set $G$           |
| $t$                  | Positive integer | Time-step in time set $T$                         |
| $k$                  | Positive integer | Index of contingency state in contingency set $C$ |
| $b$                  | Positive integer | Index of bus in bus set $B$                       |
| $i$                  | Positive integer | Area index parameter                              |
| $g_{min,g}$          | Real             | Minimum real power output of generator $g$ (MW)   |
| $g_{max,g}$          | Real             | Maximum real power output of generator $g$ (MW)   |
| $\epsilon_{fuel,g}$  | Positive real    | Fuel cost of generator $g$ (£/MWhr)               |
| $\epsilon_{start,g}$ | Positive real    | Startup cost of generator $g$ (£/MWhr)            |
| $\epsilon_{shed,g}$  | Positive real    | Curtailment cost of load $l_o$ (£/MWhr)           |
| $g_{ramp,g}$         | Positive real    | Ramp rate of generator $g$ (MW/min)               |
| $\epsilon_{trip,g}$  | Positive real    | Trip cost on generator $g$ (£)                    |
| $H_{s,g}$            | Positive real    | Inertia constant of generator $g$                 |

|                     |                  |  |
|---------------------|------------------|--|
| $S_g$               | Positive real    | S rating of generator $g$ (MWs)  |
| $w$                 | Positive integer | Index of wind generator in set $W$                                     |
| $w_{CF,t,w}$        | Real             | Capacity factor of wind generator $w$ at time $t$                      |
| $w_{cap,w}$         | Real             | Total capacity of wind generator $w$ (MW)                              |
| $\epsilon_{curt,w}$ | Positive real    | Curtailement cost of wind generator $w$ (£/MWhr)                       |
| $lo$                | Positive integer | Index of load in set $LO$  |
| $d_{lo}$            | Positive real    | Real gross power demand of load $lo$ (MW)                              |
| $d_{lo}^+$          | Positive integer | Load “area” of load $lo$   |
| $li$                | Positive integer | Index of line in set $LI$  |
| $X_{li}$            | Real             | Reactance of line $li$ (p.u.)  |
| $F_{nom,li}$        | Real             | Nominal (continuous) line real power rating of $li$ (MW)               |
| $F_{c,li}$          | Real             | Short term emergency (STE) real power rating of $li$ (MW)              |
| $F_{24,li}$         | Real             | Long term emergency (LTE) real power rating of $li$ (MW)               |
| $\gamma_{k,t,li}$   | Binary           | Service status of line $li$ at time $t$ in state $k$                   |
| $\epsilon_{x,lo}$   | Real positive    | Value of lost load (VoLL) of load $lo$ (£/MWhr)                        |
| $\epsilon_{dr,lo}$  | Real positive    | Cost of Flexible Demand Response on load $lo$ (£/MW)                   |
| $\tau$              | Positive integer | Time constant to change granularity of simulation w.r.t time           |
| $M$                 | Real positive    | Base (100MVA)  |
| $\tilde{a}$         | Real positive    | Estimated flexible demand attrition (p.u.)                             |
| $a$                 | Real positive    | Actual flexible demand attrition (p.u.)                                |
| $\alpha_{k,t,g/w}$  | Binary           | Service status of asset $g$ , $w$ , or $li$ , at time $t$ in state $k$ |
| $g_{min,g}$         | Real             | Minimum power output of generator $g$ (MW)                             |
| $g_{max,g}$         | Real             | Maximum power output of generator $g$ (MW)                             |
| $D_{k,t,lo}$        | Real positive    | Net real power demand on $lo$ at $t$ in case $k$                       |

### 5.5.1.2 Dispatch-SCOPF formulation – variables

As with the parameters, Table 5.2 shows a mix of standard DC-SCOPF variables and atypical values which represent the association with a frequency-response model and the need to schedule appropriate primary, secondary, and tertiary frequency response. These will be described in further detail both in context of the constraints to which they apply and how they interact with the SFR model.

Table 5.2 - variables used in DC-SCOPF formulation

| Variable            | Type          | Description   |
|---------------------|---------------|---|
| $w_{0,t,w}$         | Real          | Nominal dispatch of wind generator $w$ at time $t$ (MW)                       |
| $F_{k,t,li}$        | Real          | Flow across $li$ at time $t$ in state $k$ (MW)                                |
| $s_{k,t,lo}$        | Real negative | Load curtailment at load $lo$ at time $t$ in state $k$ (MW)                   |
| $\phi_{k,t,b}$      | Real          | Voltage angle at bus $b$ at time $t$ in state $k$                             |
| $w_{curt,k,t,w}$    | Real          | Wind curtailment on generator $w$ at time $t$ in state $k$ (MW)               |
| $\rho_{t,g}$        | Real negative | Primary frequency response scheduled on generator $g$ at time $t$ (MW)        |
| $\beta_{t,g}$       | Real negative | Secondary response scheduled on generator $g$ at time $t$ (MW)                |
| $\beta^*_{t,g}$     | Real negative | Net secondary response scheduled on generator $g$ at time $t$ (MW)            |
| $\chi_{t,g}$        | Real negative | Tertiary frequency response scheduled on generator $g$ at time $t$ (MW)       |
| $p_{k,t,g}$         | Real          | Real power from generator $g$ in at time $t$ in state $k$ (MW)                |
| $g_{0,t,g}$         | Real          | Real power dispatch from generator $g$ at time $t$ (MW)                       |
| $d_{k,t,lo}$        | Real positive | Net real power on load $lo$ at time $t$ in case $k$ (MW)                      |
| $up_{k,t,g}$        | Real negative | Upwards redispatch on generator $g$ at time $t$ in case $k$ (MW)              |
| $down_{k,t,g}$      | Real positive | Downwards redispatch on generator $g$ at time $t$ in case $k$ (MW)            |
| $\lambda_{k,t,g/w}$ | Binary        | Trip variable at for generator $g$ or $w$ at time $t$ in case $k$ (1=tripped) |
| $\omega_{t,lo}$     | Real positive | Flexible demand which returns in secondary phase at time $t$ (MW)             |

|                   |               |  |
|-------------------|---------------|--|
| $\Omega_{t,lo}$   | Real positive | Flexible demand linearly restored in tertiary phase at time $t$ (MW)   |
| $A_{t,g}$         | Binary        | Decision variable representing generator $g$ being used as primary frequency response at time $t$                      |
| $B_{t,g}$         | Binary        | Decision variable representing generator $g$ being used as secondary frequency response at time $t$                    |
| $C_{t,g}$         | Binary        | Decision variable representing generator $g$ being used as tertiary frequency response at time $t$                     |
| $\gamma_{t,g}$    | Binary        | Decision variable representing if $g$ is committed (=1) at time $t$  |
| $off_{t,g}$       | Binary        | Decision variable indicating generator $g$ has been switched from in service to out of service in dispatch at time $t$ |
| $on_{t,g}$        | Binary        | Decision variable indicating generator $g$ has been switched from out of service to in service in dispatch at time $t$ |
| $\bar{T}_g$       | Binary        | Minimum up time of generator $g$   |
| $\underline{T}_g$ | Binary        | Minimum down time of generator $g$   |
| $\Psi_{t,g}$      | Real negative | Frequency response inadequacy (MW)   |
| $r_p$             | Real positive | Primary frequency requirement (MW)   |
| $r_s$             | Real positive | Secondary frequency requirement (MW)   |
| $o_{t,i}$         | Real          | Inter-area transfer at time $t$ from area $i$  |

### 5.5.1.3 DC-SCOPF formulation – network-related constraints

$$-a_{k=0,t,li}F_{nom,li} \leq F_{k=0,t,li} \leq a_{k=0,t,li}F_{nom,li} \quad (5.1)$$

$$-a_{k,t,li}F_{c,li} \leq F_{k,t,li} \leq a_{k,t,li}F_{c,li} \quad (5.2)$$

$$\frac{M(\varphi_{k,t,a} - \varphi_{k,t,b})}{X_{li}} = F_{k,t,li} \forall \text{ lines if } a_{k,t,li} = 1 \quad (5.3)$$

$$\sum_{a=1\dots lo} D_{k,t,a} + \sum_{b=1\dots g} p_{k,t,b} + \sum_{c=1\dots li} F_{k,t,c} - \sum_{d=1\dots li} F'_{k,t,d} + \sum_{e=1\dots w} w_{k,t,e} = 0 \quad (5.4)$$

$$a_{k,t,g}\gamma_{t,g}g_{max,g} \geq g_{0,t,g} \geq a_{k,t,g}\gamma_{t,g}g_{min,g} \quad (5.5)$$

$$g_{max,g}a_{k,t,g}(1 - \lambda_{k,t,g}) \geq p_{k,t,g} \geq a_{k,t,g}(1 - \lambda_{k,t,g})g_{min,g} \quad (5.6)$$

$$p_{k,t,g} = g_{0,t,g} + up_{k,t,g} + down_{k,t,g} \quad (5.7)$$

$$up_{k,t,g} \geq -\gamma_{t,g}\tau g_{ramp,g}a_{k,t,g}C_{t,g} \quad (5.8)$$

$$down_{k,t,g} \leq \gamma_{t,g}\tau g_{ramp,g}a_{k,t,g}C_{t,g} - \lambda_{k,t,g}g_{min,g} \quad (5.9)$$

$$p_{k=0,t,g} = g_{0,t,g}a_{k=0,t,g} \quad (5.10)$$

$$a_{k,t,g}\gamma_{t,g}g_{max,g} \geq g_{0,t,g} + up_{k,t,g} + down_{k,t,g} \geq a_{k,t,g}\gamma_{t,g}g_{min,g} \quad (5.11)$$

$$a_{k,t,g}\lambda_{k,t,g} = 0 \quad (5.12)$$

$$D_{k,t,lo} = d_{t,lo} \quad (5.13)$$

$$w_{k=0,t,w} = w_{0,t,w} \quad (5.14)$$

$$w_{k,t,w} = w_{0,t,w} a_{k=0,t,w} - \lambda_{k,t,w} w_{CF,t,w} a_{k,t,w} w_{cap,w} + w_{curt,k,t,w} \quad (5.15)$$

$$\lambda_{k,t,w} a_{k,t,w} = 0 \quad (5.16)$$

$$w_{curt,k,t,w} \leq -w_{CF,t,w} w_{cap,w} a_{k,t,w} \quad (5.17)$$

$$\begin{aligned} -g_{ramp,g}\tau + on_{t,g} g_{min,g} &\geq g_{0,t,g} - g_{0,t-1,g} \\ &\geq g_{ramp,g}\tau - of_{t,g} g_{min,g} - \lambda_{k=0,t,g} g_{min,g} \end{aligned} \quad (5.18)$$

$$\gamma_{t,g} - \gamma_{t-1,g} = on_{t,g} a_{k=0,t,g} - of_{t,g} a_{k=0,t,g} \forall t > 0 \quad (5.19)$$

$$on_{t,g} + of_{t,g} \leq 1 \quad (5.20)$$

$$\begin{cases} \gamma_{0,g} + on_{t,g} + \sum_{a=t \dots \overline{T_g}} of_{a,g} \leq 1 \forall t < \overline{T_g} \\ on_{t-\overline{T_g},g} + \sum_{a=t-\overline{T_g} \dots t} of_{a,g} \leq 1 \forall t + \overline{T_g} \leq T_{max} \\ on_{t,g} + \sum_{a=t \dots T_{max}} of_{a,g} \leq 1 \end{cases} \quad (5.21)$$

$$\begin{cases} \gamma_{0,g} + \sum_{a=t \dots \overline{T_g}} on_{a,g} \leq 1 \forall t < \overline{T_g} \\ of_{t-\overline{T_g},g} + \sum_{a=t-\overline{T_g}-1 \dots t} on_{a,g} \leq 1 \forall t + \overline{T_g} < T_{max} \\ of_{t,g} + \sum_{a=t \dots T_{max}} on_{t,g} \leq 1 \end{cases} \quad (5.22)$$

These constraints describe a reasonably typical Unit Commitment DC-SCOPF with redispatch and varying line flow limits, but also with wind-varying and curtailable wind generation. For clarity, unless otherwise stated or described herein it is assumed the constraints act for all variables associated with the given indices in the constraint (e.g. (5.5) applies  $\forall k$  states,  $t$  times, and  $g$  generators). These constraints form the backbone of the “network” side of the dispatch problem. That is, the granularity is set to 10 minutes and effectively the model dispatches the generator dispatch in the  $k=0$  state to minimise the cost of running the network for a given hour while ensuring all of the security criteria are met. The objective function shall be discussed later as some aspects of it remain to be described.

(5.1 and 5.2) constrain the flow of lines in nominal or contingency states. These constraints ensure that in normal, continuous operation the continuous line flows are within the limits set, whereas these limits are relaxed in contingency states ( $k \neq 0$ ) to the branch STE ratings.

(5.3) determines the voltage angle and flow between bus  $a$  and  $b$  in set B based on the flow between the respective nodes across branch  $li$  assuming said branch is functional in the contingency state  $k$  at time  $t$ .

(5.4) is the node balance constraint, which ensures the power balance at every node is equal to zero. That is, the sum of the net demand, the power from generators connected at a given node, the flow into and out of the node, and the net power from wind generators connected to that node must always equal zero. The indices  $a, b, c, d$ , and  $e$  refer to all of the relevant asset classes connected at the given node.

(5.5) to (5.12) enforce the constraints on generation in the dispatch problem. That is, the generator dispatch can only be nonzero if it is committed, functional, and not tripped. The net final output of the generator must also always be between its minimum and maximum, if it is operational.

The adjustment of the output of the generator to restore the supply-demand balance is constrained by the ramp rate of the generator and the time constant. In this case, in going from the nominal state  $k=0$  to a contingency state  $k$  the output of a generator can only be increased or decreased by up to  $a_{k,t,g} \gamma_g \tau_g \text{ ramp}_{g,C_g}$ , either positively or negatively, but if the generator faults its output can be forced to zero if and only if it is faulted and the trip variable is set to 1. This effectively prevents generators in the dispatch from being allowed to trip off in “normal”, planned for, conditions to maintain system security.

(5.13) tells the model that, in all cases, the net demand must equal that of the expected demand on the system on that node at a given time. That is, no load curtailment is allowed and all load must be supplied for the security conditions described.

(5.14) to (5.17) regulate the wind power infeed on the system. Wind power cannot exceed the maximum capacity of the wind farm multiplied by the capacity factor determined by the incident weather conditions on that wind farm. Further, there cannot be more wind power curtailed than is actually available at a given node. Finally, there is no equivalent limitation on the tripping of wind generators as it is assumed the power electronics used to connect a wind farm have the ability to reconnect or disconnect the generation from the MITS at time scales far smaller than an equivalent synchronous or conventional machine - they can however still be “tripped”. (5.18 to 5.22) control the unit commitment of generators and the ramp rates.

These are conservative assumptions in many cases, but the aim here was not to represent ideally a market with generators freely coming in and out of service, but reasonable hypothetical situations where generators can come into service and disconnect but would not reasonably expect to consistently be dropping in and out of service. Rather, they would operate at minimum stable generation rather than disconnect, if they could, and still gain revenue and the operator would wish to avoid repeatedly paying startup/connection costs to generators.

#### 5.5.1.4 Dispatch-SCOPF formulation – frequency related generator constraints

Crucially, these constraints have not yet alone fully incorporated the frequency-response side of the problem, which shall now be described as regards the frequency response provision from *generators*.

$$\rho_{t,g} + \beta_{t,g} + g_{0,t,g} \geq g_{min,g} \gamma_{t,g} \forall \text{ non-sustaining } g \quad (5.23)$$

$$\rho_{t,g} + g_{0,t,g} \geq g_{min,g} \gamma_{t,g} \forall \text{ sustaining } g \quad (5.24)$$

$$\rho_{t,g} \geq 0.1 \gamma_{t,g} g_{min,g} \forall \text{ primary capable } g \quad (5.25)$$

$$\rho_{t,g} \geq 0.1 A_{t,g} g_{min,g} \quad (5.26)$$

$$\rho_{t,g} = 0 \forall \text{ non-primary } g, w \quad (5.27)$$

$$\beta_{t,g} \geq 0.1\gamma_{t,g}g_{min,g} \forall \text{ secondary capable } g \quad (5.28)$$

$$\beta_{t,g} \geq 0.1B_{t,g}g_{min,g} \forall \text{ secondary capable } g \quad (5.29)$$

$$\beta_{t,g} = 0 \forall \text{ non-secondary } g,w \quad (5.30)$$

$$\beta_{t,g}^* \geq \rho_{t,g} \forall \text{ sustaining } g \quad (5.31)$$

$$\beta_{t,g}^* = \beta_{t,g} \forall \text{ non-sustaining } g \quad (5.32)$$

$$\chi_{t,g} \leq up_{k,t,g} \quad (5.33)$$

$$A_{t,g} + B_{t,g} + C_{t,g} \leq 1 \forall \text{ non-sustaining } g \quad (5.34)$$

These constraints then begin to link the frequency response adequacy problem, while not specifying the actual frequency response requirements themselves. This formulation assumes the model is dispatching generation for loss of infeed events, and that the system can handle loss of demand events straightforwardly via down-ramping and footroom in generators across the system, and thus does not need to schedule response to meet them as such.

(5.23 and 5.24) connect the dispatch of primary and secondary frequency response to the output limitations of the generators themselves, in much the same manner as (5.11) which connects the maximum power output of a given generator to its upwards or downwards redispatch. The difference being between these equations that the presumption is any generator which can sustain its primary response into secondary and/or tertiary response will do so (e.g. hydroelectric).

(5.25 and 5.26) limit the maximum possible frequency response deployable by a primary-frequency responding generator of any kind to 10% of its maximum output, and link this to the binary decision variable assigning the given generator to primary frequency response and to that generator's commitment status. That is, a generator can only contribute primary frequency response if it is committed and operational in the first instance and it has been assigned to do so.

In constraints (5.27 and 5.30) the available primary and secondary frequency response deployable is, as one would expect, limited to zero if the generators are presumed to be incapable of primary response or AGC/secondary frequency response.

The constraints (5.28 and 5.29) calculate the net contribution of secondary response from a given generator. This is to avoid double-counting of primary and secondary response in the formulation should a response provider sustain its primary response as secondary response (e.g. interconnectors, hydro in this implementation). (5.33) determines the maximum deployed tertiary response from any single generator across all contingency states, and hence how much tertiary reserve needs to be scheduled for that generator (assuming enough is scheduled ahead of time to meet the maximum necessary adjustment upwards of that generator).

Finally, for this group of constraints, (5.34) ensures that generators cannot be assigned to multiple different stages of response – that is, that primary response generators require time to recover from providing frequency response and cannot provide secondary or tertiary response and return to their original output as they are replaced by secondary response, and so on for secondary generators. That is, unless the generator is specifically able to provide frequency response across frequency domains (at least for the timescales involved in frequency response), such as run of river or adequately prepared pumped storage hydro.

These constraints describe the limitations on generators' abilities to contribute frequency response to the system, but they do not describe or constrain how much is actually required within the system itself.

Constraints (5.25, 5.26, 5.28, and 5.29) which state that only 10% of the maximum output of a generator can be used as frequency response, will in themselves naturally cause some distribution of frequency response across the system, but that in itself may not be adequate for some of the situations described. This is particularly an issue given the potential for localised effects of wind-storms which could see significant variability in wind power across boundaries or due to ramping effects.

Two different sets of constraints for determining frequency response requirements are therefore proposed for comparison and use in the simulations, which reflect potential different mindsets or approaches which an operator may take, and are defined with their respective constraints also given.

$$\sum_{a=1\dots a} -\rho_{t,a} - \sum_{b=1\dots b} \omega_{t,b} - \sum_{b=1\dots b} \Omega_{t,b} - \sum_{b=1\dots b} \Psi_{t,b} \geq r_{p,t} \quad (5.35)$$

$$\sum_{a=1\dots a} -\beta_{t,a} + \sum_{b=1\dots b} \omega_{t,b} - \sum_{b=1\dots b} \Psi_{t,b} \geq r_{s,t} \quad (5.36)$$

This first pair of constraints mandates that all the deployed primary and secondary response on the system be met by a combination of generation response (primary and secondary, reflected by the  $\rho$  and  $\beta$  variables) and FDR  $\omega$  and  $\Omega$  deployed at loads  $1\dots b$ . FDR is, in this model, assumed to take two forms: that which must be restored by secondary response (i.e. short term response from sources which may be sensitive to anything more than interruption for a few tens of seconds or for which anything more than such an interruption may cause customer inconvenience, e.g. EV chargers) or demand response which can be restored over longer timescales, such as non-critical thermostatic loads.

A correction factor can also be added to  $\omega$  and  $\Omega$ . This would serve the purpose of representing a reduction in the effective amount of FDR of that nature deployed. For example, a factor of 0.5 would mean half as much demand response was contributing to the net frequency response requirement as was scheduled – effectively the model would be dispatching twice as much as that which was expected to turn up as a way of hedging.

Subscript  $a$  and  $b$  represent subsets of generators and loads. These could be sets which include all generators across the system, or subsets of generators or loads within specific predefined areas. The use of FDR which must be restored in secondary response timescales increases the secondary frequency response required, which is reflected in (5.36), whereas this same FDR increases the amount of primary response deployable, as observed in (5.35).

The  $\Psi$  variable represents a value to allow some slack in the calculations given the conservative nature of the frequency response dispatch requirements. Its effect is that it decreases the net frequency response requirement but this is associated with a significant cost. This relaxation is only used in some scenarios and the variable can otherwise be considered fixed to zero.

The reason such an allowance could be deemed acceptable is that the dispatch formulation does not consider the fact that loads can be affected by frequency deviations themselves and system load will drop during times when frequency drops, which can be thought of as an inherent response of the system from demand which can be a useful property.

Where there is inadequate frequency response available to meet primary and secondary frequency response requirements and the SCOPF solution is infeasible for a given scenario, this variable can be nonzero to allow convergence even if there is insufficient frequency response in the system to meet a stated requirement, but an associated penalty will be levied in the objective function.

A nonzero  $\psi$  means that the frequency following a loss of infeed  $\geq r$  will rest at a value  $< f_{nom}$ . However, so long as this value is kept appropriately small, this means that the frequency should still be able to be restored to  $f_{nom}$  so long as there is adequate tertiary response scheduled.

For typical frequency response dispatches, this should be an insignificant figure on a system-scale compared to the scheduled frequency response from generators. The intention of this methodology is to understand the significance of varying the scheduling of frequency response itself. This is also based on the assumption that, for N-1 scenarios on realistic, well-developed networks in reasonably expected situations, there should reasonably be enough frequency response to handle a typical system perturbation in reasonable operating conditions.

Unless otherwise stated, this value is constrained to 0 and can be ignored. However, if convergence issues in the dispatch emerge this was allowed to be limited to  $< 50\text{MW}$ - small enough to be effectively negligible on system scale, but allowing a slight flexibility in the problem formulation itself to test extreme cases, as this formulation is designed to do.

This is a suboptimal representation of such a problem, but as with many issues in the formulations presented it represents a solution that is in place and can be replaced in future. It should be remembered that the point of the initial SCOPF here is to generate a dispatch state which could, under the criteria determined and presented, represent, at least, a reasonable approximation for the state in which the system might find itself before a perturbation. For reasons which shall become obvious, ultimately the initial dispatch itself is not nearly as significant as the restrictions on aspects such as minimum up, down time, and which assets fail at what times.

Returning to the dispatch problem under discussion, the requirement  $r$  can be determined in various ways. It can be set as an absolute parameter (e.g. 1320MW, representing single largest infeed at maximum output – to represent a large nuclear plant for example) or set based on the actual single largest output from a generator  $g$  or wind farm  $w$ .

This pair of constraints can be considered as an *absolute value* (AV) frequency response requirement. That is, the frequency response requirement is set simply based on a single parameter value. This may over (or under) estimate the actual frequency response requirement across the system, but is in line with deterministic security standards such as the grid code which mandate that the system has to be able to deal with the largest single loss of infeed on the system.

Alternatively, to deal with situations where one wishes there to be a given distribution of frequency response across an interconnection, the following constraints can be used to determine the inter-area transfer across a given boundary.

$$o_{t,i} = \sum_{a=1\dots a} d_{t,a} + \sum_{b=1\dots b} g_{0,t,b} + \sum_{c=1\dots c} w_{0,t,c} \quad (5.37)$$

$$\sum_{i=1\dots i} o_{t,i} = 0 \quad (5.38)$$

These determine the inter-area transfer between two pre-defined areas. A net negative  $O$  value infers the area is exporting, while a net positive infers import (as the positive demand exceeds negative supply). The indices  $a, b$ , refer to loads and generators respectively. The  $r$  value for primary or secondary response within an area can then be set such that it is greater than, for example, 1) the import into that area from the other network 2) the single largest wind infeed 3) the single largest generator or interconnector infeed. A truly N-1 secure system should have enough frequency response to deal with all of these issues.

A supply excess on the supplying network could be met by tripping excess wind generation during windy periods, whereas extra frequency response could be commissioned in the receiving network to ensure any loss of infeed could be adequately met. Case studies examining this and the impact of changing these frequency response requirements will be examined in further detail in due course.

#### 5.5.1.5 Dispatch-SCOPF formulation – objective function

Finally, the objective function for the DC-UCSCOPF is given.

$$\begin{aligned}
 \min \quad & \sum_{g=1\dots g} \sum_{t=1\dots t} (-\epsilon_{fuel,g}(g_{0,t,g} + \rho_{t,g} + \beta_{t,g} + \chi_{t,g}) \\
 & + \epsilon_{startup,g}on_{t,g}) \\
 & + \sum_{lo=1\dots lo} \sum_{t=1\dots t} (-\epsilon_{dr,lo}(\omega_{t,lo} + \Omega_{t,lo})) \\
 & + \sum_{w=1\dots w} \sum_{t=1\dots t} -\epsilon_{curt,w}w_{curt,t,w} - \sum_{lo=1\dots lo} \Psi_{t,b}\epsilon_{shed,lo}
 \end{aligned} \tag{5.39}$$

This effectively works to minimise the cost of generation dispatch, the cost of frequency response, and cost of wind curtailment (as wind is assumed to have zero marginal fuel cost), and the cost of demand response, while all the above security constraints are met. An objective function generally can be understood as reflecting the priorities of an operator on a system.

If  $\Psi$  is zero, the associated term can be ignored and the OF works to minimise the costs associated with a dispatch state (the cost of frequency response, the cost of fuel, the startup costs of generators). If there are convergence issues and the  $\Psi$  is allowed to be nonzero, the first priority of the OF is likely to be to minimise the cost associated with this as it is weighed by the cost of load curtailment, valued at £17,000MWh<sup>-1</sup>. Now that the formulation of the dispatch problem is complete, the formulation of the SFR problem can be undertaken.

#### 5.5.1.6 System Frequency Response simulation

The SFR simulation (represented within the flow diagram as “Frequency Response Model”) is a time-resolved quasi-steady-state based representation of a standard system frequency response simulation. It was developed in a format which can be relatively straightforwardly implemented in a language such as python which does not have the support of GUI-based simulation software other languages may provide. In the development phase this presents difficulties, particularly in linking the problem to the wider simulation platform, but the benefit of creating the model in a bespoke manner such as has been done here is that custom algorithms can be implemented and modified in a way other software solutions may not support, and the interactions between the SFR model and other aspects of the simulation can be controlled more directly. The granularity of the simulation can also be easily changed by varying a time constant.

This simulation is deployed in the SFR-load flow loop, as indicated in Figure 5.5, with the SFR model operating in the block indicated.

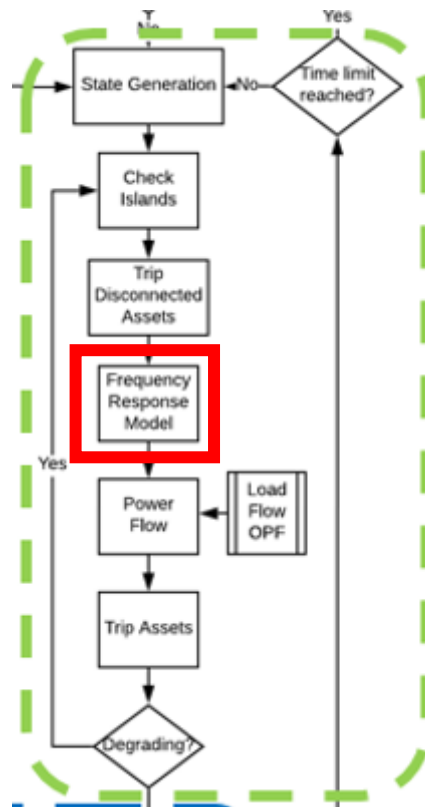


Figure 5.5 - location of frequency response simulation in wider model framework

This offers an improvement on the inclusion of frequency in conventional SFR-OPF models as it allows time-sensitive generator tripping and load shedding which can consider load shedding schemes such as those set out in the Grid Code, rather than the need to use heuristics such as those which were deployed in Chapter 3. This is a clear advancement in realism in the simulation being implemented and allows a far greater variety of events and a greater complexity in simulation than previously was implemented. The parameters and variables used in the SFR simulation are provided below.

| Quantity     | Type          | Description   |
|--------------|---------------|---|
| $f_t$        | Real positive | System frequency at time $t$ (Hz)                               |
| $L_t$        | Real positive | Net total system demand at time $t$ (MW)                        |
| $P_t$        | Real positive | Net total system power infeed at time $t$ (MW)                  |
| $P_{max}$    | Real positive | Net maximum real power on system (MW)                           |
| $P_{min}$    | Real positive | Net minimum real power on system (MW)                           |
| $\Delta d_t$ | Real positive | Net total system frequency demand adjustment at time $t$ (MW)   |
| $\Delta P_t$ | Real          | Net total system power imbalance at time $t$ (MW)               |
| $\delta P_t$ | Real          | Power adjustment signal (MW)                                    |
| $R_{droop}$  | Real positive | System droop  |
| $\delta_p$   | Real positive | Deadband of primary frequency response (Hz)                     |
| $\delta_s$   | Real positive | Deadband of secondary frequency response (Hz)                   |
| $f_{nom}$    | Real positive | Nominal system frequency (Hz)                                   |
| $\bar{f}$    | Real positive | System frequency used in load flow to minimise error (Hz)       |
| $\hat{f}$    | Real positive | Output system frequency from frequency response simulation (Hz) |
| $\Delta$     | Real positive | System error value  |

|              |               |  |
|--------------|---------------|--|
| $\Delta L_t$ | Real          | Frequency-related load adjustment (MW)             |
| $H_{s,t}$    | Real positive | Inertia constant at time $t$ (s)                   |
| $S_{t,g}$    | Real positive | S rating of generator $g$ at time $t$ (MW)         |
| $T_{rh}$     | Real positive | Reheat time constant                               |
| $F_{hp}$     | Real positive | High pressure fraction                             |
| $T$          | Real positive | Time step size to change granularity of simulation |
| $\delta f_t$ | Real          | Quasi-steady-state rate of change of frequency     |

The relevant formulae used are shown.

$$\delta f_t = \frac{\Delta P_t f_{nom}}{2H_t T} \quad (5.40)$$

$$\Delta P_t = P_t - L_t - \Delta L_t \quad (5.41)$$

$$\Delta L_t = K \frac{f_{t-1} - f_{nom}}{f_{nom}} L_t \quad (5.42)$$

$$\delta P_t = \begin{cases} \frac{(f_t - f_{nom})}{f_{nom}} \frac{F_{hp} P_t}{R_{droop} T_{rh} T} & \forall P_{min} < P_t < P_{max}, \\ 0 & \text{otherwise} \end{cases} \quad (5.43)$$

$$H_t = \frac{(\sum_i S_{t,i} H_i)}{\sum_i S_{t,i}} \quad (5.43)$$

These are derived from standard low order SFR models such as [67], literature on frequency response such as [60], and an implementation of a straightforward SFR model as shown in [68]. (5.40) describes the calculation of quasi-steady-state changes in frequency on the system. (5.41) calculates the power imbalance on the system at any given time. (5.42) calculates the adjustment in system load associated with deviations from nominal system frequency. (5.43) is the adjustment in output power on the system associated with frequency deviations based on standard SFR models and treating the entire aggregated system model as a single bus representation of a thermal generator. That is, all generators on the system are aggregated in the SFR and, if they are frequency responsive in the relevant section of the simulation (i.e. primary or secondary frequency response), their net contribution to changes in the system power output is calculated using (5.43), which caps any net power output based on maximum or minimum limits in headroom or footroom.

The values of  $L$ ,  $P$ , and  $H$  are calculated based on the generation connected at a given island. Effectively the model calculates the frequency deviation, determines the response from load, determines the response from flexible demand, and then calculates the net power imbalance, and iterates this as the model moves forward through quasi-steady-states and calculates the change in frequency at each timestep, re-calculating the variables in situ.

The exact algorithm will be described in the *System Frequency Response Features* section.  $P_{max}$  is determined by taking the absolute value of the sum of generators on the system and adding the total scheduled primary or secondary frequency response of the contributing generators.  $H_t$  also varies with time as, when generators trip, inertia on the system will be lost.  $P_{min}$  is determined by taking either 1) 10% of the net generator output contributing to frequency response's output or 2) the difference between the generator's individual power contribution at time  $t$  and its minimum total output (or, given the dispatch formulation treats generation infeed as a negative value, its "maximum").

Frequency response is generally dispatched on the basis of assuming it is handling loss of generation rather than excess demand on the assumption that generation can adjust downwards to handle overloads, so that approach is taken here.  $L$  is the net demand derived from the sum of all connected loads and can be reduced by either load shedding or demand response, the capacity of which is derived from the dispatch SCOPF.

Once the frequency response of the system has been calculated, a load flow is performed to determine if any line overloading and tripping occurs. The formulation of this power flow is now given.

### 5.5.1.7 Load Flow OPF formulation

In the load flow optimisation, all the generator output values, demand curtailment, and wind generation are fixed in the solver as a feature of *pyomo*. This OPF is solved following the SFR simulation, as indicated in Figure 5.6.

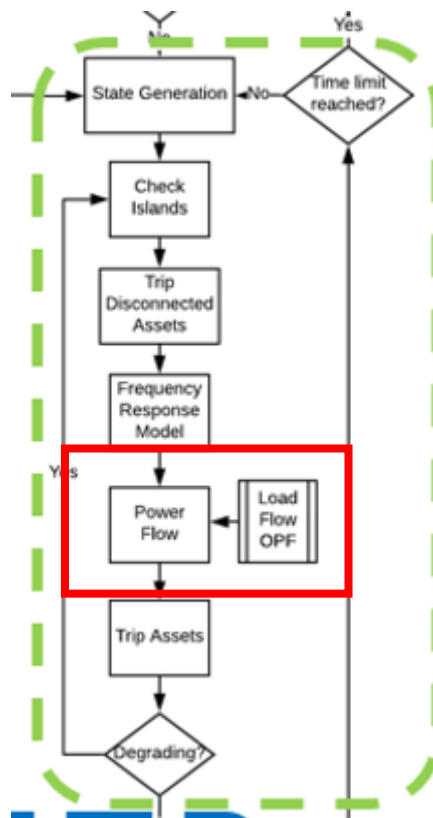


Figure 5.6 - location of load flow OPF in context of wider framework

Therefore, the majority of the constraints limiting generator output etc. used in the UC-DC-SCOPF are redundant. To that end, only the constraints pertaining to line flow limits, voltage angle, and node balance are required (5.3 and 5.4) to be carried forward. However, in this case, the only constraints on line flows are that lines out of service are constrained to line flows of zero and the voltage angle constraints which act across those lines do not apply. The net demand on a node can be represented by the constraint:

$$D_{k,t,l} = d_{l_0} + x_{l_0} + \Omega_{l_0} + K(d_{l_0} + x_{l_0} + \Omega_{l_0}) \frac{(\tilde{f} - f_{nom})}{f_{nom}} \quad (5.45)$$

which reflects the fact that the load curtailment and deployed frequency response is fixed, based on the values extracted from the dispatch and frequency response. Indices  $K, t = 0$  in this instance. The

net demand can only be changed by varying the  $\tilde{f}$  value to change the net load. This value is linked to the constraint (5.46).

$$-\Delta \leq \frac{\bar{f} - \tilde{f}}{\bar{f}} \leq \Delta \quad (5.46)$$

This allows some discrepancy between the frequency extracted from the SFR simulation and that which corrects the demand on the system, to account for rounding or floating point errors which could cause feasibility issues in the solver. The objective function is then simply the following

$$\min \Delta \quad (5.47)$$

which minimises the discrepancy between the load flow and the results of the SFR to map the results of one onto the other.

After this is completed, the model checks for lines which are overloaded and trips any which are or attempts to re-close any which have already been re-closed. That will be discussed in the *Line Overload Simulation* section. The assumption being that if the loads, reference buses, and power infeed from generators are consistent – and frequency-related demand adjustment is consistent – the load flows should reflect a realistic scenario for each island. The reference bus for each load flow is fitted based on being assigned to the node with the greatest power infeed. All loads and generators with zero routes to the reference bus are ignored. Each island’s frequency response is modelled in turn in this manner.

Assuming the system has settled into a state where there is no subsequent load shedding or overloads, the model progresses to modelling the deployment of tertiary response/removal of secondary response. That is, the islands’ frequency response and cascade simulations are performed in turn, and each island’s SFR-load flow loops are iterated until there are no remaining overloads or unacceptable frequency excursions.

#### 5.5.1.8 Redispatch OPF formulation

The results from the earlier simulations are collated and combined such that the initial conditions of the redispatch simulation match the ending states of the islands created by the SFR and perturbation simulations. In this case, only one case is simulated for 10 minutes (i.e.  $\tau = 1$ , set T is size 11 including 0). This is to replicate tertiary support replacing generation which has adjusted inputs to restore frequency during secondary response and to replace demand curtailed by operators. This is labelled as “Restoration Operations”, as indicated by the following section of the framework:

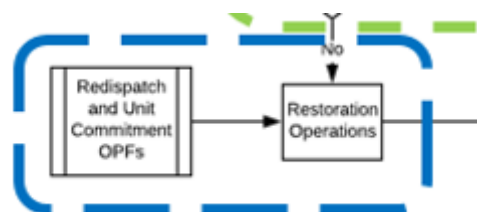


Figure 5.7 - location of redispatch, UC-OPFs in simulation framework

It is assumed that no new generators can come online in this time period, and so the results of the Unit Commitment and SFR are used to determine what generators are online, and at what output. Primary frequency generation has its outputs fixed across the redispatch simulation (on the

assumption the generator is recovering and no further adjustment of output is possible. Secondary frequency-responding generation linearly decreases (or increases) back to its nominal dispatch value. Tertiary response is free to adjust its output as required. The frequency used in this stage of simulation is a fixed parameter that gradually changes from the value determined on each island in the SFR to the nominal value at  $T_{max}$ . The standard DCOPF formulae from the original formulation are used with the exception of the unit commitment constraints. That is, constraints (5.3, 5.4, 5.6, 5.8, 5.9, 5.14, 15.15, and 5.17) are used from the original dispatch. The following additional or modified constraints are also deployed.

$$-a_{k=0,t,li}FC_{,li} \leq F_{k=0,t,li} \leq a_{k=0,t,li}FC_{,li} \quad \forall t > 0 \quad (5.48)$$

$$D_{k=0,t,a} = d_{k=0,t,a} + x_{k=0,t,a} + \Omega_{t,a} \quad (5.49)$$

$$+ K(d_{k=0,t,a} + x_{k=0,t,a} + \Omega_{t,a}) \frac{(f_{t,b} - f_{nom})}{f_{nom}}$$

$$D_{k=0,T_{max},a} = d_{k=0,T_{max},a} + x_{k=0,T_{max},a} \quad \forall t = T_{max} \quad (5.50)$$

$$p_{k=0,t,g} = p_{k=0,t-1,g} + up_{t,g} + down_{t,g} \quad \forall t > 0 \quad (5.51)$$

$$up_{t,g} \geq -g_{ramp,g} \tau \gamma_{t,g} a_{k=0,t,g} \quad (5.52)$$

$$\forall A_{t,g} + B_{t,g} = 0$$

$$down_{t,g} \leq g_{ramp,g} \tau \gamma_{t,g} a_{k=0,t,g} - \lambda_{t,g} g_{min,g} a_{k=0,t,g} \quad (5.53)$$

$$\forall A_{t,g} + B_{t,g} = 0$$

$$\lambda_{k=0,t,g} \geq \lambda_{k=0,t-1,g} \quad \forall t > 0$$

$$p_{k=0,t,g} = g_{0,t,g} (1 - \lambda_{k=0,t,g}) \quad (5.53)$$

$$\forall A_{t,g} + B_{t,g} = 1$$

This then represents a reasonably conventional DC-OPF with the exception that the net demand of a load is corrected for load, FDR, and frequency-related effects. The model dispatches such that at  $T_{max}$  the frequency is equal to the nominal frequency so the K-adjacent terms in (5.49) disappear. The line flow limits are assumed to be the STE (30 minute) limits of the lines as the system is operating in a contingency state. The generators and wind infeed are free to change in  $t = 1$  onwards but are fixed at  $t = 0$ . The index  $a$  refers to the subset of loads in set  $l_0$  which lie within the island  $i$  at frequency  $f$ . Index  $b$  classifies assets on the island  $i$  experiencing the given frequency  $f$  at time  $t$ .

Generators which are unassigned from any frequency response, are classed as sustaining, or are assigned as tertiary response, are the only ones which are assumed to be able to redispatch in a controlled manner in this stage. Primary and secondary frequency responding generators' outputs are fixed in this stage using the value  $g_{0,t,g}$  so their outputs are either those determined by their change in output associated with their frequency response tailing off, that is, the value fed into the model from the SFR simulation.

If necessary, generators can "trip off" to zero output at this stage but remain tripped for the rest of the simulation until, in the Unit Commitment, the minimum down time for that type of generator has

been exceeded after the trip event. This is a somewhat conservative assumption but ensures a feasible solution can always be found in the redispatch.

The objective function is as follows:

$$\begin{aligned}
 \min \quad & \sum_{t=1 \dots t} \sum_{g=1 \dots g} \lambda_{t,g} \epsilon_{trip,g} \\
 & + \sum_{t=1 \dots t} \sum_{a=1 \dots a} \epsilon_{fuel,a} (down_{t,a} - up_{t,a}) \\
 & - \sum_{t=1 \dots t} \sum_{lo=1 \dots lo} x_{t,lo} \epsilon_{shed} \\
 & + \sum_{t=1 \dots t} \sum_{w=1 \dots w} w_{curt,t,w} \epsilon_{curt,w}
 \end{aligned} \tag{5.55}$$

This minimizes the “cost” of generator tripping, readjustment to generators not otherwise scheduled as tertiary response but otherwise available, and load curtailment costs. Adjustment costs on tertiary generators are assumed to already be considered from the original dispatch and are not “double charged” in that sense in the redispatch. The index  $a$  represents the subset of generators which were unassigned as frequency response. Generators which are unassigned have a redispatch cost assumed, as a conservative estimate, as equivalent to the fuel cost/hr rate. As the cost of load curtailment and generator tripping (assumed as £17,000MWhr<sup>-1</sup> for VoLL and £10,000/action for tripping) vastly outweigh the fuel and redispatch cost, getting exact figures for the redispatch costs was deemed less important so such conservative assumptions could be deemed appropriate.

Now that the tertiary response has replaced secondary response, the final stage of the simulation can take place – the unit re-commitment and restoration.

#### 5.5.1.9 Restoration UC OPF formulation

This represents the final stage of the simulation loop, whereby the model starts trying to plot a restoration vector on the system to restore the supply-demand balance. In effect it uses the same constraints as those used in the original formulation, with the exception that they all apply only from  $t > 0$  as all values at  $t = 0$  are fixed based on the results of the redispatch simulation. The values of frequency response assigned to each generator are fixed based on the original dispatch (or, if the simulation is from a secondary fault, carried forward again). Generators which have tripped or are faulted are assumed to stay offline until their minimum restoration time in hours has elapsed.

Generators which were originally off – or have exceeded their minimum “down time” had they been on and then subsequently been deactivated – have their outputs fixed to zero until their minimum down time has elapsed as well.

Lines which were tripped and locked out after reclose operations are assumed to be reconnected after an hour. Frequency response is assumed to recover the hour after the fault event simulated. Generators which have tripped are assumed to contribute no further primary or secondary response.

The frequency response requirements are not enforced, rather the amount of frequency response deployed on the system is carried forward with the outputs of generators constrained appropriately. Once this has been solved, the loop can begin again with each asset sampled again.

If there is insufficient supply to meet demand, it is assumed load can be freely curtailed with an associated cost based on VoLL and is scheduled ahead of time. The net demand at each node is then

reduced should automated LFDD be deployed in subsequent SFR simulations. That is, the demand constraint represented by (5.13) is replaced with the following constraint, which allows demand curtailment.

$$D_{k=0,t,lo} = d_{t,lo} + x_{t,lo} \quad (5.56)$$

To reflect the fact some generators have tripped off and may be required to reconnect, a new variable is introduced to represent a binary switching on of a generator from tripped status following the redispatch simulation. In effect it has the same effects as the *on* variable but has zero cost associated with it. This is based on the assumption that a generator which faulted off would try and reconnect as quickly as possible and is not considered an “additional” commitment and so does not have the associated cost in the objective function. Further, the down time unit commitment constraints are enforced, but modified, but it is assumed that, in an emergency, a generator may be tripped off before its minimum up time had passed. The modified Unit Commitment constraints are shown below.

$$\begin{aligned} -g_{ramp,g}\tau + (on_{t,g} + re_{t,g})g_{min,g} &\geq g_{0,t,g} - g_{0,t-1,g} \\ &\geq g_{ramp,g}\tau - off_{t,g}g_{min,g} \\ &\quad - \lambda_{k=0,t,g}g_{min,g} \end{aligned} \quad (5.58)$$

$$\begin{aligned} \gamma_{t,g} - \gamma_{t-1,g} &= (on_{t,g} + re_{t,g})a_{k=0,t,g} \\ &\quad - (off_{t,g} + \lambda_{k=0,t,g})a_{k=0,t,g} \forall t > 0 \end{aligned} \quad (5.59)$$

$$\left\{ \begin{aligned} \gamma_{0,g} + \sum_{a=t \dots T_g} (on_{a,g} + re_{a,g}) &\leq 1 \forall t < T_g \\ off_{t-T_g,g} + \sum_{a=t-T_g-1 \dots t} (on_{a,g} + re_{a,g}) &\leq 1 \forall t + T_g \leq T_{max} \\ off_{t,g} + \sum_{a=t \dots T_{max}} (on_{a,g} + re_{a,g}) &\leq 1 \end{aligned} \right. \quad (5.60)$$

$$\sum_{t=1 \dots t} re_{t,g} \leq \lambda_{k=0,t=0,g} \quad (5.61)$$

One challenge with this UC problem is the fact that, generally, unit commitments have to make assumptions about the availability and up and down times of generators before the dispatch window in which they are solving. That is, assumptions are made about how long generators have been on or off before  $t = 0$  of the window in which they are solved. This is no problem for the original dispatch – it can be assumed that generators have been on long enough before the UC problem such that they can turn off at any point after  $t > 0$ , and conversely that generators have been off long enough before the UC problem such that they can turn on at any point after  $t = 0$ . This is difficult to capture in the formulation for subsequent problems. This was circumnavigated by counting for how many hours generators had been offline or tripped when the restoration UC problem is solved and fixing the *on* and *re* variables to zero for all values where the total time a generator had been offline was less than the minimum down time of the given generator, preventing the generator from switching on.

After every iteration of the simulation loop, generators which are online are counted as having 0 hours offline. Generators which are off have 1 added to a cumulative total and the first  $n$  hours on each offline generators have their *on* and *re* variables fixed to zero so the generator cannot switch off, notwithstanding the other unit commitment variables. That is, if a fault occurs at  $t = 2$  hours and a

generator has been off for those 2 hours and has a minimum down time of 4 hours, the generator cannot be activated until  $t = 2$  or later in the restoration UC which equates to 4 total hours after the initialization of the simulation. This is another example of the strength of separating the separate aspects of simulation – it allows recording of aspects such as this and creative solutions to address them – but also a consequence of more detailed modelling; if the problem was not so comprehensive, these issues would not have to be considered in the first place.

The objective function is given below.

$$\begin{aligned} \min \quad & \sum_{t=1 \dots t} \sum_{g=1 \dots g} (\lambda_{k=0,t,g} \epsilon_{trip,g} + \alpha n_{t,g} \epsilon_{startup,g}) \\ & - \sum_{t=1 \dots t} \sum_{lo=1 \dots lo} x_{t,lo} \end{aligned} \tag{5.62}$$

This is based on the presumption that, following a large outage event such is being simulated here – and, given frequency response and reserve generators already have their outputs fixed based on the original or previous dispatches problem solutions, the model uses the assets available to it to minimise generator tripping costs, the number of generator “on” actions, and load curtailment across the system. Given the costs of these features dwarf any associated cost with fuel costs of generators they were deemed negligible given much of the generation outputs across the system were in some way fixed anyway.

This ends the mathematical formulation of the simulation model.

#### 5.5.1.10 Summary of OPF formulation

The DC-UC-SCOPF can be understood as a mixed integer linear problem (MILP) with binary and real values as solutions to the linearized equations described, linked to a nonlinear quasi-steady-state frequency response simulation, load flow calculation, redispatch simulation, and UC-OPF.

The formulation of the DC-SCOPF itself is based on conventional optimisation problems used in power system analysis as referenced, but the additional requirements of the model deployed here and the number of variables incorporated in the simulation mean there are several unconventional nomenclatures within the formulation (e.g. frequency response problems are not typically wrapped within linearised DC network representations, and so  $f$  and  $F$  represent very different aspects of the simulation).

The simulation complexity grows with both model scale and the security rules deployed or desired by the user to represent different security requirements. That is, the set  $k$  depends on the list of contingencies which the user (representative of a system operator) may wish for the system to secure against. At a high level, the SCOPF in effect attempts to schedule generation and frequency response across the system such that:

- 1 No load curtailment happens within the predefined dispatch states in the nominal state
- 2 The cost of generation dispatch and commitment is minimised
- 3 The cost of wind curtailment in the nominal case is minimised
- 4 No line overloads occur following redispatch of generation
- 5 Adequate frequency response (primary, secondary, and tertiary) is available to meet requirements subject to requirements and the contingency list
- 6 Generators do not trip out of service during normal operation

- 7 Wind generation cannot be used for primary or secondary frequency response but can be curtailed and then un-curtailed to be used as tertiary response following the deployment of conventional frequency response

The frequency response requirements and contingency lists can then be defined by the user based on whichever security conditions or rules are desired. The efficacy of these can then be compared in the results.

What is also new in this formulation is the capacity of the network operator (the agent represented by the SCOPF minimising the objective function) to be able to schedule and utilise flexible demand response as primary frequency response which could be adapted in future to be more realistic and subject to different constraints dependent on a classification between e.g. “essential”, “non-essential” loads.

Frequency response problems are difficult to reconcile with SCOPFs due to the fact they typically rely on a single-bus representation of a system with aggregated reservoirs of load and generation which interact in some manner with a system frequency response model. Further, including frequency-adjusting loads in a power system simulation could introduce nonlinear constraints which are computationally expensive to handle and may require more specialised optimisation algorithms.

In this case, the frequency response constraints and more standard OPF constraints were associated with each other, indirectly linking the network-side problem to the frequency-response side problem which has not previously been done in SCOPFs, particularly when weather-sensitive generation is also included in the formulation.

Various features should be noted at this stage. Firstly, the sheer volume of variables is indicative of the complexity of the simulation subject. There are over 60 variable types mentioned between the frequency response and dispatch problems alone, with more being added at subsequent stages. This is the primary reason for some of the variables being used utilising unconventional nomenclature – there are only so many Greco-Roman characters available that would make sense to be used in the formulation. The model is dispatching frequency response across three different time-domains 0-30s after fault, 30s~15m after the fault, and ~15m – 1hr after. The model attempts to reconcile very different areas of analysis in an ensemble in a way which has not been done before, and of course this first such implementation is non-ideal.

The optimisation is performed and solved using the *pyomo* [106] library in the *python* programming language. The *gurobi* [107] optimisation suite is used to solve the problem. This solver returns both an objective function value (that is, the cost of the dispatch) and the variable values as output from the initial solving of the dispatch problem. Computation time scales with increased contingency list size as well as changing frequency reserve rules. The different frequency response rules and different contingency list sizes will be compared and the consequences of these will be discussed as well as what these represent.

The aim of the dispatch DC-SCOPF is to capture as many different phenomena and features of a dispatch problem as possible. This then means that the subsequent frequency response simulations represent as reasonably as possible a sensible dispatch policy that could be expected on a power system. Generators are assigned to different types of frequency response and load flows are enforced with reasonable security standards.

With the generation of a reasonable starting state, analysis can then be performed on that state to examine the different potential fault states which could emerge. The remainder of this section shall discuss the separate aspects of the simulation as they pertain to the overall simulation structure.

The fuel cost associated with each generator type was derived from [57]. Though generally speaking generator bid/offer actions will have different costs associated with them, in this case in the simplified representation of generation dispatch only an approximation of fuel cost was directly considered in the formulation. The fuel cost of generation was not the main priority of the dispatch scenario in this research.

Different sections of the modelling framework – which herein may also be referred to collectively as the *Extreme Weather Perturbation Simulator* (EWPS) – operate over different timescales, representative of the fact different hazards and phenomena on the power system also operate over different time horizons. These are summarised in the following table and associated figure.

Table 5.3 - summary of simulation timescales and features

| Simulation                | Resolution    | Time horizon   |
|---------------------------|---------------|----------------|
| Dispatch SCOPF            | Hourly        | 12 hours       |
| System Frequency Response | Milliseconds  | 60 seconds     |
| Load flow OPF             | Instantaneous | Zero           |
| Redispatch OPF            | Minutes       | ~15m           |
| Unit Commitment OPF       | Hourly        | Up to 12 hours |

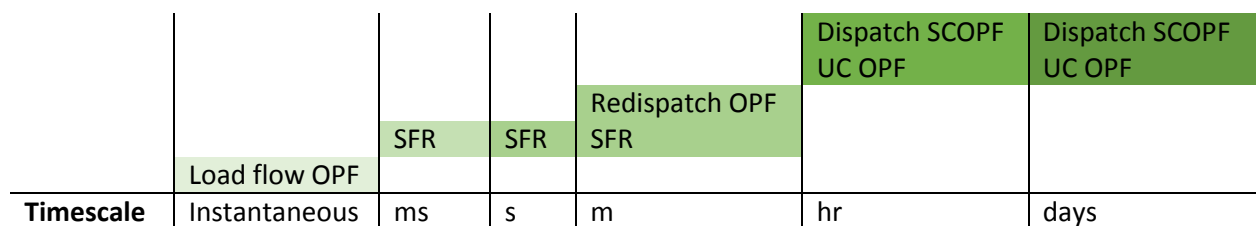


Figure 5.8 - timescales of different simulations within framework

### 5.5.2 Perturbation State Generation

Before any simulation can be run on a given situation to evaluate the consequences of a given outage, credible outage scenarios have to be generated. The subject matter under consideration in this study is that of extreme wind’s impact on resilience and reliability, and so that was the focus of the simulation. The methodology developed in Chapter 4 was used to determine failure rates across individual lines and estimate wind power across the system, but for failure rates of wind farms and power stations different approaches had to be made.

It was assumed that generator and wind generator failure rates were independent of wind, and the failure rates used were derived from data from the 1996-RTS [61]. Failure rates for wind farms required different assumptions. As wind farms are distributed resources – that is, a single “generator” in the power system model does not in fact represent a single turbine but an aggregated grouping of turbines, it is assumed that losses of individual turbines within that group would be captured by the assumptions inherent in the derivation of the power curves themselves. Therefore, the only way an entire wind “generator” could be lost would be associated with loss of infeed to the system from the single critical point in the system – the interconnector from infeed to grid. This is assumed to act like a power-electronic based converter to the main grid but in reality wind turbines may also have their own power inverters such that their connection to the grid is in AC. Substation faults were not considered, and so in lieu of that the failure rate for windfarms was assumed to be comparable to that

of a DC line interconnector converter. Therefore, the failure rate associated with each wind farm was assumed to be comparable to that of a DC line converter, also taken from the 1996-RTS.

The failure rates used are given in Table 5.4. Failure rates for lines are derived by the methods shown in Chapter 4 and thus are not shown.

Table 5.4 - failure rates used in model

| <b>Generator Type</b> | <b>Failure rate (/hr)</b> | <b>MTTF (hr)</b> |
|-----------------------|---------------------------|------------------|
| <i>Wind</i>           | $2.00 \times 10^{-5}$     | 50000            |
| <i>Hydro</i>          | $5.05 \times 10^{-4}$     | 1980             |
| <i>CCGT/OCGT</i>      | $9.09 \times 10^{-4}$     | 1100             |
| <i>Nuclear</i>        | $8.70 \times 10^{-4}$     | 1150             |
| <i>Coal</i>           | $8.70 \times 10^{-4}$     | 1150             |
| <i>CHP/other</i>      | $2.22 \times 10^{-3}$     | 450              |
| <i>Interconnector</i> | $2.51 \times 10^{-5}$     | 39825            |

These act as broad approximations – different types of gas and nuclear generators will naturally have different failure rates. However, like many other aspects of the simulations used herein, they are assumed to act as an appropriate first approximation.

Now that failure rates are assumed for generators and wind turbines, and a methodology for quantifying OHL risk has been assumed, the generation of a fault state for analysis can be undertaken. This can be described using the following pseudocode.

---

***In each hour of each sample:***

*For line in list of lines:*

*For section in subsections of line:*

*Generate random number*

*If random number < probability of failure of subsection*

*Take line out of service*

*For generator in generators:*

*Generate random number*

*If random number < probability of failure of generator class:*

*Take generator out of service*

*For wind farm in wind farms:*

*Generate random number*

*If random number < probability of failure of generator class:*

*Take wind farm out of service*

---

The primary concern in these simulations concerns the consequences of a failure on the power system. Therefore, for purposes of determining an EFL value as discussed in Chapter 4 the location of a given fault could also be recorded- but that was not done for these simulations.

This section of the model operates entirely independent of the dispatch problem itself and is intended to perturb an already “known” system state. Once the dispatch information is known and the exact

faults caused on the system are known, the consequences of that fault scenario can then be investigated via simulation.

### 5.5.3 Check Islands and Trip Disconnected Assets

The primary reason for linking together a network-based optimal power flow type problem with a frequency response simulation problem was to investigate the relationships between the spatial distribution of frequency response and the ability of that frequency response to be delivered during system perturbations.

Generally, frequency response is dispatched based on the assumption that the response across the system will be distributed in such a way that it can be fully delivered to the system as and when it needs to be without incurring further system problems such as line overloads and cascading outages. This is difficult to capture in a standard OPF formulation but the proposed approach directly addresses that by wrapping both problems into the same model.

The reason network failures may inhibit the ability to deliver frequency response to the system is twofold – lines connecting generation to the system which is scheduled to provide frequency response may fail, or islands may be created separating generation-heavy areas from demand-heavy areas – such as the loss of the B6 boundary (which shall be described in greater detail in section 5.6.2) between Scotland and England on a particularly windy day. Therefore, two approaches present themselves.

In Chapter 3, it is assumed that the loss of two specific nodes from the main system represents the loss of the B6 boundary and hence the loss of everything North of that. In reality this may not necessarily be the case and Scotland may be able to sustain itself entirely unharmed. Therefore, within the simulation model there needs to be the ability for the model to consider different islands in turn and then recombine those islands when suitable. In reality, resynchronising grids following an outage will be challenging, requiring the use of synchro-check relays. This shall be discussed in the Restoration Simulation section.

If an outage event creates multiple islands these are each analysed in turn, but if subsequent line overloads create more islands after the initial event, these are assumed to blackout. This is based on the assumption that reference buses are generally assigned to nodes with the greatest amount of power generation connected to them, and that the loss of the two largest power output nodes for a given island would almost certainly result in a total loss of that island due to instability or power loss.

Once a perturbation state has been created and is fed into this module, first, the model has to determine if multiple islands have been created. As a first order approximation, it is assumed if the perturbation state only consists of generator or windfarm faults, there is no initial islanding on the network and it remains contiguous.

The algorithm for identifying and generating the islands used for subsequent analysis is described in the following pseudocode.

---

*Run system search using NetworkX to find nodes with zero connectivity to ref. bus*  
*Generate list of islanded nodes*  
*Determine power infeed at each node*  
*While list of islanded nodes not empty:*  
    *Determine node at which maximum power infeed connected*  
    *Assign as new reference bus*  
    *For node in list of islanded nodes:*  
        *If node connected to new reference bus:*  
            *Remove from list of islanded nodes*

---

This script effectively builds a list of islanded nodes, assigns new reference nodes, and tries to determine the connectivity of the subsequent subnets until all nodes are accounted for. This then provides a set of subnets which can be subsequently analysed with frequency response to determine if any further system degradation occurs in these subnets and how severe the system degradation is.

#### 5.5.4 System Frequency Response features

Now that the simulator has a series of islands to analyse, each of these islands will have their own supply-demand balance, inertia properties, and available frequency response. Therefore, the frequency response of each will have to be simulated in turn.

The formulation of the frequency response simulator and relevant parameters, variables, and equations are described in 5.5.1 The derivation of the frequency response model was a consolidation of work developed in [68] and from first principles referred to in work such as [60]. Each island in the system is considered in turn. Different facets of the frequency response simulation and the implementation shall be described herein. It acts as a series of quasi-steady-state simulations with the assumption of 10ms timesteps between quasi-steady-states.

##### A. Generator Tripping Behaviour

As well as the general formulation of the system frequency response simulation, various rules and assumptions had to be made about how different generators actually respond during system frequency changes. The representations for different actions automated systems and network operators might take during a major frequency deviation event also have to be considered, particularly how generators and demand may respond to a major fall or spike in frequency.

An approach similar to that used in [78] is used to determine generator tripping probabilities during the system frequency response simulation. That is, above a given threshold there is assumed a probability of 1 that a generator will trip, and below a certain threshold it is assumed there is a zero probability a connected generator will trip. Between these thresholds the trip probability is linearly interpolated, as illustrated by Figure 5.9, taken from [78].

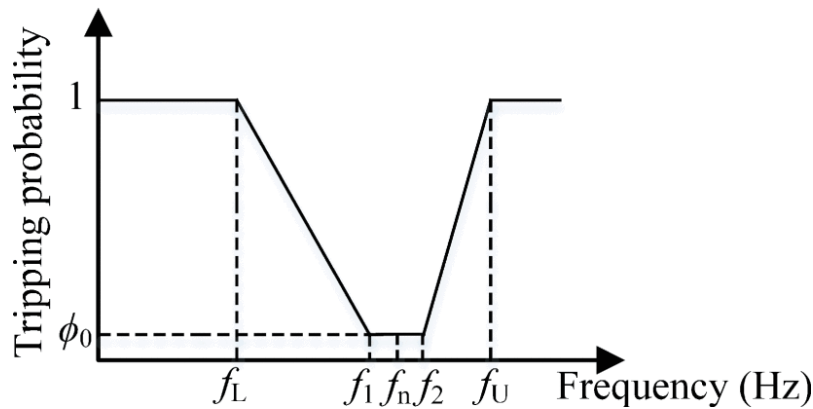


Figure 5.9 - Typical generator tripping scheme

In the implementation of the model deployed, only over-frequency tripping of generators is considered. Instead, an absolute minimum frequency is defined in the model and if the frequency drops below that level the system is assumed to black out.

The maximum frequency threshold, referred to as  $f_u$  in the chart, on the system is assumed to be 52Hz. This is a conservative assumption, as generators in GB are permitted to trip independently once frequency rises above 52Hz. The frequency  $f_2$  indicated on the figure, beyond which generators start tripping, is assumed to be 50.5Hz (i.e. the statutory limit for frequency on GB). The blackout frequency on GB is assumed to be 47.8Hz. Frequency response actions are intended, fundamentally, to keep generators on the system – if all generators are lost, the system has to be entirely restarted (i.e. a black start condition). To prevent that, generators can reduce their output downwards in high frequency situations, before they trip. In low-frequency situations, there are a wide variety of assets available to operators to restore supply-demand balance – and hence frequency. The last resort is performed LFDD; pre-determined disconnection of loads at locations distributed across the country. This is to prevent frequency falling below thresholds at which generators begin to trip and disconnect, leading to further cascading outages.

One challenge with representing load curtailment is that, in simulations, various heuristics tend to be used to represent this load curtailment – such as were used in Chapter 3. Other actions before LFDD-related curtailment are also possible (e.g. use of voltage control to reduce net demand), but such features are not included. The heuristics used in Chapter 3 do not reflect what actually would occur during a supply-demand imbalance – load will be curtailed as a last resort as LFDD relays at Grid Supply Points (GSP) detect a deviation significant enough to trip, and these will trip. Rota disconnections can be planned and implemented in a more co-ordinated manner by operators, but that is well outwith the timescale in which the initial frequency deviation will occur.

#### B. Low Frequency Demand Disconnection

Given frequency response is being modelled there also has to be consideration for LFDD in-situ. The shed scheme used in the model for LFDD is shown in Figure 5.10, taken from the Grid Code [73].

| Frequency Hz          | % Demand disconnection for each Network Operator in Transmission Area |           |           |
|-----------------------|---|-----------|-----------|
|                       | NGET  | SPT       | SHETL     |
| 48.8                  | 5   |           |           |
| 48.75                 | 5   |           |           |
| 48.7                  | 10  |           |           |
| 48.6                  | 7.5   |           | 10        |
| 48.5                  | 7.5   | 10        |           |
| 48.4                  | 7.5   | 10        | 10        |
| 48.2                  | 7.5   | 10        | 10        |
| 48.0                  | 5   | 10        | 10        |
| 47.8                  | 5   |           |           |
| <b>Total % Demand</b> | <b>60</b>   | <b>40</b> | <b>40</b> |

Table CC.A.5.5.1a

Figure 5.10 - LFDD scheme used in model

Buses were assigned to each area accordingly in the system model.

It is expected that LFDD schemes operate with 96% reliability in accordance with Grid Code requirements, and so within the simulation, when a tripping action is performed in a stochastic context, each load is sampled with a probability of 96% of a given load being curtailed in a given time step when it is called upon. Of course, another problem with this is that the actual percentage of load being tripped in such a simulation may not reflect the actual load being disconnected.

As discussed and investigated by NG ESO in [72], changes in demand and consumer behaviour and the fact LFDD relays are set annually could mean a disparity between what response is expected when opening an LFDD array and the actual load disconnected. That is, a distribution network with significant infeed from solar PV in the summer may actually be a net exporter during the summer but a net importer during the winter, meaning that disconnecting such load would have very different consequences not just seasonally but also across diurnal cycles.

Disconnecting distribution networks with significant DER may not only disconnect load but may also trip DG, exacerbating energy imbalance on the system in hard-to-predict ways. This is difficult to capture in simulations – one approach could be to designate a certain amount of wind capacity at each node as being connected at a distribution level and reducing net infeed from wind at that node accordingly. This was not directly addressed in the proposed methodology, however. In future, though, the approach does mean it could be in similar studies.

LFDD is designed as a last-resort scheme to keep frequency above levels at which generation starts to disconnect for self-preservation; short term pain for a relatively small number of customers in order to preserve service to the remainder on the system such that the remaining MITS can be used to restore the degraded network more easily than had the entire network been lost. An alternative to this approach, however, could be to utilise demand more creatively in the system. Rather than gross shedding of load, using assets on the system as demand response to reduce load without disconnecting customers unnecessarily while maintaining system stability.

### C. Flexible Demand Response

The exact amount of FDR available for the system to deploy is scheduled and determined in the initial dispatch SCOPF as illustrated in Figure 5.2. In this case, it is assumed that each load has a reservoir of

aggregated FDR which can be called upon during a major frequency deviation as a non-inconvenience to end-users when a frequency threshold is exceeded or when the frequency sits below a certain threshold for a given amount of time. This operates as a “second line of defence” deployed in the SFR simulation after conventional frequency response from generators but before LFDD is fully deployed on the system. This is intended to replicate the potential utility of services such as demand aggregation to utilities.

Generally speaking, the availability of such resources will change with the diurnal demand cycle, ambient temperature, and other weather conditions, as well as consumer behaviour and demand. Further, whilst, for poorer consumers the versatility of allowing devices to be used for such “smart” response capabilities may be appealing, for better-off consumers the potential (or perceived) inconvenience of allowing a device to be used as flexible demand response may simply not outweigh what may be a relatively trivial cost associated with increased energy or device usage prices during high-stress situations on the power system.

The model requires three different values in deploying devices as flexible demand response in this manner.

1. The total capacity, as a percentage, of load on the system which is assumed to be able to be used as flexible demand response
2. The expected return rate of devices, used when scheduling
3. The return rate of devices which is actually deployed in the SFR simulation

The reasons for this approach are linked to a study into actual potential for the deployment of wet appliances as demand response in Belgium [74]. In this study it was found that, in the test area, around 4% of total demand could be curtailed using demand reduction of wet appliances assuming 29% population participation in such a scheme. The actual demand that is available to respond to a signal from the system will be inherently stochastic, and the amount needed may simply not be available for any number of reasons and so this should be taken into consideration when scheduling any demand response solution, and so should consideration be made in the simulation itself for the potential of demand response failing to respond during system events as expected.

Over-reliance on such schemes could actively exacerbate adverse network conditions during situations where the system is most in need of its assets to be functioning reliably if expected demand response does not perform appropriately. Conversely, flexible demand response at a device level has significant potential for fast frequency response if devices can respond quickly enough to signals from the system (even if that “signal” is simply the observed system frequency at the point of connection). Hence, such rapid response devices could contribute to a reduced requirement for inertia.

Therefore it was deemed necessary to include at least a very basic representation of such phenomena in the simulation. This is represented by a percentage reduction in net load in nodes affected by frequency deviations where either a frequency boundary has been breached or frequency has been outwith minimum frequency limits for a given amount of time.

#### 5.5.5 System Frequency Response simulation

The frequency response simulation itself is contained within a loop, as described in the general framework of the software model. That is, the SFR model takes in system information from the dispatch state and system perturbation data, and returns data on the adjusted outputs of the generators on the system, the change in load observed at network nodes, and any generation or load which has been tripped. This in turn can be fed forward to a load flow to determine if any lines have subsequently been overloaded as a result, and whether any further network degradation occurs.

The volume of data mentioned in this section is indicative of the challenges of linking an SFR to multiple OPFs, and the creation of the SFR model in the wider context of the simulation model was particularly time consuming and challenging. Typically programs such as *MatLab SimuLink* are used for such simulations due to their user-friendly GUI. In this case, due to the bespoke requirements of the simulation model, an extensible model which could be modified to include all of the discussed features and facilitate integration with a wider OPF framework had to be devised. The SFR simulation was written in the *python* language and can be described, at a high level, with the following pseudocode (shown overleaf). For the purposes of clarity in reading and simplicity reference to the specific mathematical symbols used are omitted but are referred to in general terms.

---

Import generator dispatch state  
 Import frequency state of system  
 Calculate available primary frequency response  
 Calculate available secondary frequency response  
 Calculate system inertia of island  
 Initialise simulation  
 Set power adjustment signal to zero  
 Set all timers to zero  
 For timestep in time series if not blackout conditions:  
     Calculate net power infeed using power adjustment signal  
     If  $t < 29s$  and in "primary response" mode and no blackout:  
         Calculate power imbalance  
         Calculate new power adjustment signal  
     Otherwise if  $t = 29s$ :  
         Change mode to "transition"  
         Set power adjustment signal to zero  
         Calculate power imbalance  
         Calculate secondary response requirement  
         Calculate rate of change of power as primary transitions to secondary  
     Otherwise if in "transition" mode:  
         Calculate power imbalance  
     Otherwise if  $t = 30s$  and mode = "transition":  
         Change mode to "secondary"  
         Calculate power imbalance  
         Calculate new power adjustment signal  
     Otherwise if in "secondary" mode:  
         Calculate power imbalance  
         Calculate new power adjustment signal  
     Calculate frequency adjusted load  
     Calculate rate of change of frequency  
     Calculate new system frequency  
     If frequency below given lower threshold and mode is not "transition":  
         If threshold for demand response deployment breached:  
             Run **demand response algorithm**  
             Change threshold  
         Else:  
             Run **load tripping algorithm**  
             Change threshold  
     Otherwise if frequency above tripping threshold  $f_u$  and mode not "transition":  
         Run **generator tripping algorithm**  
     Next timestep

---

For perspective, the pseudocode represents approximately 1,000 lines of *python* code and is an attempt to keep the representation as simple as possible and highlight the key aspects.

Algorithms which are referred to are described in more specific detail elsewhere, where relevant. From this model, all information is then fed forward into a load flow calculation.

If one of the following conditions is met, the system is assumed to go into blackout, and all values in the simulation are set to zero except load curtailment, which is gross total load of the analysed island, and the “blackout” status of the SFR is recorded:

- Frequency exceeds absolute maximum or minimum values
- All connected generators trip
- Zero inertia remaining on system (e.g. if all synchronous machines trip and only windfarms are left)
- All connected load disconnected or tripped off

In such cases the load flow for the given island is not performed and the model immediately moves onto simulation of the next intact island. It should also be noted that in this implementation, the frequency response of every independent island is analysed in turn. This creates challenges for the implementation of DC links between islands – international DC interconnectors are modelled as generators with zero inertia but which utilise droop control, whereas windfarms are assumed in this implementation are assumed to be nonresponsive to frequency control.

A DC link between two islands would have different frequency responses on either side of that connection, and the connection itself would be susceptible to frequency-related tripping in a way cable or OHL would not. In the implementation of the model used, there are no DC interconnections on the MITS so this was not a direct concern (the Western Link and “Bootstrap” in the GB model were not considered).

The outputs of the SFR were compared with papers such as [68] and discussions with peers and those working in the area to ensure results were acceptable for reasonable test cases. It is very difficult to validate frequency response models on systems such as GB, however, due to the lack of data pertaining to large losses of infeed and case studies. An example frequency response on the system with a loss of ~1.3GW and gross demand of ~34GW is shown in Figure 5.11.

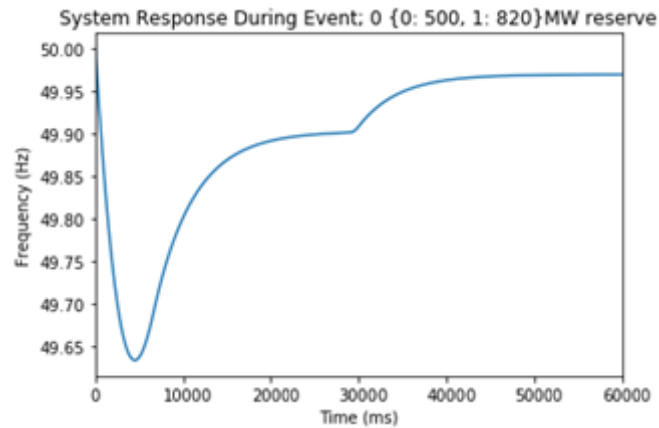


Figure 5.11- representative frequency response curve from model

In this case 500MW of frequency is dispatched in the area north of the B6 boundary (further detail on this is detailed in section 5.6.2), with 820MW dispatched south of this boundary, and no demand response.

The initial frequency deviation can be seen, as well as the deployment of secondary response at  $t = 30s$ , and subsequent frequency stabilisation. This case has no demand response.

This can be compared with a situation where 1320MW net frequency response is scheduled across the system in the same manner, but inclusive of demand response capability, for the same scenario.

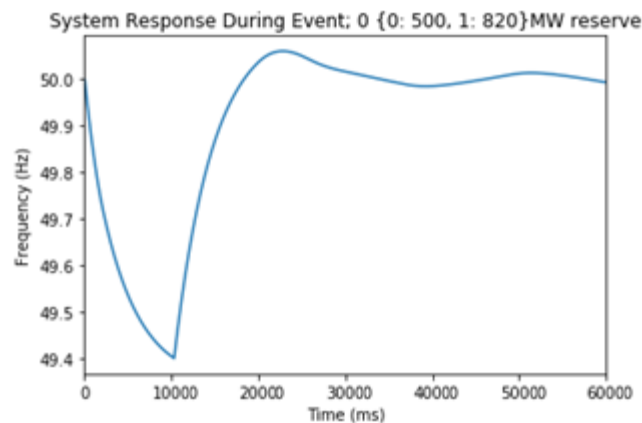


Figure 5.12 - representative frequency response curve inclusive of flexible demand response

The near-instantaneous, more directly targeted deployment of DR can be observed when the frequency drops below 49.4Hz, with secondary frequency response taking over to restore the nominal system frequency thereafter. In this case only enough demand response is scheduled to arrest the frequency below 49.4Hz, and the demand response used is assumed to be able to be restored during tertiary response via the redispatch OPF, described elsewhere.

The demand response deployment algorithm can be deployed with the following pseudocode.

---

*Calculate imbalance between demand and supply*  
*Calculate available demand response*  
*Adjust secondary response requirement*  
*Adjust tertiary response requirement*  
*Reduce system total load by min(amount to restore balance, total available)*

---

The load shedding algorithm itself can be described in the following terms.

---

*For load in loads:*  
*Determine load area*  
*If demand response deployed at load:*  
*Set demand response deployment at load to zero*  
*Correct secondary response requirement*  
*Correct tertiary response requirement*  
*Get load curtailment ratio from lookup table or use predetermined amount*  
*Reduce load at node by appropriate amount*

---

Finally, the (stochastic) generation tripping algorithm.

---

*Calculate trip probability from model and trip rate*  
*For generator in generators:*  
*Generate random number*  
*If random number < probability:*  
*Add generator to tripped generator list*  
*For generator in tripped generator list:*  
*Set generator output to zero*  
*Reduce available primary headroom and footroom*  
*Reduce available secondary headroom and footroom*  
*Set trip variable on generator to 1*  
*Reduce system inertia*

---

There are multiple different generator tripping algorithms which could be employed. For instance, an optimistic model could assume that generators are intelligently tripped and the generator whose output most closely matches the power surplus on the system could be employed. More conservative models could assume generators of a given class trip concurrently at different tripping thresholds rather than randomly. The approach chosen was chosen because it resembled those already deployed in the literature. This offers an advancement in methodology compared to e.g. [78] because the generators are tripped in-situ with the frequency response model, and secondary frequency response is considered in the simulation, whereas in the referred-to paper actions are taken in 100s steps. In EWPS the model performs these actions while the frequency response simulation is ongoing,

capturing the dynamics of the event in a more representative fashion at the cost of computational expense.

Windfarms and interconnectors are assumed to contribute nothing towards system inertia but the power electronics of interconnectors are assumed to be able to change outputs within the frequency response simulation in line with the deployed droop control and headroom/footroom limitations. Wind farms' outputs do not change w.r.t. frequency in the simulation itself but in the tertiary response simulation their curtailment can be adjusted as required with assumed cost.

#### 5.5.6 Load flow calculation and optimisation

Once a given iteration of the system frequency response simulation is carried out, the results are translated onto a load flow. That is, the dispatch condition for the given island is taken and the trip status and adjusted output of generators across the system are applied. So too is the frequency-related load adjustment (positive or negative). The generator outputs are then fixed and cannot be changed when the optimisation is solved. Load curtailment, too, is fixed across the system for this simulation, as is generator trip status.

All that can be changed when this optimisation is solved then, are the following values:

- Voltage angle
- Net load
- Line flows
- "Observed" frequency

A small discrepancy between the frequency determined in the SFR simulation and that used in the load flow calculation is allowed. This is to account for potential floating point errors or rounding point errors in translating the results from the linear programmed model into an optimisation model. So although the load flow is being calculated and load curtailment itself is fixed, minor discrepancy is allowed in the net load at each point to represent demand response associated with island frequency, which is subject to the associated constraints and objective function.

It is assumed that frequency response is distributed proportionately across loads and generators. That is, if 10% of the total scheduled frequency response is deployed at a given point of time, a generator with 100MW of frequency response and one with 10MW would contribute 10MW and 1MW respectively. Similarly, frequency is assumed to be homogenous across islands during the simulation.

These are themselves relatively broad simulations – like voltage, frequency can vary locally with different supply-demand states across a system. Areas with significantly lower than average inertia will have more severe frequency deviations than those with high inertia e.g. Northern Scotland vs the English Midlands, where there are significant gas and coal generation plants. The purpose of this is to estimate the load flow conditions of lines across the system and determine whether any line overloads, and hence further system deterioration, has occurred and whether further preventative or mitigation actions need to be taken.

#### 5.5.7 Trip Assets simulation block

Combining the SFR and load flow simulations provides an estimation of the post-frequency-response state of the system. In such cases, it may arise that areas with significant frequency response resources have deployed their response at times where there is reduced network capacity (say during a localised wind storm which has taken down connections to load centres). Situations may therefore arise where this increased power output on reduced network capacity leads to line overloads and the necessary deployment of protection schemes on overloaded lines. Line protection schemes, like generator

intertrips, can be simulated in either a deterministic or stochastic manner, but in the context of this simulation a stochastic line protection deployment algorithm is deployed comparable in nature to those demonstrated in [78] or [77]. Effectively it is assumed that, within the context of the SFR simulation loop, all actions are automated and unless mitigation actions (e.g. intertrip protection schemes on wind farms) are deployed, lines will have a given probability to trip by operator action as soon as they exceed their contingency line flow limit, estimated as 130% of their continuous seasonal value (based on typical values on the SHETL system).

Any lines which have been tripped due to overload can be attempted to be reconnected to see if flows have returned to within operational limits, but this is generally only done a limited number of times before the lines are “locked out”. This is assumed to be limited to three operations in the implementation. Overload protections vary in style between voltage levels and network but are assumed to be installed on all transmission lines in this implementation.

What also concerns operators is the possibility of incorrect actions or sympathetic tripping. That is, lines tripping when they are not supposed to. This is assumed to be a suitably low value as a first order approximation- 0.001.

A probability for correct protection operation must be assumed. In this implementation that value is taken as 0.999. The line tripping algorithm can be described as follows:

---

*Determine lines connected to reference bus of island being investigated*  
*For line in list of already tripped lines:*  
    *If reclose counter < 3:*  
        *Try and reconnect line*  
        *Increase reclose counter*  
*For line in list of lines:*  
    *If line overloaded:*  
        *Generate random number*  
        *If random number < protection action probability:*  
            *Trip line*  
            *For line in list of lines in same island:*  
                *Generate random number*  
                *If random number < probability of incorrect action:*  
                    *Trip line*

---

This then incorporates both line overload tripping by operator action, and sympathetic tripping within the model structure.

After the load flow calculation and line tripping algorithms have run, the model then performs a check. If no lines have been tripped, and frequency is within statutory limits, the model ends the SFR-loop. If not, some action is taken. In this case, either an “override” is triggered and a signal is fed forward to tell the model to trip more load or run the SFR again and see if a generator trips, or if a line is tripped due to overload a connectivity check is performed again to see if any new islands are formed and the SFR-loadflow simulation is performed again. This loop continues until all lines are within limits and frequency is within bounds, at which stage the state is assumed to be “stable” (i.e. fully degraded but not expected to degrade any further) and further restoration and corrective actions can be taken.

### 5.5.8 Restoration action simulation – Redispatch OPF

After primary and secondary frequency response has been deployed across all of the islands and they have settled down into a perturbed, but stable, state, it is assumed that the model moves from automatic-actions, and periods of time in which events are generally progressing too rapidly for humans to control (seconds to single-minutes), to a time domain in the scale where humans can begin to make operational decisions such as controlled generator adjustments. As previously mentioned, this inherits the results of the SFR-load-flow loops of each island and consolidates it into one system model. This occurs in the “Check Islands...Degrading” loop.

In this case, secondary frequency response trails off via AGC and is replaced over time by generator redispatch/tertiary response. Secondary response is generally assumed to trail off 15-30m after the initial fault event, being replaced with tertiary response in an, ideally, stable and controlled manner. This means *another* optimal power flow needs to be performed to replicate this action in the simulation while considering factors such as load curtailment and power curtailment of windfarms, which can be controlled in the scale of minutes just as output from generators unable to be used for frequency response can be.

Primary and secondary frequency response generators, unless they are specifically assigned as being capable of doing so (such as the case with interconnectors, hydro), are assumed to be unable to contribute to generator redispatch as generators require time to recover having delivered such frequency response.

In this optimisation, the information from perturbed sections of the system are imported from the SFR-loadflow loops. Time constant  $\tau$  is set to 1, such that the OPF is in the scale of minutes. The initial state where  $t = 0$  has generator and net demand states set based on the output of the SFR-loadflow loop but for the next 10 minutes can freely redispatch and curtail load as required subject to other system constraints.

The aim of this part is for the operator to minimise the cost of load curtailment, generator trips, and generator adjustments, while restoring supply-demand balance. The significant cost of load curtailment, assigned at a cost of £17,000MWhr<sup>-1</sup>, incentivises the solver to prioritise minimisation of load curtailment.

All of the individual islands’ frequency response pathways are simulated and used to generate the  $t=0$  state. In  $t = 0$ , all generator outputs and load states are fixed from based on the results of the SFR loops associated with each island. It is assumed that system frequency linearly recovers from the post-SFR frequency to the nominal system frequency with generator redispatch and load curtailment operating accordingly. Frequency can therefore be fixed in the formulation after  $t = 0$  avoiding a nonlinear problem formulation and reducing computation times.

It is assumed lines which are “locked out” due to the SFR-load flow loop simulation are not in service for this stage of the simulation, and generators that are tripped are also locked out of service – with the exception of windfarms which are assumed to be able to infeed power whenever desired (that is, whenever economically optimal given the formulation of the problem).

This then, in total forms a more complete representation of the simulation of an outage even from the causal perturbation to the first stages of the restoration. That is, from lines or generators dropping out of service, the simulation of the disruption and the initial system degradation, and then the initial attempts to stabilise the system.

Taking into consideration how the events themselves are generated w.r.t the spatial disaggregation of line risk, this forms a further advancement in the modelling of power system risk and a comprehensive tool for simulating wind-related outages. The final step for this would be to then begin to consider system restoration – that is, scheduling of repairs, bringing lines back into service, and restoring supply-demand balance as generators come back onto the system and as demand changes with the diurnal cycle, before the next system perturbation.

#### 5.5.9 Restoration action simulation – Unit Commitment

The next – and final – stage of the simulation is to begin to incorporate more significant restoration actions into the system, such as bringing tripped generators back online or bringing new generators into operation. Generators which have tripped or are sitting offline will require a given amount of time to either resynchronise with the network or be ready to connect and contribute power to the system as required.

Further, as generators adjust their outputs up and down and reconnect, it is assumed that load curtailment can be freely controlled, as can wind power curtailment. Extending the simulation model in this manner was done to be able to investigate the cumulative impact of many outages associated with a single storm or largescale outage event.

Similarly, for example, if a fault happens at peak demand there will be less surplus generation available to come online following the fault event in order to support system restoration and stability more generally- but greater system inertia due to the amount of connected generation. Such simulations have not been performed with the type of detail and refinements offered in this model, especially not when considering the associated impact of changes in wind generation.

This is illustrative of the fact that resilience will mean different things in different timescales. The ability to react and respond quickly to reduce the impact of results is more significant if one is also considering the restoration timeline of the system – which is to say, a long outage with a low impact will, in absolute terms of ENS, have a comparable consequence relative to an event which has a very significant impact but for a shorter time period. Socioeconomically, the impacts could be very different if, for example, a small community is left without electricity for a long time in an inaccessible or geographically isolated location, such as can be found in the Highlands and Islands of Scotland. Quantifying the cost associated with outages, therefore, becomes increasingly difficult the longer events extend, because the uncertainties about factors such as human behaviour, electricity demand, and even social cohesion may impact the ability of operators and, potentially, restoration teams to restore the system to a state of nominal functionality.

Tripped conventional generators stay out of action for a predetermined minimum “downtime” assumed based on the 1996-RTS. Wind generators that trip are assumed to be able to reconnect whenever possible and can freely curtail otherwise.

This simulation is represented by a unit-commitment OPF defined above, with the model granularity set in hours, and only one case being considered (so  $t$  is a set from 0 to  $T_{max}$ , and  $k = 0$ ). Lines are reintroduced as soon as they are functional, and generators can connect as soon as their minimum down time has elapsed.

For clarity, further elaboration is provided in Appendix 7.2 – Example EWPS Case.

## 5.6 Case Studies – Cyclone Friedhelm

As referred to in Chapter 4, Cyclone Friedhelm was a large storm system which affected Scotland around the 8<sup>th</sup> December 2011. The significantly increased complexity of the simulation model

described and the features that this enable to be simulated mean that new sensitivities are added into the resilience study which have not conventionally been an issue – particularly frequency response.

The question then is whether this increased level of granularity is necessary and whether it provides sufficiently useful information to be a worthwhile addition to resilience studies or whether the added complexity and computational expense is not a worthwhile investment of time and effort. Various case studies will be used to investigate this based on using the same specific weather events as described in Chapter 4, with different power system setups and scenarios.

As demonstrated in Chapter 4, and implemented here, high wind speeds mostly affect the ability of the electricity system to transmit power and the availability of wind power itself. There is also a clear methodology for simulating HILP events and associated cascade effects on the system. This shall now be used to investigate the potential effects of changing how these aspects are used in resilience studies to see if there is a material difference in the results across studies for the same event when these models are changed. If there is significant variation in results, this suggests that omission of e.g. frequency response may not be appropriate as it suggests significant divergence in results from what can reasonably be expected during such events.

For example, typically resilience studies assume that the system can redispatch, curtail load, or trip off generation in an ideal manner to maintain system stability such as in [57], not considering the potential for frequency deviations to lead to generator trips or UFLS before any such actions can be taken. If the network was dispatched via an OPF without the consideration of frequency response requirements, in reality this may mean that there would simply not be adequate frequency response available to contain system perturbations before the events can cascade to something worse.

However, if the ENS associated with a major network-side fault on a system is largely caused by disconnection of loads or islanding of sections, the effect of simulating the frequency response on either side of that disconnection may not significantly differ from OPF-based models with appropriate assumptions – such as those deployed in Chapter 3. The case studies herein, therefore, will be used to investigate whether changing the frequency response dispatch scenario or security rules used fundamentally changes the results one can reasonably expect from such studies.

Various different studies are implemented to understand this. In each study, a “base case” was performed with 1,000 samples each comprising of a 12-hour window, with different dispatch scenarios. The load profile used is derived from the 1996-RTS paper describing a winter peak day. Different case studies will use different time windows.

One drawback of using a wide variety of different simulations and OPFs is that translating one format to another can introduce formatting and floating point errors, which can in turn cause infeasibilities in the results of these OPFs (primarily, it was found, due to generator values being fixed marginally outside of their maximum/minimum ranges by vanishingly small values e.g.  $5 \times 10^{-14}$ ). This was only found to affect approximately 1 in 1,000 hours. In such cases the perturbation was simply repeated.

From each “base case”, a dictionary describing the “timeline” of each sample was recorded – that is, what faults were recorded and when. When the simulation was repeated with a different dispatch scenario, this predefined set of cases was used for analysis. This was to reduce the variance in results attributable to randomness and sampling and ensure any change in results was predominantly due to changes in the dispatch scenario rather than the inherent randomness in what events are sampled – this is a very basic example of a variance reduction technique known as *correlated sampling*.

Various case studies and their results shall now be demonstrated using the simulation model. The following load profile in Figure 5.13 is used in all cases, with different start/stop times over the given 12-hour windows.

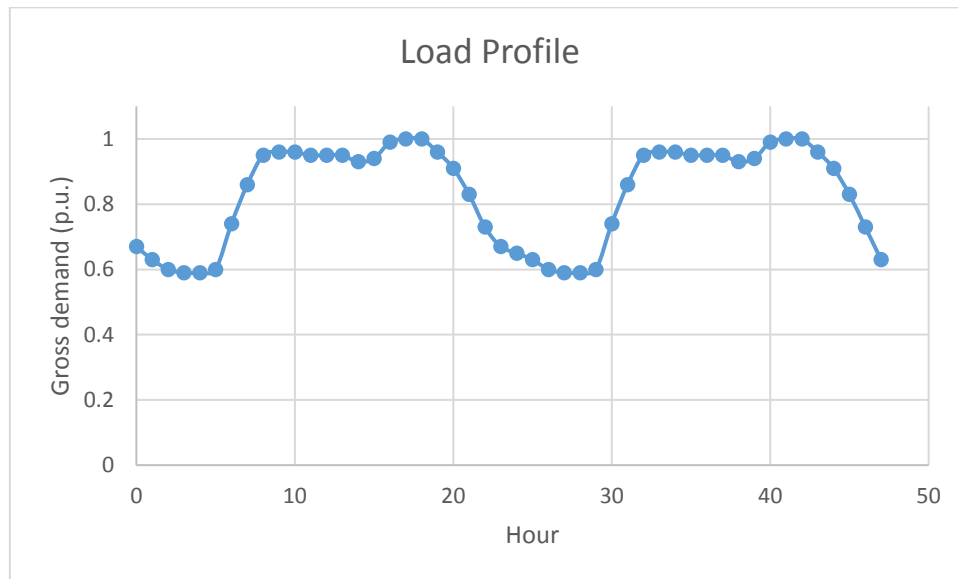


Figure 5.13 - load profile used in case studies, representing a winter peak day

The wind speed was corrected in each case to bring it closer to the values used in the derivation of the fragility curves, and to make the model more conservative and induce more faults, by multiplying the wind speeds on every point by 1.28, in accordance with guidelines from [108] to convert a wind speed from hourly average to 60s gust duration.

A summary of the tabulated results of all simulation parameters used and additional figures can be found in Appendix 7.3 - EWPS Outputs, along with additional analysis. The discussion offered in this section is offered as a high level summary and interpretation of results.

For clarity, there are two separate “case/contingency lists” which may be alluded to which should be considered separately. The “contingency list” refers to the set of events fed into the Dispatch SCOPF to determine the dispatch and lever of security. A “case list” of weather-related and other faults is also generated on the first pass of each case study before the subsequent changes in dispatch scenarios which reflect the different timelines of fault events being inflicted on the test system, which are performed using these generated timelines to compare how the system reacts differently to a consistent set of events with different dispatch scenarios.

#### 5.6.1 Baseline: economic dispatch, very vulnerable double circuits

In order to form a baseline, worst-case set of results with a variety of lossy states a particularly conservative scenario is used. This will be used to determine the potential significance of frequency response dispatch in resilience studies in the most extreme cases.

These case studies focus on major network-side losses, rather than direct loss of infeeds. In this instance, if there is a loss of a single circuit on a dual circuit, it is assumed that the adjacent circuit also always faults as well concurrently (i.e. all single circuit faults lead to dual circuit faults on that branch). The system will be dispatched in various different modes. First, the system is dispatched in economic dispatch mode, meaning:

- The Dispatch-SCOPFT contingency list is empty, so no faults are being secured in the initial system dispatch
- No frequency response is scheduled

These studies take place between 1200 and 0000 (hours 12 and 24). The results for the “base case” scenario are shown in Figure 5.14. In all histograms the red and blue (left, right) lines represent the calculated VaR, cVaR values. As a reminder, the definition of VaR, cVaR used here is taken from [56]: “with respect to a specified probability level  $\beta$ , the  $\beta$ -VaR of a portfolio is the lowest amount  $\alpha$  such that, with probability  $\beta$ , the loss will not exceed  $\alpha$ , whereas the  $\beta$ -CVaR is the conditional expectation of losses above that amount  $\alpha$ .” The “loss” value alluded to in VaR and cVaR may be, for instance, a dollar amount or a value of ENS. The charts on the left show the histograms for all recorded events, with the histograms on the right showing only N-2+ events. Two charts being similar or identical, as in this case, implies that a significant proportion, or even all, the events causing loss of supply are already N-2+. It should be noted that the y axis in all histograms is logarithmic, and attention should be paid to the x axis scales also. Further, it should be recalled that the leftmost bars in the histogram represent all occurrences of ENS values *less than* the limit of the first bin, and are not automatically all values which represent zero ENS.

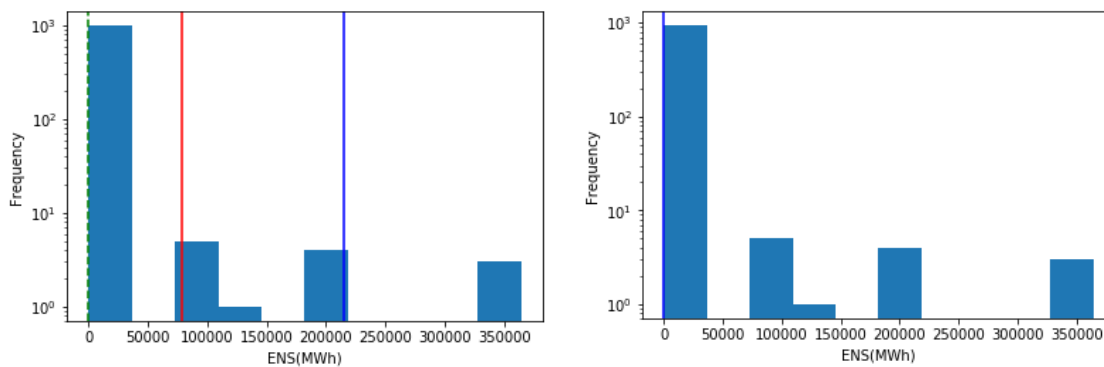


Figure 5.14 - ENS histograms for “base case” economic dispatch scenario

Next, as second “base case” is created with the system dispatched N-1 security. The initial approach to this attempted to use independent N-1 events at each time-step, such that if there were 100 events in the contingency list, there would  $100^2$  cases to solve for two time-steps and  $100^3$  cases for three timesteps. Applying this approach to an N-1 dispatch for loss of lines, generators, and wind farms brought with it significant computational cost and memory requirements – feeding in an N-1 contingency list for 24 hours’ dispatch resulted in the model immediately filling the RAM of the computer during setup (with 64Gb of data) and the computer crashing.

Therefore, to create a proxy of an N-1 dispatch that considered frequency response, and N-1 security on system assets, the model was solved for independent time-steps (i.e. N-1 dispatch at each timestep with frequency response requirements set but only  $t=0, 1$  – that is only using two hours, one for the hour being considered, and one for the hour immediately after). These dispatches were then linked together using the dispatch SCOPF problem with the frequency response requirement set as per the specific requirements of the case study in question but only  $k=0$  as the contingency set and the associated unit commitment-related generator constraints. The timesteps used represent key points in the load-profile –  $t = 4, 6, 15,$  and  $19$ . These are extremes of load (highs, lows) or points of inflexion- also known as Cardinal Points.

This approach is not what would typically be referred to as an “N-1” secured dispatch but acts as a proxy that is tractable and usable here and all references made in the context of this simulation herein are assumed to be stated with that caveat in mind.

The results of this second “base case” results using an N-1 dispatch shown in Figure 5.15. 1320MW of frequency response was included, scheduled across the system, with  $\Psi$  (that is, the ‘slack parameter’ allowing the model to dispatch less frequency response to allow convergence if needed as described in Section 5.5) was zero.

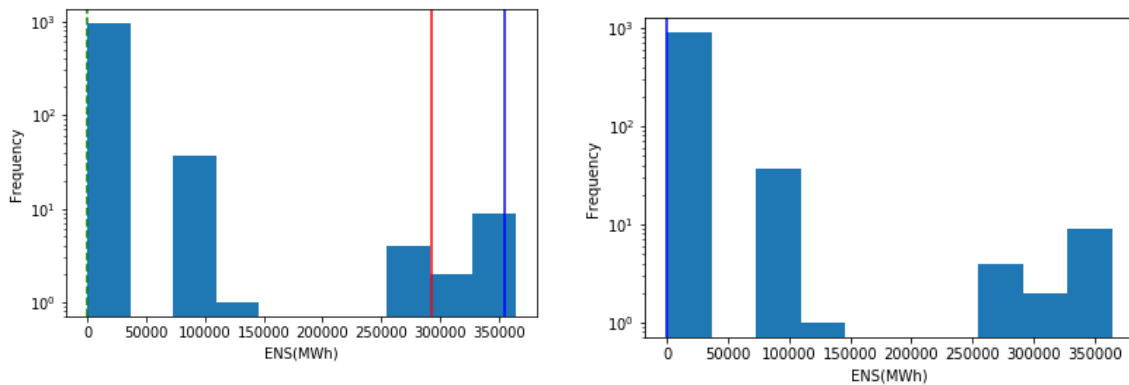


Figure 5.15 - ENS histograms for "base case" N-1 dispatch scenario, 1320MW of reserve spread across system, no FDR,  $\Psi = 0$

Next, in Figure 5.16, a case study is performed with frequency response increased from 1320MW to 2000MW (scheduled across the system) and with Flexible Demand Response (FDR) available. In accordance with the expected response rate of LFDD relays, FDR is scheduled such that it is assumed only 96% of commissioned FDR will respond to any signal sent. That is, as previously discussed, a correction factor of 0.96 is applied to the FDR deployment constraints in the SCOPF to reduce the effective contribution of gross FDR during scheduling. 100% of this FDR was then expected to turn up. In future, sensitivity tests could also be carried out to investigate the randomness associated with this, but such features were not considered here.

Up to 5% of total load at each load point was deemed available for FDR, but zero cost was attached to incentivise the model to use as much as possible. Note the difference in x axes.  $\Psi$  was relaxed to allow up to 50MW of frequency requirement reduction.

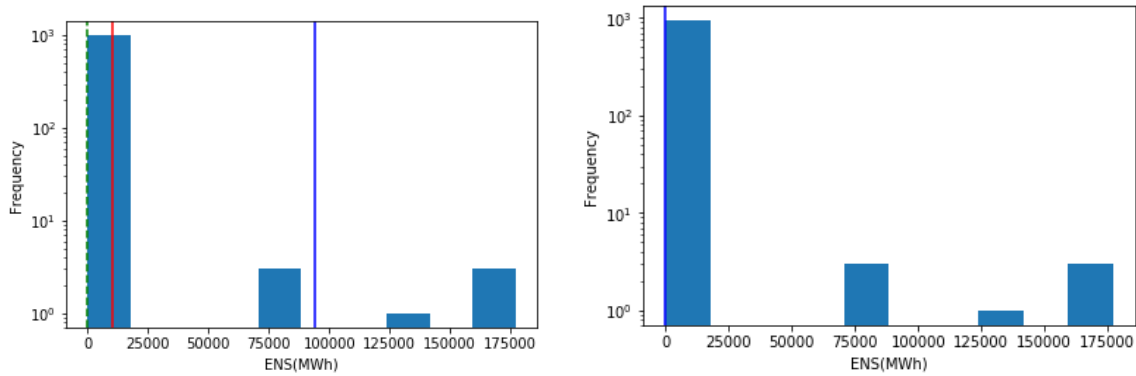


Figure 5.16 - ENS histograms for case with 2000MW frequency response and FDR, no locational constraints,  $\Psi = 50\text{MW}$ , empty contingency list

Next, a study is performed but, in this case, the location of frequency response is considered. Due to the storm primarily affecting Scotland, in this case study frequency response was dispatched such that 2000MW of response was dispatched across all nodes south of the B6 boundary (i.e. England and Wales), with zero assigned in buses which happened to be north of the B6 boundary (i.e. Scotland).  $\Psi$  was relaxed to allow up to 50MW of frequency response requirement reduction but was found to be zero anyway. The results are shown in Figure 5.17.

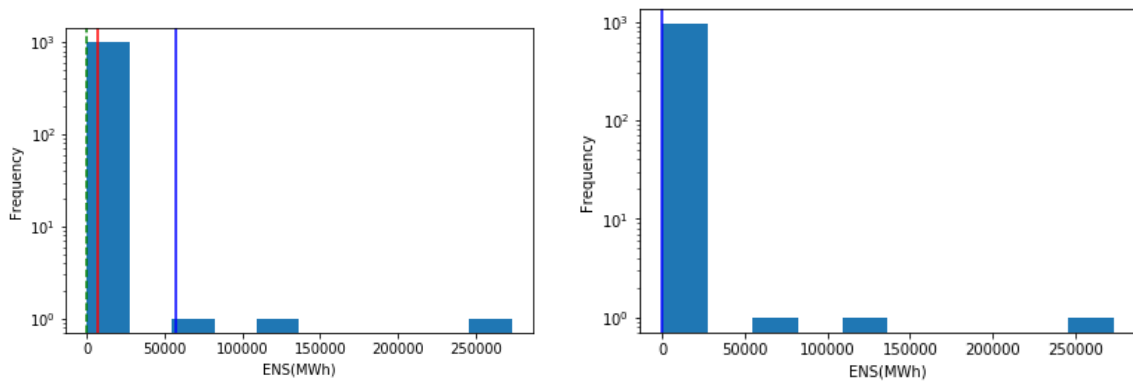


Figure 5.17 - ENS histograms for case with 2000MW of frequency response south of B6, empty contingency list,  $\Psi = 50\text{MW}$ , no FDR

Finally, a simple comparison can be drawn between the interpolated data being used as a base for the simulation and the coarse MERRA-2 dataset. In this case, the interpolated dataset is used for simulation instead of the raw data, and a new case list is generated accordingly. N-1, 1320MW frequency reserve dispatch is used to maximise the number of lossy cases such that any change in output is most pronounced, shown in Figure 5.18. There is no FDR and  $\Psi$  is locked to zero. There is no locational restriction on frequency response dispatch. Note again the difference in x axes. Also, a new case list was generated as the perturbation generation mechanics had changed. That is – the probabilities of line failures were different, and so the lines had to be re-sampled.

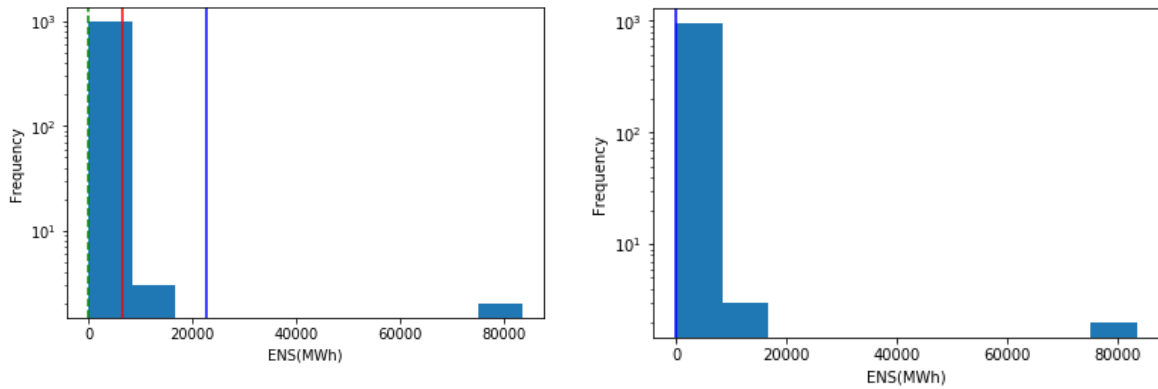


Figure 5.18 - ENS histograms for "base case" dispatch scenario, N-1 dispatch, interpolated weather data, 1320MW frequency response, no FDR,  $\Psi = 0$ , no locational constraint, interpolated data set

### 5.6.2 Loss of B6

B6 refers to the interconnection boundary between Scotland and England, as illustrated by Figure 5.19, extracted from [95].

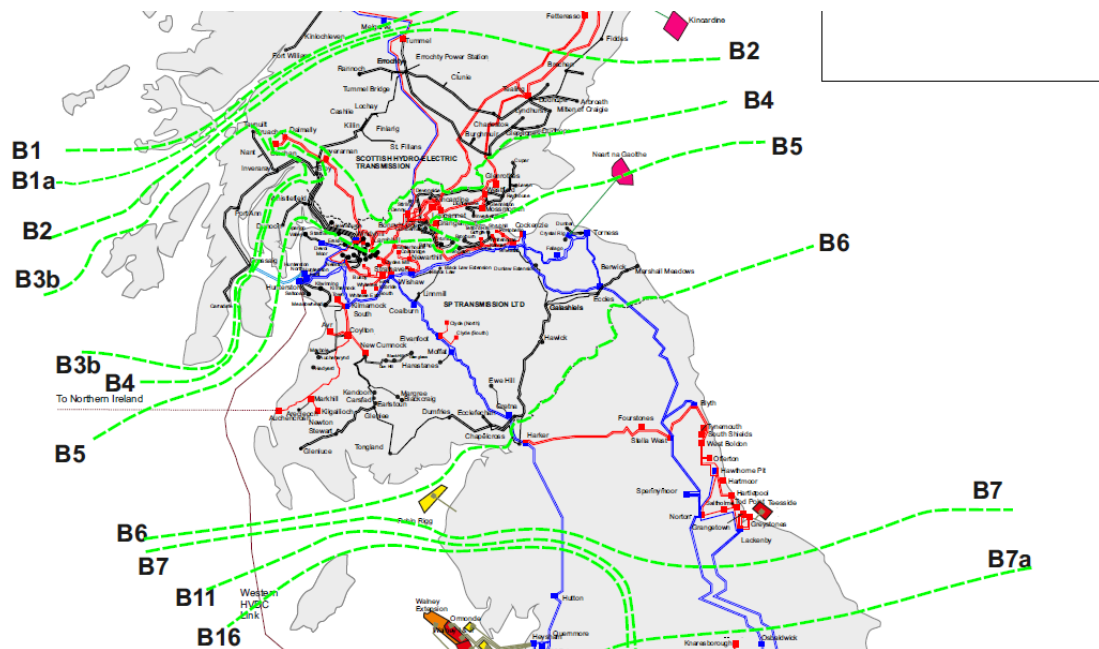


Figure 5.19- boundaries around the Central Belt of Scotland, South of Scotland, and North of England

This case study differs from the last, in that it specifically models the loss of a large interconnection at a given time on top of the stochastically generated events already simulated. Various different frequency response dispatch and flow constraint scenarios will be considered. B6 is important because the (stability limit constrained) flow limit across this boundary is approximately 2.6GW which, on a windy day, the flows can regularly approach. Any loss of this interconnection during such times without suitable remedial actions in place North and South of the boundary could lead to rapid system deterioration for and cascading outage events in both the supplying and receiving systems. All subsequent simulations in this case utilise the interpolated data set.

In this case, a less conservative representation of dual circuit faults is adopted. Anecdotally, approximately 1 in 50 single circuit faults on the GB system can be associated with a dual circuit fault happening. Therefore, if a single line in a double circuit faults, it is assumed there is a 2% chance the

adjacent line also faults for this and successive simulations. The loss of B6 is modelled at hour 5 (1700) with the simulation occurring in the same window as the previous case studies (1200-0000).

In this case, the weather data and grid resolution is correspondingly interpolated by a factor of five, as it was for the research in Chapter 4, and will be for all subsequent simulations as well. Flexible demand response is not considered in these cases. A new set of fault states is therefore again generated for this study.

The first set of results shown correspond to a dispatch where there is 1320MW of frequency response dispatch with an N-1 contingency list.  $\Psi$  was restricted to <50MW for all subsequent simulations in this set. It should be noted that this value only ever typically approaches the upper limit during peak demand for one hour but is otherwise universally zero. As stated in the model definition, it acts as slack to improve the model's robustness and ability to find convergence in extreme scenarios such as this. Herein only one figure is shown as the faults are deterministically induced at the given times compounded with stochastically generated faults, so the scenario is always N-2+ and thus demarcating the figures on that basis was redundant.

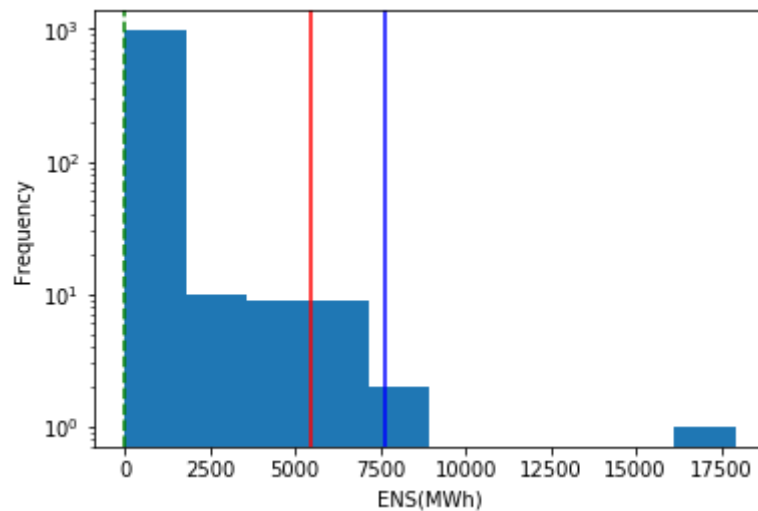


Figure 5.20 - ENS histogram of B6 scenario with N-1 dispatch and 1320MW frequency response,  $\phi = 50\text{MW}$ , no locational constraints, interpolated data, no FDR

This can then be compared with the scenario performed but in economic dispatch. Note the change in x axis.

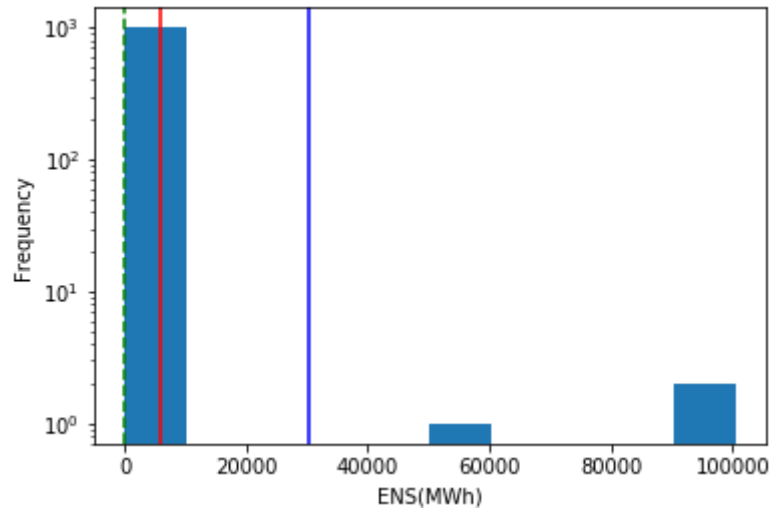


Figure 5.21 - ENS histogram of scenario with economic dispatch, empty contingency list, 0MW frequency response dispatched,  $\phi = 0$ , no FDR

In order to compare this with changing the distribution of frequency response, 500MW of frequency response was scheduled in the North, and 820MW in the South (to broadly agree with the net total frequency requirement but ensure that it is not concentrated geographically). An empty contingency list was used, this time around. The results are shown below.

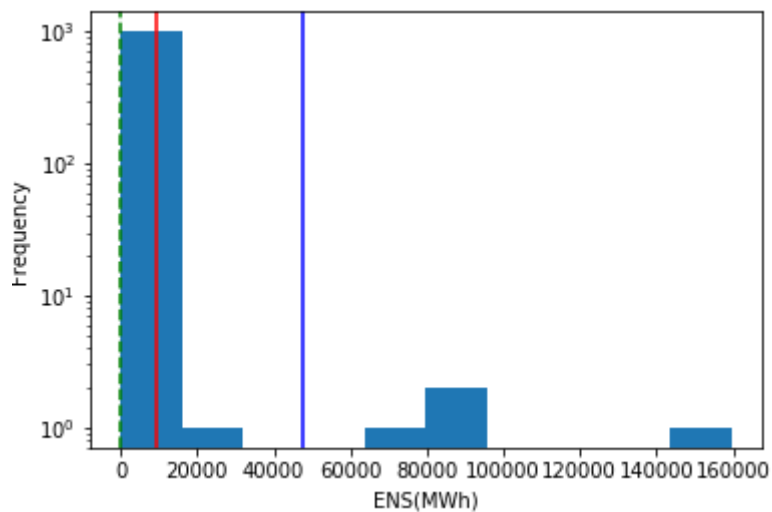


Figure 5.22 - ENS histogram for case with 500MW frequency response scheduled in North and 820MW scheduled in South,  $\phi = 0$ , no FDR, empty contingency list

To investigate how to mitigate this in the simulated cases, a constraint is put on inter-area flow across the B6 boundary such that it is limited to 500MW, or, the primary frequency response scheduled in area  $a$ , North of the B6 boundary. The results are shown below in Figure 5.23.

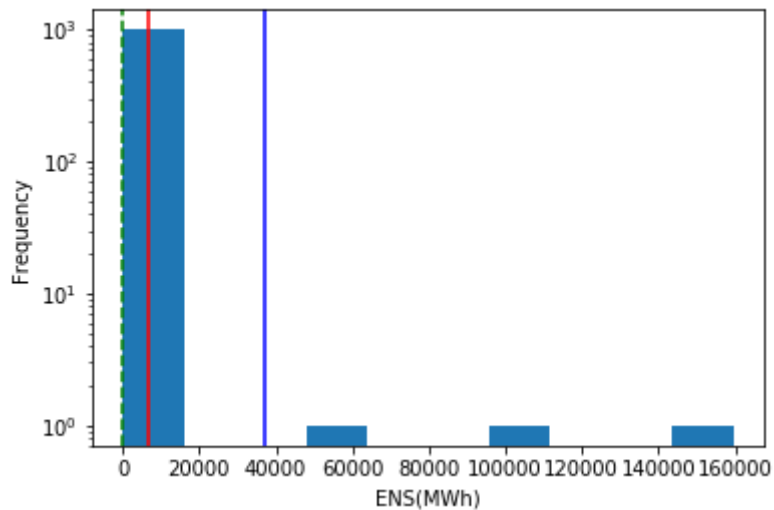


Figure 5.23 - ENS histogram with constrained flow, 500MW north of boundary, 820MW located south,  $\phi = 0$ , no FDR, empty contingency list

Finally, the simulation is performed but with 500MW of frequency response dispatched in the North, 2000MW dispatched in the South (to better reflect the scale of outage due to the loss of transfer), and, crucially, at hour 5 when both connections across B6 are deterministically tripped and interconnection is lost,  $\sim 1.5\text{GW}$  of wind power capacity in Scotland is set to trip off such that the overload scale is reduced, giving the system more time to react as the positive RoCoF should be reduced. The results are shown in Figure 5.24

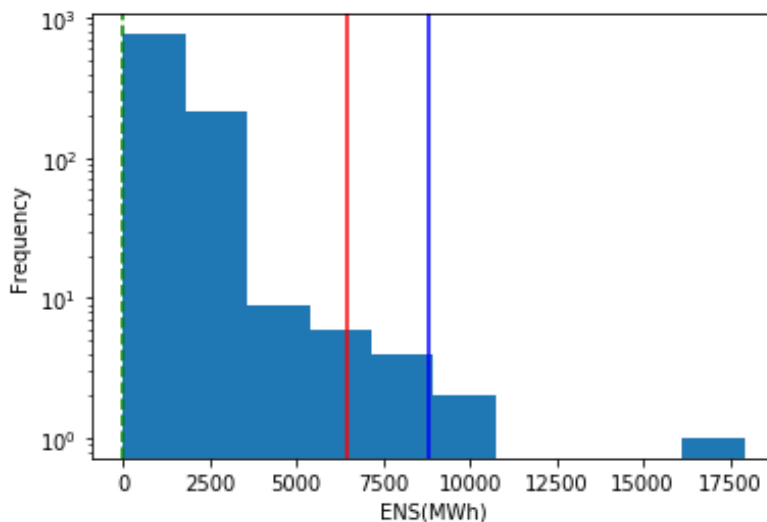


Figure 5.24 - ENS histogram with case with unconstrained flow, trips, 500MW in north, 2000MW in south, pre-programmed wind generation trips, no FDR, empty contingency list

### 5.6.3 Large loss of generation

In this case, to specifically create cases where there is a significant loss of infeed (and thus force the model to use the frequency response module for extreme cases), a large loss of generation is induced at a period of low demand (when there will be less generation on the system, less demand to respond to changes in frequency, and lower system inertia).

The specific “generators” lost are the interconnectors from Ireland, the Netherlands, and France, which equate to a total loss of capacity of  $\sim 3.5\text{GW}$  in this representation of the system. The actual

output of the interconnectors at these times will be scheduled based on the initial dispatch but, of course, may differ at the time of fault due to redispatch and unit commitment re-solves following earlier fault events. All cases are in this section dispatched with an empty contingency list.

As with the other case studies, this is chosen to represent a low probability event at a particularly inconvenient time to model extreme system response to the event. In this case, exacerbated by low demand periods where the total gross demand is approximately only 38GW, with the loss of infeed therefore representing approximately 10% of supply. It is during these times when the system is at its “bounciest” – that is, most susceptible to frequency deviations during loss of infeed and highest magnitudes of RoCoF. Therefore, in these cases the system is most susceptible to the negative consequences associated with frequency deviations such as LFDD and generator tripping. In this case, the model is run from hours 0 to 12 with the faults deterministically occurring at hour 4 compounded with stochastically generated perturbations. The first set of samples is performed in an economic dispatch mode, shown in Figure 5.25.

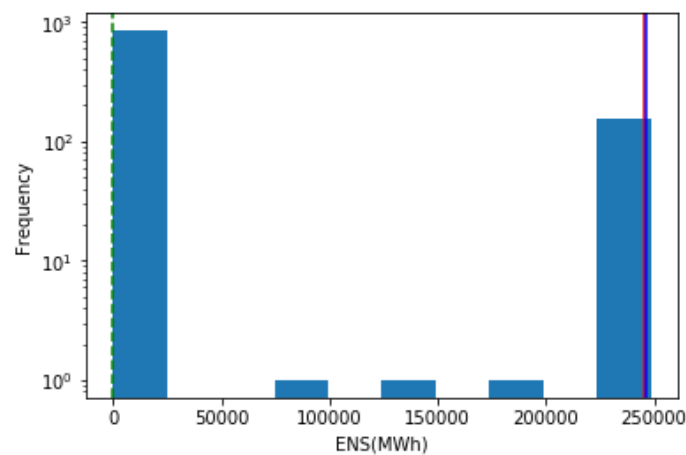


Figure 5.25 - ENS histogram for case with large generation loss and system in economic dispatch,  $\phi = 0$ , no frequency response, empty contingency list, no FDR

Similar to the B6 case study, another simulation is performed but, this time, with frequency response concentrated south of B6. That is, with 2000MW of frequency response dispatched South of B6 and 0MW North of it. There is no FDR in this case.  $\Psi$  was limited to 50MW, and will be for all subsequent cases. The results are illustrated in Figure 5.26.

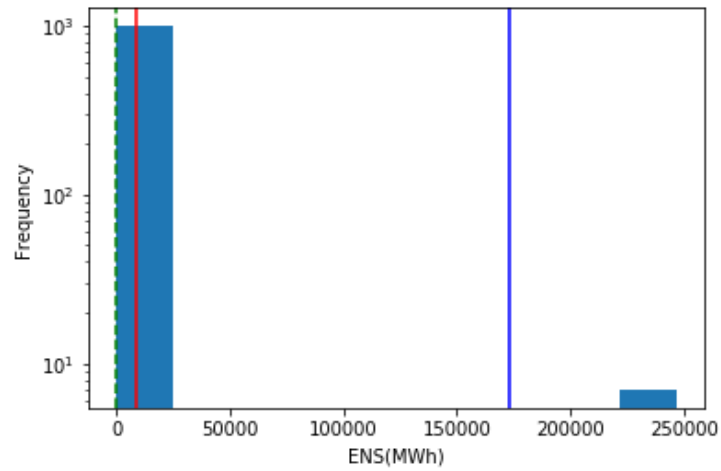


Figure 5.26 - ENS histogram for scenario with 2000MW of net response in South,  $\phi = 50\text{MW}$ , no FDR

A simulation is then performed, with results illustrated in with 500MW of net frequency response dispatched in the North of the system, 2000MW in the South, and FDR is available to see the benefits of having additional frequency response closer to the scale of outage observed. The results are shown in Figure 5.27.

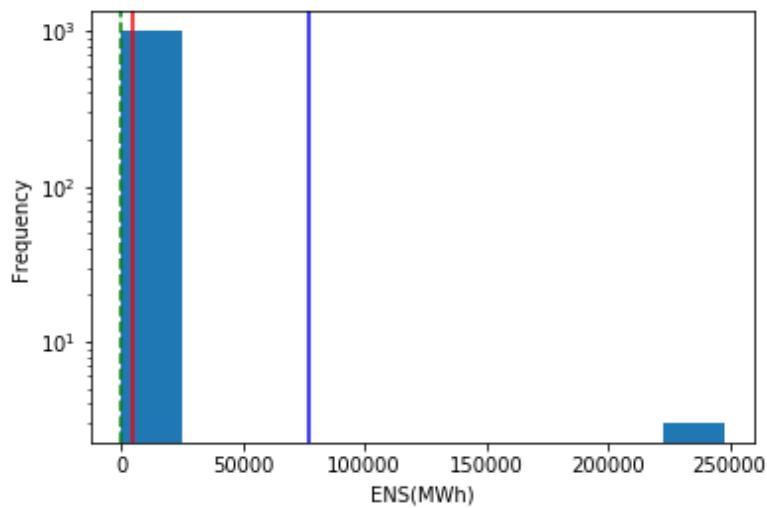


Figure 5.27 - ENS histogram of results from case with 500MW net frequency response in North, 2000MW in South, with FDR

This can be compared with Figure 5.28, and the same dispatch scenario, but with zero demand response allowed.

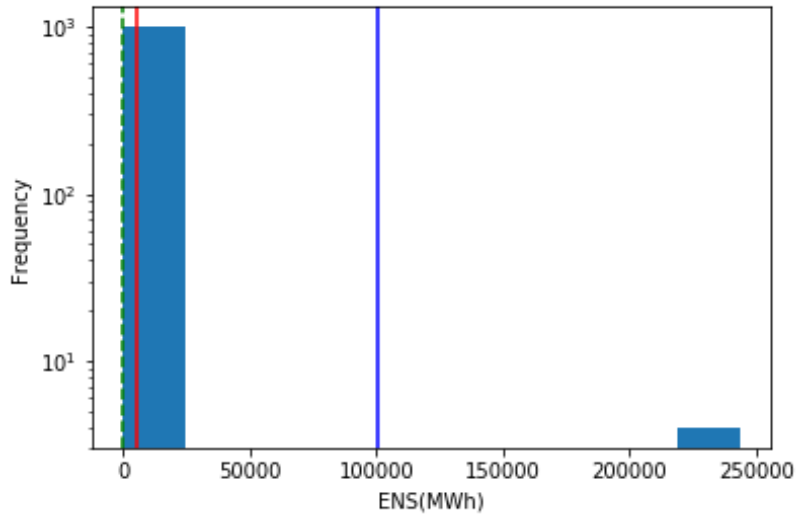


Figure 5.28 - ENS histogram of results from case with 500MW net frequency response in North, 2000MW in South, no FDR

As the next, and final, comparison, the significance of the unit commitment constraints will be briefly investigated. The work in Chapter 3 made various assumptions about the ability of generators to redispatch following perturbations to the system. In reality, generators have restrictions on their ability to ramp up and down based on factors such as reheating, available water for hydroelectricity, and electromechanical restrictions. Enforcement of unit commitment restrictions could have significant consequences for the ENS in simulations over longer events as more generators drop offline if other generators cannot be brought online to ameliorate this.

A stochastic simulation is run again but without enforcing the unit commitment constraints (in essence allowing generators to freely switch in and out with no time restrictions) to demonstrate the potential significance on the risk metrics used with the histogram shown below in Figure 5.29.

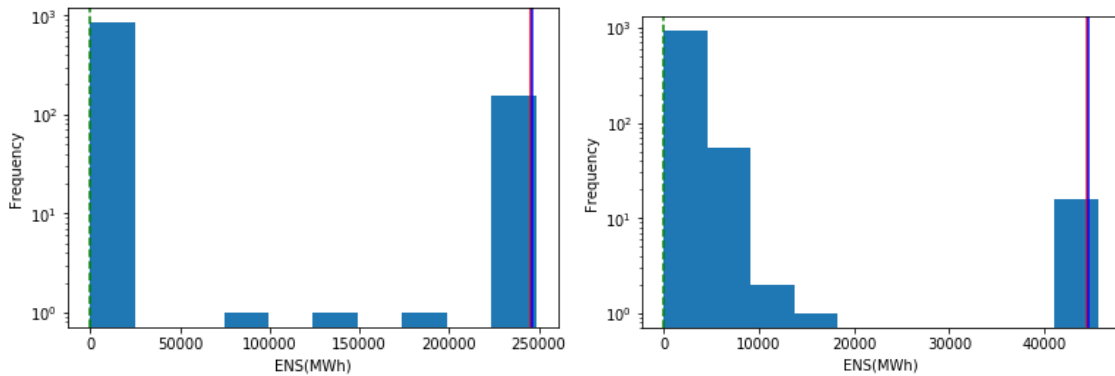


Figure 5.29 - ENS histogram [right] for case where there is a large loss of infeed but no constraint on generator up/down times, compared with baseline case in economic dispatch

## 5.7 Discussion and key findings

Collating the results from the various case studies in to a single table for quick reference produces the following (cases are given in the table in the same order in which they were performed) in Table 5.5 (an expanded version of which can be found in the Appendix 7.3).

Table 5.5 - tabulated results of case studies

| <b>Case</b>                    | <b>EENS (MWh)</b> | <b>VaR (99%. MWh)</b> | <b>cVaR (99%, MWh)</b> | <b>LOLP (%ge)</b> |
|--------------------------------|-------------------|-----------------------|------------------------|-------------------|
| <i>Baseline/Econ. Dispatch</i> | 2552±767          | 79128                 | 215142                 | 33.9±1.5          |
| <i>Baseline/N-1</i>            | 8249±1362         | 292223                | 355303                 | 60.8±1.5          |
| <i>Baseline/2000/FDR*</i>      | 1204±359          | 10417                 | 93827                  | 67.9±1.5          |
| <i>Baseline/2000/South*</i>    | 745±314           | 6645                  | 56810                  | 64.7±1.5          |
| <i>Baseline/Interpolated*</i>  | 418±118           | 6459                  | 22660                  | 67.9±1.5          |
| <i>B6/N-1</i>                  | 213±32            | 5488                  | 7628                   | 54.0±1.6          |
| <i>B6/Econ. Dispatch</i>       | 456±154           | 6016                  | 30198                  | 31.6±1.5          |
| <i>B6/1320MW</i>               | 840±218           | 9402                  | 47601                  | 46.1±1.6          |
| <i>B6/Constrained*</i>         | 530±197           | 6899                  | 37234                  | 32.2±1.5          |
| <i>B6/Trips*</i>               | 661±42            | 6476                  | 8791                   | 85.6±1.1          |
| <i>Gen Loss/Econ. Dispatch</i> | 37738±2762        | 245244                | 246337                 | 38.1±1.5          |
| <i>Gen Loss/South*</i>         | 2703±642          | 9062                  | 173601                 | 52.9±1.6          |
| <i>Gen Loss/FDR*</i>           | 1293±493          | 4439                  | 77117                  | 55.3±1.6          |
| <i>Gen Loss/No DR*</i>         | 1771±485          | 5556                  | 100891                 | 86.7±1.1          |
| <i>Gen Loss/No UC*</i>         | 1569±182          | 44428                 | 44581                  | 51.9±1.6          |

\*= situation where  $\Psi$  was limited to <50MW rather than 0

Interpreting the results of a simulation framework as complicated as EWPS is challenging in and of itself because of the volume of assumptions and the challenges associated with model implementation that come with it. The novelty, and major challenge, with EWPS was in the attempt to bring together disparate simulation methodologies and techniques with different data requirements so as to first understand the challenges associated with such a task.

Compromises at each stage were necessary to make the simulations work, and each stage on its own will have associated weaknesses which more specialised analysis could address, but the novelty of the work lies in the ensemble effort. No such simulations attempted previously have combined the scale of simulations and data handling, paired with the disaggregation of line risk that was undertaken in this modelling. Discussions were consistently held with peers and contacts in industry such as J. Kelly of SSE, who contributed to the work in Chapter 4 to ensure the work was a reasonable approximation of more detailed modelling.

Validation then is difficult, because models with the complexity of EWPS simply do not exist with the same functionality and complexity, particularly as regards the combination of weather conditions, spatial risk across OHL, and frequency response simulation. The model was developed from first principles using conventional representations of features of power system simulation, adapted to the differing contexts as well as possible. It is therefore reasonable to expect that, at each stage, the results should be taken as at least representative or reasonable approximations. The mantra “all models are wrong, but some are useful” from George Box should be remembered here.

What is important in any study where different cases are performed is that the simulation framework and assumptions that are used are done so consistently across case studies such that it is clear and obvious what is different in the inputs so the effects on outputs can be reasonably understood.

It should be remembered that, despite having over 70 nodes, and a combined total of over 340 lines and generators, the system model being used still represents a significant reduction on the actual GB system. The distribution networks are likely to be significantly weaker than the main transmission system, and also feature less redundancy and resilience due to the reduced economy of scale associated with distribution networks and the radial nature of typical distribution systems. Therefore, the results of the simulations provided should be understood in that context.

Further, to more fully quantify the impacts of this, more thorough analysis needs performed on the pathways which actually lead to the events associated with energy loss. The use of exaggerated OHL risk to intentionally create extreme network fault scenarios was intended in part to create lots of network outage states to more fully investigate the impacts of frequency response scheduling in situations where there are major network outages, but the exact fault scenarios and cascade events which lead to the largest values of ENS in the simulations are worth more comprehensive investigation than was able to be performed in this analysis.

Further, the use of correlated sampling also helps to reduce the randomness to facilitate better comparisons between the results of similar system scenarios. At a high level, the variation in results is more directly associated with the changes in input data rather than any difference in the events captured by random sampling. This effectively serves as a means of reducing the state-space and randomness of the investigations and studies carried out.

It should be noted that the size of the state-space for the analyses carried out here is significant, given the randomness assorted with the MCMC simulation of faults themselves (>340 assets over 12 hours), combined with the stochastic tripping behaviour of generators and lines, as well as with the stochastic behaviour of UFLS. Correlated sampling works to reduce the randomness and associate any change in ENS more directly with changes in dispatch scenarios as opposed to changes in fault scenarios, but there is still underlying uncertainty and randomness in the models.

Given, in some cases, the long tail of models may be also affected by as few as one extreme event associated with e.g. total system blackout at peak load, which will affect both the cVaR and VaR values significantly, this emphasises the difficulty of finding HILP events to model. When the contributory factors are combined in quantifying the probability of such events, net probability of such events is small (in a weather event itself already in the single digit percentiles annually). However, such events only need to happen once and cause a black start to cause major socioeconomic damage.

Identifying more obvious preventative measures which reduce the EENS (a reminder that EENS is an averaged value of ENS across simulations, while ENS itself represents the aggregated PNS across an individual scenario) well outwith the margins of error and minimise the long tail are useful aims, but the existence of such extreme HILP events emphasises that there is always residual low probability extreme events that cannot be picked up by random sampling.

All results then should be understood in that context – that the changes in ENS distributions are useful indicative measures of changes in performance, but that accuracy and precision can always be improved. Specifically, random sampling is likely a suboptimal approach for identifying such events beyond reasonable doubt unless the sample sizes are significantly larger than those used here, in which case filtering or variance reduction techniques would be imperative to improve model efficiency. Identifying which events are associated with these 1 in 12,000 sampled hours events and the pathways leading to the extreme high impact events and profiling the lower impact events would nevertheless be a useful and obvious next stage for investigation and simulation.

### 5.6.1 Baseline cases

Changing the frequency response-related parameters and constraints within the dispatch has a profound effect on the measured performance metrics. The use of suboptimal frequency response scheduling leads to worse, more extreme, and more probable adverse operational states dependent on how that frequency response is actually deployed. One potential reason for this is that, in the GB model, Scotland has very little thermoelectric generation and very little frequency responsive generation. In the “economic dispatch” case investigated, therefore, little generation is generally scheduled (and relatively little even exists any more) in Scotland – which has significant wind output even in the storm scenarios simulated with HWSS depressing power output on the relevant wind farms, and so loss of nodes tends not to result in loss of infeed on the remaining network.

One interpretation here is that placing frequency response in areas which are affected by significant storm events or is reliant on weak connections to the MITS means that line outages associated with network losses can have significant net impacts on the wider system. That is, on weaker networks, loss of network connectivity can lead to loss of connections to demand (and hence associated ENS), but with the increasing prevalence of distributed generation the system is also losing generation in such events. In situations where these networks are net exporters, while islanding of the subsections of network may cause automated disconnection of DG and therefore total blackouts on these disconnected network, the remaining MITS will “see” this as a net loss of generation at a time where other generators may simultaneously be losing network connections to the grid compounding the negative operational conditions.

Moving the frequency response away from the worst of the storm – at a very basic level, moving it from England to Scotland – ameliorates this, as can be seen when comparing the various performance metrics - but, given some of the North of England is still affected by the worst of the storm, does not entirely mitigate the consequences of network losses.

Flexible demand response, as implemented in this simulation, has a significant contribution to overall system security, and results in an almost halving of the cVaR and EENS values. This is likely because it does not rely in any way on needing network connections to demand centres and can act independently, and also because it acts almost instantaneously as implemented. More work needs to be conducted to determine a hypothetical fiscal value for this, and to more realistically represent such technologies, but it is clear demand response at a transmission scale can provide significant system operability benefits. Another potential future avenue of research would be to randomise the amount of FDR which actually turns up when demanded to investigate potential risk associated with this.

Finally, the effect of interpolating the weather data used in the simulation is considered. This has an effect on two aspects of the simulation – the wind power on the system (as the weather conditions at a given node to which wind generation is connected will change), and the distribution of risk across OHL on the system. This results in lower EENS, lower VaR, and lower cVaR values. This should not be surprising – by interpolating the data, less of the system is exposed to the most extreme values of wind speed proportionally, and so the probability of OHL faults happening concurrently at points in the system with the most extreme wind speeds is correspondingly lower. This also can be understood as vindication for the approach taken in Chapter 4 to disaggregate OHL risk on the system.

If only the most extreme wind speeds were used across all lines on the system and all nodes, this would serve as a distinctly conservative assumption and would likely overestimate the outage risk on lines across the system. The significant difference in performance metrics between the interpolated and uninterpolated data serves as a basic approximation for a comparison between conventional methods of quantifying OHL failure rates associated with weather and the novel techniques

demonstrated here, and given the difference in performance metrics between the two suggests a more thorough investigation is warranted.

A notable result is the depreciation in performance between the economic dispatch baseline case and the case with N-1-type dispatch. Without further analysis of the extreme results and the causal perturbations, it is difficult to understand why, precisely, the system performs worse in a situation where theoretically it should be better prepared. However, it is likely an effect associated with the islanding effects created by the concentration of faults associated with the coarse granularity of the incident dataset and the extreme nature of the perturbations caused. That is, if there is significant frequency-responsive generation, and generation of any kind, assigned to areas with extreme weather conditions prone to islanding, moving generation to these areas may simply exacerbate the consequences of outages, especially if economic dispatch is more likely to utilise generation in southerly regions away from the most extreme weather conditions but the N-1 dispatch tries to move more generation to Scotland, putting more frequency response in areas subject to more extreme weather. Further study is warranted to investigate this.

### 5.6.2 B6 cases

It can be observed that there is a serious degradation in performance across the analysed states when the contingency list is reduced from the N-1 proxy to zero, which has the impact of removing the consideration of network faults entirely from the dispatch of frequency reserve, with performance drop worse even than that of economic dispatch versus N-1.

As was found in the Baseline cases, the relationship between the dispatch of frequency response and system performance during adverse events is not as straightforward as “more equals better”, at least for the 1,000 sampled states considered in this scenario. The location and nature of this frequency response also matters. It can still be observed that it does have a material impact on the dispatch scenarios generated which in turn affects system performance in adverse states.

The inter-area flow in the various scenarios was found to be as high as 2.1GW in scenarios where there was no constraint on inter-area flows, and thus a loss of this connection would have serious consequences on system operability following a fault of those lines without adequate preparation.

The probability of just such a fault is low – but the severity of the impacts render it worth study nonetheless and the long tail of the potential outcomes following such an event can clearly be seen in the various histograms of results shown and reflected in the risk metrics observed.

Constraining the flow across these lines in the dispatch did not markedly improve performance outwith error bounds – although this could also be associated with the fact that, if any faults happened before the B6 fault event, the original dispatch information would be obfuscated by subsequent simulations and line flows at the time of fault may have been significantly larger than originally set in the first SCOPF.

This is a feature of the redispatch and re-commitment OPFs and reflects the challenges associated with this analysis – maintaining inter-area transfer restrictions after other faults may in itself cause load curtailment before the loss of B6, and so preparation for such eventualities is in itself not as straightforward as setting initial restrictions and ignoring them in subsequent simulations as may happen in the simulations performed here.

However, dispatching the system and programming in that a large amount of wind generation trips following the loss of B6, and correspondingly increasing frequency response south of the boundary,

does show a significant improvement in performance in the analysed states- most notably in the VaR, cVaR values. The EENS is otherwise not significantly improved beyond the margin of error.

What can be implied here is that the tripping action prevents the worst events from cascading to more severe and damaging outage events in the Northern section, as does the commissioning of extra frequency response in the area where there may be a corresponding the loss of infeed. Further, the increase in LOLP but consistent EENS implies that there are more nonzero ENS events, but that they are less severe on a case-by-case basis. This has a net neutral impact on EENS, but in material terms trying to mitigate the impact of more severe events may be deemed preferable to eliminating altogether less harmful ones.

### 5.6.3 Large generation loss cases

The results in all of the large generation loss cases show significant variation across all measured variables. It is noteworthy that results are heavily influenced by the long tail of the results with a small number of outliers being present in all cases but the magnitude of these outliers varying significantly.

Using extra frequency response dispatched across the boundary (500MW in North/2000MW in South, set arbitrarily to reflect the upper end of frequency response capacity on each system while still allowing for solution convergence) has a significant impact on both the “average” events and those that could be considered the “extreme” events (or top 1%, in this case). This is insofar as the averaged results across the test states are reduced well below the error of the first sets of results and the VaR and CVaR results reflect a significant shift in the distribution of faults and their extremeness.

Comparison can also be drawn between the use of the approximation of flexible demand response and the use of “conventional” scheduled frequency response. FDR does not rely on the transmission system to get power to where it needs to be, and acts instantaneously to deliver a targeted response. In contrast, the frequency response from generators as modelled here responds to a signal (power imbalance) on the system as a proportional controller with the associated time delay, which may not act rapidly enough to prevent frequency deviations associated with UFLS.

With the same gross amount of frequency response scheduling across the system, when comparing cases with or without DR, the EENS is not only significantly greater in cases where there is no DR, but the top 1% of events are non-negligibly worse as well. This illustrates that flexible demand response of this nature is useful for both moderate-severity events and more extreme ones.

Finally, removing the minimum up/down time constraints for generators (thus meaning the unit-commitment of generators is ignored and generators can switch in and out with zero limit other than ramping limitations across hours) has a mixed impact on the measured metrics. New generators can be brought online after the system has been perturbed by the loss of infeed and high-power generators such as nuclear can come online and offline rapidly. In reality, they are far more constrained in their ability to respond to system events. Increasing flexibility of generation, represented very approximately in this sense, can improve system resilience and reliability by allowing more generation to come online after outage events to balance supply and demand. However there is also a shift in where and what generation is dispatched, and though the cVaR is significantly reduced – representing a reduction in severity of the rarest events - the EENS and VaR are actually broadly consistent with the other results (that is, within the margins of error) and the VaR is actually above average.

There is a mid-point between the (rather conservative) assumptions about generation commitment and minimum up/down times used in most of the simulations versus having no unit commitment constraints whatsoever, and it can be observed that changing this significantly affects system

performance as measured here. Comparing these results to those attained in Chapter 3 emphasises the fact that the simulations in Chapter 3 were overly optimistic in this regard so cannot be judged as an accurate representation of a real system’s response, but still offers a useful comparison in relative terms across the different scenarios modelled.

5.6.4 Summary of cases and resilience quantification

Another metric that was recorded across all the simulations was a measurement of the proportion of states in a given simulation which exceed some absolute value of ENS for N-2 states. This was used as a proxy for a potential metric for the “resilience” of a system given a set sample size or scenario, reflective of the ability of the system to contain the negative consequences of an event which falls outwith the boundaries of a conventional “reliability” (i.e. N-1) paradigm. These results are collated into a table, in the same order as shown in Table 5.6.

A high number implies lots of “unresilient” simulations in an ensemble, but does not say anything about how bad the outcome of those simulations were. For example, changing the dispatch setting could see a significant reduction in the VaR, cVaR, and EENS values but could see an increase in the unresilience metric used here. This would imply that rather than a small number of extreme events, there could be a large number of less-severe events. Analysis could then be performed on the balance between these two metrics.

Table 5.6 - tabulated results for "unresilience metric" from simulations

| <b>Case</b>                    | <b>N-2+ "unresilience" (%ge)</b> |
|--------------------------------|----------------------------------|
| <i>Baseline/Econ. Dispatch</i> | 87.0±1.1                         |
| <i>Baseline/N-1</i>            | 82.2±1.2                         |
| <i>Baseline/2000/DR*</i>       | 82.5±1.2                         |
| <i>Baseline/2000/South*</i>    | 78.4±1.3                         |
| <i>Baseline/Interpolated*</i>  | 78.4±1.3                         |
| <i>B6/N-1</i>                  | 78.6±1.3                         |
| <i>B6/Econ. Dispatch</i>       | 78.9±1.3                         |
| <i>B6/Constrained*</i>         | 85.8±1.1                         |
| <i>B6/Trips*</i>               | 59.9±1.6                         |
| <i>Gen Loss/Econ. Dispatch</i> | 64.3±1.5                         |
| <i>Gen Loss/South*</i>         | 63.5±1.5                         |
| <i>Gen Loss/DR*</i>            | 56.9±1.6                         |
| <i>Gen Loss/No DR*</i>         | 30.5±1.5                         |
| <i>Gen Loss/No UC*</i>         | 56.5±1.6                         |

The resilience “threshold” in these cases is arbitrarily set to 10MW – i.e. nonzero but small. A zero value here would simply represent the LOLP. This performance metric is the proportion of states N-2 or worse where the ENS is higher than the threshold. Via this metric it is clear to see that the system is most susceptible and performs worst in scenarios where there are significant cases of islanding as was the case in the baseline cases. The variation in outcomes is much more severe in the Gen Loss cases - e.g. there is a difference of ~34 percentage points between the best and worst performing scenarios compared to the Baseline cases where there is at most 9 percentage points.

Two noteworthy results can be taken from these results. Interpolating the data has a significant effect on the results of the simulation in terms of the “resilience” of the system, due to the reduced level of system exposure to the most extreme weather parameters and hence less islanding associated with wind faults (compare the first and fifth cases in the table above, without and with interpolated data

respectively). Also, the significant variation in results associated with a large loss of infeed. This is because of the link between the loss of infeed, dispatch of frequency response, and the magnitude of the outages which are incurred. The loss of infeed from the interconnectors not only affects the load-supply balance at the time of fault, but also the ability of the system to respond to other faults by diminishing the reserve of frequency response on the system.

It should also be noted how important the ability to separate analysis of reliability-typical metrics (e.g. EENS) from resilience-driven metrics (e.g. VaR) could be. EENS inherently depends on averaging results across the entire population of a simulation ensemble, whereas VaR, cVaR, and the new metric proposed allow examination of the more severe, rare events' effects on results.

The resilience metric proposed allows one to determine the proportion of events which may fall into an "acceptable" or "unacceptable" boundary of risk whereas cVaR and VaR allow an exploration of how the most extreme events drive wider performance metrics which would otherwise be lost in more gross estimators.

## 5.8 Conclusion

The demonstrated approach in this chapter is, by necessity of the nature of the simulations being undertaken, complicated, computationally expensive, and, in terms of the software implementation, decidedly extensive. The sum total of the *python* model is circa 8,000 lines of code over several scripts and took almost 2 years of development. However, the results that can be gleaned from this are useful and demonstrate various important concepts.

The probability of events as significant as the loss of B6 and the loss of interconnectors as modelled in the case studies is difficult to quantify because there is little historical precedent or data to quantify the probability of such events. Faults on the French interconnector, for instance, are not uncommon, and interconnectors themselves are vulnerable to tripping and disconnections as seen in the South Australian Blackout [14] which has been discussed previously. Similarly, the August Blackouts in the UK [13] originated from a fairly innocuous lightning strike on a line which was restored appropriately, but which led to concurrent outages of wind generation and distributed generation, and coincided with a trip on gas fired generation. Therefore, the net impact of the event was still extreme but the inducing event was actually reasonably predictable and should have been low impact.

The events chosen for simulation in these cases all reflect HILP scenarios and are difficult to contextualise in the normal running of a power system. The storm used was specifically chosen for its extremity and rarity, and the extreme events in the case studies represent a compounding of both an uncommon inducing event and an uncommon set of outages corresponding to that inducing event.

The compounding low probabilities of these events make the simulations performed here representative of a small proportion of the kinds of events which will happen to a power system in typical operational conditions and so, again, the results should be understood in the context of the relative differences between the simulations and case studies and how both the frequency and intensity of outage events change.

What has been demonstrated is that frequency response scheduling has an impact on both the distribution of ENS during fault events, and the potential extremeness of these events- for correlated simulations. This can be due to the location of where frequency response is scheduled, or if generation is dispatched in such a way that frequency response is scheduled in areas subsequently affected by storm conditions. The speed of response also matters – in cases where demand response was used, where frequency response was less reliant on the network and acted instantaneously, the system performance metrics were notably improved.

Intuitively it makes sense that events which jeopardize the integrity of the transmission system are better secured against using resources which are not then reliant on the transmission system being affected by the incident natural hazard, be that an extreme wind event, seismic event, or any other inclement operational conditions. The results here demonstrate quite clearly that is indeed the case.

What should be noted, also, is the significance in the models of very small numbers of extreme events and their impacts on the observed results. In many of the histograms, the results indicated the vast majority of results being in the first bin, with <10 observed states in larger bins. This meant that the VaR, cVaR results were particularly sensitive to changes in the distribution of these results, and also that, by inspection, the histograms are difficult to extract results from directly, in their own right, with the scale of bins used. In future, there may be better, alternative, ways of showing the results of these simulations less sensitive to single-digit numbers of extreme events obscuring the visualisation of the distribution of less-severe events.

However, despite the large scale of the simulation and the significant number of features the simulation includes, there are still significant abstractions and approximations which take the model away from an ideal representation of the system.

Voltage is not directly considered, neither is reactive power. Wind direction, too, is ignored. Rotor angle stability is also not addressed, nor is localised frequency changes. Similarly, the effects of wind speed on a line are likely very different between a gust perpendicular to, and one parallel to, an OHL – but there is a lack of work understanding this.

Further, solar power is not considered and considered negligible. Given the case studies used are in the UK during the peak of winter, this then is not unreasonable as an approximation – but for summer storms, or storms in warmer climates, this may be a less appropriate assumption.

In the frequency response simulation, RoCoF tripping is not considered, nor is under-frequency tripping by generators. Again, in reality this means that some features are missed which, in reality, can have a significant impact on system stability following system perturbations. Other factors which can cause disconnection such as vector shift protection are also not considered, which is still present on the GB network. This means generation vulnerable to deviations in frequency caused by other loss of infeed events, potentially leading to cascading outage events such as those seen in August 2019. The formulation of the simulation in the manner as performed here, however, means that it is possible in future to incorporate these features into future simulation methodologies.

Another factor not considered in significant detail is the resilience of substations, generators, or other point assets themselves. Substations usually have more than one route through which power can be transmitted and the node-branch representation of the network cannot capture this. Further, in this model fault states are characterised as binary “in service” representations of an asset. Functionally, assets may be able to be utilised in reduced capacity if damaged by a natural hazard. Wind faults on substations were not considered at all in this implementation but falling vegetation and extreme gusts can also impact substations, however the impact may not be as severe as that on OHL.

The type of frequency-related protection on connected generation may be significant and is not fully considered in this analysis – GB at the time of writing typically uses 0.125Hz/s as a RoCoF protection setting but with decreasing system inertia this may be overly conservative and may exacerbate negative operational conditions following outage events, and so this setting is under review. Comparison between the effects of using these settings or less strict ones may be a further useful analysis to undertake.

Further, the impact of the direction of wind and comparison between homogenous representations of OHL and disaggregated representations as used in these studies would also be useful to determine the significance of the difference across methodologies. A comparison between interpolated and uninterpolated cases prima facie indicate significant differences in system performance in this simulation, but only over one case. Future case studies could be used to perform a more comprehensive comparison between the datasets as was done in Chapter 4.

There are various aspects which can and should be improved in future iterations of this work, particularly incorporating RoCoF tripping for assets in the frequency response, and using more efficient and realistic representations of the redispatch algorithm, for example. However that does not take away from the significant part of the work, which is demonstrating how these different aspects of system restoration interact with each other to understand their significance.

Future iterations of this research could operate over long time periods, for instance, perhaps incorporating system repairs and restoration of generators more generally, but this would necessitate efficiency savings across the model. There are two main processing bottlenecks in this implementation – the island finding algorithm following network faults, and the repair UC-OPF. These were necessary in this implementation to allow the cumulative effect of storms on the system to be simulated as well as to replicate the fact that system operators would be concerned not simply with meeting supply and demand but ensuring line flows across the system were secured to prevent further cascading. Future work would have to find a way of improving the efficiency of these aspects of the work.

The results should also be understood in the context that the sample sizes are very small for an MCMC type study, with typical Markov Chain Monte Carlo (MCMC) style simulations typically having a lower limit of ~10,000 samples- especially given the complexity of the simulation means a much larger state space size than typical security assessments.

More detailed studies would therefore need to improve on the efficiencies within the model to allow larger, potentially more accurate and precise result sets to be generated. Nonetheless, the relative changes between the result sets are useful as indicative comparators even if the specific contingency states generated represent only a small subsample.

Another potential output for this methodology is to identify sections of the network or individual assets associated with particularly high risk metrics to either identify weaknesses in the system or particularly critical assets. This could be paired with the methodology used in Chapter 4 to visualise risk properly across the system over a given time horizon to aid in planning decisions e.g. where to dispatch generation, where to place backup generation, etc.

# Chapter 6 Conclusions and future work

## 6.1 Summary of contributions and achievements

This thesis has demonstrated over its course various novel approaches and methods for use in quantifying and understanding the impact of extreme weather on power systems. Quantification has been done using metrics such as EENS and VaR with another metric EMLS also demonstrated to quantify the expected severity of a particular scenario.

Various different simulation approaches have been deployed on different scales of network, e.g. a truncated version of the Reduced GB representation, a representation of the Northern Scottish transmission network, and a more detailed version of the Reduced GB model updated with more recent wind generator data.

Further, various different simulation methods have been incorporated in a way which has not been done before, allowing investigation of different kinds of fault events and different operational modes for the mitigation of high impact events on the power system. It is acknowledged that even these do not represent an ideal representation of a power system, but nonetheless it is useful for demonstrating the concepts which this thesis concerns and in many cases are an advancement of existing approaches.

This thesis has demonstrated advancements in approaching modelling of HILP events, quantification of OHL risk during extreme weather events, and integration of disparate simulation methods to investigate the impact of dependent faults on the power system associated with extreme weather conditions.

The main contributions and findings of the completed research can be described in the following.

### 6.1.1 Defining approaches and frameworks in which to simulate dependent, weather induced faults in a power system and investigate model sensitivities

As demonstrated in Chapter 3, modelling power system faults during extreme weather events is a complicated task requiring significant quantities of data from several sources. The interactions between different data types and models is clearly illustrated and the sensitivity of the output metrics to changes in these data sources and relationships is demonstrated.

Though the model representations are simplified in this case – such as it is with frequency response being neglected, load shedding being performed using heuristics, and other simplifications – a comparison between different fault-wind relationships clearly illustrates that approximations or errors in data or modelling can have a profound effect on the outputs of such models.

Using frameworks such as this allows individual aspects of the model to be modified individually to evaluate the sensitivity of model outputs to the data and simulation models used within so that either aspects of the modelling can be improved to increase the simulation accuracy or precision, or such that network performance can be quantified in different operational scenarios.

When modelling the impact of natural hazards on a power system, at multiple stages in the thesis what constitutes an “event” has been a matter of discussion. This is because how an “event” is interpreted can have significant implications: typically in extreme weather simulation scenarios, weather is seen as an external factor affecting the power system. A weather system is an external “event” in its own right, acting independently on the power system based on some postulated relationships.

The failure of a line is, in its own way, also an “event” - a line taken out of service is agnostic to whatever causes its failure when it is out of service in a security assessment, except to the extent of what type of fault or outage has occurred. I.e. in a generic DCOPF it does not matter whether a lightning bolt or gust of wind has taken a line out of service, the line is out of service when the calculations are performed. In a transient or dynamic simulation, however, a lightning strike acts over timescales which are significantly impacted by automated protection actions which are not generally captured in OPFs (e.g. auto-recloser actions). The quantification of the impacts of that outage are tied to the failures of lines, but only indirectly associated with the wind. Similarly, the amount of wind infeed on the system is determined by the wind capacity factor given to the model. This is calculated externally, and again the DCOPF does not take consideration of what is generating the levels of wind “generation” – it only interprets it as a maximum and minimum power output, irrespective of what is actually determining these values.

In Chapter 5, the effects of perturbations after this can then be examined – UFLS, frequency response, and generator trips, for example. In the system frequency response simulation, again, the network and its failures are not considerate of the network at all beyond the aggregated pool of generation, demand response, and load. So when talking about “HILP” events one needs to be clear about from where the probability and impact is actually being derived – is the causal weather event itself low probability, or the effects on the power system associated with failures associated with that event? This emphasises the need to have clear frameworks for modelling natural hazards and extreme weather such that these factors can be understood.

In conventional security studies examined in the literature (e.g. [54], [102]), frequently the simulation of such events extends as far as taking lines out of service and e.g. running a DCOPF to quantify its impact on the system via metrics such as EENS – such as was demonstrated in Chapter 3. Chapter 3 investigates the relationship between an external weather event, a relationship between a natural hazard and a failure rate on OHL, and the impact a change in this relationship can have on subsequent results. Chapter 4 investigates the significance of the changes in data granularity and disaggregation when modelling OHL and wind power distributions across the power system. Chapter 5 looks at the relationship between different aspects of simulation after any set of perturbations has actually been generated and their relationship with changing security criteria. In these cases the weather event itself is consistent, but the interpretation of the weather event’s impacts on the power system varies. Visually this can be represented at a high level as what is shown in Figure 6.1.



Figure 6.1 - chain of causality for effects of weather on power system

This is alluded to in the framework developed in Chapter 3 and more fully developed in Chapter 5. The natural hazard perturbs the system in some way – be that by determining the wind power infeed, the collection of line faults, etc. The SFR/OPF loop evaluates the consequences of this more fully. An SFR model does not take into consideration what has caused the supply-demand imbalance only that one exists; much like if a wind-induced line fault happens it is unlikely the loading of the line will have any impact on the actual probability of that line failing. A key contribution, and overriding theme, of this

work is demonstrating the relationships between these different aspects of resilience modelling and how they interact with each other.

### 6.1.2 Demonstrating sensitivity of power system analysis to changes in failure rate-weather relationships

In Chapter 4, a change in fault probability for the most extreme case on the system (normalised down) by a factor of 2 has an impact in orders of magnitude on resultant EENS in the case studies performed, and both the probability and severity of outage events which occur.

That is, more things break, more things break at the same time, and the consequences are more severe. This demonstrates the need for caution when using stochastic simulation methods reliant on techniques such as fragility curves because even minor changes in these relationships can have significant impacts on the outputs of such models. If the results of these simulations are then to be used for investment or operational decisions, any errors could lead to significant negative consequences (be that stranded assets, inefficient investments, or widespread blackouts depending on the type of decision-making).

Using synthetic relationships such as those demonstrated in Chapter 3 clearly is not appropriate for real world investment decisions, but are shown as useful for indicating the sensitivity of stochastic modelling of its nature to the veracity of any data-driven models used.

The key for any comparison study is to ensure consistency in approach across different case studies such that any difference in outcomes can be clearly attributed to changes in the input data, hence the importance of clearly defining the relationships and models used within and applying them consistently. This work has at various stages demonstrated the significant impact changes on incident data can have whether that be changing the resolution of the data used, changing the parametric relations, or changing more technical aspects such as the contingency lists and parameters in an SCOPF.

The individual components of work such as performed in Chapter 5 can be improved, but the fundamental aspects are a contribution to modelling HILP events attributable to natural hazards insofar as they clearly demonstrate the kinds of interactions and simulations which may be necessary to comprehensively quantify the potential impacts of extreme wind events on transmission systems like GB.

### 6.1.3 Illustrating potential correlations between overhead line fault risk and wind power

Chapter 5 focuses on elaborating on some of the themes investigated in Chapter 3 and better understanding overhead line risk during storm events. Given overhead lines are not point assets – unlike generators or substations, which can be assumed such – current approaches which tend to assume they are or treat them as such are clearly inadequate when modelling the impact of extreme weather. This is because weather acts over large regions spatially and over different temporal ranges depending on geographic conditions and weather types. Treating OHL as point assets with a single failure rates over their range – as was done in Chapter 3 – fails to capture the diversity of weather conditions to which an OHL may be exposed as well as the different geographical conditions.

The variation across networks of overhead line failure risk is demonstrated clearly with failure rates being shown to vary across power systems and individual lines, with observations also made about potential linkages between wind power infeed and OHL risk. This merits further investigation to quantify more fully such risk to ameliorate it due to increasing penetration of wind across distribution networks and power systems globally.

There are socioeconomic reasons why the system has been designed in this manner in Scotland which has the unintended consequence of creating the potential for serious common-mode faults and correlated outages of lines and windfarms associated with HWSS and line faults, be they transient or permanent. This should have implications for future systems development – if resilience is to become a component of system planning, diversity of asset type as well as location has to be considered, on the basis of work such as Chapter 4 which clearly illustrates that concentrations of transmission infrastructure increase the probability of faults happening in any given location. The comparison between interpolated and uninterpolated data emphasises this – if significant amounts of system assets are concentrated where the weather is most extreme, significant portions of the system are subject to the risk associated with that natural hazard.

#### 6.1.4 Linking spatially resolved weather data to power system modelling and simulation

Integrating disparate simulation and modelling techniques associated with power systems proved to be a difficult, complex task. Converting netCDF4 data from NASA sources to formats usable in a python simulation required extensive conversion and scripting across multiple platforms. In Chapter 3, the effect of wind on generation was not considered which is simply not representative of the modern GB network given the high levels of wind penetration on the system. This was the reason for the simplified consideration of wind data. As is consistent across the work in this thesis, a basic first principle was established, and then subsequently developed and improved. In the case of the weather data used in Chapter 3, a conventional representation of how wind speeds are used to quantify OHL risk was used. This was deemed inadequate, and subsequently improved in Chapter 4. The simulation of the actual system response, demonstrated in Chapter 3, was also then improved in Chapter 5 to represent a comprehensive advancement on the simpler methods shown in Chapter 3.

Linking reanalysis data to wind generation, frequency response dispatch in an SCOPF, and OHL risk projection has not been done before as it was demonstrated in this work. This still represents only a first approximation of fully considering wind's effect on power system risk, however – directionality was not considered, and various corrections were necessary on the weather data to make it suitable for use in the different components of simulation. Each iteration of improvement in the methodology demonstrated in the research conducted is nonetheless a progression of the state of the art, in discrete terms and in aggregate.

What is also worth mention is the linking of wind generation, OHL failure risk, and spatially distributed natural hazards over an extended timeframe. In Chapter 3 the simulation was over a 24 hour window but using simplified representations of weather and the power system. Chapter 4 extended the modelling of OHL but only examining representations of the system within a single hour. This was because the fragility curves and wind power curve used were equally in per-hour terms. A major part of why weather-dependent faults are problematic, though, is the cumulative effect of such outages over an extended period of time, hence the need to, in Chapter 5, combine these analyses to model cumulative outages on the power system over a known storm system on a known network. Ideally in future historic fault events could be modelled in this manner with known load balance data to validate the model, but such data was not forthcoming at the time of research. Nonetheless, a future avenue of study is clear.

#### 6.1.5 Integrating simulation of frequency response with weather fault simulation and demand response

Standard resilience modelling described in the literature generally makes assumptions about how the system responds to perturbations and faults – idealised redispatch of generators, tripping of generators and actions of intertrips, etc. In reality, the system can respond to perturbations in a

chaotic, unpredictable manner. The implementation in Chapter 5 builds upon the weaknesses identified in Chapter 3 and combines that with the novel methodologies demonstrated in Chapter 4 to perform various case studies to identify how important improved detail in simulations could be. This includes the combination of a frequency response model and line overload simulation model attached to the wider framework, which, in the context of resilience studies, has not been done before in the manner demonstrated.

The model implementation considers all stages of system restoration to different levels of granularity. Again, though individual aspects of this simulation may be more broad approximations and abstractions than others, the net impact is a comprehensive simulation that identifies how these different aspects of power system simulation may interact with weather conditions and the associated impacts and risks for the power system.

This is a clear advancement on existing conventional techniques and acts as a first step towards better understanding how to mitigate HILP events associated with extreme weather. Further, the consideration, even at a basic level, of flexible demand response was used to illustrate the significant potential benefits such schemes – which are not reliant on wider system security – could provide to system reliability and resilience. The advancement is in pulling together these factors in an orderly way and establishing a working model of considering all of them in a simulation framework.

#### 6.1.6 Establishing methods for assessing the effect of changing frequency response regimes on system reliability and resilience performance

Given the complicated nature of the simulation model used, complete validation of results was not possible because the data does not exist which can be compared with the findings from the simulation model. However, using techniques such as correlated sampling to compare similar scenarios was used to compare the effect of changing dispatch scenarios on the system to at least give a relative, or indicative, representation of the effect of changing how the network is set up ahead of unpredictable or extreme events. The significant variation in results when different frequency response or demand response scheduling is used is indicative that such factors can have a significant impact on results even if only because it changes the location and scheduling of generators on the system.

Further, it demonstrates that for some types of fault scenarios frequency response scheduling may have more significant impacts than in others. Generation infeed events are most sensitive to changes in frequency response scheduling, particularly comparing between using demand response and not. One potential reason for this is that, in the Baseline cases demonstrated, ENS was associated with islanding events which could not be contained with frequency response alone, and so changing the scheduling of frequency response had fewer direct impacts. That is, the effects of changing frequency response were associated with the location of generation and whether it was placed in at-risk regions of the system. Placing generation in these areas meant islanding of nodes in such areas would result in net loss of infeed on the MITS and according stability effects. If generation was accordingly concentrated in areas impacted by the storm, this could lead to particularly negative consequences.

Such phenomena could only be investigated using a simulation platform as demonstrated due to the number of factors which must be considered to perform such analysis. Though different aspects of the simulation can be improved in future to make the simulation methods more realistic or representative, the framework and approach demonstrated here marks a clear and productive first step to more complete and holistic simulation of such events.

### 6.1.7 Demonstrating significance of spatial disaggregation and interpolation of weather data for use in power system simulations

In both Chapters 4 and 5, interpolated and un-interpolated weather data sets were used, meaning the results of analysis using these different datasets could be compared to interrogate their significance. As would reasonably be expected, in Chapter 5 it was shown that interpolating the data means that the performance of the system during the case studies was better when the interpolated data was used. This was due to the lower concentration of system assets experiencing the most extreme values of wind speed. Given the significant sensitivity of wind failure rates, wind power output to changes in wind speed above  $25\text{ms}^{-1}$  as demonstrated in Chapter 4, these results corroborate each other's findings that the weather data set used should be of appropriate granularity for the network under investigation.

The coarser, 50x50km MERRA-2 dataset is in itself likely too broad to appropriately model networks as condensed and concentrated as GB with significant regional meteorological variation. Despite the added computational expense associated with having to sample more sections of line and the added pre-processing it was shown that the results differ enough such that such improvements in granularity are necessary on a GB level to ensure accuracy of results. It should also be noted that distribution-network level studies may require even more precise weather data for suitable analysis. Given distribution OHL and associated assets can reasonably be expected to be even more fragile than transmission assets, this suggests a potential area meriting further investigation.

This also clearly emphasises the inadequacy of treating OHL as homogenous assets during analysis involving natural hazard resilience studies pertaining to wind, because the variation in wind across these assets is lost.

### 6.1.8 Demonstrating the potential value of Flexible Demand Response solutions for containing HILP events or large loss of infeed events in frequency response simulations

As implemented in Chapter 5 – though an idealised and simplistic representation – flexible demand response could provide crucial services during force majeure events where network integrity is compromised to help stave off the initial hit of a major loss of infeed or interconnection. Primary and Secondary frequency response can be understood as mechanisms by which the system buys time to respond using larger scale, controllable system features such as redispatch or bringing other generators online. The flexible demand response could also be understood as an idealised representation of non-generation frequency response that acts in a precisely targeted manner.

In conventional resilience studies which do not directly consider frequency behaviour, such simulations could be interpreted as simulations in which frequency response acts in a perfect, targeted manner to control frequency almost instantaneously (by disconnecting the exact amount of demand required to balance demand with generation) – which is not completely different from FDR as represented in the case studies in Chapter 5. Ergo, the clear difference in results in cases where FDR was used versus where it was not used is indicative of the fact that speed of response, and the precision of its response, does indeed matter, and cannot simply be ignored and approximated out of studies. This mattered particularly in cases where there was concentrated loss of infeed, or in the cases where there was major loss of infeed across the system but was shown to be a significant benefit regardless of context.

Finding a market value for such solutions, of course, and demonstrating their efficacy is another field of study altogether. Flexible demand response was encouraged in the system to be deployed as fully as possible by assigning zero cost to it in the objective function, and so the dispatch SCOPF model was

incentivised to use it heavily as primary response. It was not limitless in its use, however, given secondary and tertiary response were still required and so flexible demand response alone could not be used to sustain the system following perturbations.

#### 6.1.9 Understanding the potential importance of features such as Unit Commitment restrictions in resilience simulations

As discussed in Chapters 3 and 5, factors such as how quickly generators can switch in and out of operation can have a significant impact on a system's operability during adverse conditions. Having a flexible fleet of generators means less need for load curtailment if generators can be brought quickly online where they are needed to meet demand. This does not directly affect the frequency response on its own – though the frequency response will be indirectly affected by the inertia of the generators which can be brought back online and the net demand remaining on the system.

Nonetheless, the variation in results when the Unit Commitment constraints are not enforced (or, to view it another way, when the minimum up and down time of the generators is reduced to zero) is in itself noteworthy and emphasises the need to take consideration of such factors in resilience studies. Being able to modify and take consideration of such factors was a key benefit of the approaches taken in Chapter 5 – doing so in more proprietary software would simply not be possible with the same degree of flexibility. Having control over every aspect of the simulation allows many degrees of freedom in how simulations are controlled to account for different features and despite the extensive case studies undertaken there are more still potential avenues to explore different case studies and features.

#### 6.1.10 The significance of initial dispatch when subsequent fault events happen

Due to the way the model works, when the system redispatches and the restoration unit commitment OPF is performed, effectively the initial dispatch that is generated in the SCOPF is discarded. Beyond that, the only retained information or bearing on subsequent hours in the simulation is the allocation and location of frequency response. Otherwise, the model uses whatever generation is available to minimise the load curtailment, for example. Therefore, the benefits of using any sort of specialised SCOPF are immediately lost other than the use of the frequency response allocation and the generator commitment at the start of the simulation and the information about the minimum down time of generators. Adding further complexity at this stage would add further computational burden in an already complicated and computationally expensive simulator. However, for each case study the SCOPF was only performed once to generate a feasible dispatch scenario, there may still be room to expand it dependent on other factors (e.g. memory, the scale of contingency list and implementation, etc.)

However, what can be appreciated at the very least from this is the fact that, in reality, during an extreme event it is not unreasonable that the first priority of any operator during a force majeure event would be to keep the system online and then try and secure the system against a subsequent event. Given that the simulated events can go further than N-10 in terms of the number of faulted assets during the storm, it is reasonable to assume a focus on just keeping the network operational as a first priority, and so the assumption made that an operator would try and maintain frequency response from key generators and just try and otherwise minimise system disruption and load curtailment otherwise seems a reasonable approximation to use in modelling.

#### 6.1.11 Industrial co-operation and academic impact

Much of the work was conducted either with guidance or support from industrial partners. The earlier stages of the work had support from *S&C Electric* who were, at the time, industrial partners of the

project and supported the project work at the University of Strathclyde which formed the basis of this research.

When they moved on, support was provided by J. Kelly and F. Irwin of SSE who provided technical guidance and data necessary for the assembly of the network models used in Chapters 4 and 5. In return, the work was presented at various stages to SSE at their Perth headquarters to workers involved with the use of weather data and asset management.

The CDT itself was assembled on the basis of encouraging interdisciplinary co-operation among researchers and involvement of industrial partners to ensure work was relevant to the modern power sector and grounded in applicability to real world needs of the power system. This was a driving feature of the undertaken research and is what guides many of the future directions of the research: guiding planning for reliability and resilience work involving the electricity system grounded in realistic representations of the power system generated from extensive consultation with industrial partners.

The tools developed, especially in Chapter 4, are designed to be extensible and reproducible for planners or operators to understand the risk extreme weather poses to their systems during inclement weather conditions. For example, using the work in Chapter 4 planners could run daily calculations overnight using weather forecasts to generate risk profiles for their sections of the network to aid in deployment of restoration teams and operational risk management measures., especially before e.g. storms. This would be particularly useful at a transmission level where the scale of impacts can be far more significant.

Presentation of the research at events like the EPSRC HubNet Risk Days, or the ETP Conference 2019 in Dundee (at which the prize for best presentation in session was awarded for material used in this thesis) was done to disseminate knowledge to peers. Material was also presented to the UK's energy market regulator Ofgem and to consulting company *Risk Management Solutions (RMS)*, London in 2019, a company heavily involved with what is known as cat (catastrophe) modelling. This emphasises the broad utility of the work conducted in this thesis.

The work presented in this thesis has been presented at academic and industrial conferences for knowledge dissemination, as previously mentioned. Two academic, peer-reviewed publications have also been produced based directly on the research conducted, which have already been discussed and are referred to in the relevant sections. The work which formed the content of Chapter 3 was presented at the IET's International Conference on Resilience of Transmission and Distribution Networks, with the work in Chapter 4 being published in the IET Smart Grid journal at the end of 2019, in a high-quality open-access Special Issue on system resilience.

In total, then, this emphasises the industrial and academic value of the undertaken research and its potential value for future endeavours as a basis for more detailed analyses.

## **6.2 Future work**

Though a thorough approach to modelling the impact of weather on power systems has been undertaken, significant amounts of further areas of research remain that can be pursued to build upon and expand the research completed. Here follows a non-exhaustive discussion of some potential areas of improvement and further development can be pursued.

### **6.2.1 Incorporation of alternative kinds of distributed renewables generation**

Presently, the modelling does not take consideration of the impacts of renewable generation such as solar. It was assumed this could be ignored as the modelling was carried out in winter when, in the UK, days are particularly short and dark, so there is unlikely to be significant infeeds of solar PV on the

system. However, it is entirely possible for high wind conditions to occur during otherwise sunny conditions and, when combined with wind infeed, there may be significant renewables penetration and little inertia to support system security, making the system substantially more vulnerable to shocks and disturbances.

Given solar PV is also grid-connected via power electronics, there is also risk of RoCoF-related disconnections following less serious system perturbations which could cascade into more serious events. Therefore, one desirable future area of study would be to include modelling of solar PV and weather impacts such as cloud cover in the analysis, particularly given the spatially distributed impacts of e.g. cloud cover on solar PV.

### 6.2.2 Improved frequency response modelling

The frequency response modelling used represented a very basic approximation of what a real system would do following a frequency disturbance. As happened in the August 9<sup>th</sup> blackouts, as well as LFDD there can be loss of infeed from distributed generation associated with vector shift protection or RoCoF protection on devices, which can feed into cascading events and cause widespread outages. This was not directly considered in the modelling.

Further, load shedding – though representative of approaches taken in real life on the GB grid – made no distinction between “essential” and “non-essential” loads. Though the flexible demand response algorithm at a very superficial level acted as a proxy for this, it represented a very idealised and optimistic approach of load shedding that also did not represent a particularly controlled deployment after the initial response. It may be desirable to feed in a methodology for the model to assign loads to “essential” (heating, cooling in life-critical contexts) and “non-essential” (wet devices, non-critical thermostatic) classifications.

Given there is also a link between demand and ambient temperature, it is reasonable to expect that at colder temperatures there will be more heating deployed on the system – but not all of that heating may be necessary at the same time and there may be a way of harnessing such heating demand in a controlled manner non-intrusively to support system security.

The model also assumed a homogenous, single bus representation of frequency response. All available evidence suggests, though there can be assumed an “averaged”, representative system-wide frequency response, there are pronounced localised effects, particularly when comparing areas such as Scotland and the midlands of England where in the latter there is significantly greater inertia than in Highland Scotland where years of decommissioning of thermoelectric generation has significantly weakened system strength. As a first step and improvement of existing techniques, using a homogenous frequency profile marks a solid first step, but many improvements could be made to make this more realistic dependent on the context being examined.

In the system frequency response simulation, various assumptions about the behaviour of individual generators also had to be assumed – all generators were bundled into a single generator with “representative” controller behaviour. In reality, the behaviour of a hydroelectric scheme and e.g. an interconnector will vary significantly and the assumption that the net effect of averaging the individual contributions of all these multiple infeeds on the system may not be appropriate. Further study is warranted.

### 6.2.3 Incorporating the investment-side problem

Modelling the system response to perturbations is only a minor aspect of the challenge in performing security studies. Planners and operators must also then tackle the problem of “so what?” Incorporating simulations with investment-side optimisations is a complicated problem and has been

tackled in the literature, but not with simulations as complicated as those undertaken here. Resilience-based investments and reliability-based investments may differ – for example the latter may incorporate features such as backup generation, spare transformers, etc, with reliability perhaps leaning more towards redundancy or reinforcement. Reliability investment, however, can also improve resilience – but quantifying the benefits of such investment is a challenge in itself because of the various issues highlighted here: how does one decide which events the system needs to “secure” against, and how does one quantify the cost-benefit behind the decision-making? A balance also needs to be struck between the complexity of the simulation algorithm versus the computational expense of the optimisation, and any further expansion of the optimisation SCOPF in the first instance would require significant efficiency savings in the simulation.

#### 6.2.4 Examining effects of other weather impacts on the power system

For the reasons stated in the introduction and literature review sections of this thesis, wind has been the primary concern for its impacts on the power system, but many other natural hazards threaten the power system and require similar quantification – and many of those natural hazards themselves coincide with wind and compound its risk.

In the analysis carried out, wind direction was omitted as a factor as it was not considered in the original fragility curves. Similarly, line faults were assumed to be permanent rather than transient. In reality, wind can cause a wide range of faults and problems for operators beyond simply taking a line out of service. Transient faults such as short circuits from falling vegetation or clashing conductors can also cause issues for system security. This could particularly be a risk for lines which have a similar bearing experiencing similar weather patterns. As a very simple example, a strong Southwesterly gust in Scotland could cause transient faults across lines perpendicular to that bearing associated with clashing lines, and if these coincide across a network and multiple line outages happen simultaneously before lines can be brought back in service by DAR actions this could lead to outages and islanding. Such events were not captured in the analyses performed thus, but could be a worthwhile future area of analysis.

Another potential direction would be to combine wind data with temperature data. On exposed, high elevation grids such as SHETL there is significant risk of line icing in colder months in winter. This can be affected by line loading, which is in itself determined by generation dispatch and system demand. Combining a simple OPF with the visualisation and weather modelling demonstrated in Chapters 3 and 4 could be used to visualise OHL risk associated with extreme cold or heat. Line heating via heavy loading can be used to reduce the risk of line collapse associated with line icing, but increasing ambient temperatures can also affect the loading of lines and necessitate de-rating in summer months or during heatwaves.

With increased penetration of renewables on distribution networks during summer months associated with PV or with wind during windier days this could become acutely problematic for more congested networks, and so application of these methods to identify particularly at-risk regions of the system could be a useful avenue of future research.

#### 6.2.5 Effects of climate change and other externalities on system resilience

Externalities such as socioeconomic drivers of system design have been discussed, but climate change mitigation itself is set to become a major driver of system design as well as the need to prepare for a more renewables-heavy grid. Hypothetically, the methods demonstrated in Chapter 4 could be used with annualised data to determine at-risk areas of network such that hypothetical future network extensions or new connections could be optimised to minimise weather-risk and avoid particularly windy regions. Of course, as highlighted in Appendix 7.1, there are many reasons why such

optimisations may not be as simple as finding the lowest-risk areas for network connections, but this information could feed into network design at least as a consideration and to help make evidence-based cases for connection pathways.

Given climate change is also liable to change the frequency and intensity of extreme weather events, such tools adapted to other weather phenomena such as flooding (for substation, generator risk) or lightning events (for any overground exposed infrastructure) could also prove vital for network planners and operators going forward, particularly if resilience becomes a major factor in price control mechanisms such as RIIO.

Climate change compounds pre-existing risks in a complex manner and so extension of the methods deployed in this thesis to other weather patterns may be particularly useful for other spatially distributed weather events affecting the power system.

With metrics to quantify system resilience such as the very basic ones demonstrated here there are ways and means of comparing hypothetical resilience improvement strategies going forward – after all, improvement cannot be measured if there is no metric by which to quantify it.

#### 6.2.6 Comparator studies

In Chapter 4 the methodology to represent lines as 2-dimensional arrays rather than point-to-point homogenous assets is demonstrated but it is not compared to existing methodologies directly, rather the varying failure rates are shown as proof unto itself that present approaches are inadequate. Clearly in future a more direct comparison study could be carried out, in tandem with a developed simulation model, to elaborate on this.

Using a smaller network model such as Iceland would also ease validation of results and avoid the risk of results being obfuscated by the scale and magnitude of the test network. The Ryan model as used was chosen as it was available and complete and broadly representative of the modern GB network, but for demonstration purposes sometimes it is better to use smaller, simpler networks to illustrate important concepts. A study comparing homogenous representations of OHL to spatially disaggregated models as deployed here would therefore be a useful output.

#### 6.2.7 Improvement of model efficiency

The model as deployed in Chapter 5 represents many compromises brought together to prove that the integration of the wide array of areas of study is possible. There are various weaknesses in the formulation and deployment of the model as demonstrated, which have all been discussed, and in future these should be addressed to allow model validation and verification. Nonetheless, the generalised framework still has value.

Most immediately the linkage between the SFR loop and the subsequent Unit Commitment problem needs to be improved and made more efficient, with the representation of tertiary response improved. The representation used is significantly idealised, though, crucially, was applied consistently across all test cases used and so any error introduced would be consistent across all cases.. This part of the model in particular should be investigated to improve model realism and efficiency.

#### 6.2.8 Optimal OHL routing planning

For systems such as GB, where infrastructure development is significantly constrained by socioeconomic constraints such as public opposition and environmental concern, the routing of OHL is an intricate and complex challenge with many stakeholders. Nonetheless, the methods developed in Chapter 4 introduce another potential factor for planners to consider. The routing of lines is also

related to the risk presented to those lines from natural hazards, particularly when considering the bearing of prevailing winds and geographic conditions or vegetation.

Geographic conditions can provide wind shadows for OHL which, while in the context of wind generation would prove problematic, could be useful for reducing the risk associated with extreme wind conditions based on the prevailing wind directions of an incoming storm. Studies examining the potential improvements in reliability which could be achieved by planning future developments in larger scale grids – or rebuilding existing routes – could be informative for future planning decisions if resilience becomes a pressing concern. The complementarity of OHL risk and wind power infeed implies that future planners should seek to situate windfarms in areas which are exposed to as much wind as possible while ensuring long distance exposed OHL are exposed to as low risk from natural hazards as possible, but there will be a cost-benefit balance to be found.

#### 6.2.9 Improved mitigation planning

With the techniques demonstrated in Chapters 4 and 5, there is the possibility not only to make projections about high risk areas of the network but to then put in place suitable preventative or corrective measures for when there are particularly acute adverse operating conditions. Once high risk areas of the system are identified using the visualisation techniques demonstrated, interventions such as back-up generation, additional frequency response reserve, or rapid response teams could be put in place to optimise system restoration following any major outage which happens in the vicinity of the at-risk areas.

This emphasises the strength of the methodology in that it can be used across different timescales with the simulation framework proposed to examine different kinds of interventions and responses to different natural hazards in inclement operational conditions.

#### 6.2.10 Three-dimensional OHL modelling and wind direction consideration

As mentioned at length in Chapter 4, when geographic features are considered the representation and visualisation of OHL failure risk can naturally be extended from 2 dimensions to 3 dimensions to incorporate the elevation and altitude of OHL. Further, if such features are being considered, factors such as wind shadow from hills and wind tunnels can then begin to be incorporated into simulations to more fully understand the implications of the inclusion of such features. It is also worth noting that wind direction could also matter in this context given the bearing of prevailing winds versus that of the OHL being considered and the associated geographic features of mountain ranges within the study areas.

### 6.3 Concluding remarks

The completed research forms a comprehensive examination of the potential impacts of extreme wind on the power system and how to model these impacts, with various case studies performed to examine the significance in any given analysis of the different abstractions and data used in such modelling.

The distributed impacts of extreme wind have been demonstrated on representations of real networks, as has the sensitivities of the performance of these systems to changes in the models used to represent failure-weather relationships.

The modelling illustrates that increased system flexibility – either via flexible demand response or the ability to switch generators in and out of service more rapidly – has a significant impact on system resilience and reliability for the types of test cases shown, particularly in cases where there is significant loss of infeed.

Changing the relationships between weather and failure rates is shown to have an impact in terms of orders of magnitude on the performance metrics used in security studies, as does the representations used more generally to aggregate risk on OHL. Further, it has been shown that more granular data results in significantly better system performance in security studies performed as less of the network is deemed to be exposed to the most extreme weather conditions. This was demonstrated both via visualisation of the data in question and via simulation using the underlying models. This is important to note because it is the same fundamental underlying data, interpreted differently, producing very different results, for the very same incident weather events.

Incorporating the spatial impacts of weather on wind power availability as well as on OHL security demonstrated the potential correlations between these phenomena and marks a first step towards more fully quantifying and mitigating these impacts with a reasonable understanding of potential areas of improvement, but also demonstrated the significant uncertainty in these types of studies, even when corrections are added to account for e.g. wind gust velocity, asset altitude, etc.

A quote attributed to George Box, and already mentioned previously in this thesis, is that “all models are wrong, but some are useful”. The problem with modelling the impact of weather on power systems is that it is not known exactly how wrong our models are, and until something goes wrong it is difficult to know exactly how useful they were in the first place. The work done here is at least a step towards trying to understand how wrong they actually may be and, crucially, in what ways.

## References

- [1] Energy Research Partnership, 'Future Resilience of the UK Electricity System' (Energy Research Partnership, United Kingdom, 2018), pp.
- [2] 'Scientific consensus: Earth's climate is warming ',<https://climate.nasa.gov/scientific-consensus/>, accessed 23 April 2019
- [3] Entriken, R. and Lordan, R., 'Impacts of extreme events on transmission and distribution systems', in, *2012 IEEE Power and Energy Society General Meeting*, (2012, San Diego, USA)
- [4] 'Storm Desmond',<https://www.enwl.co.uk/site-search/?q=storm%20desmond#!?page=1>, accessed 14/06/2019
- [5] 'Scotland Hit By 165mph Winds As Twitter Dubs Storm 'Hurricane Bawbag' (Photos) (Video)',[https://www.huffingtonpost.co.uk/2011/12/08/scottish-winds-hurricane-bawbag\\_n\\_1136460.html](https://www.huffingtonpost.co.uk/2011/12/08/scottish-winds-hurricane-bawbag_n_1136460.html), accessed 15 April 2019
- [6] Dawkins, L.C., 'Weather and Climate Related Sensitivities and Risks in a Highly Renewable UK Energy System: A Literature Review' (The Met Office, United Kingdom, 2019), pp.
- [7] McColl, L., Palin, E.J., Thornton, H.E., et al., 'Assessing the potential impact of climate change on the UK's electricity network', *Climatic Change*, 2012, 115, (3), pp. 821-835.
- [8] Masson-Delmotte, V., Zhai, P., Pörtner, H., et al., 'IPCC, 2018: Summary for Policymakers', *Global Warming of*, 2018, 1.
- [9] 'Digest of UK Energy Statistics (DUKES): Solid Fuels and Derivatives' 2018), pp. 37
- [10] United States National Academies, 'Enhancing the Resilience of the Nation's Electricity System' United States, 2017), pp.
- [11] 'Storm Desmond damage across Cumbria estimated at £500m ',<https://www.theguardian.com/uk-news/2015/dec/08/storm-desmond-damage-cumbria-estimated-500m>, accessed 14/06/2019
- [12] 'The 2003 Northeast Blackout--Five Years Later',<https://www.scientificamerican.com/article/2003-blackout-five-years-later/>, accessed 14/06/2019
- [13] 'Investigation into 9 August 2019 Power Outage',<https://www.ofgem.gov.uk/publications-and-updates/investigation-9-august-2019-power-outage>, accessed 5 June 2020
- [14] 'BLACK SYSTEM SOUTH AUSTRALIA 28 SEPTEMBER 2016 - FINAL REPORT',[https://www.aemo.com.au/-/media/Files/Electricity/NEM/Market\\_Notices\\_and\\_Events/Power\\_System\\_Incident\\_Reports/2017/Integrated-Final-Report-SA-Black-System-28-September-2016.pdf](https://www.aemo.com.au/-/media/Files/Electricity/NEM/Market_Notices_and_Events/Power_System_Incident_Reports/2017/Integrated-Final-Report-SA-Black-System-28-September-2016.pdf), accessed 20/06/2019
- [15] Jamieson, M., Strbac, G., Tindemans, S., et al., 'A simulation framework to analyse dependent weather-induced faults', in, *IET International Conference on Resilience of Transmission and Distribution Networks (RTDN 2017)*, (2017, Birmingham, UK)
- [16] Jamieson, M., Strbac, G., and Bell, K., 'Quantification and Visualisation of Extreme Wind Effects on Transmission Network Outage Probability and Wind Generation Output', *IET Smart Grid*, (Institution of Engineering and Technology, 2019)
- [17] Liang, G., Weller, S.R., Zhao, J., et al., 'The 2015 Ukraine Blackout: Implications for False Data Injection Attacks', *IEEE Transactions on Power Systems*, 2017, 32, (4), pp. 3317-3318.
- [18] Teng, F., Dupin, R., Michiorri, A., et al., 'Understanding the Benefits of Dynamic Line Rating Under Multiple Sources of Uncertainty', *IEEE Transactions on Power Systems*, 2018, 33, (3), pp. 3306-3314.
- [19] 'Enabling Resilient UK Energy Infrastructure: Natural Hazard Characterisation ',<https://www.imeche.org/policy-and-press/energy-theme/enabling-resilient-uk-energy-infrastructure>, accessed 12 July 2019
- [20] National Grid Electricity Transmission Plc, 'Climate Change Adaptation Reporting: Second Round Response' (National Grid Electricity Transmission Plc, 2016), pp.

- [21] 'IEEE Guide for Improving the Lightning Performance of Electric Power Overhead Distribution Lines', *IEEE Std 1410-2010 (Revision of IEEE Std 1410-2004)*, 2011, pp. 1-73.
- [22] Napolitano, F., Tossani, F., Borghetti, A., et al., 'Lightning Performance Assessment of Power Distribution Lines by means of Stratified Sampling Monte Carlo Method', *IEEE Transactions on Power Delivery*, 2018, 33, (5), pp. 2571-2577.
- [23] Kuntz, P.A., Christie, R.D., and Venkata, S.S., 'Optimal vegetation maintenance scheduling of overhead electric power distribution systems', *IEEE Transactions on Power Delivery*, 2002, 17, (4), pp. 1164-1169.
- [24] Romps, D.M., Seeley, J.T., Vollaro, D., et al., 'Projected increase in lightning strikes in the United States due to global warming', *Science*, 2014, 346, (6211), p. 851.
- [25] Piper, D. and Kunz, M., 'Spatiotemporal variability of lightning activity in Europe and the relation to the North Atlantic Oscillation teleconnection pattern', *Natural Hazards & Earth System Sciences*, 2017, 17, (8).
- [26] Rowbottom, M.D., 'Method of calculating the vulnerability of an overhead transmission line to faults caused by galloping', *IEE Proceedings C - Generation, Transmission and Distribution*, 1981, 128, (6), pp. 334-341.
- [27] Murray, K. and Bell, K.R.W., 'Wind related faults on the GB transmission network', in, *Probabilistic Methods Applied to Power Systems (PMAPS), 2014 International Conference on*, (2014, Durham, UK)
- [28] Morris, E.A., Bell, K.R.W., and Elders, I.M., 'Spatial and temporal clustering of fault events on the GB transmission network', in, *2016 International Conference on Probabilistic Methods Applied to Power Systems (PMAPS)*, (2016)
- [29] Macdonald, H., Hawker, G., and Bell, K., 'Analysis of wide-area availability of wind generators during storm events', in, *2014 International Conference on Probabilistic Methods Applied to Power Systems (PMAPS)*, (2014, Durham, UK)
- [30] Karauskas, K.B., Lundquist, J.K., and Zhang, L., 'Southward shift of the global wind energy resource under high carbon dioxide emissions', *Nature Geoscience*, 2018, 11, (1), pp. 38-43.
- [31] Brayshaw, D.J., Troccoli, A., Fordham, R., et al., 'The impact of large scale atmospheric circulation patterns on wind power generation and its potential predictability: A case study over the UK', *Renewable Energy*, 2011, 36, (8), pp. 2087-2096.
- [32] Hosking, J.S., MacLeod, D., Phillips, T., et al., 'Changes in European wind energy generation potential within a 1.5 °C warmer world', *Environmental Research Letters*, 2018, 13, (5), p. 054032.
- [33] Cannon, D.J., Brayshaw, D.J., Methven, J., et al., 'Using reanalysis data to quantify extreme wind power generation statistics: A 33 year case study in Great Britain', *Renewable Energy*, 2015, 75, pp. 767-778.
- [34] Sinden, G., 'Characteristics of the UK wind resource: Long-term patterns and relationship to electricity demand', *Energy Policy*, 2007, 35, (1), pp. 112-127.
- [35] Grams, C.M., Beerli, R., Pfenninger, S., et al., 'Balancing Europe's wind-power output through spatial deployment informed by weather regimes', *Nature Climate Change*, 2017, 7, p. 557.
- [36] Colantuono, G., Wang, Y., Hanna, E., et al., 'Signature of the North Atlantic Oscillation on British solar radiation availability and PV potential: The winter zonal seesaw', *Solar Energy*, 2014, 107, pp. 210-219.
- [37] 'Electricity Distribution Company Performance 2010 to 2015', <https://www.ofgem.gov.uk/publications-and-updates/electricity-distribution-company-performance-2010-2015>, accessed 05 June 2020
- [38] Michelle, T.H.v.V., Justin, S., David, W., et al., 'Impacts of recent drought and warm years on water resources and electricity supply worldwide', *Environmental Research Letters*, 2016, 11, (12), p. 124021.
- [39] 'California wildfires', <https://www.bbc.co.uk/news/topics/cjyq4rd3x3zt/california-wildfires>, accessed 6 December 2019

- [40] 'PG&E Shuts Power to California Resort Area to Prevent Wildfires', <https://www.wsj.com/articles/pg-e-shuts-power-to-california-resort-area-to-prevent-wildfires-11560046802>, accessed June 11 2019
- [41] Dian, S., Cheng, P., Ye, Q., et al., 'Integrating Wildfires Propagation Prediction Into Early Warning of Electrical Transmission Line Outages', *IEEE Access*, 2019, 7, pp. 27586-27603.
- [42] Koufakis, E.I., Tsarabaris, P.T., Katsanis, J.S., et al., 'A Wildfire Model for the Estimation of the Temperature Rise of an Overhead Line Conductor', *IEEE Transactions on Power Delivery*, 2010, 25, (2), pp. 1077-1082.
- [43] 'Capacity Market', <https://www.gov.uk/government/collections/electricity-market-reform-capacity-market>, accessed 22 May 2020
- [44] Yaji, K., Homma, H., Sakata, G., et al., 'Evaluation on flashover voltage property of snow accreted insulators for overhead transmission lines, part I - field observations and laboratory tests to evaluate snow accretion properties', *IEEE Transactions on Dielectrics and Electrical Insulation*, 2014, 21, (6), pp. 2549-2558.
- [45] Pernebayeva, D., James, A., and Bagheri, M., 'Live line snow and ice coverage detection of ceramic insulator using Gabor image features', in, *IET International Conference on Resilience of Transmission and Distribution Networks (RTDN 2017)*, (2017)
- [46] Thornton, H.E., Hoskins, B.J., and Scaife, A.A., 'The role of temperature in the variability and extremes of electricity and gas demand in Great Britain', *Environmental Research Letters*, 2016, 11, (11), p. 114015.
- [47] Auffhammer, M., Baylis, P., and Hausman, C.H., 'Climate change is projected to have severe impacts on the frequency and intensity of peak electricity demand across the United States', *Proceedings of the National Academy of Sciences*, 2017, 114, (8), p. 1886.
- [48] Wilson, I.A.G., Rennie, A.J.R., Ding, Y., et al., 'Historical daily gas and electrical energy flows through Great Britain's transmission networks and the decarbonisation of domestic heat', *Energy Policy*, 2013, 61, pp. 301-305.
- [49] De Sa, A. and Al Zubaidy, S., 'Gas turbine performance at varying ambient temperature', *Applied Thermal Engineering*, 2011, 31, (14), pp. 2735-2739.
- [50] Steinhauser, G., Brandl, A., and Johnson, T.E., 'Comparison of the Chernobyl and Fukushima nuclear accidents: a review of the environmental impacts', *Science of the Total Environment*, 2014, 470, pp. 800-817.
- [51] 'Transmission Availability Data System (TADS)', <http://www.nerc.com/pa/RAPA/tads/Pages/default.aspx>, accessed 10/04/2017
- [52] Slugeň, V., Nuclear Safety', *Safety of VVER-440 Reactors*, (Springer, 2011)
- [53] Wu, B., Soares, C.G., Zhan, D., et al., 'A sequential barrier-based model to evaluate human reliability in maritime accident process', in, *2015 International Conference on Transportation Information and Safety (ICTIS)*, (2015)
- [54] Panteli, M., Mancarella, P., Trakas, D., et al., 'Metrics and Quantification of Operational and Infrastructure Resilience in Power Systems', *IEEE Transactions on Power Systems*, 2017, PP, (99), pp. 1-1.
- [55] 'System Operator Incentives', <https://www.ofgem.gov.uk/electricity/wholesale-market/market-efficiency-review-and-reform/system-operator-incentives>, accessed 22 May 2020
- [56] Rockafellar, R.T. and Uryasev, S., 'Optimization of conditional value-at-risk', *Journal of risk*, 2000, 2, pp. 21-42.
- [57] Moreno, R.: 'Reliability and Cost-Benefit-Based Standards for Transmission Network Operation and Design', PhD, Imperial College London, 2012
- [58] Strbac, G., Djapic, P., Moreno, R., et al., 'Review of Distribution Network Security Standards' (Consulting, N., London, 2015), pp. 233-253
- [59] 'Security and Quality of Supply Standard (SQSS)', <https://www.nationalgrideso.com/industry-information/codes/security-and-quality-supply-standards>, accessed 22 May 20
- [60] Weedy, B.M., Cory, B.J., Jenkins, N., et al., *Electric power systems*, (John Wiley & Sons, 2012)

- [61] Grigg, C., Wong, P., Albrecht, P., et al., 'The IEEE Reliability Test System-1996. A report prepared by the Reliability Test System Task Force of the Application of Probability Methods Subcommittee', *IEEE Transactions on Power Systems*, 1999, 14, (3), pp. 1010-1020.
- [62] Billinton, R., Wu, C., and Singh, G., 'Extreme adverse weather modeling in transmission and distribution system reliability evaluation', in *Power Systems Computation Conf.(PSCC)*, (2002, Seville, Spain)
- [63] Gaver, D.P., Montmeat, F.E., and Patton, A.D., 'Power System Reliability I-Measures of Reliability and Methods of Calculation', *IEEE Transactions on Power Apparatus and Systems*, 1964, 83, (7), pp. 727-737.
- [64] Fan, F. and Bell, K.R.W., 'Fragility Curves and Fault Outage Prediction for Overhead Lines' (University of Strathclyde, United Kingdom, 2019), pp.
- [65] Ofgem, 'Electricity Capacity Assessment Report 2013' 2013), pp. 83-84
- [66] TradeWind, 'Integrating Wind - Developing Europe's power market for the large-scale integration of wind power' (EWEA, Denmark, 2009), pp. 23-25
- [67] Anderson, P.M. and Mirheydar, M., 'A low-order system frequency response model', *IEEE Transactions on Power Systems*, 1990, 5, (3), pp. 720-729.
- [68] Vogler-Finck, P.J. and Früh, W.-G., 'Evolution of primary frequency control requirements in Great Britain with increasing wind generation', *International Journal of Electrical Power & Energy Systems*, 2015, 73, pp. 377-388.
- [69] 'Mandatory response services ',<https://www.nationalgrideso.com/balancing-services/frequency-response-services/mandatory-response-services>, accessed 9 July 2019
- [70] Virmani, S., 'Security impacts of changes in governor response', in *IEEE Power Engineering Society. 1999 Winter Meeting (Cat. No.99CH36233)*, (1999)
- [71] Zhang, G. and McCalley, J., 'Optimal power flow with primary and secondary frequency constraint', in *2014 North American Power Symposium (NAPS)*, (2014)
- [72] 'Low Frequency Demand Disconnection',<https://www.nationalgrideso.com/sites/eso/files/documents/SOF%20-%20LFDD%20-%20July%202017.pdf>, accessed 11 July 2019
- [73] 'Grid Code',<https://www.nationalgrideso.com/codes/grid-code>, accessed 18/06/2019
- [74] Labeeuw, W., Stragier, J., and Deconinck, G., 'Potential of Active Demand Reduction With Residential Wet Appliances: A Case Study for Belgium', *IEEE Transactions on Smart Grid*, 2015, 6, (1), pp. 315-323.
- [75] Davarzani, S., Pisica, I., and Taylor, G., 'A novel methodology for predicting potential responsiveness in residential demand', in *IET International Conference on Resilience of Transmission and Distribution Networks (RTDN 2017)*, (2017)
- [76] Ela, E., Gevorgian, V., Tuohy, A., et al., 'Market Designs for the Primary Frequency Response Ancillary Service&#x2014;Part I: Motivation and Design', *IEEE Transactions on Power Systems*, 2014, 29, (1), pp. 421-431.
- [77] Rios, M.A., Kirschen, D.S., Jayaweera, D., et al., 'Value of security: modeling time-dependent phenomena and weather conditions', *IEEE Transactions on Power Systems*, 2002, 17, (3), pp. 543-548.
- [78] Ju, W., Sun, K., and Yao, R., 'Simulation of Cascading Outages Using a Power-Flow Model Considering Frequency', *IEEE Access*, 2018, 6, pp. 37784-37795.
- [79] Kjølle, G.H. and Gjerde, O., 'Vulnerability analysis related to extraordinary events in power systems', in *2015 IEEE Eindhoven PowerTech*, (2015)
- [80] 'pandapower - Convenient Power System Modelling and Analysis based on PYPOWER and pandas',[http://pandapower.readthedocs.io/en/v1.2.2/\\_downloads/pandapower.pdf](http://pandapower.readthedocs.io/en/v1.2.2/_downloads/pandapower.pdf), accessed 20/01/2017
- [81] 'NCDC Climate Data Online',<https://www.ncdc.noaa.gov/>, accessed 09/03/17
- [82] Bell, K.R.W. and Tleis, A.N.D., 'Test system requirements for modelling future power systems', in *IEEE PES General Meeting*, (2010, Minneapolis, USA)

- [83] Panteli, M. and Mancarella, P., 'Influence of extreme weather and climate change on the resilience of power systems: Impacts and possible mitigation strategies', *Electric Power Systems Research*, 2015, 127, pp. 259-270.
- [84] Panteli, M., Mancarella, P., Hu, X., et al., 'Impact of climate change on the resilience of the UK power system', in *IET International Conference on Resilience of Transmission and Distribution Networks (RTDN) 2015*, (2015)
- [85] Panteli, M. and Mancarella, P., 'Modeling and Evaluating the Resilience of Critical Electrical Power Infrastructure to Extreme Weather Events', *IEEE Systems Journal*, 2015, PP, (99), pp. 1-10.
- [86] 'Modern-Era Retrospective analysis for Research and Applications, Version 2', <https://gmao.gsfc.nasa.gov/reanalysis/MERRA-2/>, accessed 11 April 2019
- [87] 'MERRA-2 tavg1\_2d\_flux\_Nx: 2d,1-Hourly,Time-Averaged,Single-Level,Assimilation,Surface Flux Diagnostics V5.12.4', [https://disc.gsfc.nasa.gov/datasets/M2T1NXFLX\\_V5.12.4/summary](https://disc.gsfc.nasa.gov/datasets/M2T1NXFLX_V5.12.4/summary), accessed 17 January 2019
- [88] 'MERRA-2 inst1\_2d\_asm\_Nx: 2d,1-Hourly,Instantaneous,Single-Level,Assimilation,Single-Level Diagnostics V5.12.4', [https://disc.gsfc.nasa.gov/datasets/M2I1NXASM\\_V5.12.4/summary](https://disc.gsfc.nasa.gov/datasets/M2I1NXASM_V5.12.4/summary), accessed 30 March 2019
- [89] 'SRTM 90m DEM Digital Elevation Database ', <http://srtm.csi.cgiar.org/>, accessed 5 April 2019
- [90] 'open-elevation', <https://open-elevation.com/>, accessed 11 April 2019
- [91] 'Renewable Energy Planning Database quarterly extract ', <https://www.gov.uk/government/publications/renewable-energy-planning-database-monthly-extract>, accessed 15 April 2019
- [92] Staffell, I. and Pfenninger, S., 'Using bias-corrected reanalysis to simulate current and future wind power output', *Energy*, 2016, 114, pp. 1224-1239.
- [93] Jones, E., Oliphant, T., and Peterson, P., 'SciPy: Open source scientific tools for Python', 2001.
- [94] 'Electricity Ten Year Statement (ETYS) Appendix A' (National Grid ESO, 2017), pp. 2-8
- [95] 'Electricity Ten Year Statement (ETYS) Appendix A' (National Grid ESO, 2018), pp. 2-8
- [96] 'The Matplotlib Basemap Toolkit User's Guide', <https://matplotlib.org/basemap/users/index.html>, accessed 15 April 2019
- [97] Hunter, J.D., 'Matplotlib: A 2D graphics environment', *Computing in science & engineering*, 2007, 9, (3), p. 90.
- [98] Hagberg, A., Swart, P., and S Chult, D., 'Exploring network structure, dynamics, and function using NetworkX' 2008), pp.
- [99] 'Batch coordinate transformation tool ', <https://www.ordnancesurvey.co.uk/gps/transformation/batch#>, accessed 3 April 2019
- [100] Backshall, J., Manley, J., and Rebane, M., *The upland management handbook*, (English Nature Peterborough, United Kingdom, 2001)
- [101] Pipelzadeh, Y., Moreno, R., Chaudhuri, B., et al., 'Corrective Control With Transient Assistive Measures: Value Assessment for Great Britain Transmission System', *IEEE Transactions on Power Systems*, 2017, 32, (2), pp. 1638-1650.
- [102] Clements, D. and Mancarella, P., 'Fragility curve based storm modelling of distribution networks with staff constraints', in *IET International Conference on Resilience of Transmission and Distribution Networks (RTDN 2017)*, (2017, Birmingham, UK)
- [103] 'Three Mile Island Incident', <https://www.world-nuclear.org/information-library/safety-and-security/safety-of-plants/three-mile-island-accident.aspx>, accessed 16 July 2019
- [104] 'Realtime', <https://extranet.nationalgrid.com/RealTime>, accessed 18 July 2019
- [105] Staffell, I. and Pfenninger, S., 'The increasing impact of weather on electricity supply and demand', *Energy*, 2018, 145, pp. 65-78.
- [106] Hart, W.E., Laird, C.D., Watson, J.-P., et al., *Pyomo-optimization modeling in python*, (Springer, Germany, 2012)
- [107] Optimization, G., 'Inc., "Gurobi optimizer reference manual," 2015', URL: <http://www.gurobi.com>, 2014.

- [108] Harper, B., Kepert, J., and Ginger, J., *Guidelines for converting between various wind averaging periods in tropical cyclone conditions*, (WMO Geneva, Switzerland, 2010)
- [109] Jamieson, M.: 'The Challenges Facing Renewable Energy Developments in the Highlands and Islands of Scotland', MSc Energy, Water, and Environmental Management MSc Thesis, University of Abertay Dundee, 2015
- [110] 'Storm Desmond', <https://www.metoffice.gov.uk/weather/warnings-and-advice/uk-storm-centre/storm-desmond>, accessed 25/11/19
- [111] DECC, 'Progress in Preparing for Climate Change' (Committee on Climate Change, London, United Kingdom, 2015), pp. 76-86
- [112] 'Limekiln wind farm', <https://www.johnmuirtrust.org/about/resources/330-limekiln-wind-farm>, accessed 25 November 2019

## Chapter 7 - Appendices

### 7.1 Socioeconomic constraints on energy developments in Scotland

As is illustrated in Chapter 4 throughout, the energy infrastructure in Scotland particularly tends to be concentrated around the coasts and urban centres in the Northeast (Aberdeen), and South (where the vast majority of the population and economic development in Scotland is concentrated). There are multiple socioeconomic reasons for this which are explored in depth in [109]. The general themes addressed therein shall be discussed at a high level in this section due to the indirect consequences this has for power system resilience and reliability, and are drawn from the source referenced.

#### 7.1.1 Historical underdevelopment

As can be implied from the various maps illustrating the SHETL system in Scotland, industrial development and development of renewable energy resources tends to focus on the coasts and developed areas. This is a consequence of generations of historical underdevelopment and depopulation of rural areas in Scotland known historically as the *Highland Clearances* which began in the 19<sup>th</sup> century but the consequences of which are still felt in rural communities throughout Scotland. People were forcibly removed from rural areas either to the British colonies or to urban centres away from Highland Scotland. The consequence for this in a power systems context is that there are very few people in these rural areas, and hence little to no demand. However, it is in these regions where the greatest renewable energy potential for onshore wind is, creating conflicts of interest as to how to best utilise historically underdeveloped but aesthetically attractive “wilderness”.

There is a perception that much of the Highlands should remain “wild” – or, rather, in the state it has been left in since the mid-19<sup>th</sup> century – as that is more “natural” than the sight of wind turbines or pylons. This is problematic because, as mentioned in [6], the key to improving resilience of renewable energy resources is diversity of both type and location. If assets are concentrated in developed areas, this makes them vulnerable to common mode failures or fluctuations assorted with extreme weather events. Diversity cannot be improved if significant portions of the landmass are excluded from development.

Rural areas – across the UK, not simply in the Highlands and Islands of Scotland – are underdeveloped in part because of the legacy of the industrial revolution and generations of depopulation, and are caught between being underdeveloped because of this depopulation, and new developments being opposed because of that depopulation and the resultant “wildness” of the land. Therefore, attaining any planning permission for power system developments faces significant opposition by lobbyists who wish to maintain rural areas as a “wild” place.

Development of renewable energy developments and infrastructure developments are then easiest in areas which are already developed and do not face the same hurdles. Alternatively, developments can also rely on modifying or retrofitting existing infrastructure, which can itself lead to problems. One of the issues that led to widespread outages following Storm Desmond was the inundation of a low-lying substation [110] which was converted from an old power station. The cost of land in the UK and planning challenges in rural areas mean this is often an economically necessary solution as land is frequently sub-optimally utilised given the needs for security and resilience in the context of climate change [111] and rural areas in the UK are not exempt from this.

#### 7.1.2 Perceptions of the rural environment

The perception of Scotland as a wilderness is emphasised by government and tourist organisations, as well as wealthy landowners who benefit from the use of their land for the purposes of leisure (e.g. grouse hunting) as the land is perceived as having greater economic value being left underdeveloped

– so as to bring in tourists and associated revenue – rather than the potential income associated with energy developments.

This is related to the earlier themes already discussed. The Highlands and Islands are underdeveloped because they have been historically depopulated and the concentration of land ownership (approximately 600 people own almost 50% of Scotland’s landmass) means further development is difficult or outright opposed by those who own the land. The state of “wilderness” is not only seen as natural, but desirable. There are also contrasting opinions of what “wildness” even means – in [109] it is reported and discussed that many people saw ruins and rubble from ancient dwellings as more “natural” than tree farms. Further, opposition to energy developments emerges not just from landowners or local inhabitants but from lobbying organisations in favour of maintaining natural spaces.

An example of the confused approach to development of the Highlands and Islands can be seen in the Limekiln wind farm development in Thurso. It faced opposition from lobbyists despite being less than five miles from the Dounreay nuclear material decommissioning plant [112].

### *7.1.3 Consequences of underdevelopment and opposition to development*

Faced with conflicting interests between landlords, local citizens, and stakeholders such as hillwalkers and tourists, developing in rural areas is a complex and controversial issue but one which materially impacts power system stability and decarbonisation efforts for the Scottish – and hence wider GB – system, given the sheer quantity of wind resource concentrated in rural areas in Scotland.

Development of power infrastructure is focussed on coastal regions and those regions which are already developed, creating increased common-mode failure risk for assets in those regions due to the resistance to developments in areas which are not already developed.

Even should planning permission for wind generation be approved in contentious areas, the grid infrastructure to transport the power from the areas in which it is generated to regions in which it may be used – particularly during windier periods – may be particularly vulnerable and susceptible to faults as identified in Chapter 4. Wind generation tends to be built in windier regions to optimise profitability from investments and power output, but this necessarily increases the associated risk with the transport of power from these regions as the impact of outages associated with these lines increases as the network is being tasked with delivering services it may not have been originally designed to do.

Areas of the network which were historically low demand regions, and hence required little generation and could import from more developed parts of the system in radial networks, are now being utilised as generation networks due to the rapid increase in wind generation on the system, grids like SHETL being a prime example of this phenomenon. This then has implications for the wider network – fault events which damage areas of network which previously would only have had demand connected – and so the MITS system as a whole would be largely unaffected – now also have connected distributed generation meaning that, if these areas are exporting during fault events, the system may see a net loss of infeed and the corresponding degradation in system stability associated with that.

Ideally, to improve the resilience of the Scottish, hence GB, system, wind power should be distributed across the whole of Scotland and whichever areas are suitable in the wider UK. However, the perception of land, its ownership patterns, and how it is presently used act as inhibitors to reform of land usage and optimal strategic usage of land. The techniques demonstrated in Chapter 4 could be used to investigate areas across Scotland and GB which are less hazardous for overhead lines to plan out network expansions. Given the potential links between elevation, wind speeds, and OHL risk, there

may be significant reliability and resilience gains to be made. However, line expansions are not driven primarily by strategic utility but by aspects such as cost and public amenability to infrastructure developments which, in the context of the areas in which Scotland has particularly rich wind resource, is a complex socioeconomic and political problem.

As it stands, it is easiest to develop areas which have already been developed, and so wind farms and generation are pushed towards demand centres and already existing areas of infrastructure. There is some distribution of resources across the system, mitigating risk associated with local fault events, but, as demonstrated in Chapter 4, there is still significant overlap between wind generation, OHL infrastructure, and demand centres which can be problematic during HILP events.

Resilience lies in diversity and independence of resource vectors and wind affects both the ability to generate and transport power, undermining the independence of system security and increasing interdependencies on the system. This will become increasingly problematic as synchronous machines and inertia continues to be lost on the system.

Such issues cannot be simply ameliorated by undergrounding lines or moving wind offshore, however – undergrounding lines is expensive and cables have different electrical properties from overhead lines and so are not a like-for-like replacement. Stakeholders, investors, and citizens, if we are serious about decarbonisation, sustainability, and system resilience, have to find common ground to most effectively utilise land in an economically advantageous way while still allowing efficient exploitation of renewable energy vectors in under-developed regions like the Highlands and Islands of Scotland- and this will undoubtedly necessitate uncomfortable decisions regarding planning decisions, costs, and aesthetic effects on ostensibly “natural” land. In many ways this reflects the fact that the power system can never fully isolate itself from the socioeconomic context of the customers which it serves and the environment in which it is built.

## 7.2 Model deployment on simple test case

For this case, to demonstrate the fundamental workings of the model, two different perturbations shall be incurred at two separate times. These represent deterministic perturbations fed into EWPS to demonstrate the relationship between different aspects of the model so as to clarify its operation.

### 7.2.1 Scenario summary

First, the “dispatch” state is created. In this case, the dispatch is set such that 1320MW of frequency response is dispatched across the system. This test case involves use of the B6 boundary in the simulation. The boundary’s approximate location is indicated in Figure 7.1 with a solid line.

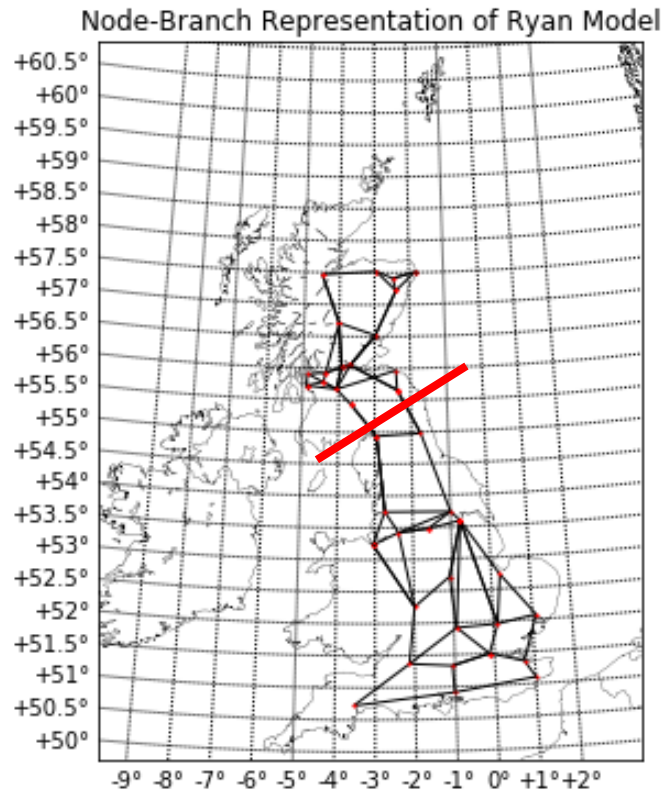


*Figure 7.1- approximate location of B6 boundary shown on "Ryan Model"*

The first of the faults simulated will be the loss of both double circuits which cross this line. The second, will be a loss of two large nuclear generation units in the southwest peninsula. These are indicated in Figure 7.2.

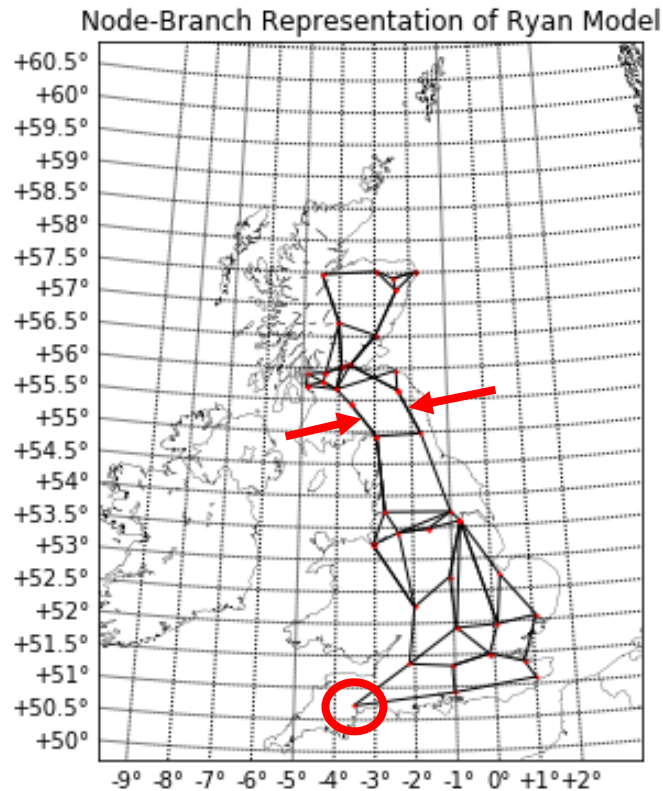


Figure 7.2 - outage locations indicated on Ryan Model

The system is dispatched with an empty contingency list. As a reminder, in this case the “contingency” list in the dispatch refers to the events against which the SCOPF is tasked with securing. That is, for an N-1 dispatch, for every single asset on the system which can fault (i.e. branches, wind generators, generator units), a state would be generated for asset  $n$  faulting at time  $0, 1, 2, 3, \dots, T$  on the presumption there are no repairs in the time horizon being assessed.

An empty contingency list, used in many of the case studies sampled, implies no such contingency list is generated or used in solving the problem and set  $k$  only has  $k = 0$  rather than a  $k$  for every hour of simulation, in this implementation 12, and for every asset on the system (>340).

The simulation performed in this case is over 12 hours from 1200 to 0000 on December 8<sup>th</sup> 2011.

### 7.2.2 Stage 1 - Dispatch

First, then, the Dispatch SCOPF is solved with these parameters as the first “stage” of simulation as described here.

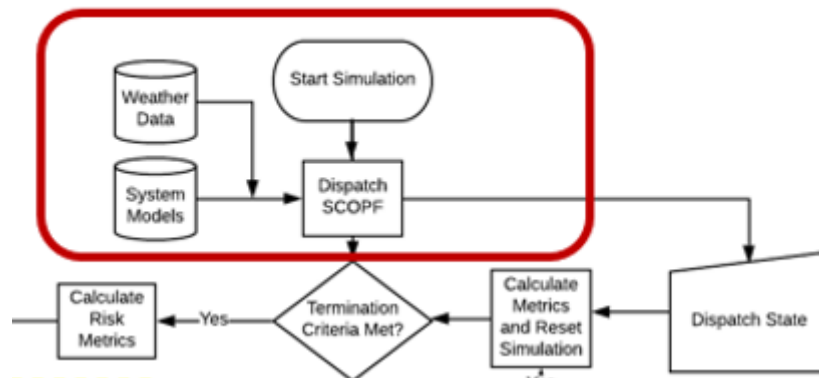


Figure 7.3 - stage 1 of simulation; dispatch and storage of dispatch state

The dispatch state of the SCOPF is stored in memory such that, were this a stochastic simulation, the state could be re-loaded for subsequent simulations. A loop would also be started over how many samples/simulations the model wished to perform. Since this is a deterministic test case, the loop is only a single pass, but nonetheless the flow direction and termination check is shown.

### 7.2.3 Stage 2 – Perturbation generation

The model moves onto stage 2, hour zero, and a loop begins over the time limit of a single simulation (12 hours) as illustrated in Figure 7.4.

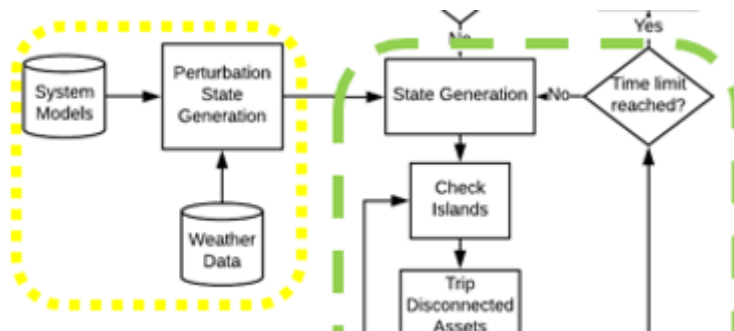


Figure 7.4 - stage 2; generation of perturbation state

In this case the model inherits the state of the system from the original dispatch. In a stochastic simulation, each asset would be sampled to determine if it has faulted or not. Deterministic faults may also be introduced dependent on the case study in question.

The asset outages are generated and imposed on the system state. Since the first fault in this test case does not occur until hour 4 (1600), the first 3 hours of the loop will be skipped.

### 7.2.4 Stage 3 – SFR-load-flow loop

At hour 4, the fault on the lines across B6 is introduced deterministically and imposed on the state model inherited from  $t=3$ . The model then enters the cascade simulation. This is the large green hatched box from the original framework, and is illustrated in Figure 7.5

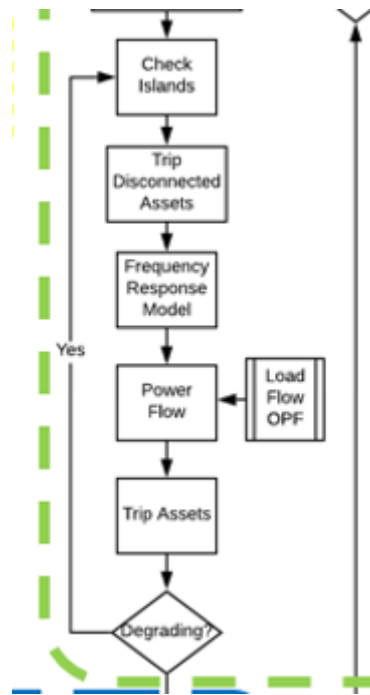


Figure 7.5 - cascade simulation loop

The first action the model takes is to determine the contiguous islands on the system and how those islands are connected. The model does this, then runs the SFR simulation on all of those islands identified. The results from the case in question are shown in Figure 7.6.

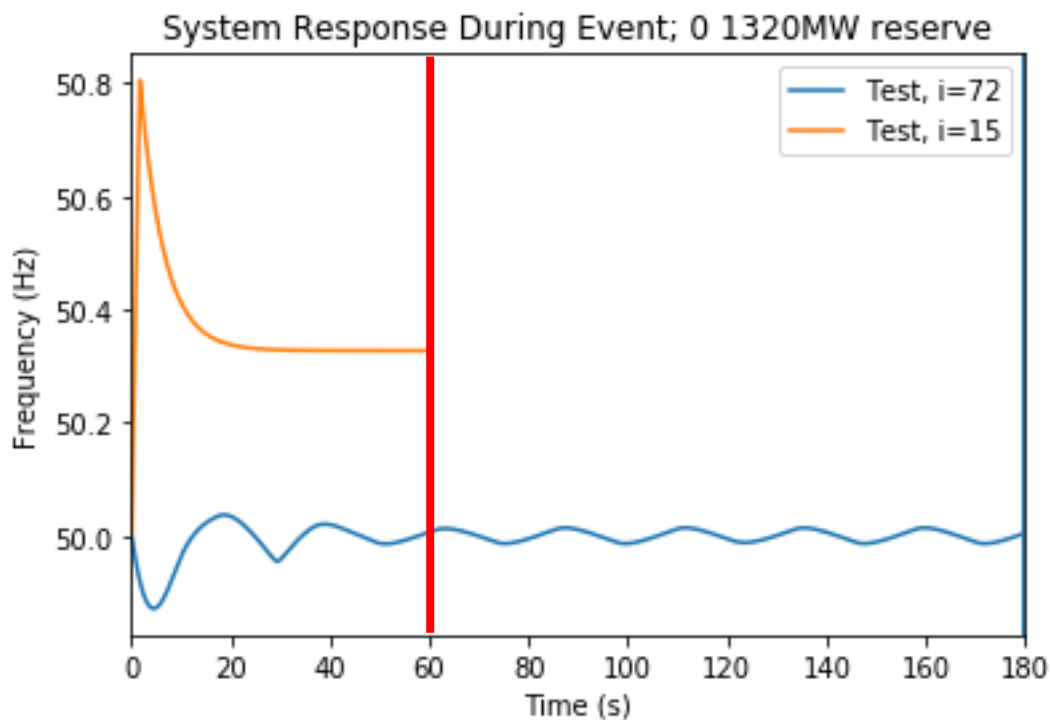


Figure 7.6 - SFR simulation for loss of B6 event

In this case, on island  $i=15$  (north of B6), there is a surplus of power so frequency rapidly rises. This leads to a generation trip, before frequency recovers to within statutory limits. On island  $i = 72$ , there is a corresponding loss of infeed and slight frequency excursion, which is easily controlled.

After the SFR simulation is run, the load flow is performed. This determines a line overload somewhere on the southern surviving network. As the frequency is controlled within bounds in the northern system, the cascade simulation stops for this island. It continues for the southern island as an overload is detected on the system.

As a consequence a line overloads and is disconnected then reconnected over two subsequent iterations. It is not possible from the output data to determine exactly which line, once the simulation has concluded.

No further overloads or excursions are detected, so the model proceeds to the next stage.

#### 7.2.5 Stage 4 – Redispatch and Unit Commitment OPFs

This section aggregates all of the results from the individual islands simulated in the previous stage and consolidates them for the redispatch and unit commitment OPFs. These are performed sequentially but bundled into one “module” in the framework.

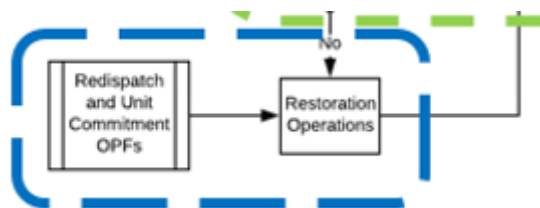


Figure 7.7 - redispatch/UC OPF locations in framework

Once these simulations have been performed, simulation for the individual hour is completed and the model cycles back to stage 1. The results of the UCOPF are then inherited by the next hour of the simulation.

For situations where no perturbations are detected, all intermediate sections can be skipped in the cascade simulation module and no actions are taken. The model simply moves onto the next hour and uses the dispatch scenario from the previous solution of the UCOPF to determine the state of the system.

The next fault in this scenario occurs at 1900, with the loss of a large generator on the southern island. The previous stages as described occur. The differences are described.

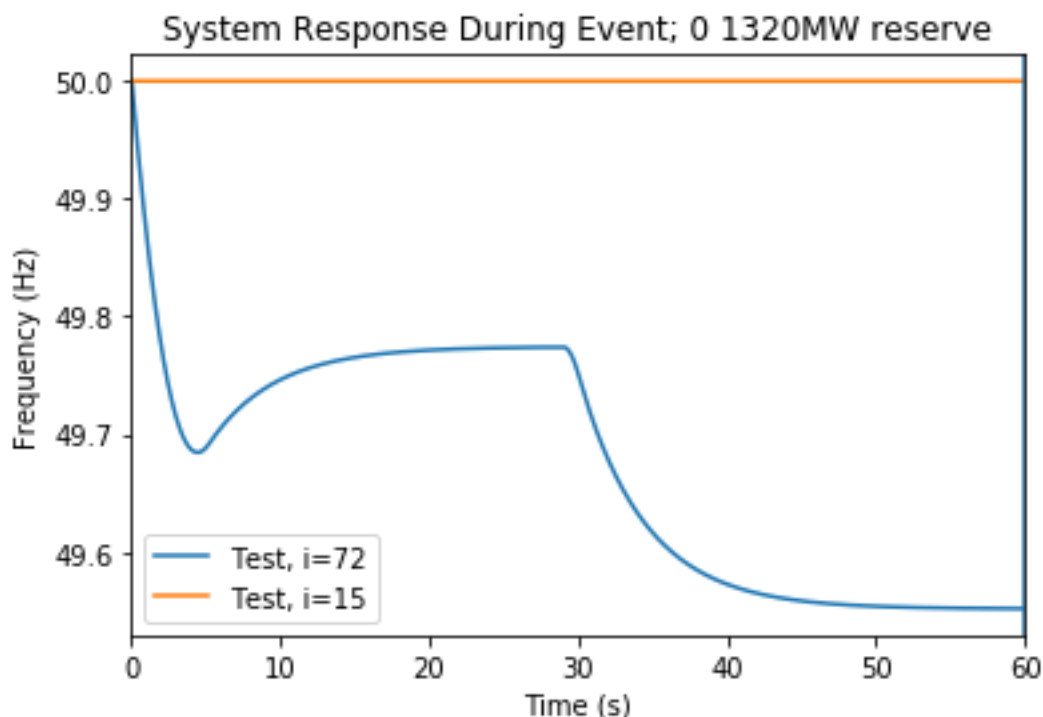


Figure 7.8- frequency response for second perturbation event

In this case, the model is able to detect that a loss of infeed only occurs on one island and so it does not need to simulate any frequency excursion on the other one. In contrast, the large loss of infeed is detected on the southern island, but there is adequate frequency response to keep frequency within statutory limits, though not restore it fully to the nominal value of 50Hz.

### 7.2.6 Stage 5 –Results and termination

No further perturbations are recorded over the subsequent hours, and so the model reaches the end of the time limit and can terminate.

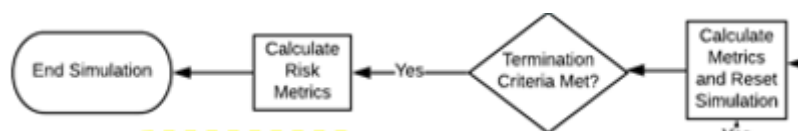


Figure 7.9 - termination of model

The ENS from this run of the model is 360MWh. This is the aggregated load curtailment across the whole 12-hour simulation. This is not associated with LFDD but rather load curtailment associated with losing a large infeed at peak time in the system and not having adequate scheduled tertiary response. In a full stochastic simulation this run would be reinitialized with the original dispatch and sampling performed again, but for this case the simulation ends.

## 7.3 EWPS Outputs

This sections provides additional figures and results for extra analysis of the case studies.

### 7.3.1 Tabulated results

Consolidating all of the cases into a single table the following table is generated and shown overleaf. Scenarios which utilise FDR are given with “FDR” in their name in the table and “DR” in the forthcoming figures.

Table 7.1 - tabulated summary of case studies

| Case                | N-1? | Reserve (MW) | North (MW) | South (MW) | Phi (MW) | EENS (MWh) | Error (MWh) | Var (MWh) | CVaR (MWh) | LOLP (%) | Error | Performance (%) | Error |
|---------------------|------|--------------|------------|------------|----------|------------|-------------|-----------|------------|----------|-------|-----------------|-------|
| Baseline_econ       | 0    | 0            | 0          | 0          | 0        | 2552       | 767         | 79128     | 215142     | 33.9     | 1.5   | 87              | 1.1   |
| Baseline_1          | 1    | 1320         | 0          | 0          | 0        | 8249       | 1362        | 292223    | 355303     | 60.8     | 1.5   | 87              | 1.1   |
| Baseline_2000_FDR   | 0    | 2000         | 0          | 0          | 50       | 1204       | 359         | 10417     | 93827      | 67.9     | 1.5   | 82.2            | 1.2   |
| Baseline_2000_South | 0    | 2000         | 0          | 2000       | 50       | 745        | 314         | 6645      | 56810      | 64.7     | 1.5   | 82.5            | 1.2   |
| Baseline_interp     | 1    | 1320         | 0          | 0          | 0        | 418        | 118         | 6459      | 22660      | 67.9     | 1.5   | 78.4            | 1.3   |
| B6_1                | 1    | 1320         | 0          | 0          | 50       | 213        | 32          | 5488      | 7628       | 54       | 1.6   | 78.4            | 1.3   |
| B6_econ             | 0    | 0            | 0          | 0          | 0        | 456        | 154         | 6016      | 30198      | 31.6     | 1.5   | 78.6            | 1.3   |
| B6_split            | 0    | 1320         | 500        | 820        | 50       | 840        | 218         | 9402      | 47601      | 46.1     | 1.6   | 78.9            | 1.3   |
| B6_flows_limit      | 0    | 1320         | 500        | 820        | 50       | 530        | 197         | 6899      | 37234      | 32.2     | 1.5   | 85.8            | 1.1   |
| B6_trips            | 0    | 2500         | 500        | 2000       | 50       | 661        | 42          | 6476      | 8791       | 85.6     | 1.1   | 59.9            | 1.6   |
| Gen_econ            | 0    | 0            | 0          | 0          | 0        | 37738      | 2762        | 245244    | 246337     | 38.1     | 1.5   | 64.3            | 1.5   |
| Gen_South           | 0    | 2000         | 0          | 2000       | 50       | 2703       | 642         | 9062      | 173601     | 52.9     | 1.6   | 63.5            | 1.5   |
| Gen_South_FDR       | 0    | 2500         | 500        | 2000       | 50       | 1293       | 493         | 4439      | 7117       | 55.3     | 1.6   | 56.9            | 1.6   |
| Gen_south_noFDR     | 0    | 2500         | 500        | 2000       | 50       | 1771       | 485         | 5556      | 100891     | 86.7     | 1.1   | 30.5            | 1.5   |
| Gen_noUC            | 0    | 0            | 0          | 0          | 0        | 1569       | 182         | 44428     | 44581      | 51.9     | 1.6   | 56.5            | 1.6   |

These can also be graphically represented as shown in Figure 7.10.

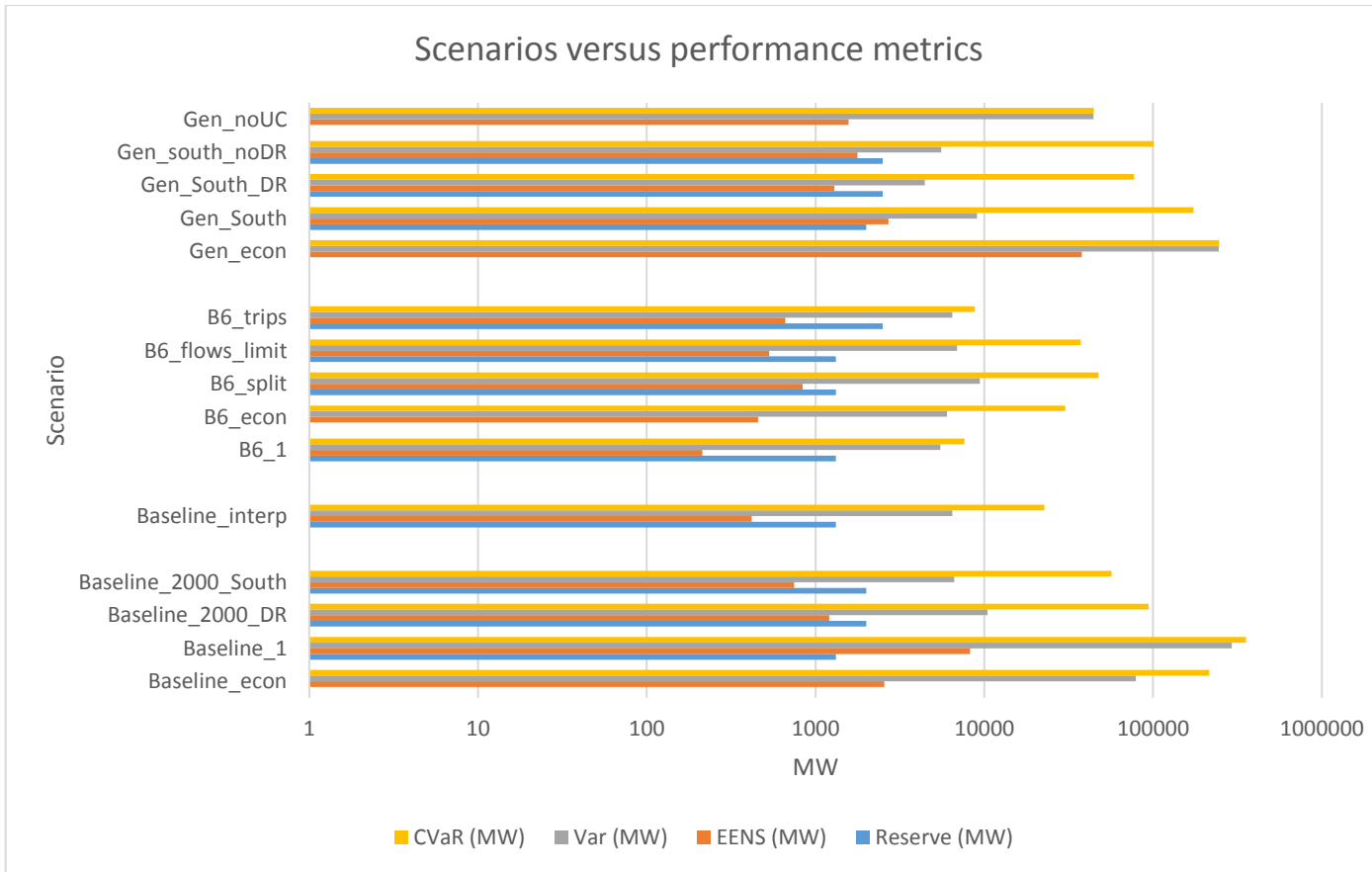


Figure 7.10 - performance of different scenarios with given metrics

Given the significant difference between the tested scenarios care should be taken in interpreting the results. However, one clear interpretation that can be made is that the interpolated data in the baseline cases shows significantly better performance across all metrics. This is associated with the lessened islanding effects and less “clustering” of line faults around nodes with the most extreme weather values.

The economic dispatch cases also generally perform much worse than the other dispatch scenarios, with the exception of the B6 cases.

In future, further analysis of the events which drive the most extreme results and the tail of the distributions could be useful to understand the phenomena which are most significant in driving these results.

### 7.3.2 Comparison of flexible demand versus non-flexible demand

Four scenarios and their performance metrics are given below.

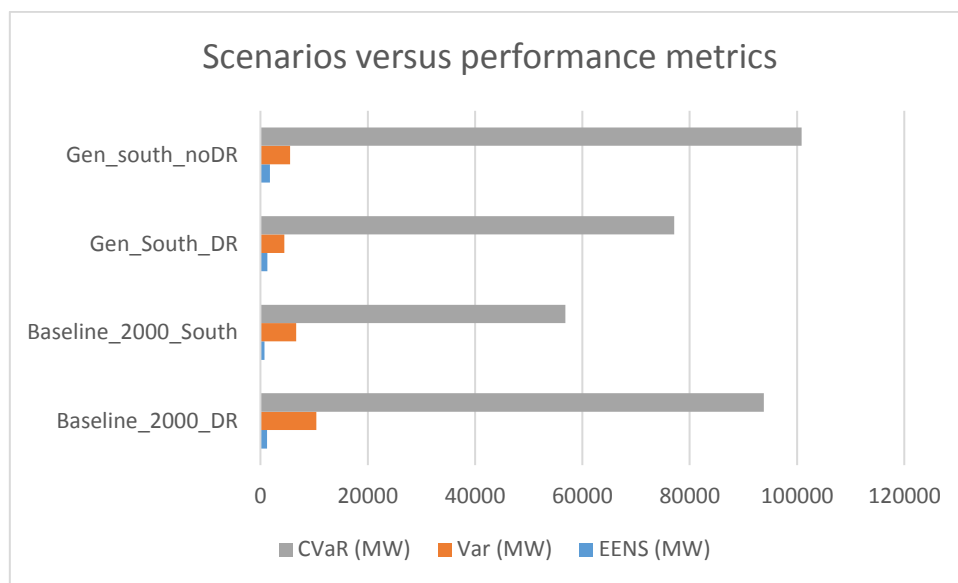


Figure 7.11 - performance metrics for given scenarios

What can be ascertained from these results is twofold. The first two cases compare scenarios where the top case has no FDR, but the second does, as well as additional frequency response available in the North (made possible because of the additional response available because of the FDR). The second compares a case where locational considerations are taken into account when dispatching frequency response, and one without.

Firstly, there are clear performance benefits to utilisation of FDR and additional frequency response in the cases with high generation infeed loss in the scenarios studied. Second, there are also performance benefits to locational restrictions/requirements in the optimisation in those cases. However, this should be understood in the context of the small sample sizes involved and the significantly different scenarios examined, and cannot definitively be understood as a generalizable policy without further study.

### 7.3.3 Frequency response versus EENS

In absence of all information about the case studies behind the data and the utilisation of FDR, a plot of EENS versus net frequency response dispatched is provided.

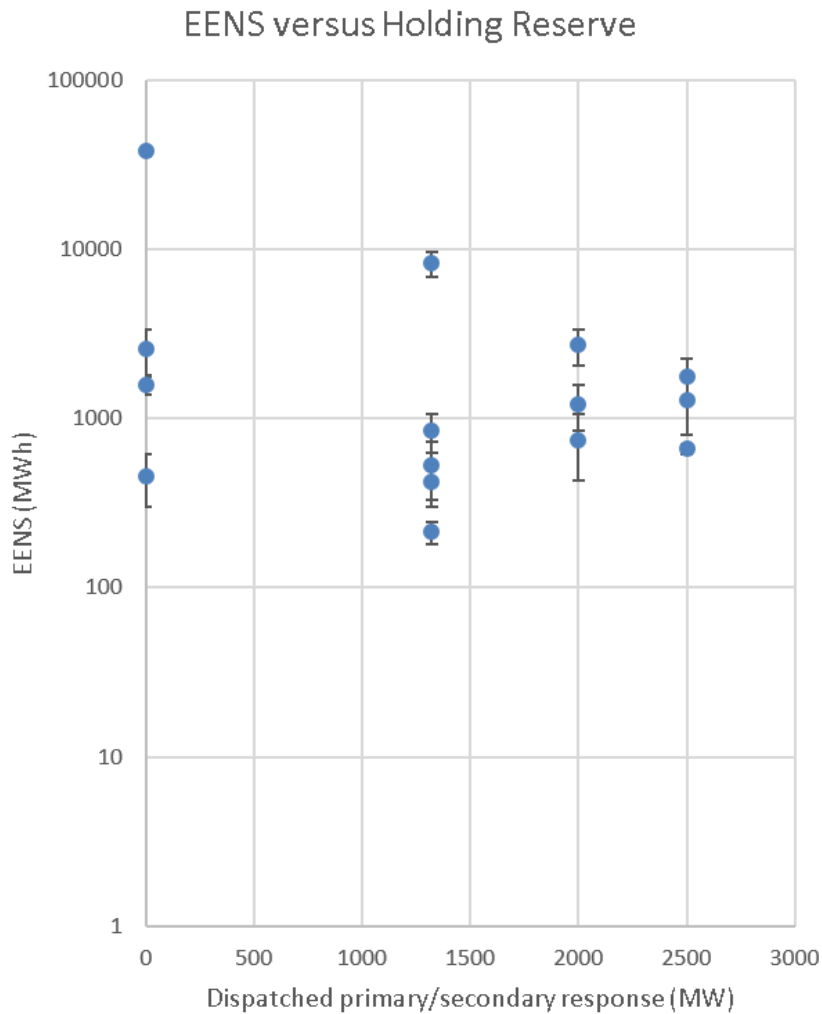


Figure 7.12 - frequency response dispatched versus EENS

Given the data and modelling limitations it would be unwise to draw too significant a generalised conclusion from such a set of results, however, what can broadly be concluded is that the presence of *some* frequency response limits the severity of outliers considerably for the examined cases, which should be unsurprising given the nonlinear impacts associated with cascading events such as those studied. That is, “something is better than nothing”, but as is demonstrated in other sets of results, suboptimal location of those interventions (particularly the distribution of frequency response or deployed generators) can also be unhelpful.